# Effect of molecular markers HIF-1α and *IDH1* on the radiobiological behavior of human malignant glioma cell lines in normoxia and hypoxia

## Dissertation

zur Erlangung des akademischen Grades

*doctor rerum naturalium* (Dr. rer. nat.)

der

Naturwissenschaftlichen Fakultät I

-Biowissenschaften-

der Martin-Luther-Universität Halle-Wittenberg,

vorgelegt

von Frau Diplom-Biologin Jacqueline Keßler

geboren am 28.Oktober 1981 in Apolda

Gutachter:

Herr PD. Dr. rer. nat. Ralph Golbik (Halle)

Herr Prof. Dr. med. Dirk Vordermark (Halle)

Herr Prof. Dr. med. Daniel Zips (Tübingen)

Tag der öffentlichen Verteidigung: 28.10.2016

Für meine Familie

# TABLE OF CONTENTS

# LIST OF ABBREVATIONS AND SYMBOLS

| | |
|---|---|
| AcCoA | acetyl coenzyme A |
| AFM | atomic force microscopy |
| AKT | protein kinase B |
| AhR | aryl hydrocarbon receptor |
| ARNT | aryl hydrocarbon nuclear translocator |
| ATP | adenosine triphosphate |
| bHLH | basic-helix-loop-helix motif |
| BNIP3 | BCL2/adenovirus E1B 19 kDa interacting protein 3 |
| BNIP3L | BCL2/adenovirus E1B 19 kDa interacting protein 3-like |
| BSA | bovine serum albumin |
| bp | base pair |
| C-TAD | C-terminal transactivation domain |
| CA9/CAIX | carbonic anhydrase 9 |
| CDKN2A | cyclin-dependent kinase inhibitor 2A |
| CHI3L1 | chitinase-3-like protein 1 |
| cm | centimeter |
| CNS | central nervous system |
| CTM | chetomin |
| cDNA | copy DNA |
| D-2-HG | D-2-hydroxyglutarate |
| kDa | kilodalton |
| DAPI | 4′,6-diamidino-2-phenylindole |
| DFO | desferrioxamine |
| DMF10 | dose modifying factor 10 |
| DMSO | dimethyl sulfoxide |
| DNA | deoxyribonucleic acid |
| DNase | deoxyribonuclease |
| ECL | enhanced chemiluminescence |
| EDTA | ethylenediaminetetraacetic acid |
| EGFR | epidermal growth factor receptor |
| EGTA | ethylene glycol tetraacetic acid |
| EGLN | egg-laying defective nine |

| | |
|---|---|
| eIF-4E | eukaryotic translation initiation factor 4E |
| ERK | extracellular signal-regulated kinase |
| FBS | fetal bovine serum |
| FIH | factor inhibiting HIF |
| GABRA1 | gamma aminobutyric acid A receptor alpha 1 |
| GBM | glioblastoma multiforme |
| GLUT-1 | glucose transport protein, isoform 1 |
| GSH | glutathione |
| Gy | gray |
| h | hour |
| HEPES | 2-[4-(2-hydroxyethyl) piperazin-1-yl] ethanesulfonic acid |
| HIF-1α | hypoxia-inducible factor-1α |
| HPRT1 | hypoxanthine phosphoribosyltransferase 1 |
| HR | hazard ratio |
| HRP | horseradish peroxidase |
| IAA | iodoacetate |
| IC50 | half-maximal inhibitory concentration |
| IDH1 | isocitrate dehydrogenase 1 |
| kb | kilo base |
| LB Agar | Luria-Bertani Agar |
| MAP | mitogen-activated protein |
| MEK | MAPK/ERK kinase |
| MERTK | c mer proto oncogene tyrosine kinase |
| MES | 2-(N-Morpholino) ethanesulfonic acid |
| Mdm2 | mouse double minute 2 homolog |
| mg | milligram |
| MG | malignant glioma |
| min | minutes |
| mL | milliliter |
| mM | millimolar |
| MNK | MAP kinase interacting kinase |
| MRI | magnetic resonance imaging |
| mRNA | messenger ribonucleic acid |
| mTOR | component mammalian target of rapamycin |
| NADP$^+$ | nicotinamide adenine dinucleotide phosphate |

| | |
|---|---|
| NADPH | nicotinamide adenine dinucleotide phosphate hydrogen |
| NEFL | neurofilament light polypeptide |
| NF1 | neurofibromin 1 |
| ng | nanogram |
| nM | nanomolar |
| N-TAD | N-terminal transactivation domain |
| OER | oxygen enhancement ratio |
| ODDD | oxygen-dependent degradation domain |
| PAGE | polyacrylamide gel electrophoresis |
| PARP | poly (ADP-ribose) polymerase |
| PBS | phosphate-buffered saline |
| PCR | polymerase chain reaction |
| PDGFRA | platelet-derived growth factor receptor alpha |
| PET | positron emission tomography |
| PHD | HIF prolyl hydroxylase |
| PI3K | phosphatidylinositol-4,5-bisphosphate-3-kinase |
| POLR2A | Homo sapiens polymerase (RNA) II (DNA directed) polypeptide A |
| PTEN | phosphatase and tensin homolog, deleted on chromosome 10 |
| qPCR | real-time quantitative PCR |
| RAF | rapidly accelerated fibrosarcoma |
| RAS | rat sarcoma |
| RB1 | retinoblastoma 1 |
| ROS | reactive oxygen species |
| rpm | revolutions per minute |
| RT | room temperature |
| s | sense |
| S6K | ribosomal protein S6 kinase |
| SDS | sodium dodecyl sulfate |
| PAGE | polyacrylamide gel electrophoresis |
| sec | second |
| siRNA | small interfering RNA |
| SLC12A5 | potassium-chloride co-transporter member 5 |
| SYT1 | synaptotagmin 1 |
| TBE | Tris-Borate-EDTA |
| TBS | Tris-buffered saline |

| | |
|---|---|
| TET | Ten-eleven translocation |
| TP53 | tumor protein p53 |
| Tris | Tris (hydroxymethyl) aminomethane |
| Tris-HCl | Tris (hydroxymethyl) aminomethane hydrochloride |
| U | unit |
| UV | ultraviolet |
| VEGF | vascular endothelial growth factor |
| VHL | von Hippel-Lindau |
| vs. | versus |
| WB | Western blot |
| WHO | World Health Organization |
| Wnt | wingless-related integration site |
| wt | wild type |
| α-KG | α-ketoglutarate |
| 4E-BP1 | 4E binding protein 1 |
| α | alpha |
| β | beta |
| γ | gamma |
| μg | microgram |
| μL | microliter |
| μM | micromolar |

# 1 INTRODUCTION

## 1.1 Gliomas classification, clinical and molecular characteristics and standard therapy of glioma

### 1.1.1 Classification and clinical characteristics of gliomas

Nowadays cancer is an enormous burden on society in more and less economically developed countries and is the second most deadly disease after heart condition (Torre et al., 2015). The incidence of cancer increased during the last decades due to the growth and aging of the world population as well as an elevated prevalence of risk factors such as genetic predispositions, personal circumstances (e.g. smoking, overweight, physical inactivity) and chemicals (e.g. aromatic amines, alkylating agents), physical (e.g. UV light, X-ray, radioactive radiation) or biological sources (human papilloma viruses, hepatitis B and C viruses, Epstein-Barr virus, bacteria *Helicobacter pylori*) (Torre et al., 2015; Harris, 1991; Poirier, 2004; Parkin, 2006, De Flora and Bonanni, 2011).

In 2012 over 14 million new cases of cancer and 8.2 million cancer deaths were recorded worldwide and the World Health Organization (WHO) predicts that the annual number of cancer cases will reach 19.3 million by the year 2025 (WHO/International Agency for Research of Cancer, GLOBOCAN 2012, date of last access 18.03.2016). Cancer is a disease that can affect nearly every organ and system (e.g. immune, blood, lymphatic system) in the human body. Several different types of benign and malignant tumors have been identified, whereas lung and breast cancer are the most common types worldwide. In contrast, primary tumors of the central nervous system (CNS) are relatively rare, with an annual incidence of 15/100,000 adult individuals, whereas the two most abundant forms in adults are tumors from the neuroepithelial tissue, called gliomas, and tumors of the meninges called meningiomas (Poeck and Hacke, 2013; Louis et al., 2001).

Gliomas are named after the glial cells, also called neuroglia or simply glia, from which they arise (Bigler and Clement, 1997). The brain consists of two major types of cells, neurons and glial cells. Glial cells surround neurons to hold them in place, provide nutrients, oxygen and electrical insulation, destroy pathogens, participate in the signal transmission and help to maintain homeostasis in the nervous system (Kettenmann and Verkhratsky, 2011). The glial cells were discovered in the middle of the 19th century by a group of scientists including Robert Remak, Theodor Schwann and Rudolf Virchow. Glial cells of the central nervous system are classified into microglia cells, oligodendrocytes and astrocytes (Kettenmann and Verkhratsky, 2011). Microglia cells are the immune cells of the central nervous system and have been considered as pathological sensors of the brain as they perform phagocytic functions (Kettenmann and Verkhratsky, 2011). Oligodendrocytes in the central and

Schwann cells in the peripheral nervous system form myelin sheaths to coat the neuronal axons, allowing high nerve conduction velocity in axons of vertebrates. Astrocytes are the most abundant and most heterogeneous neuroglial cell type in the CNS and are involved in several physiological processes. For example, these cells store and distribute energy substrates, control the development of other neural cells and define the micro-architecture in the brain (Kettenmann and Verkhratsky, 2011).

The first pathological description of gliomas was proposed by Virchow in 1863, who differentiated common types of intracranial malformations (Safavi-Abbasi et al., 2006). In 1926 Bailey and Cushing provided the first histopathological classification of gliomas, based on parallels between putative developmental stages and histological appearances of glial tumors (Bailey and Cushing, 1926).

Nowadays a classification established by the WHO is used in the clinical routine, which categorizes gliomas according to the histologically equivalent normal cell type and malignancy (Louis et al., 2007). Therefore, in accordance with the different glial cell types, gliomas are classified into astrocytomas, oligodendrogliomas, mixed gliomas such as oligoastrocytomas, ependymomas, choroid plexus tumors and other neuroepithelial tumors (Table 1.1). However, if gliomas indeed arise from differentiated glial cells remains a matter of debate. The cellular origins of gliomas are still undefined and experimental *in vivo* data have shown that different cell types of the central nervous system may be capable of being the source of glial neoplasia, including differentiated glial cells like an astrocyte or an oligodendrocyte, a more immature precursor cell or a neural stem cell (Jiang and Uhrbom, 2012; Modrek et al., 2014).

With respect to their malignancy, gliomas are classified into WHO grade I to grade IV. Grade I or II tumors are termed low-grade gliomas. Grade I tumors preferentially develop in children and young adults (Tonn et al., 2006). They grow very slowly, have a limited potential for malignant progression and can often be cured by surgical resection. Grade II gliomas (low-grade gliomas) preferentially, but not exclusively, occur in young adults (age peak: 30-40 years). These grade II gliomas are well-differentiated and also grow slowly. However, they diffusely infiltrate in the adjacent brain parenchyma, which impairs the possibility of treatment by resection. Therefore, grade II gliomas have an inherent tendency for local recurrence and malignant progression to a higher grade (Tonn et al., 2006; Louis et al., 2007). The majority of grade II gliomas are diffuse astrocytomas, oligodendrogliomas as well as oligoastrocytomas and patients suffering from these subtypes typically survive more than five years (five-year survival rate of 93 %). However, 52 % of the patients also progress within these five years (Soffietti et al., 2010; Louis et al., 2007). Grade III and grade IV gliomas are considered as high-grade gliomas. Grade III gliomas have incidence peaks between 40-45 years and are anaplastic (i.e. dedifferentiated) tumors, which grow fast and diffusely infiltrative. These gliomas are histologically characterized by increased cellularity, nuclear atypia and distinctive mitotic activity, whereas microvascular proliferation and necrosis are missing (Tonn et al., 2006; Louis et al.,

2007). In general, grade III gliomas require adjuvant treatments after resection. However, the median survival for patients with grade III gliomas is two to three years (Louis et al., 2007). Grade IV, the most malignant form of gliomas, also known as glioblastoma multiforme (or just glioblastoma), is the most common subtype of brain tumors (Maher et al., 2001). This tumor type can develop at any age, but adult patients are predominantly affected (peak incidence: 50-60 years). Glioblastomas are histologically characterized by high cellularity, marked cellular pleomorphism, nuclear atypia and increased mitotic activity (Tonn et al., 2006; Wesseling et al., 2011). Furthermore, the presence of microvascular proliferation and/or necrosis is a typical feature for the diagnosis of these tumors. The prognosis of patients with glioblastomas depends largely upon the availability of effective treatment regimens, consisting of surgery and adjuvant therapies (Louis et al., 2007). Patients suffering from glioblastomas have a median survival time of 14-17 months (Okada et al., 2009; Chen et al., 2012; Westermark, 2012; Gilbert et al., 2013).

Glioblastomas mostly arise *de novo* (primary glioblastoma) without clinical or histopathological evidence of a pre-existing less malignant precursor lesion (Newton, 2007; Taylor, 2010). On the contrary, secondary glioblastomas develop from a lower grade glioma over the time through malignant progression. Despite their molecular differences, primary and secondary glioblastomas are morphologically indistinguishable and respond similarly to conventional therapy (Maher et al., 2006).

**Table 1.1 The WHO classification and grading of gliomas of the CNS (adapted from Louis et al., 2007).**

| Tumors of the neuroepithelial tissue | Grading | | | |
|---|---|---|---|---|
| **Astrocytic tumors** | **I** | **II** | **III** | **IV** |
| Pilocytic astrocytoma | • | | | |
| Subependymal giant cell astrocytoma | • | | | |
| Pilomyxoid astrocytoma | | • | | |
| Diffuse astrocytoma | | • | | |
| Pleomorphic xanthoastrocytoma | | • | | |
| Anaplastic astrocytoma | | | • | |
| Glioblastoma | | | | • |
| Giant cell glioblastoma | | | | • |
| Gliosarcoma | | | | • |
| **Oligodrendroglial tumors** | **I** | **II** | **III** | **IV** |
| Oligodendroglioma | | • | | |
| Anaplastic oligodendroglioma | | | • | |
| **Oligoastrocytic tumors** | **I** | **II** | **III** | **IV** |
| Oligoastrocytoma | | • | | |
| Anaplastic oligoastrocytoma | | | • | |
| **Ependymal tumors; Choroid plexus tumors; Other neuroepithelial tumors** | | | | |

**1.1.2    Diagnosis, standard therapy and molecular characteristics of gliomas**

Gliomas account for 82 % of malignant primary brain and CNS tumors (Ostrom et al., 2015). In general, glioma patients present symptoms, which vary by tumor type, tumor size, location and tumor growth rate. Common symptoms of gliomas are headache, cognitive limitations (e.g. memory loss, personality changes, confusion, speech problems) and seizures, which are caused by disorganized electrical activity in the brain (Buckner et al., 2007). Diagnosis of gliomas usually involves gathering the patients' medical history, a physical exam, a neurological exam (e.g. vision, hearing, balance, coordination and reflexes) and scans of the brain by magnetic resonance imaging (MRI) and computed tomography (CT) to define the anatomic extent of the tumor (Kieffer, John Hopkins Medicine, date of last access 20.03.2016; Taylor, 2010; Buckner et al., 2007). Finally, the differential and final diagnosis is based on histological analyses of the tumor tissue obtained from biopsies or resections.

Surgery, if applicable, represents the primary therapy of gliomas and aims at debulking of the tumor (Hartmann and von Deimling, 2005; Desjardins et al., 2008). However, in some cases (e.g. young patients with small low-grade gliomas) a number of surgeons have recommended to consider the "watch and wait policy", which means to postpone surgery and instead to control the tumor radiographically, due to the potential surgical morbidity (Soffietti et al., 2010; Recht et al., 1992; Olson et al., 2000; Reijneveld et al., 2001). Moreover, the option of adjuvant treatment following surgery depends on the tumor classification and grade of resection. In this context surgical resection and radiotherapy are the mainstays of treatment of malignant gliomas (Stupp et al., 2005). For these gliomas or recurrent gliomas, radiotherapy is frequently accompanied or followed by chemotherapy using the alkylating agent temozolomide (TMZ).

Irrespective of the aggressive therapy options available, high-grade gliomas remain lethal diseases with dismal prognosis (Jiang and Uhrbom, 2012). Thereby, the failure of therapy for malignant gliomas is attributed to different factors. On the one hand, the diffusely infiltrative growth of malignant gliomas impedes their complete resection. (Tonn et al., 2006; Louis et al., 2007). Additionally, gliomas are generally immunosuppressive tumors due to the secretion of soluble immune inhibitory factors by microglia, astrocytes and tumor cells, such as transforming growth factor β (TGF-β) and interleukin (IL-10) (Wick et al., 2006; Rabinovich et al., 2007). Furthermore, the most malignant grade IV gliomas exhibit areas of necrosis and/or hypoxia, whereas the latter is described as an important limiting factor for the efficacy of radiotherapy (Vaupel et al., 2001; Höckel and Vaupel, 2001). The failure of current therapies has mainly been ascribed to the heterogeneity of gliomas with respect to clinical presentation, pathology and response to treatment (Jovčevska et al., 2013).

One reason for this heterogeneity of gliomas is most certainly the variety of epigenetic and genetic alterations (Jiang and Uhrbom, 2012). Therefore, several studies highlighted the importance of the epigenetic changes and the mutual signature of gliomas to improve the knowledge of their

development, progression and resistance to therapy (Parsons et al., 2008; Noushmehr, 2011 van den Bent et al., 2009; van den Bent et al., 2013a). Furthermore, molecular analysis of gliomas is an alternative approach to improve diagnosis and tumor classification by distinguishing glioma subtypes based on a molecular level. In a recent study it has been demonstrated that gliomas can be classified by their epigenetic changes due to the discovery of the CpG island methylator phenotype (G-CIMP) (Noushmehr et al., 2010). This phenotype defines a distinct subgroup of gliomas based on global promotor methylation patterns (i.e. concerted hypermethylation at a large number of loci).

In addition, low-grade and high-grade gliomas can also be grouped into different subtypes based on their molecular signature. By means of a comprehensive, integrative genomic analysis, the clustering of mutations revealed three prognostically significant subtypes of lower grade gliomas that were categorized more accurately by codeletion of chromosome arms 1p and 19q as well as *isocitrate dehydrogenase* (*IDH*) and *tumor protein p53* (*TP53*) status compared to histological classification (Cancer Genome Atlas Research Network, 2015).

On the other hand in a further study, a molecular classification of glioblastomas into neural, classical, mesenchymal and proneural subtypes was compiled based on their molecular and genetic alterations (Verhaak et al., 2010; Brennan et al., 2013) (Figure 1.1). Based on these studies the neural glioblastoma subtype exhibits a genetic signature almost like normal brain tissue and was typified by the expression of neuronal markers, such as *neurofilament light polypeptide* (*NEFL*), *gamma-aminobutyric acid A receptor alpha 1* (*GABRA1*) and *synaptotagmin 1* (*SYT1*). The classic glioblastoma subtype demonstrates chromosome 7 amplification, loss of heterozygosity on chromosome 10, amplification/overexpression/mutation of *epidermal growth factor receptor* (*EGFR*), homozygous deletion of the *cyclin-dependent kinase inhibitor 2A* (CDKN2A) and no alterations in *TP53*. The mesenchymal glioblastoma subtype can be identified by the expression of mesenchymal and astrocytic markers (e.g. *chitinase-3-like protein 1* (CHI3L1), *CD44* and c-mer *proto-oncogene tyrosine kinase* (*MERTK*)) as well as *neurofibromin 1* (*NF1*) deletions or mutations and *phosphatase and tensin homolog* (*PTEN*) mutations. Moreover, the two main features of the proneural glioblastoma subtype are alterations of *platelet-derived growth factor receptor alpha* (*PDGFRA*) and point mutations in the gene encoding the IDH1 enzyme. This subtype showed high expression of oligodendrocytic development genes and contained several proneural development genes. Furthermore, it has been demonstrated that G-CIMP gliomas belong to the proneural subtype (Noushmehr et al., 2010).

Verhaak and colleagues also investigated the effect of more intensive treatment regimes, consisting of concurrent chemo- and radiotherapy or more than three subsequent cycles of chemotherapy, on survival of the different glioblastoma subtypes (Verhaak et al., 2010). The results showed that

increasing the aggressiveness of the treatments reduced mortality in classical, mesenchymal and neural subtype, whereas it did not alter the survival times of patients with proneural glioblastomas.

In summary, based on their genetic and epigenetic alterations it is possible to divide gliomas into specific subgroups with different molecular and clinical phenotypes. These molecular classifications have consequences on the tumor diagnosis and therapeutic options for glioma patients. Hence, molecular markers provide additional information about tumorigenic processes to gain deeper insights into the development and progression of gliomas. Moreover, molecular markers represent a useful tool for the development of personalized therapeutic options for targeted therapies as one of the main research objectives in the next years.
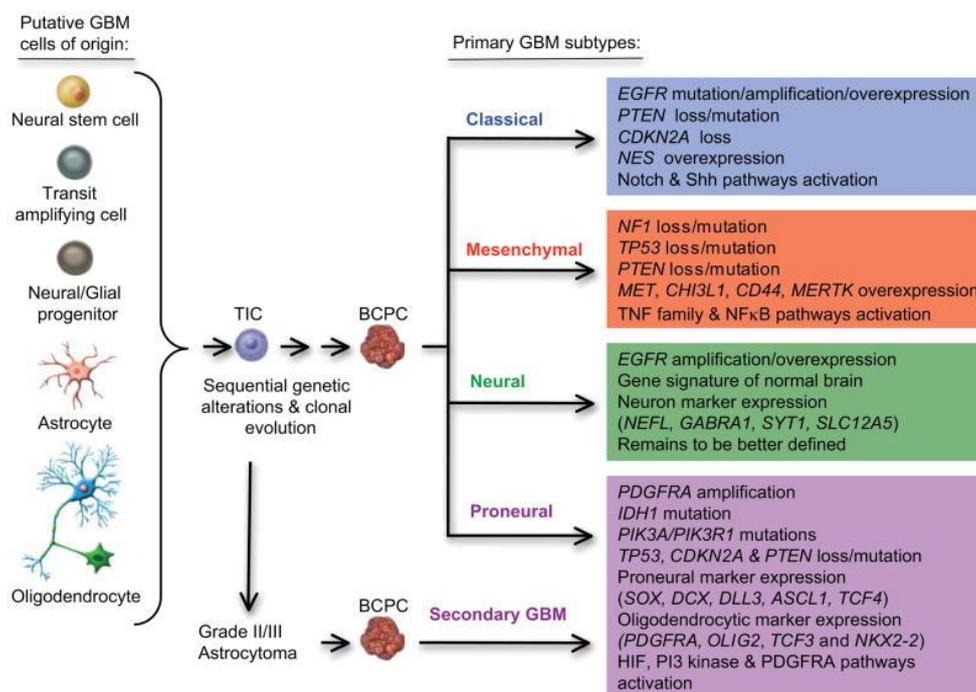


**Figure 1.1. Molecular classification of glioblastomas (glioma grade IV) into neural, classical, mesenchymal and proneural subtypes.** The cellular origins of gliomas are still undefined and it has been supposed that different cell types of the central nervous system may be capable of being the source of glial neoplasia by undergoing genetic alterations, which leads to a population of tumor–initiating cells (TICs). These TICs can then further accumulate genetic and epigenetic changes and become brain cancer–propagating cells (BCPC), which have than the ability for the formation of glioblastomas. GBM: glioblastoma multiforme, *EGFR*: *epidermal growth factor receptor*, *PTEN: phosphatase and tensin homolog*, *CDKN2A: cyclin-dependent kinase inhibitor 2A*, *NES*: *nestin*, *Shh*: *sonic hedgehog*. *NF1*: *neurofibromin 1*, *TP53*: *tumor protein 53*, *MET*: *mesenchymal-epithelial transition*, *CHI3L1*: *chitinase-3-like protein 1*, *CD44*: *CD44 molecule*, *MERTK*: *c-mer proto-oncogene tyrosine kinase*, TNF: tumor necrosis factor, NFκB: nuclear factor of kappa light polypeptide gene. *NEFL*: *neurofilament light polypeptide*, *GABRA1*: *gamma-aminobutyric acid A receptor alpha 1*, *SYT1*: *synaptotagmin 1*, *SLC12A5*: *potassium-chloride co-transporter member 5*. PDGFRA: platelet-derived growth factor receptor alpha, *IDH1*: *isocitrate dehydrogenase 1*, *PIK3: phosphatidylinositide 3-kinase*, *SOX*: *SRY-box*, *DCX*: *doublecortin*, *DLL3*: *delta-like 3 (Drosophila)*, *ASCL1*: *achaete-scute family basic-helix-loop-helix (bHLH) transcription factor*, *TCF4*: *transcription factor 4*, *OLIG2*: *oligodendrocyte lineage transcription factor 2*, *TCF3*: *transcription factor 3*, *NKX2-2*: *NK2 homeobox 2*, HIF: hypoxia-inducible factor (Van Meir et al., 2010).

## 1.2 Radiation and hypoxia

Conventional treatment of malignant gliomas, comprising surgery, radiotherapy and chemotherapy, requires a multidisciplinary team, including neurosurgeons, medical neuro-oncologists, radiation therapists and pathologists (Stupp et al., 2006). An optimal care for patients is ensured by an individual treatment plan based on several tumor characteristics, such as histology, genetic status of specific biomarkers as well as location and stage of the brain tumor. In addition, the medical history and the current living conditions of the patient are considered when planning the individualized therapy.

Radiation therapy is one of the most common and effective strategies to treat cancer. Thus at least 50 % of all patients receive radiotherapy at some stage during the course of their disease (Bernier et al., 2004; Delaney et al., 2005; Begg et al., 2011; Balcer-Kubiczek, 2012). In general, one can distinguish between two main types of radiotherapy (Baskar et al., 2012). The most widespread approach in the clinical setting is external beam radiation, which is applied from outside the body by irradiating the location of the tumor with high-energy rays (photons, protons or particle radiation). On the other side, for the routine treatment of gynecological and prostate malignancies internal radiation therapy or brachytherapy is delivered inside the body directly to the tumor site by radioactive sources, sealed in catheters or seed implants (Baskar et al., 2012).

In general, conventional radiotherapy is performed in a fractionated scheme, where the required total dose to kill the tumor cells is delivered in small doses per fraction, usually 1.8–2 Gy five times per week, over several weeks (Balcer-Kubiczek, 2012; Hellevik and Martinez-Zubiaurre, 2014; Mariotti et al., 2013; Teresa Pinto et al., 2016). In this way, the specific time intervals between the single treatments allow healthy tissue to recover. The aim of radiotherapy, i.e. destroying cancer cells with ionizing radiation while limiting the damage to nearby healthy tissue, has been significantly improved during the last decade by advances in imaging techniques, computerized systems for treatment planning, linear accelerators (with improved X-ray production and treatment delivery) as well as deeper understanding in the field of radiobiology (Bernier et al., 2004; Baskar et al., 2012; Balcer-Kubiczek, 2012).

Exposure of tumor cells to clinically relevant doses of ionizing radiation induces DNA damage directly through ionization of the DNA backbone or indirectly by forming free radicals through the hydrolysis of water molecules (Baskar et al., 2012; Mariotti et al., 2013). In both cases the most relevant induced DNA lesions, besides base damage and single-strand breaks, are double-strand breaks (DSBs), because these lesions are more complex and difficult to repair (Sancar et al., 2004; Suzuki et al., 2003). Consequently, unrepaired and misrepaired lesions of the DNA affect the genomic integrity and further induce death of the irradiated cells. However, it has been shown that the mechanisms of cell death caused by irradiation are complex (Baskar et al., 2012). In general, two main processes,

namely apoptosis and mitotic catastrophe, account for the majority of ionizing radiation-induced cell death (Dewey et al., 1995; Rupnow and Knox, 1999; Cragg et al., 2009; Jonathan et al., 1999). In addition, also necrosis, senescence and autophagy have been shown to induce cancer cell death in response to radiation (Hotchkiss et al., 2009; Schmitt, 2007; Roninson, 2003; Kondo et al., 2005; Baskar et al., 2012). However, although the knowledge concerning the various molecular pathways involved in the radiation-induced cell death has been rapidly increased in recent years, the precise mechanisms have still not been fully elucidated (Baskar et al., 2012).

Generally, treatment of high-grade gliomas is primarily aimed at alleviation of disease symptoms and control of growth or elimination of the tumor by means of surgery, to achieve tumor debulking, radiation and/or chemotherapy. (National Cancer Institute, date of last access 14.03.2016 and Kieffer, John Hopkins Medicine, date of last access 14.03.2016). In most cases radiotherapy is recommended following surgery to kill remaining tumor cells. Moreover, radiotherapy is also applied to treat recurrent, metastatic or inoperable gliomas, which are located in high-risk regions of the brain, to finally increase the survival of the patients (Kieffer, John Hopkins Medicine, date of last access 14.03.2016).

It is well known that tumors differ in their sensitivity to radiation. In this context, a critical factor for radiotherapy resistance is tumor hypoxia (Vaupel et al., 2001; Höckel and Vaupel, 2001; Moeller et al., 2005; Vaupel and Mayer, 2007). While normal tissue exhibits a partial oxygen pressure of approximately 40 mmHg, solid tumors are often characterized by hypoxic areas with partial oxygen pressures below 10 mmHg (Jordan and Sonveaux, 2012). In these regions, hypoxia is a limiting factor for the efficacy of radiotherapy (Vaupel et al., 2001; Höckel and Vaupel, 2001; Vaupel and Mayer, 2007). Main reason for this phenomenon is that the DNA damage caused by reactive oxygen species (ROS), which are produced indirectly by ionization radiation through the hydrolysis of water, is easily reversible unless oxygen stabilizes the radiation-induced lesions (Ewing, 1998; Jordan and Sonveaux, 2012). This radioprotective effect of hypoxia can be expressed quantitatively by the oxygen enhancement ratio (OER), which means that anoxic cells need a two- to threefold higher radiation dose compared to well-oxygenated cells in order to achieve the same biologic effects, i.e. DNA damage and subsequent cell death (Gray et al., 1953; Duncan, 1973).

Malignant gliomas exhibit intratumoral hypoxia due to their rapid proliferation and a highly abnormal dysfunctional vascularization (Dimberg, 2014). The blood vessels of high-grade gliomas are morphologically and functionally different from normal brain blood vessels. Due to stimulating factors, such as rapid growth and hypoxia, the tumor endothelium becomes dysregulated, resulting in fragile and leaky blood vessels with irregular diameters and an abnormal blood flow (Vaupel, 1996; Vaupel et al., 1989; Gambarota et al., 2008; Dudley, 2012).

In addition to an altered DNA repair and angiogenesis, hypoxia induces further changes in various cellular processes to adapt tumor cells to the harsh micromilieu of the tumor, including proliferation, differentiation, apoptosis and metabolism (Graeber et al., 1996; Semenza, 2000; Gatenby and Gillies, 2004). For example, one of the most universal characteristics of solid tumors is the so called "Warburg effect". In contrast to normal differentiated cells, which almost exclusively rely on mitochondrial oxidative phosphorylation to generate the energy for their cellular processes, most tumor cells instead rely on aerobic glycolysis to produce energy (Warburg, 1956; Weinhouse, 1956). It has been proposed that the switch from oxidative to glycolytic metabolism in tumor cells occurs in order to provide sufficient energy (adenosine triphosphate (ATP)) as well as nutrients for their rapid growth and proliferation and further to reduce the generation of ROS that might otherwise damage replicating DNA and inhibit their proliferation (Spitz et al., 2000; Semenza, 2000; Vander Heiden et al., 2009).

Indeed, hypoxia response elements (HRE) have been identified in the promoters of different genes encoding *glucose transporters* (*GLUTs*) and glycolytic enzymes (Ebert et al., 1995; Firth et al., 1994; Firth et al., 1995; Semenza et al., 1994; Semenza et al., 1996). Therefore, hypoxia induces cellular adaption and provides a physiological pressure to select cells (clonal selection), which are able to survive the harsh microenvironment in the tumor (Semenza, 2000). Thus, tumor-specific mutations do not result from targeted mutagenesis, but instead represent the effect of selection. Ultimately, tumor progression occurs as a consequence of the clonal selection of cells, in which somatic mutations have activated oncogenes or inactivated tumor suppressor and mutator genes leading to increased proliferation and/or survival within the hypoxic tumor microenvironment (Nowell, 1976; Semenza, 2000; Graeber et al., 1996). Hence, hypoxia promotes the aggressiveness of tumor cells and has been associated with poor outcome in several tumor entities, including malignant gliomas (Vaupel et al., 2001; Höckel and Vaupel, 2001; Vaupel and Mayer, 2007; Evans et al., 2010). Moreover, it has been demonstrated that the level of oxygenation is critical for the efficacy of radiotherapy and chemotherapy of malignant gliomas (Pérès et al., 2014).

The relationship between hypoxia and tumor progression as well as prognosis and resistance to therapy, especially in high-grade gliomas, underlines the clinical importance of assessing hypoxia in these tumors. Based on the characterization of the oxygen status it could be possible to refine prognosis and evaluate the therapeutic efficacy in order to adapt the treatment regimen of malignant tumors (Corroyer-Dulmont et al., 2015). In the literature several techniques have already been described to detect and quantify clinical relevant hypoxia within solid tumors, including direct methods (e.g. invasive polarographic needle electrode measurements), physiological methods (e.g. pimonidazole, magnetic resonance imaging (MRI), positron emission tomography (PET)) and by endogenous markers of hypoxia (e.g. hypoxia-inducible factor-1α (HIF-1α)) (Collingridge et al., 1999; Höckel et al., 1993; Bell et al., 2015; reviewed in Walsh et al., 2014). In fact, the invasive

polarographic electrode measurements remain the gold standard for the detection and quantification of tumor hypoxia, but several less invasive approaches have also shown to be feasible (reviewed in Walsh et al., 2014). Moreover, noninvasive detection methods seem to be beneficial especially for patients with malignant gliomas, since the application of invasive methods is limited in clinical routine. In this context, several studies have also been focused on proteins as endogenous markers of hypoxia. These molecules are directly or indirectly induced by hypoxia and regulate the adaptation of glioma cells to low oxygen concentrations. HIF-1α is one of the main mediators of the hypoxic response and has been shown to be a potential molecular marker of hypoxia in various tumor entities (Collingridge et al., 1999; Nordsmark et al., 2005; Brennan et al., 2006; Semenza, 2013). Moreover, the HIF-1α target genes *carbonic anhydrase 9 (CA9)* and *GLUT-1* as well as the extracellular matrix protein osteopontin have been linked to hypoxia and are therefore also considered as endogenous markers of hypoxia in different types of cancer (Vordermark and Brown, 2003a; Vordermark et al., 2004; Said et al., 2007a; Bache et al., 2006; Bache et al., 2008; Said et al., 2007b; Bache et al., 2015). Besides their promising potential for assessing the tumoral oxygen status, endogenous markers of hypoxia represent useful tools to gain a deeper understanding of the relationship between hypoxia and cancer biology and may serve as suitable targets to develop new therapeutic options for a more personalized treatment of individual patients.

## 1.3 The transcription factor HIF-1

### 1.3.1 Discovery of HIF-1α and clinical relevance

For the development of novel strategies for cancer therapy recent studies highlighted the HIF-1α pathway as an important survival pathway of solid tumors. The discovery of the hypoxia responsive element (HRE), an oxygen-regulated DNA sequence required for transcriptional activation of the erythropoietin gene (EPO), lead to the identification of the transcriptional factor HIF-1 (Semenza et al., 1991; Goldberg et al., 1988).

HIF-1 governs the cellular adaption to oxygen deficiency by regulating tumor-relevant genes involved in energy metabolism, angiogenesis, migration and invasion, cell proliferation, differentiation and apoptosis (Carmeliet et al., 1998; Semenza, 2003; Wenger et al., 2005; Keith et al., 2011; Semenza, 2014; Vaupel and Mayer, 2014). For example, HIF-1α has been shown to contribute to the Warburg effect through the induction of enzymes involved in the glycolysis pathway and overexpression of GLUTs, which increase the glucose import into tumor cells (Denko, 2008; Weinhouse, 1956; Masoud and Li, 2015). Therefore, HIF-1α "helps" hypoxic tumor cells to shift their glucose metabolism from mitochondrial oxidative phosphorylation to aerobic glycolysis (Weinhouse, 1956; Masoud and Li, 2015). Compared to the respective normal tissues, the overexpression of HIF-1α protein was observed in multiple tumor types, including colon, breast, gastric, lung, skin, ovarian, pancreatic, prostate, renal

and brain tumors (Zhong et al., 1999). Different studies demonstrated that elevated HIF-lα protein correlates with poor patient outcome in head and neck cancer, nasopharyngeal carcinoma, lung cancer, breast cancer, colorectal cancer, cervical cancer, pancreatic cancer, renal carcinomas, meningiomas of higher WHO grade and malignant gliomas (Rankin and Giaccia, 2008; Li et al., 2013a; Kaya et al., 2012; Baba et al., 2010; Dellas et al., 2008; Ye et al., 2014; Minardi et al., 2015; Reszec et al., 2013; Kaynar et al., 2008). Zhong and coworkers also identified increased gene expression of HIF-1α at tumor margins and in surrounding areas of neovascularization (e.g. in small cell lung carcinoma, glioblastoma and hemangioblastoma) as well as in distinct metastases (e.g. in lymph node metastasis from breast adenocarcinoma), whereas benign and noninvasive tumors (breast and uterus) were negative for HIF-1α overexpression (Zhong et al., 1999). The existence of a link between HIF-1α and invasion or metastasis has been confirmed in several studies of different tumor types (Harris, 2002; Semenza, 2003; Semenza, 2007; Dai et al., 2011). In patients with astrocytic tumors, HIF-1α gene expression has also been demonstrated as a prognostic biomarker (Mashiko et al., 2011). In this study, the median survival time of patients with HIF-1α gene expression was 17 months, whereas it was 80 months for patients without HIF-1α gene expression (Mashiko et al., 2011). A recent meta-analysis of 24 studies about the prognostic significance of HIF-1α in glioma showed that HIF-1α gene expression was significantly associated with high WHO grade (III+IV), microvascular density and overall survival of glioma (Liu and Cao, 2015). This suggests that HIF-1α might predict prognosis and can provide clinical benefit for the therapeutic strategy for patients with glioma.

Furthermore, HIF-1α and HIF-2α have also been demonstrated to play a role in stem cell biology (Semenza, 2016). Interestingly, it has already been shown that stem cells are often localized in specific hypoxic niches in tissues. Within these hypoxic niches HIFs have been shown to maintain the pluripotent and multipotent phenotype of stem cells as well as cancer stem cells, which are also known as tumor-initiating cells (Semenza, 2016). Several studies have suggested that cancer stem cells may be the primary mediators of resistance to chemo- and radiotherapy, leading to failure in cancer therapy and recurrence of tumors (Dean et al., 2005; Malik and Nie, 2012; Conley et al., 2015; Semenza, 2016).

Moreover, HIF-1α has been shown to be involved in the regulation of autophagy in malignant gliomas (Hu et al., 2012). Autophagy is a catabolic process aimed at recycling cellular components and damaged organelles in response to diverse stimuli, including nutrient deprivation, viral infection and genotoxic stress (Filomeni et al., 2015). Through this cytoprotective mechanism, glioblastomas coordinate their energy metabolism, availability of metabolites, adaption to oxidative stress or damage and also promote their treatment resistance (Kroemer et al., 2010; Filomeni et al., 2015). For example, in gliomas of high-grade malignancy, vascularization is often excessive and supports tumor progression (Linkous and Yazlovitskaya, 2011). Therefore, targeting the tumor vasculature by

antiangiogenic drugs or vascular-targeting agents has been considered as a promising approach for the treatment of malignant gliomas. Moreover, several studies, proposed the use of antiangiogenic therapy as therapeutic approaches in preclinical and clinical trials (Millauer et al., 1994; Kim et al., 1993; Cheng et al., 1996; Jain, 2008). However, the initial successes of these studies was mitigated by the clinical failure of antiangiogenic drugs through hypoxia-induced tumor cell autophagy (Hu et al., 2012). Moreover, HIF-1α-dependent expression of BNIP3/BNIP3L (BCL2/adenovirus E1B 19 kDa interacting protein 3 and BCL2/adenovirus E1B 19 kDa interacting protein 3-like) is a key mechanism in the activation of hypoxia-induced autophagy, indicating that inhibition of autophagy may help to prevent resistance to anti-angiogenic therapy used in the clinic (Bellot et al., 2009; Dodson et al., 2013; Hu et al., 2012).

### 1.3.2 Structure of HIF-1α

HIF-1 is a heterodimeric transcription factor, consisting of two subunits, the hypoxia-induced HIF-1α and the oxygen-independent HIF-1β subunit (Wang et al., 1995). HIF-1α gene expression is dependent on the oxygen concentrations, whereas HIF-1β is constitutively expressed (Wang et al., 1995). The HIF-1β subunit is also known as aryl hydrocarbon nuclear translocator (ARNT) and facilitates the translocation of HIF-1 into the nucleus via binding to the aryl hydrocarbon receptor (AhR) (Reyes et al., 1992; Wang et al., 1995). Both, HIF-1α and HIF-1β are members of the bHLH-PAS protein family, which contain a basic-helix-loop-helix (bHLH) motif (Jiang et al., 1996; Wang and Semenza, 1995). The small subgroup of bHLH proteins share recognizable motifs (bHLH, PAS and TAD), which can regulate their own transcription as well as the gene expression of other family members (Masoud and Li, 2015) (Figure 1.2).
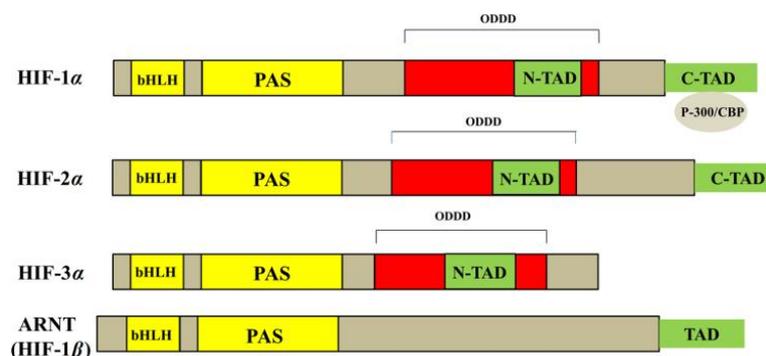


**Figure 1.2. Structure of HIF-α and HIF-1β proteins.** Functional domains at the C-termini: bHLH and PAS; Functional domains at the N-termini: N-TAD and C-TAD. HIF-1α and HIF-2α exhibit a high degree of similarity in the amino acid sequence of their DNA (bHLH), in the HIF-1β (PAS) binding domains and the C-TADs. In contrast, HIF-3α only shows N-TAD at the N-terminus. bHLH: basic-helix-loop-helix motif, PAS: PER (period circadian protein)-ARNT (aryl hydrocarbon nuclear translocator)-SIM (single minded protein), N-TAD: N-terminal transactivation domain, C-TAD: C-terminal transactivation domain, ODDD: oxygen-dependent degradation domain (adapted from Masoud and Li, 2015).

In general, bHLH and PAS are motifs at the N termini of HIF-1 and they are required for heterodimer formation between the HIF-1α and HIF-1β subunits and for binding to the HRE sequence on the target genes (Crews, 1998; Jiang et al., 1997) (Figure 1.2). The C termini of HIF-1α is subdivided into a N-terminal transactivation domain (N-TAD) and a C-terminal transactivation domain (C-TAD), which are responsible for the transcriptional activity of HIF-1α (Li et al., 1996; Ruas et al., 2002; Jiang et al., 1997; Pugh et al., 1997) (Figure 1.2). Both transactivation domains are important for optimal HIF transcriptional activity (Hu et al., 2007). In this context, the C-TAD has been shown to interact with coactivators such as CBP/p300 to activate gene transcription (Lando et al., 2002). N-TAD is responsible for stabilizing HIF-1α against proteasomal degradation, since it overlaps with the oxygen-dependent degradation domain (ODDD), which in turn mediates the oxygen regulation stability (O'Rourke et al., 1999; Bruick and McKnight, 2001).

Among the three HIF-α isoforms (HIF-1α, HIF-2α and HIF-3α) HIF-1α and HIF-2α are closely related proteins, sharing 48 % amino acid sequence identity and possess a number of structural and biochemical similarities (Ema et al., 1997; Flamme et al., 1997; Hogenesch et al., 1997; Tian et al., 1997). All isoforms dimerize with the HIF-1β subunit and bind to HREs (Ema et al., 1997; Gu et al., 1998). HIF-1α has been shown to be ubiquitously expressed in the body, whereas gene expression of HIF-2α is restricted to specific tissues, including the lung, endothelium and carotid body (Ema et al., 1997; Tian et al., 1997; Tian et al., 1998; Ke and Costa, 2006). On the other hand, HIF-3α is also expressed in a variety of tissues, including adult thymus, lung, brain, heart and kidney (Gu et al., 1998). Moreover, inhibitory PAS (IPAS) is known as an alternative splice variant of HIF-3α, which lacks the intrinsic transactivation activity (Makino et al., 2001). IPAS has been demonstrated to act as a dominant-negative regulator of HIF-1α, whereas it prevents HIF-1 DNA binding by interacting with the amino-terminal region of HIF-1α (Makino et al., 2001).

### 1.3.3 Regulation of HIF-1α

The transcriptional activity and accumulation of HIF-1α protein is regulated at different levels throughout its life cycle inside the cells (Masoud and Li, 2015). *HIF-1α* mRNA is constitutively expressed independent of the oxygen status, while its protein level is regulated through a series of signaling events, including various growth factors or signaling molecules (Kallio et al., 1997). Under normal oxygen conditions, HIF-1α protein has a short half-life of five minutes and is quickly degraded through the proteasome (Wang et al., 1995; Salceda and Caro, 1997). On the contrary, in hypoxia, HIF-1α becomes stabilized and translocates from the cytoplasm to the nucleus, where it dimerizes with the HIF-1β subunit to form the transcriptionally active HIF-1 complex. (Kallio et al., 1997; Huang et al., 1996) (Figure 1.3).
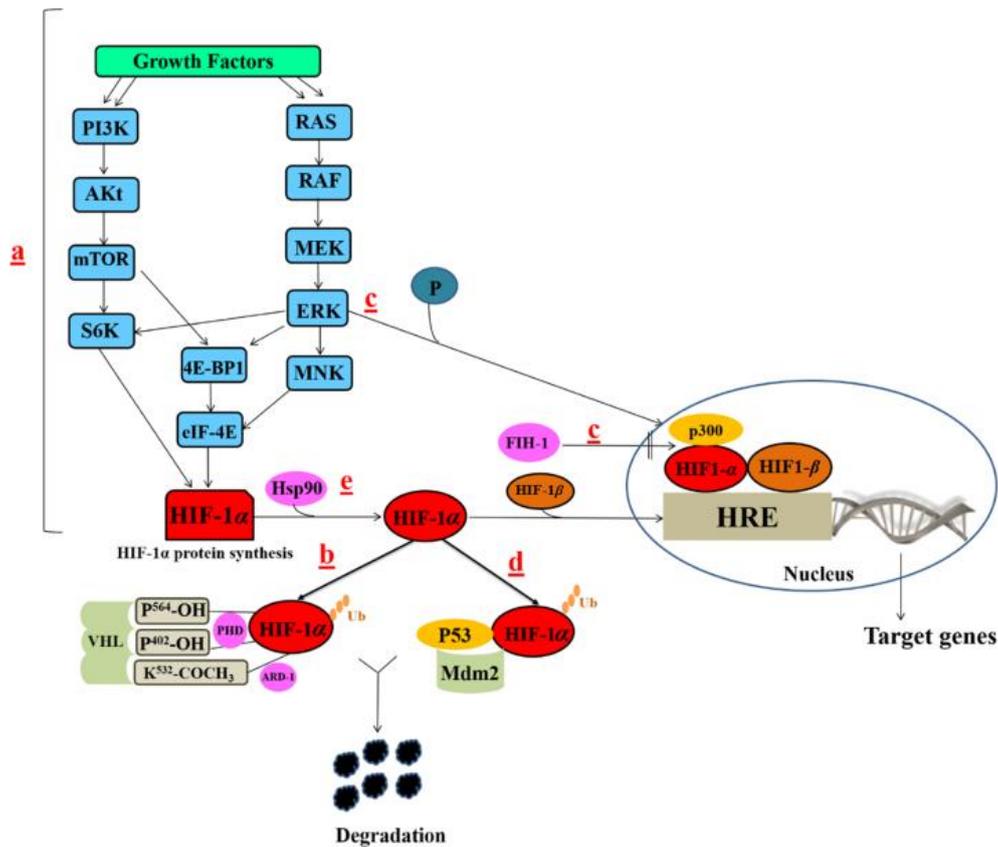
**Figure 1.3. Regulation of the HIF-1α pathway.** (a) Growth factors related pathways; (b) VHL related pathways; (c) FIH-1pathway; (d) Mdm2/p53-mediated ubiquitination and proteasomal degradation pathway; (e) Hsp90 stabilization. HIF-1α activity is regulated by: regulating HIF-1α synthesis (a), HIF-1α stability (b, d, e) or HIF-1α transcriptional activity (e, c). PI3K: phosphatidylinositol-4,5-bisphosphate-3-kinase, AKT: protein kinase B, mTOR: component mammalian target of rapamycin, S6K: ribosomal protein S6 kinase, 4E-BP1: 4E binding protein 1, eIF-4E: eukaryotic translation initiation factor 4E, RAS: rat sarcoma, RAF: rapidly accelerated fibrosarcoma, MEK: MAPK/ERK kinase, ERK: extracellular signal-regulated kinase, MNK: MAP kinase interacting kinase; (adapted from Masoud and Li, 2015).

The activated HIF-1 complex translocates into the nucleus, where it recruits transcriptional coactivators and induces the gene expression of its transcriptional targets via binding to their HREs (Lando et al., 2002). The stability and transcriptional activity of HIF-1α is strictly regulated by its post-translational modifications, such as hydroxylation, acetylation, ubiquitination and phosphorylation, which occur within several domains (Salceda and Caro, 1997; Brahimi-Horn et al., 2005). In the presence of oxygen, hydroxylation of two proline residues ($P^{402}/P^{564}$) is carried out by enzymes called prolyl-4-hydroxylases (PHDs) or HIF-1 prolyl hydroxylases (HPH) (Srinivas et al., 1999; Masson et al., 2001; Masson and Ratcliffe, 2003). These molecules are iron- and 2-ketoglutarate (KG)-dependent dioxygenases, which require adequate amounts of oxygen to maintain their hydroxylation activity (Bruick and McKnight, 2001; Epstein et al., 2001). Moreover, oxygen-independent acetylation of a specific lysine residue ($K^{532}$) in the ODDD, by an acetyl

transferase called arrest-defective-1 (ARD-1), promotes the interaction of the modified HIF-1α with the von Hippel-Lindau (VHL) ubiquitin E3 ligase complex (Srinivas et al., 1999; Masson et al., 2001; Jeong et al., 2002). By this process the VHL complex tags HIF-1α with ubiquitin and thereby marks it for proteasomal degradation (Maxwell et al., 1999) (Figure 1.3b).

In addition, oxygen-independent hydroxylation of the asparagine residue $N^{803}$ in the C-TAD, by factor inhibiting HIF-1 (FIH-1), impairs the cooperative binding of HIF-1α with the co-activator CBP/p300 (Figure 1.2c). Thus, this asparaginyl hydroxylase impairs the transcriptional activity of HIF-1α (Lando et al., 2002b).

HIF-1α has also been shown to be regulated oxygen-independent via growth factor signaling pathways through activation of phosphatidylinositol-4,5-bisphosphate-3-kinase (PI3K), which increases the protein translation of the protein (Jiang et al., 2001; Semenza, 2002a; Conrad et al., 1999) (Figure 1.2a). Furthermore, HIF-1α is regulated by the mouse double minute 2 homolog (Mdm2) pathway, by means of p53/Mdm2-mediated ubiquitination and subsequent proteasomal degradation (Ravi et al., 2000) (Figure 1.2d). Hence, it has been demonstrated that loss or mutations in these two tumor suppressor genes resulted in elevated HIF-1α levels in certain types of tumors (Bae et al., 2002). On the other hand, HIF-1α is also controlled by the Heat shock protein 90 (Hsp90), which directly binds to the protein and protects it from its non-VHL dependent degradation (Gradin et al., 1996; reviewed in Masoud and Li, 2015) (Figure 1.2e).

In summary, HIF-1 regulates over 200 genes and promotes tumorigenesis by the regulation of several cancer characteristics, including angiogenesis, metabolism, proliferation, metastasis and differentiation (Schödel et al., 2011; Masoud and Li, 2015). In view of the intratumoral hypoxia of high-grade gliomas, which impairs the effectiveness of radiotherapy as well as the multiple roles of HIF-1 in progression and invasiveness of these tumors, inhibition of HIF-1α appears to be a promising treatment strategy and may therefore sensitize human malignant gliomas to radiotherapy.

## 1.4   The *IDH* Mutations

### 1.4.1   Discovery of the *IDH* mutations and clinical relevance

Over the last decade the understanding of glioma tumorigenesis was revolutionized due to the discovery of mutations involving the gene encoding isocitrate dehydrogenase (IDH) enzymes. Using whole-genome sequencing, Parson and colleagues first identified recurrent mutations in the active site of IDH1 in 12 % of glioblastoma (GBM) patients (Parsons et al., 2008). Interestingly, patients with *IDH1* mutations had a very high frequency of *TP53* mutations and a very low frequency of mutations in *PTEN*, *retinoblastoma 1 (RB1)*, *EGFR* or *NF1*, suggesting a biologically specific subgroup of glioblastoma patients (Parsons et al., 2008). A subsequent genome-wide mutational analysis of gliomas revealed somatic mutations of the *IDH1* gene or the related *IDH2* gene in a mutually

exclusive manner in over 80 % of WHO grade II/III astrocytomas, oligodendrogliomas and oligoastrocytomas (Yan et al., 2009). *IDH* mutations occur in the vast majority of grade II and grade III gliomas and secondary glioblastomas (grade IV) that evolved from these lower grade tumors, but not in primary glioblastomas (Yan et al., 2009; Balss et al., 2008; Ichimura et al., 2009; Lai et al., 2011; Brennan et al., 2013). Similarly, *IDH* mutations are frequently found in a number of other tumors, including acute myeloid leukemia (AML), intrahepatic cholangiocarcinoma, melanoma and cartilaginous tumors (Paschka et al., 2010; Borger et al., 2012; Lopez et al., 2010; Shibata et al., 2011; Amary et al., 2011).

*IDH* mutations are thought to be an initiating event in gliomagenesis, probably occurring before *TP53* mutation or 1p/19q codeletion, as gliomas carrying only an *IDH* mutation are more frequent than those which only show *TP53* mutation or loss of chromosome 1p/19q (Yan et al., 2009; Ohgaki and Kleihues, 2013). Thus, *IDH* mutations seem to dictate a particular path for oncogenic progression, preferentially occurring in younger patients compared to patients with *IDH1* wild type WHO grade II/III gliomas and glioblastomas (Parsons et al., 2008; Yan et al., 2009; Lai et al., 2011; Balss et al., 2008). Furthermore, the presence of *IDH1/2* mutations are associated with increased progression-free and overall survival for patients with glioma irrespective of their grade (Parsons et al., 2008; Yan et al., 2009; Hartmann et al., 2009; Ichimura et al., 2009; Sturm et al., 2012; Weller et al., 2012). In contrast, this study also indicated that *IDH1* mutations are not related to the temozolomide response. Thus, *IDH1* mutation can be used as a prognostic marker in gliomas, but not as predictive value for treatment decisions (Dubbink et al., 2009; Sanson et al., 2009; van den Bent et al., 2009; Weller et al., 2012; Dubbink et al., 2015). On the other hand, it is unclear whether the positive effect of *IDH* mutation on survival of patients with low-grade or high-grade gliomas is associated with a less aggressive phenotype or is directly linked to increased sensitivity to therapy treatment of these tumors.

## 1.4.2 Biochemical features and cellular effects of an *IDH* mutation

IDH enzymes catalyze the decarboxylation of isocitrate to α-ketoglutarate (α-KG). In particular, IDH1 and IDH2 use $NADP^+$ (nicotinamide adenine dinucleotide phosphate) as a cofactor to generate NADPH (nicotinamide adenine dinucleotide phosphate hydrogen) during the catalysis, whereas IDH3 uses $NAD^+$ as a cofactor to produce NADH in the process (Xu et al., 2004; Yoshihara et al., 2001). The $NADP^+$-dependent enzymes are capable of catalyzing the reductive carboxylation of α-KG to isocitrate (Siebert et al., 1957). IDH1 (chromosome 2q33.3) and IDH2 (chromosome 15q26.1) are homodimeric enzymes exhibiting a high degree of sequence similarity (70 % in human) and an almost identical protein structure with two active sites per dimer (Xu et al., 2004). IDH1 is located in the cytoplasm and peroxisomes, while IDH2 and IDH3 are located in the mitochondria where they are involved in the citric acid cycle (also known as tricarboxylic acid (TCA) cycle) (Geisbrecht and

Gould, 1999) (Figure 1.4). In addition, IDH1 and IDH2 are involved in a variety of cellular processes, including the glutamine metabolism, glucose sensing and lipid metabolism, synthesis of N-acetylated amino acids and regulation of the cellular redox status via glutathione (GSH) (Metallo et al., 2011; Wise et al., 2011; Reitman et al., 2011) (Figure 1.4).

Mutations in the *IDH* genes are generally heterozygous missense substitutions, which remarkably occur in a mutually exclusive manner affecting only the active sites of the enzymes (Reitman and Yan, 2010; Yan et al., 2009). Mutations in *IDH1* always appear in the arginine residue at codon 132 resulting in a substitution of histidine for arginine (R132H) in over 90 % of all *IDH1* mutations (Yan et al., 2009; Hartmann et al., 2009). Other *IDH1* mutations at $Arg^{132}$ occur at much lower frequencies, including R132C (4.1 %), R132S (1.5 %), R132G (1.4 %) and R132L (0.2 %) (Hartmann et al., 2009) (Table 1.2). Grade II/III gliomas and secondary glioblastomas which are not carrying an *IDH1* mutation are often positive for mutations of the *IDH2* gene. This usually affects arginine at codon 172 ($Arg^{172}$), the analogous amino acid to *IDH1* $Arg^{132}$, and is most commonly characterized by an *IDH2R172K* missense substitution (Yan et al., 2009; Hartmann et al., 2009).

**Table 1.2. Frequency of specific *IDH* mutation in gliomas.** Type of 716 *IDH1* and 31 *IDH2* mutations and frequency among mutations in 1,010 WHO grades II and III astrocytomas, oligodendrogliomas and oligoastrocytomas. Data are presented as the percentage of total *IDH1/2* mutations in glioma patients according to Hartmann and colleagues; (adapted from Hartmann et al., 2009).

| Gene | Nucleotide change | Amino acid change | Frequency (%) |
|------|-------------------|-------------------|---------------|
| *IDH1* | G395A | R132H | 664 (92.7 %) |
| | C394T | R132C | 29 (4.1 %) |
| | C394A | R132S | 11 (1.5 %) |
| | C394G | R132G | 10 (1.4 %) |
| | G395T | R132L | 2 (0.2 %) |
| *IDH2* | G515A | R172K | 20 (64.5 %) |
| | G515T | R172M | 6 (19.3 %) |
| | A514T | R172W | 5 (16.2 %) |

Mutations in the active sites of the IDH1 enzyme cause a distinctly decreased enzyme activity to isocitrate and result in a neomorphic enzyme function, which catalyzes the NADPH-dependent reduction of α-KG to the 2-hydroxyglutarate (2-HG) enantiomer, D-2-hydroxyglutarate (D-2-HG). In turn, this leads to D-2-HG accumulation and lowering α-KG as well as NADPH levels (Zhao et al., 2009; Dang et al., 2010; Gross et al., 2010; Ward et al., 2010) (Figure 1.4). However, NADPH is necessary for the regeneration of reduced GSH which functions as the main antioxidant in mammalian cells. Low levels of cytoplasmic NADPH have been linked to elevated oxidative stress through impaired reduction of GSH (Bleeker et al., 2010) (Figure 1.4). In general, oxidative stress is increased

by irradiation and chemotherapy leading to the hypothesis that *IDH1* mutations induce an enhanced response to radiotherapy and may contribute to the prolonged survival of patients harboring the mutation (Ozben, 2007).
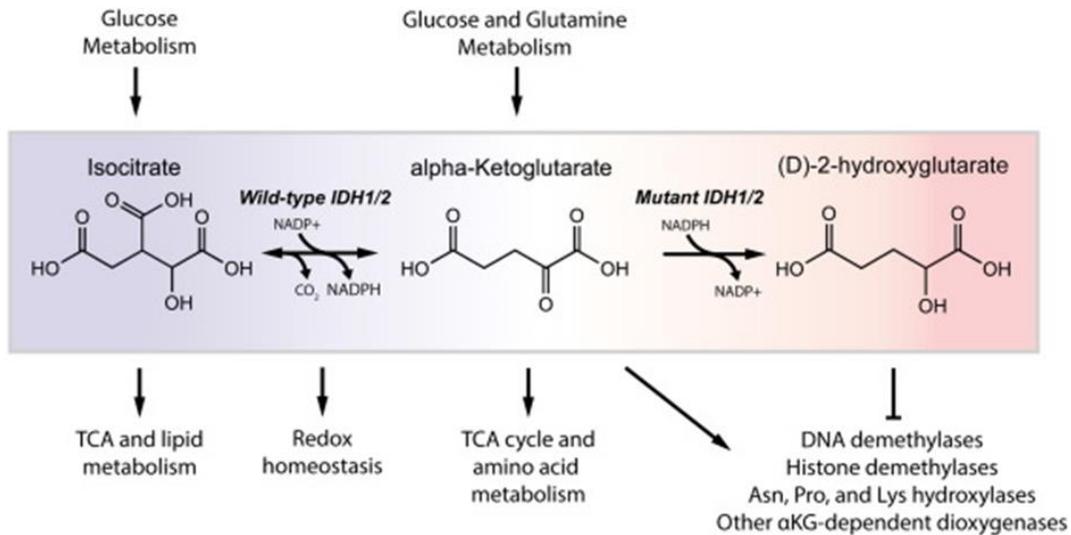


**Figure 1.4. Neomorphic enzyme activity of mutant IDH enzymes.** IDH1 and IDH2 catalyze the oxidative decarboxylation of isocitrate to generate α-KG, by using $NADP^+$ as a cofactor to produce NADPH and $CO_2$. Recurrent mutations in the active sites of IDH1 and IDH2 induce a decreased enzyme activity to isocitrate and results in a gain-of-function that catalyzes the conversion of α-KG into D-2-HG in a manner that consumes NADPH. IDH1 and IDH2 are involved in a variety of cellular processes; (adapted from Parker and Metallo, 2015).

Due to the finding that mutations in the *IDH1* gene cause an over 100-fold increase of D-2-HG concentration compared to normal tissue, it has been postulated that D-2-HG act as an oncometabolite in glioma and leukemia cells (Xu et al., 2011). D-2-HG and α-KG are nearly identical metabolites, except that the oxygen atom linked to C2 in α-KG is replaced by a hydroxyl group in D-2-HG (Xu et al., 2011). Thus, it was suggested that D-2-HG may bind and function as a competitive inhibitor of α-KG-dependent dioxygenases (Iyer et al., 2009; Loenarz and Schofield, 2008; Chowdhury et al., 2011; Xu et al., 2011) (Figure 1.4 and Figure 1.5).

These enzymes are involved in a number of important cellular processes by hydroxylating target proteins while utilizing α-KG as a cosubstrate, including Jumonji C-(JmjC)- domain-containing proteins of histone demethylases and Ten-eleven translocation (TET) family members (Chowdhury et al., 2011; Xu et al., 2011) (Figure 1.5). TET 5-methylcytosine hydroxylases are a family of α-KG-dependent enzymes that catalyze the first step in an active DNA demethylation process, which converts 5-methylcytosine (5mC) to its unmethylated form 5-hydroxylmethycytosine (5hmC) (Xu et al., 2011; Kohli and Zhang, 2013) (Figure 1.4 and Figure 1.5). In glioma patients, *IDH* mutations are strongly linked to the glioma CpG island methylation phenotype (G-CIMP), suggesting that *IDH* mutations are capable of establishing the G-CIMP phenotype in glioma cells (Lai et al., 2011; Brennan

et al., 2013; Turcan et al., 2012). Collectively, *IDH* mutations seem also to cause a dysregulation of chromatin modification and thus a profound change in the cellular epigenetic status, resulting in a blockage of cell differentiation and promotion of cell proliferation, two frequent harbingers of tumorigenesis (Turkalp et al., 2014) (Figure 1.5).
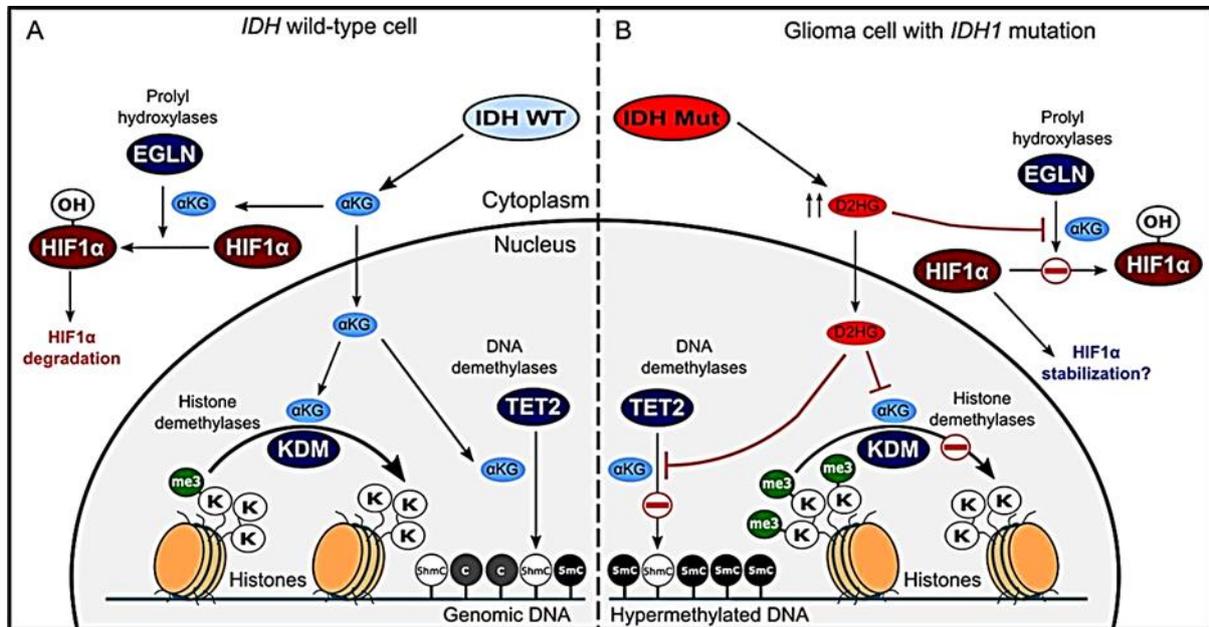


**Figure 1.5. Cellular effects of increased D-2-HG levels on dioxygenases in glioma cells.** Under physiological conditions, IDH1 catalyzes the reversible oxidative decarboxylation of isocitrate to α-KG (Metallo et al., 2011). The neomorphic enzyme function of mutated IDH enzymes drives cells to elevated D-2-HG levels (to ~100-fold) in *IDH* mutated cancer tissues compared to normal tissue. α-KG functions as a cofactor for several cellular dioxygenases, including histone demethylases, TET 5-methylcytosine hydroxylases and HIF prolyl hydroxylases. Excessive D-2-HG accumulation disrupts the normal function of α-KG-dependent enzymes causing an altered chromatin modification and hence changes in the cellular epigenetic status. D-2-HG potentially influences HIF hydroxylases, HIF-1α degradation and HIF-1α-dependent transcription (adapted from Waitkus et al., 2016).

In the literature, a relationship between mutant IDH1 and the actions of HIF-1α in gliomas has been discussed. Further, HIF-1α protein stability and therefore its transcriptional activity are controlled by proline and asparagine hydroxylation mediated by PHD2 and FIH-1, respectively (Hirota and Semenza, 2005) (Figure 1.4). HIF-1α hydroxylases are α-KG-dependent enzymes. Hence, accumulation of D-2-HG and decreased levels of α-KG may modulate HIF-1α protein stability by competitive inhibition. Several studies support this hypothesis. Zhao and colleagues reported an elevated HIF-1α accumulation induced through decreased α-KG levels due to gene expression of an IDH1[R132H] transgene in U-87MG and HEK293T cells (Zhao et al., 2009). A subsequent study confirmed this finding and further demonstrated that knocking down *IDH1* by shRNA, inhibition of endogenous IDH1 by oxalomalate or treatment with cell-permeable D-2-HG increased HIF-1α gene expression, whereas ectopic expression of wild type IDH1 decreased HIF-1α gene expression in

U-87MG cells (Xu et al., 2011). In contrast, this study also demonstrated that D-2-HG weakly competes with α-KG. In addition, Chowdhury and colleagues reported also a weak inhibitory effect of D-2-HG on HIF-1α prolyl and asparaginyl hydroxylases *in vitro*, with IC50 (half-maximal inhibitory concentration) values higher than 1 mM (Chowdhury et al., 2011). In other words, D-2-HG is a relatively weak inhibitor of HIF hydroxylation and hence it would be probably ineffective in inducing HIF-1α accumulation (Chowdhury et al., 2011). Moreover, D-2-HG has been reported to specifically increase the activity of PHD2 in human astrocytes and colorectal cancer cells, leading to decreased levels of HIF-1α protein (Koivunen et al., 2012). However, further studies are necessary in order to fully elucidate the relationship between D-2-HG accumulation and the actions of HIF-1α in gliomas. Taken together, *IDH* mutations affect several cellular processes, including lipid metabolism, DNA repair via GSH regeneration, glutaminolysis, DNA and histone modifications and protein modifications by prolyl hydroxylases (Metallo et al., 2011; Chowdhury et al., 2011; Xu et al., 2011) (Figure 1.6). It is, therefore, important to investigate the role of an *IDH1* mutation and IDH1R132H-mediated processes in oncogenic progression and therapy treatment of malignant gliomas.
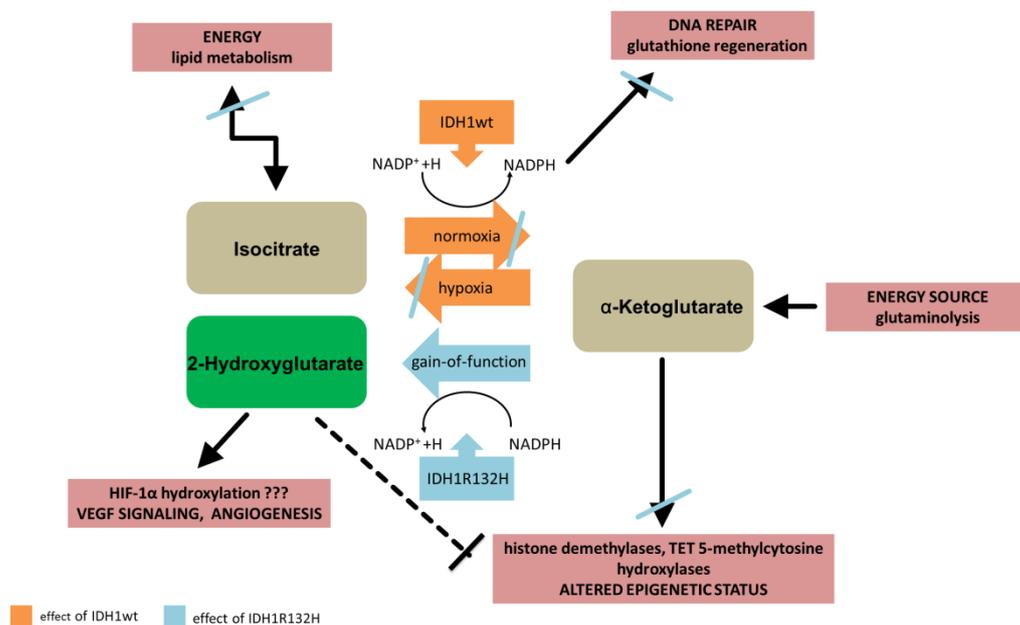


**Figure 1.6. Overview of cellular processes influenced by IDH1 wild type or IDH1R132H.** The oxidative decarboxylation of isocitrate to α-KG is active in most cell lines under normal culture conditions, but cells grown under hypoxia rely almost exclusively on the reductive carboxylation of glutamine-derived α-KG for *de novo* lipogenesis. Mutation of *IDH1* influences several cellular processes, including lipid metabolism, DNA repair, chromatin modification and potentially the HIF-1α pathway.

## 1.5 Objectives of this thesis

Malignant gliomas, especially anaplastic astrocytomas and glioblastomas, generally respond poorly to modern multimodality treatment approaches combining standard therapies such as surgery, radiotherapy and chemotherapy. In this context, intratumoral hypoxia is considered as a crucial characteristic of malignant gliomas because it induces the activation of the HIF-1 pathway. Especially the transcription of *HIF-1α*, one of the main steps of this process, represents an essential mediator for the adaptive response to hypoxia and has been associated with resistance to radiotherapy and poor outcome.

On the contrary, the *IDH1* mutation has been shown to be a strong positive prognostic factor in gliomas and was thus proposed as a genetic marker for their classification on a molecular level. *IDH1* mutations occur in the vast majority of grade II and grade III gliomas as well as in secondary glioblastomas, where they seem to predispose a particular path for oncogenic progression resulting in an increased, progression-free and overall survival of patients, irrespective of tumor malignancy. Therefore, characterization of molecular tumor markers appears to be a useful tool to gain a deeper understanding of progression, aggressiveness and radioresistance of high-grade gliomas. Hence, the aim of the present thesis was to investigate the effect of HIF-1α inhibition as well as of an *IDH1* mutation on cellular behavior and response to radiation of different malignant glioma cell lines under both normoxic and hypoxic conditions.

The primary aims of this study were:

1. To investigate the effect of HIF-1α inhibition via specific small interfering RNA (siRNA) or chetomin (CTM) on the mRNA and protein expression of HIF-1α and its target gene *CA9* in U-251MG and U-343MG malignant glioma cells under normoxic and hypoxic conditions.

2. To analyze the influence of reduced HIF-1α transcriptional activity on the induction of apoptosis via PARP cleavage, on the clonogenic survival and on radiosensitivity of U-251MG and U-343MG cells under normoxic and hypoxic conditions.

3. To examine the effect of *IDH1* reduction via specific siRNA on the mRNA and protein expression of IDH1 and to further analyze the influence of reduced IDH1 activity on the clonogenic survival and radiosensitivity of U-251MG, U-343MG and LN229 cells under normoxic and hypoxic conditions.

4. To generate IDH1$^{wt}$ and IDH1$^{R132H}$ constructs and to establish U-251MG, U-343MG and LN-229 cells with stable expression of IDH1$^{wt}$ or IDH1$^{R132H}$ protein.

5. To investigate the effect of IDH1$^{R132H}$ gene expression on cell biological behavior (i.e. proliferation, viability, growth properties in 3D culture, cell migration and cellular stiffness) of U-251MG, U-343MG and LN-229 malignant glioma cells under hypoxia and normoxia.

6. To analyze the effect of IDH1$^{R132H}$ expression on radiobiological behavior (i.e. radiosensitivity, DNA damage and induction of apoptosis) of U-251MG, U-343MG and LN-229 malignant glioma cells under hypoxic and normoxic conditions.

7. To validate the relationship between expression of IDH1$^{R132H}$ on the mRNA and protein level of HIF-1α and its target gene *CA9*.

# 2 MATERIALS

## 2.1 Devices and consumables

| | |
|---|---|
| Analytical lab scale | Sartorius (Göttingen, DE) |
| Anaerocult® A mini | Merck, (Darmstadt, DE) |
| Anaerocult® P | Merck, (Darmstadt, DE) |
| Axio Vert 25 microscope | Carl Zeiss (Jena, DE) |
| AxioVert 135 microscope | Carl Zeiss (Jena, DE) |
| AxioVert 200M microscope | Carl Zeiss (Jena, DE) |
| Cell culture dishes, flasks, well plates | Greiner Bio-One (Frickenhausen, DE) |
| Centrifuge 5415R | Eppendorf (Hamburg, DE) |
| Centrifuge 32R | Hettich Lab Technology (Tuttlingen, DE) |
| Centrifuge vials, pipette tips | Greiner Bio-One (Frickenhausen, DE) |
| CL-XPosure films | Thermo Scientific (Dreieich, DE) |
| Coulter Z2 Particle Counter | Beckman Coulter (Krefeld, DE) |
| Countess™ Automated Cell Counter | Thermo Scientific (Dreieich, DE) |
| Electrophoresis unit | GE Healthcare (Chalfront St Giles, UK) |
| GENios™ plate reader | Tecan (Crailsheim, DE) |
| Heracell™ $CO_2$ Incubator | Thermo Scientific (Dreieich, DE) |
| Heraeus® Multifuge 3S-R | Thermo Scientific (Dreieich, DE) |
| Herasafe™ Biological Safety Cabinets | Thermo Scientific (Dreieich, DE) |
| Laboratory gloves | Ansell (München, DE) |
| Laboratory pH meter | WTW inoLab (Weilheim, DE) |
| Laboratory shaker | Scientific Industries, Inc. (New York, US) |
| Magnetic stirrer | IKA-Labortechnik (Staufen, DE) |
| Mini Trans-Blot Cell | Bio-Rad (München, DE) |
| Mini-cell electrophoresis system | Thermo Scientific (Dreieich, DE) |
| Micropipettes | Eppendorf (Hamburg, DE) |
| MJ Research PTC-200 Thermal Cycler | MJ Research Inc. (St. Bruno, CAN) |
| Multiband UV table TCP-20.LC | Vilber Lourmat (Eberhardzell, DE) |
| NanoDrop 2000c spectrophotometer | Thermo Scientific (Dreieich, DE) |
| PerfectBlue Gelsystem Mini M | Peqlab Biotechnologie GmbH (Erlangen, DE) |
| pH Meter | WTW inoLab (Weilheim, DE) |
| Photometer SmartSpec™ 3000 | Bio-Rad (München, DE) |

Pipette controller Pipetboy®                          Integra Biosciences (Biebertal, DE)

Reactions vials                                       Eppendorf (Hamburg, DE)

Sprout® mini centrifuge                               Biozym Scientific (Hessisch, DE)

Stuart™ digital roller mixer SRT6D                    Stuart (Stone, UK)

Thermomixer compact                                   Eppendorf (Hamburg, DE)

T1 thermocycler                                       Biometra® (Göttingen, DE)

Universal Shaker SM30 & Incubator Hood TH 30          Edmund Bühler GmbH (Hechingen, DE)

Water bath                                            GFL (Burgwedel, DE)

Specialized devices and consumables are mentioned in the corresponding method section.

## 2.2 Standard buffer, solutions and medium

Composition of solutions, buffers and medium used in this work is provided in Table 2.1. Specialized buffers and solutions are described in the corresponding method section.

**Table 2.1. Composition of standard solutions, buffers and medium used in this work.**

| Buffer/solution | Composition |
| --- | --- |
| 5x TBE (Tris-Borate-EDTA) | 445 mM Tris (hydroxymethyl) aminomethane (Tris; Carl Roth, Karlsruhe, DE), 445 mM boric acid (Carl Roth), 10 mM ethylenediaminetetraacetic acid (EDTA; AppliChem, Darmstadt, DE); pH 8.0 |
| 10x TBS (Tris-buffered saline) | 0.5 M Tris (hydroxymethyl) aminomethane hydrochloride (Tris-HCl; Carl Roth), 5 M NaCl (AppliChem); pH 7.5 |
| 1x TBST | 100 mL TBS (10x), 0.1 % Tween®-20 (Serva, Heidelberg, DE), 900 mL aqua bidest.; pH 7.5 |
| 100 mM desferrioxamine (DFO) | 131.4 mg DFO, 2 mL PBS |
| 100 mM iodoacetate (IAA) | 41.6 mg, 2 mL PBS |
| 100 mM chetomin (CTM) | 1 mg CTM, 14.066 mL dimethyl sulfoxide (DMSO) |
| Agarose gel loading buffer | 18 % Ficoll-400, 0.25 % bromophenol blue, 5 % xylene cyanol, aqua bidest. add to 10 mL |
| Cell culture medium | RPMI 1640 medium (Lonza, Walkersville, US), 10 % FBS (Thermo Scientific), 1 % sodium pyruvate (Thermo Scientific), 185 U/mL penicillin and 185 µg/mL streptomycin (Biochrom, Berlin, DE) |

## 2.3 Cell lines

The human glioma cells U-251MG (kindly provided by Dr. Ariane Söling, Department of Pediatrics, University of Göttingen, Göttingen, DE) and LN-229 (kindly provided by Annie-Claire Diserens, Laboratoire de Neurochirurgie, Lausanne, CH), which are both derived from grade IV glioblastomas as well as U-343MG (CLS Cell Lines Service, Eppelheim, DE) derived from a grade III anaplastic astrocytoma were used in this work.

## 2.4 Oligonucleotide and siRNA

Oligonucleotides used for real-time quantitative PCR (qPCR) are listed in Table 2.2. The primers were obtained from Sigma-Aldrich, St. Louis, US. The siRNA target sequences used in this work are mentioned in Table 2.3. *HIF-1α*, *IDH1* and *luciferase* (control) siRNA were synthesized by Eurofins MWG Operon (Ebersberg, DE).

**Table 2.2. Oligonucleotides used for qPCR.**

| Gene | Sequence (5'→3') | Orientation | Position | NCBI Reference Sequence |
|---|---|---|---|---|
| *HPRT1* | 5'-TTGCTGACCTGCTGGATTAC-3' | sense | 391-410 | NM_000194.2 |
| | 5'-CTTGCGACCTTGACCATCTT-3' | antisense | 652-633 | |
| *POLR2A* | 5'-CTTGCCCCGTGCCATGCAGA-3' | sense | 1358-1377 | NM_000937.4 |
| | 5'-CTCGCACCCGGCCTTCCTTG-3' | antisense | 1421-1440 | |
| *CA9* | 5'-GAAAACAGTGCCTATGAGCAGTTG-3' | sense | 895-918 | NM_001216.2 |
| | 5'-TGCTTAGCACTCAGCATCAC-3' | antisense | 1087-1106 | |
| *HIF-1α* | 5'-CCACAGGACAGTACAGGATG-3' | sense | 1203-1224 | NM_001243084 |
| | 5'-TCAAGTCGTGCTGAATAATACC-3' | antisense | 1331-1352 | |
| *IDH1* | 5'-CGGTCTTCAGAGAAGCCATT-3' | sense | 612-631 | NM_005896.3 |
| | 5'-AACACCACCACCTTCTTC-3' | antisense | 812-829 | |

**Table 2.3. siRNA target sequences used in this work.**

| Target mRNA | siRNA | Sequence (5'→3') | Orientation |
|---|---|---|---|
| *HIF-1α* | *HIF-1α* | 5'-CUGAUGACCAGCAACUUGA-3' | sense |
| | | 5'-UCAAGUUGCUGGUCAUCAG-3' | antisense |
| *IDH1* | *IDH1* | 5'-GUCUCUAUUGAGACAAUUG-3' | sense |
| | | 5'-CAAUUGUCUCAAUAGAGAC-3' | antisense |
| *Luciferase* | *Lu GL2* (control siRNA) | 5'-CGUACGCGGAAUACUUCGA-3' | sense |
| | | 5'-UCGAAGUAUUCCGCGUACG-3' | antisense |

## 2.5 Antibodies

Primary antibodies used for Western blot (WB) analysis, immunofluorescence (IF) and immunohistochemical staining (IHC) are shown in Table 2.4. The corresponding secondary antibodies utilized for immunostaining are described in Table 2.5. For the analyses of apoptosis two poly (ADP-ribose) polymerase (PARP) antibodies were used, namely Anti-PARP and cleaved PARP. Anti-PARP antibody detects endogenous levels of full length PARP (116 kDa), as well as the large fragment (89 kDa) of PARP resulting from caspase cleavage. On the contrary, the cleaved PARP (Asp214) antibody detects endogenous levels of the large fragment (89 kDa) of PARP resulting from caspase cleavage and does not recognize full length PARP.

**Table 2.4. Primary antibodies used for immunostaining.**

| Antibody | Source | Dilution | | Manufacturer |
|---|---|---|---|---|
| | | WB | IF/IHC | |
| Anti-HIF-1α | Mouse | 1:1,000 | | BD Biosciences, Heidelberg, DE |
| Anti-CAIX (MN75) | Mouse | 1:2,000 | | Bayer Healthcare, Berlin, DE |
| Anti-PARP | Rabbit | 1:1,000 | | Cell Signaling, Danvers, MA, US |
| Anti-IDH1 | Rat | 1:1,000 | 1:100 | Dianova, Hamburg, DE |
| Anti-IDH1R132H | Mouse | 1:1,000 | 1:100 | Dianova, Hamburg, DE |
| Cleaved PARP (Asp214) | Rabbit | 1:2,000 | | Cell Signaling, Danvers, MA, US |
| Anti-β-actin | Mouse | 1:5,000 | | Sigma-Aldrich, St. Louis, US |
| P-Histone H2AX (S139) | Rabbit | | 1:400 | Cell Signaling, Danvers, MA, US |

**Table 2.5. Secondary antibodies used for immunostaining.**

| Antibody | Source | Dilution | | Manufacturer |
|---|---|---|---|---|
| | | WB | IF/ICC | |
| Anti-mouse-HRP | Rabbit | 1:1,000 | | DAKO, Hamburg, DE |
| Anti-rabbit-HRP | Goat | 1:1,000 | | DAKO, Hamburg, DE |
| Anti-rat-HRP | Goat | 1:1,000 | | Santa Cruz, Santa Cruz, CA, US |
| Anti-mouse-Alexa 488 | Goat | | 1:100 | Thermo Scientific, Dreieich, DE |
| Anti-rat-Alexa 488 | Goat | | 1:100 | Thermo Scientific, Dreieich, DE |
| Anti-rabbit-Alexa 488 | Goat | | 1:400 | Thermo Scientific, Dreieich, DE |

# 3   METHODS

## 3.1   Cell culture conditions and methods

For normoxic conditions (21 % $O_2$), U-251MG, U-343MG and LN-229 glioma cells were grown in RPMI 1640 medium (Lonza), supplemented with 10 % FBS (Thermo Scientific), 1 % sodium pyruvate (Thermo Scientific), 185 U/mL penicillin and 185 µg/mL streptomycin (Biochrom) (cell culture medium) at 37 °C in a humidified-air atmosphere incubator containing 5 % $CO_2$. Monolayer (2D) cultures were grown in flasks (12.5 $cm^2$ to 150 $cm^2$), on cell culture plates (6 cm to 10 cm), 24-well, 48-well or 96-well plates depending on the experimental procedure. For three dimensional (3D) cultures cells were grown in flat bottom agarose coated 96-well plates. Cell counting was carried out with an automated Cell Counter (Coulter Z2; Beckman Coulter) using 100 µL cell suspension in 10 mL Isoton II (Beckman Coulter) . All experiments were performed with cells in logarithmic growth phase. Cell cultures were tested for mycoplasma contamination at regular intervals by using Venor®GeM Classic Mycoplasma PCR Detection Kit (Minerva Biolabs, Berlin, DE). Therefore, 500 µL of cell culture supernatant containing up to $10^6$ cells was transferred to a microcentrifuge tube, incubated at 95 °C for 10 min and centrifuged at 13,000 rpm for 5 sec. The obtained supernatant (2 µL) was used for preparation of the PCR reaction mix using a polymerase with a concentration of 5 U/µL according to the manufacturer´s protocol.

For passaging, the respective glioma cell culture was washed with PBS (Lonza) and overlaid with 3 mL of warm (37 °C) 0.05 % Trypsin-EDTA solution (Thermo Scientific). Trypsin was kept on the cells for up to 5 min at 37 °C and inactivated by cell culture medium. After collecting the cells by gentle centrifugation at 800 rpm for 4 min, the inactivated trypsin medium mixture was removed. Subsequently, the cells were resuspended in pre-warmed cell culture medium and subcultured at a split ratio of 1:5 to 1:10.

For cryopreservation the collected cells were resuspended in cell culture medium containing 20 % dimethyl sulfoxide (DMSO; Sigma-Aldrich) at the range of $2.0x10^5$ to $5.0x10^5$ cells/mL. The cell suspension was transferred to sterile cryogenic vials and freezed using a freezing rate of approximately 1 °C per min in an isopropanol chamber at -80 °C overnight. The cells were stored in the liquid phase (-196 °C) of liquid nitrogen.

For thawing the cells were warmed very quickly by placing the cryogenic vial directly from the liquid nitrogen container into a 37 °C water bath. The thawed cells were washed twice with warmed (37 °C) cell culture medium, centrifuged at 800 rpm for 4 min and plated in 25 $cm^2$ flasks.

## 3.2 Transfection of glioma cells with siRNA

Gene silencing by small interfering RNA (siRNA) was performed by transfection, using target gene-directed (*HIF-1α*, *IDH1*) double-stranded RNA oligonucleotides. For siRNA experiments a nonsense siRNA, specifically targeting the *firefly luciferase* gene, was used. This control siRNA was designed with no significant homology to any known gene in human cells. The target sequences are depicted in Table 2.3. For transfection experiments, cells ($1.5 \times 10^5$-$2 \times 10^5$) were plated in 12.5 cm$^2$ or 25 cm$^2$ flasks 24 h before treatment with siRNA. At the time of transfection, the confluency of the cell monolayer was 40-50 %. Different concentrations (25-150 nM) of siRNA and pre-incubation times (4 h-48 h) were analyzed in pilot experiments. Transfection of siRNA in glioma cell lines was carried out using INTERFERin® (biomol, Hamburg) according to the manufacturer's protocol. Reduction of the *HIF-1α* and *IDH1* gene expression was achieved using concentrations of 75 nM and 50 nM siRNA, respectively. Cells were pre-treated with the corresponding siRNA for 4 h at 37 °C under normoxic conditions. The cells were subsequently incubated under hypoxic conditions or maintained in normoxia for 20 h, respectively. The cells were then used for RNA isolation, protein isolation or irradiated under normoxic or hypoxic conditions.

## 3.3 HIF-1α inhibition by CTM

HIF-1α inhibition was further carried out using CTM (Alexis®Biochemicals, DE), an epidithiodiketopiperazine metabolite of the fungal species *Chaetomium* (Kung et al., 2004). For HIF-1α inhibition via CTM, CTM stock solutions (100 mM) were initially prepared in 0.1 % DMSO. In pilot experiments different concentrations (9-300 nM) and pre-incubation times (4-48 h) of CTM were examined in detail. The individual glioma cell lines were plated with $3 \times 10^5$ cells in 25 cm$^2$ flasks 24 h before treatment with 75 nM CTM. The effect of CTM on HIF-1α gene expression level was compared to the solvent DMSO (75 nM) and an untreated control. At the time of treatment, the confluency of the monolayer was 40-50 %. Cells were pre-incubated with CTM under normoxic conditions for 4 h. Untreated cells and cells treated with CTM or DMSO (control) were then incubated under hypoxic conditions or maintained in normoxia for 20 h, respectively. The cells were then used for RNA isolation, protein isolation or irradiated under normoxic or hypoxic conditions.

## 3.4 Generation of constructs and stable overexpression of IDH1^wt^ and IDH1^R132H^ in glioma cell lines

The establishment of stable cells overexpressing IDH1^wt^ or IDH1^R132H^ was performed using a lentivirus system (Clontech, Heidelberg, DE). Therefore, full-length human wild type *IDH1* coding sequence was amplified from cDNA of U-251MG cells using the following oligonucleotides *IDH1*

BamHI forward: 5'-GGGGATCCATGTCCAAAAAAATCAGTGGCGGTTCTGTG-3', *IDH1* XhoI reverse: 5'-GGCTCGAGTTAAAGTTTGGCCTGAGCTAGTTTGATCT-3' and High Fidelity PCR Enzyme Mix (Thermo Scientific) according to the manufacturer's protocol. Amplification was performed by running an initial denaturation for 5 min at 95 °C, followed by 35 cycles of denaturation for 10 sec at 95 °C, annealing for 30 sec at 66 °C, extension for 1 min at 68 °C and a final extension step for 10 min at 68 °C. The PCR product was purified on a 1 % agarose gel (1 mg agarose in 100 mL 0.5x TBE buffer and 5 µL ethidium bromide (10 mg/mL)) in 0.5x TBE buffer at a constant voltage of 200 V for 1 h. For the determination of molecular weights of the PCR products, PageRuler™ 100 bp Plus DNA Ladder (Thermo Scientific) was used. Following electrophoresis the PCR product was cut out, isolated from the gel slice by Zymoclean™ Gel DNA Recovery Kit (Zymo Research, Irvine, US), cloned into pCR® 2.1 Vector (Thermo Scientific) to generate pCR® 2.1-IDH1$^{wt}$ and subcloned as BamHI-XhoI (New England Biolabs) fragments into pLVX-Puro vector (kindly provided by Prof. Dr. Stefan Hüttelmaier, Institute of Molecular Medicine, Medical Faculty, Martin Luther University Halle-Wittenberg, Halle Saale, DE.). IDH1$^{R132H}$ was prepared by QuikChange® II XL Site-Directed Mutagenesis Kit (Stratagene, La Jolla, CA, US) following the manufacturer's instructions using IDH1$^{wt}$ as a template and the following oligonucleotides: 5´-CCATAAGCATGATGACCTATG-3´ and 5´-CATAGGTCATCATGCTTATGG-3´. The entire *IDH1* coding region was sequenced using pLVX-Puro forward primer: 5'-CGCCATCCACGCTGTTTTGACCTCCATA-3' and pLVX-Puro reverse primer: 5'-CCTTGGGAAAAGCGCCTCCCCTACCCGG-3' to verify its authenticity. Sequence analyses were performed by SEQLAB Sequence Laboratories Göttingen Gmbh. NucleoBond® Plasmid kit (Plasmid DNA Purification, NucleoBond® Xtra Midi/Maxi; Clontech) was used to extract and purify plasmid DNA, respectively.

For virus production, a second-generation three-plasmid packaging system was used including the envelope-coding plasmid pMD2.G and the packaging plasmid psPAX2 (addgene, Cambridge, US). The empty vector (10 µg) pLVX-Puro (clontech) or pLVX encoding IDH1$^{wt}$ or IDH1$^{R132H}$ were co-transfected with 10 µg pMD2.G and 5 µg psPAX2 into HEK293T cells using the calcium chloride DNA precipitation method. The precipitate was formed by adding the plasmids to 0.5 mL sterile buffered H$_2$O and 0.5 mL 2× HEPES buffered saline (280 mM sodium chloride (NaCl), 50 mM HEPES, 1.5 mM sodium hydrogen phosphate (Na$_2$HPO$_4$), pH 7.0). Following this, 60 µL 2.5 M calcium chloride (CaCl$_2$; Sigma-Aldrich) was added under gentle agitation of the tube. The solution was incubated for 20 min at room temperature (RT) and then added dropwise to the cells. Twelve hours later, the medium was replaced with fresh cell culture medium. The viral supernatant was harvested 48 h post-transfection and cleared by centrifugation at 1,500 rpm for 5 min at RT followed by filtration through a 0.45 µm pore cellulose acetate filter (Sartorius).

Glioma cells with different degrees of malignancy were transduced with empty vector (pLVX) or with pLVX encoding IDH1$^{wt}$ or IDH1$^{R132H}$ using 1 mL of the viral suspension, respectively. U-251MG (grade IV), U-343MG (grade III) and LN-229 (grade IV) stable cell lines (polyclonal) with empty vector (pLVX) or overexpressing IDH1$^{wt}$ or IDH1$^{R132H}$ were selected using 1.5 µg/mL puromycin (Sigma-Aldrich) from 48 h post transfection (Kessler et al., 2015).

## 3.5   Hypoxia and irradiation

Hypoxia (<0.1 % O$_2$) was achieved using an Anaerocult® A mini gas generator system (Merck, Darmstadt, DE). The gas generator system is a special incubation bag that produces an anaerobic atmosphere due to the presence of an Anaerocult® A mini sachet containing specific components (kieselguhr, iron powder, citric acid and sodium carbonate), which are activated by water and quickly bind oxygen (less than 0.1 % residual oxygen in the bag after 1 h). Four hours after siRNA transfection or incubation with CTM, the flasks with the treated or untreated cells were transferred into the Anaerocult® A mini systems. After activation of the Anaerocult® A mini sachets by wetting with 8 mL aqua bidest. the bags were closed with Anaeroclips® and placed in a humidified-air atmosphere incubator. The cells were incubated for 20 h under hypoxic conditions. Establishment of hypoxia was controlled through Anaerotest® strips on the lids of the inoculated flasks according to manufacturer's protocol.

Irradiation was carried out on logarithmically growing cultures with 6 MV photons and adequate bolus material on a SIEMENS ONCOR (Erlangen, DE) linear accelerator at a dose rate of 2 Gy/min. When normoxic conditions were applied, the cells treated with siRNA (*HIF-1α/IDH1*) or CTM were irradiated with a single dose of 0, 2, 5 or 10 Gy at RT, respectively. siRNA and CTM treated cells under hypoxic conditions were irradiated inside the Anaerocult® A mini gas generator system with a single dose of 0, 2, 5, 10 or 15 Gy at RT. After irradiation, the cells were further incubated under normoxia or hypoxia at 37 °C for 1 h before harvesting for the clonogenic assay, RNA isolation or protein isolation. In untreated cells, empty vector (pLVX) cells and IDH1$^{wt}$ or IDH1$^{R132H}$ cells, hypoxia was achieved 24 h after seeding as described above and maintained for 24 h before irradiation with 0, 2 or 5 Gy under normoxia and 0, 2, 5 or 10 Gy under hypoxia. After irradiation, cells were either incubated in normoxia or hypoxia at 37 °C for 1 h before harvesting for the clonogenic assay, RNA isolation and protein isolation or for 72 h before harvesting for PARP analysis via Western blot.

### 3.6 Quantitative real-time PCR

### 3.6.1 RNA isolation and quantitative real-time PCR

Cells were washed twice with ice-cold PBS, harvested using a cell scraper and centrifuged at 1,000 rpm for 5 min to pellet debris. Total RNA was extracted by using the RNeasy Mini Kit (Qiagen, Hilden, DE) or TRIzol reagent (Thermo Scientific) as recommended by the manufacturers. DNA digestion was included by using 30 Kunitz units of RNase-free DNase in 80 μl RDD buffer (both Qiagen). RNA concentrations were quantified in a NanoDrop 2000c spectrophotometer (Thermo Scientific). A sample volume of 2 μL was used to determine the absorbance at 260 nm and the RNA concentration was calculated by the NanoDrop software using the following formula:

$$OD_{260nm} * Dilution factor * 40 = \frac{ng}{\mu L} RNA \tag{1}$$

The ratios A260/A280 and A260/A230 were used to assess the purity of the RNA. Thereby, A260/A280 ratios between 1.8 and 2.0 as well as A260/A230 ratios around 2.0 were considered as an optimal measure for the purity of the respective RNA. cDNA was synthesized from 1 μg of RNA using RevertAid H-Minus first-strand cDNA synthesis kit (Thermo Scientific) following the manufacturer's instructions. Quantitative real-time PCR (qPCR) was performed in triplicate on a real-time PCR cycler (Rotor-Gene 6000, Qiagen) by using Maxima SYBR Green/ROX qPCR Master Mix (Thermo Scientific). The samples were prepared by mixing 6.5 μL of SYBR Green mix, 0.25 μl of each primer (20 μM), 1 μl of cDNA and 7 μl of water. Reactions were denatured for 15 min at 95 °C, followed by 40 cycles of denaturation for 30 sec at 95 °C, annealing for 30 sec at 60 °C, extension for 30 sec at 72 °C, a final extension step for 30 sec at 60 °C and a melting curve program (65 °C-95 °C with a heating rate of 0.2 °C/s). For normalization, *hypoxanthine phosphoribosyltransferase 1* (*HPRT1*) or *Homo sapiens polymerase (RNA) II polypeptide A* (*POLR2A*) were used as housekeeping genes. The primers for the amplification step were synthesized by TIB MOLBIOL (Berlin, DE) or Sigma-Aldrich. A summary of all primer sequences used in this thesis is provided in Table 2.2.

### 3.6.2 Generation of plasmid standards for qPCR

DNA plasmid standard curve was performed using TA Cloning® Kit (Thermo Scientific) to determine the absolute quantity (copy numbers, ng, mRNA) of a specific gene. The respective plasmid standard was synthesized by amplifying the PCR product from cDNA of the glioma cells using HotStarTaq DNA Polymerase (Qiagen), gel-purification by Zymoclean™ Gel DNA Recovery Kit (Zymo Research, Irvine, US) and ligation into pCR® 2.1 vector via T4 DNA Ligase (Thermo Scientific). The

constructs were transformed into One Shot®TOP10 Chemically Competent *E.coli* (Thermo Scientific) and 50-200 µL from each transformation was spread on LB Agar plates (Thermo Scientific) containing 5-Bromo-4-chloro-3-indolyl-ß-D-galactosid (X-Gal; Sigma-Aldrich) as well as 100 µg/µL ampicillin (Carl Roth) and further a blue-white screening for inserts was performed. According to the manufacturer's instructions white colonies were picked, grown overnight at 37 °C in LB Broth Base (Thermo Scientific) containing 100 µg/µL ampicillin and plasmid isolation was subsequently assessed by ZR Plasmid Miniprep™ Classic Kit (Zymo). The entire gene fragment region was sequenced using M13 forward primer: 5'-GTAAAACGACGGCCAG-3' or T7 promotor primer: 5'-TAATACGACTCACTATAGGG-3' to verify its authenticity. A detailed description of the individual steps of the plasmid standard synthesis can be found in the manufacturer's protocol of the TA Cloning® Kit (Thermo Scientific).

## 3.7  Protein isolation and Western blot analysis

For protein isolation cells were washed twice with ice-cold PBS, harvested using a cell scraper and lysed with RIPA buffer containing Tris-HCl (50 mM, pH 8.0), 200 mM NaCl (200 mM), EDTA (1 mM; AppliChem), ethylene glycol tetraacetic acid (EGTA, 1 mM; Carl Roth), 1 % TritonX-100 (Carl Roth), 0.25 % deoxycholate (AppliChem), Protease-Inhibitor-Cocktail (1:100; Sigma-Aldrich) and Halt™ Phosphatase Inhibitor Cocktail (1:100; Thermo Scientific). The lysates were incubated for 20 min on ice and centrifuged at 13,000 rpm for 10 min at 4 °C. The supernatants were collected and protein concentrations were measured via the Bio-Rad Protein-Assay (Bradford reagent) at 595 nm according to the manufacturer's instructions.

Equivalent amounts of protein (10-30 µg) were diluted in NuPAGE® LDS Sample Buffer (4x) containing NuPAGE® Sample Reducing Agent (10x) (Thermo Scientific) and denatured for 5 min at 95 °C. Protein samples and Protein Ladder (PageRuler™ Plus Prestained Protein Ladder; Thermo Scientific) were loaded on 4-12 % Bis-Tris Mini Gels and separated in NuPAGE® MES SDS running buffer (20x) using a mini-cell electrophoresis system (XCell SureLock™; Thermo Scientific) at a constant voltage of 200 V for 1 h. Proteins were transferred to a 0.45 µm PVDF membrane (Millipore, Schwalbach, DE) by tank electroblotting (Bio-Rad) at 150 V for 2 h in transfer buffer containing 50 mL NuPAGE® Transfer Buffer (20x) (Thermo Scientific), 850 mL aqua bidest. and 10 % methanol (Sigma-Aldrich).

After blocking the non-specific binding sites with 10 % milk powder (Carl Roth) in 0.1 M TBS for 1 h at RT, the membranes were incubated with the primary antibodies at appropriate dilutions in TBST-10 % milk powder overnight at 4 °C. Subsequently, staining was performed for 1 h at RT with a suitable secondary horseradish peroxidase-conjugated antibody. Details of the utilized antibodies are described in Table 2.4 and Table 2.5. The protein-antibody complexes were detected by enhanced

chemiluminescence using ECL™ Western Blotting Detection Reagent or ECL™ Prime Western Blotting Detection Reagent (both GE Healthcare, Chalfont St Giles, UK). In a darkroom, the X-ray films (Thermo Scientific) were exposed to the emitted light signal and developed by successive immersion in developing solution (Nordenta, Hamburg, DE), water, fixer solution (Nordenta) and water.

## 3.8 Immunofluorescence and immunohistochemical staining

Immunofluorescence analysis was performed to investigate the gene expression pattern of IDH1$^{wt}$ or IDH1$^{R132H}$ in glioma cells. Cells were grown for 24 h on coverslips in 24-well plates at a density of $1.5x10^5$ cells/well, fixed with 4 % paraformaldehyde (Sigma-Aldrich), permeabilized with 0.5 % Triton X-100/PBS for 10 min at RT. After blocking for 1 h with 1 % BSA (Promega) in PBS, the cells were incubated overnight at 4 °C with primary antibodies and subsequently for 1 h at RT in the dark with suitable secondary antibodies. Immunofluorescence counterstaining was performed with 4′,6-diamidino-2-phenylindole (DAPI, 0.25 µg/µL in PBS; Carl Roth) for 5 min in the dark at RT. The slides were then washed again with PBS, air-dried and mounted with ProLong®Gold Antifade Reagent (Thermo Scientific). Details of the used antibodies are listed in Table 2.4 and Table 2.5. Fluorescence imaging was carried out using an AxioVert 200M microscope (Carl Zeiss, Jena, DE).

IDH1$^{R132H}$ gene expression patterns and its influence on the HIF-1α and CAIX protein levels in glioma cells were investigated by immunohistochemical staining. Cells grown for 24 h on coverslips in 24-well plates at a density of $1.5x10^5$ cells/well were fixed with 4 % paraformaldehyde (Sigma-Aldrich). The cells were then permeabilized with 0.5 % Triton X-100/PBS for 10 min at RT. After blocking for 10 min in Antibody Diluent (ZYTOMED Systems, Berlin, DE) the cells were incubated overnight at 4 °C with primary antibodies and subsequently stained via Dako REAL™ Detection System, Peroxidase/DAB+, Rabbit/Mouse (Dako, Hamburg, DE) according to the manufacturer's instructions. After staining the target antigens, the cell nuclei were counterstained with 20 % hematoxylin in aqua bidest. for 2 min, washed with water, dehydrated in a graded ethanol (Carl Roth) series (50-100 %), air-dried and mounted in Eukitt® mounting medium (Sigma-Aldrich). Details of the used antibodies are depicted in Table 2.4 and Table 2.5.

Image analysis of the stained cells was performed with an AxioVert 200M microscope (Carl Zeiss). Quantitative analysis was performed by scoring the staining intensity and the proportion of positively IDH1$^{R132H}$, HIF-1α and CAIX stained cells. Therefore, three fields of vision were selected randomly and 200 cells were counted per field. The immunohistochemical results for HIF-1α protein were classified as follows: 0, no staining; 1, nuclear staining in 1–10 % of cells and/or with weak cytoplasmic staining; 2, nuclear staining in 11–50 % of cells and/or with distinct cytoplasmic staining; 3, nuclear staining in more than 50 % of cells and/or with distinct cytoplasmic staining and 4, nuclear

staining in more than 50 % of cells and/or with strong cytoplasmic staining (Zhong et al., 1999). Cytoplasmic immunoreactivity for IDH1$^{R132H}$ and CAIX was evaluated according to the extent of staining, with staining intensities scored as: 0, no cells stained; 1, less than 10 % of cells stained; 2, 11 % to 50 % of cells stained; 3, more than 50 % of cells show a distinct staining; 4, more than 50 % of cells show a strong staining (Zhong et al., 1999).

## 3.9 Viability and proliferation in 2D culture and 3D spheroid culture

To determine the impact of *IDH1* mutation on viability and cell growth in monolayer under normoxic and hypoxic conditions, untreated cells, cells stably transduced with empty vector pLVX, IDH1$^{wt}$- or IDH1$^{R132H}$-expressing cells were seeded in 25 cm$^2$ flasks with 2x10$^5$/flask, respectively. After 24 h at 37 °C in normoxia, flasks were either kept in normoxia or transferred to the Anaerocult® A mini gas generator system (<0.1 % O$_2$) and further incubated under hypoxia. After 24 h, 48 h, 72 h and 96 h the cells were trypsinized and the number of viable cells was determined by trypan blue (Thermo Scientific) exclusion method using a Countess™ Automated Cell Counter (Thermo Scientific).

In addition, cell growth characteristics in 3D spheroid culture were analyzed using flat bottom 96-well plates. For spheroid generation the wells were coated with 50 µL of 1.5 % agarose (Sigma-Aldrich) before plating the cells at an optimized density of 5×10$^3$ cells/well using a multichannel pipette. Plates were incubated for seven days under normoxia or hypoxia and spheroid formation was evaluated using an AxioVert 135 microscope (Carl Zeiss).

## 3.10 Cell migration

To analyze the migration of untreated cells, empty vector cells and IDH1$^{wt}$- or IDH1$^{R132H}$-expressing cells a wound-healing assay (scratch assay) was performed under normoxic and hypoxic conditions. For this, cells were grown to 100 % confluence in 10 cm petri dishes following careful creation of defined cell-free wounds using a 200 µL pipette tip. The dishes were then gently rinsed twice with PBS to remove free floating cells. The PBS was replaced by cell culture medium and images were taken just after wound creation (0 h) and again after 24 h and 48 h of incubation under normoxic or hypoxic conditions by using an AxioVert 135 microscope (Carl Zeiss). To evaluate the relative cell migration of IDH1$^{wt}$- and IDH1$^{R132H}$-expressing cells, the wound closure (µm$^2$) at the different time points was measured using the microscope software (AxioVision Rel 4.6.). The scratch assay was also performed after pre-treatment of the glioma cell lines with 10 µg/mL mitomycin C for 2 h to prevent proliferation.

Furthermore, a 3D spheroid-based migration assay was carried out. For this, individual day 5 tumor spheroids were transferred to 10 cm dishes (6-8 spheroids/dish) by using a 1 mL pipette. To evaluate

the cell migration the migration radius (µm) of untreated cells, empty vector cells and IDH1$^{wt}$- or IDH1$^{R132H}$-expressing cells at different time points (0 h, 24 h, 48 h and 72 h) was measured using AxioVision Rel 4.6. software.

## 3.11   Colony formation assay and radiosensitivity

Radiosensitivity and cell survival of glioma cell lines was investigated by colony formation assay. For this purpose, the cells were trypsinized 1 h after irradiation, plated in 25 cm$^2$ flasks at different cell densities ranging from 250-10,000 cells/flask depending on the treatment and irradiation dose. The cells were then cultured for 10-16 days under normoxic or hypoxic conditions and finally fixed with 4 % paraformaldehyde in aqua bidest. (Sigma-Aldrich). Thereafter, the colony formation (colonies of ≥50 cells) was visualized by staining with 10 % Giemsa solution (Sigma-Aldrich). The surviving fractions were defined as ratios of the plating efficiencies (PE=counted colonies/seeded cells*100) of the irradiated cells to the non-irradiated cells. Based on that the dose-modifying factor at a 10 % survival level (DMF10=radiation dose untreated cells/radiation dose treated cells) was determined to analyze the effect of reduced *HIF-1α/IDH1* gene expression or IDH1$^{wt/R132H}$ overexpression on the radiosensitivity of glioma cells. To fit the survival curves, a linear quadratic model lnS=-(αD + βD2) was applied, using origin 8.0 (Kessler et al., 2015).

## 3.12   Quantification of phospho-histone H2AX foci formation

For quantification of phospho-histone H2AX (γH2AX) foci formation, untreated cells, empty vector cells and IDH1$^{wt}$- or IDH1$^{R132H}$-expressing cells ($1 \times 10^5$) were seeded in 8-well chamber slides (Thermo Scientific). After 24 h at 37 °C in normoxia, chamber slides were either kept in normoxia or incubated in Anaerocult® A mini gas generator system (<0.1 % O$_2$) under hypoxia. After 24 h the cells were then irradiated with 0, 2 and 4 Gy and following further incubation in normoxia or hypoxia at 37 °C for 24 h, respectively. For γH2AX staining, the cells were fixed for 10 min with 4 % paraformaldehyde solution and permeabilized with 0.5 % Triton X-100/PBS for 10 min at RT. After blocking with 1 % BSA in PBS for 1 h, the cells were incubated for 2 h at RT with the specific phospho-histone H2AX antibody and subsequently for 1 h at RT with Anti-rabbit-Alexa 488 labeled secondary antibody. Cell nuclei were counterstained with DAPI (in PBS, 0.25 µg/µL; Carl Roth) for 5 min at RT in the dark, washed twice with PBS, air-dried and mounted in ProLong® Gold Antifade Reagent (Thermo Scientific). Details of the used antibodies are depicted in Table 2.4 and Table 2.5. Quantification of γH2AX foci formation was carried out using an AxioVert 200M microscope (Carl Zeiss). The foci were counted manually in the nuclei of 300-400 untreated, empty vector, IDH1$^{wt}$ or IDH1$^{R132H}$ cells under normoxia and hypoxia.

## 3.13 Atomic force microscopy

The influence of IDH1[R132H] mutant protein expression on cell adhesion energy and cell stiffness was investigated by atomic force microscopy (AFM). AFM indentation is a useful tool to analyze the mechanical properties of living cells in physiological environment at the nanoscale. Cells were plated with $5 \times 10^5$ cells/flask in 75 cm$^2$ flasks, cultured under normoxic conditions for 48 h, trypsinized to induce detachment and centrifuged at 1,000 rpm for 5 min. Cells were resuspended in 1 mL cell culture medium, plated on a 6 cm culture dish and incubated for 15 min allowing the cells to adhere slightly to the surface. For AFM indentation measurements a lithium nitride tip-less cantilever (Nanoworld, Arrow-TL2) with an angle of 10° on the cell was used (Figure 3.1). To analyze the cellular mechanical properties, single cells were indented with a force of 3 nN (Figure 3.2). Five force curves per rounded cell were recorded. The Young´s modulus $E$ (elastic modulus,) was estimated by fitting force curves with the Hertz model:

$$F = \frac{4}{3} \frac{E}{1-v^2} \sqrt{R\delta_0{}^3} \, ,$$ 

(2)

where $F$ is force detected, $E$ is the Young´s modulus, $R$ is the radius of the cell, $v$ is the Poisson´s ratio and $\delta_0$ is indentation (Hertz, 1882). In general, Poisson´s ratios between 0.3 for soft tissue to 0.5 for an incompressible material are used. The best-match of experimental and modelling data has been reported when cells are treated as almost incompressible. Thus a Poisson´s ratio of 0.47 was applied in the present study (Mahaffy et al., 2004). The total adhesion energy Eadh was derived from the calculated Young´s modulus and the contact radius $a$ of the cantilever on the investigated cell based on the Derjarguin-Muller-Topolov model (Derjaguin et al., 1975):

$$a^3 = \frac{R(1-v^2)}{E} \left( F + \frac{2RE_{adh}}{a^2} \right)$$ 

(3)

Furthermore, additional physical measurements carried out (indentation, normalized adhesion energy, jump energy, total adhesion energy, minimal force, jump force, slope of approach curve, cell radius, Young´s modulus and jump number) to quantify the relationship between several cell-specific parameters based on a network analytical approach to compile the nondimensional composite parameter "stiffness" as a weighted sum (Hohmann et al. 2016).
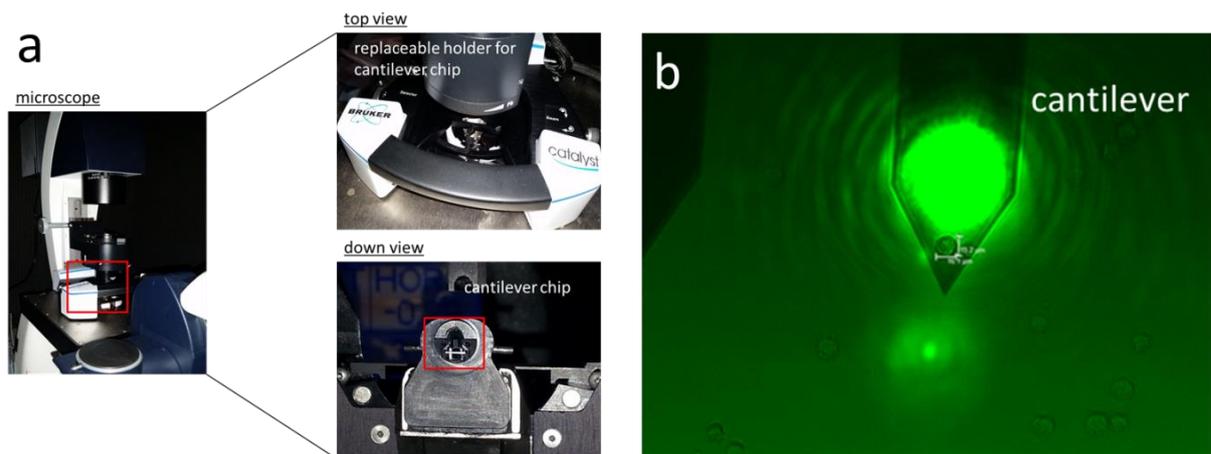
**Figure 3.1. Atomic force microscopy.** (a) Cantilever based optical microscope. Cantilever chip was mounted on a chip holder, which is placed on the stage of an inverted optical microscope. (b) Microscopic image of an indentation of a single cell by the cantilever. For each cell line (U-251MG, U-343MG and LN-229) 20 single cells of untreated, empty vector cells, IDH1$^{wt}$ or IDH1$^{R132H}$ cells were analyzed, respectively. AFM measurements were carried out in Institute of Molecular Medicine, Medical Faculty, Prof. Dr. Stefan Hüttelmaier, Martin Luther University Halle-Wittenberg, Halle Saale, DE.
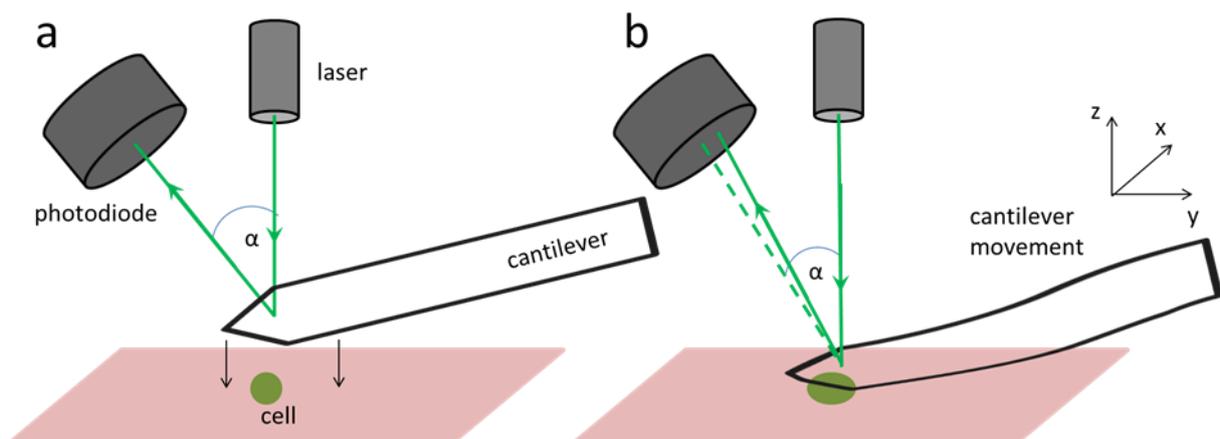


**Figure 3.2. Measurement principle of atomic force microscopy.** (a) AFM cantilever is positioned above a cell and (b) gently pressed with a force of 3 nN onto the cell. The laser (green line) is reflected off the back of the cantilever and the deflection is detected using a photodiode. The laser spot was initially positioned in the middle of the photodiode. Deformation of the cantilever occurs during indentation on a single cell; thereby deflection on the cantilever was detected as a change in output voltage.

## 3.14  Statistics

The experimental results are presented as means ±SD and represent at least three to five independent experiments, respectively. Statistical differences among various groups were assessed basd on the absolute values using an unpaired two-sided Student's t test. A p-value of less than 0.05 was considered as an indicator of significant difference.

# 4 RESULTS

## 4.1 Targeting HIF-1α via siRNA or CTM in U-251MG and U-343MG malignant glioma cells under normoxic and hypoxic conditions

Hypoxia induces activation of the HIF-1 pathway and is a critical characteristic of malignant gliomas. Thereby, the transcription factor hypoxia-inducible factor-1 (HIF-1), a dimer of HIF-1α and HIF-1β, is an essential mediator for adaptive response to reduced oxygen. HIF-1 governs cellular adaption to low oxygen concentrations by regulating tumor-relevant genes involved in energy metabolism, cell proliferation, apoptosis and angiogenesis (Semenza, 2002; Bracken et al., 2003; Goda et al., 2003). The hypoxia-induced accumulation of HIF-1α protein and thus the increased gene expression of its target gene *CA9* was analyzed in glioma cell lines with different degrees of malignancy (U-251MG, grade III and U-343MG, grade IV). Two distinct strategies have been used to investigate the impact of HIF-1α inhibition on cell survival, radiosensitivity and induction of apoptosis of U-251MG and U-343MG cells in normoxia and hypoxia. HIF-1α inhibition was achieved by siRNA targeting or via CTM, a disruptor of interactions between HIF-1α and p300 in U-251MG (grade IV) and U-343MG (grade III) under normoxic and hypoxic conditions.

### 4.1.1 Effect of hypoxia on *HIF-1α* and *CA9* mRNA expression level

HIF-1α activation by hypoxia is regulated at the level of HIF-1α subunit protein stability in an oxygen-dependent fashion. Although *HIF-1α* mRNA is constitutively expressed, HIF-1α protein is rapidly degraded by the ubiquitin-proteasome system under normoxic conditions. U-251MG and U-343MG exhibited a similar *HIF-1α* mRNA expression pattern in normoxia and hypoxia (Figure 4.1a and Figure 4.1b). During reoxygenation an increased *HIF-1α* mRNA expression up to 2.1-fold ($p<0.05$) in U-251MG and up to 1.4-fold ($p<0.05$) in U-343MG cells in comparison to the *HIF-1α* mRNA level in normoxia was observed, indicating a restocking process after consumption of HIF-1α protein under hypoxic conditions (Figure 4.1a and Figure 4.1b).

Treatment with 100 μM of the chelating agent desferrioxamine (DFO) under normoxic conditions was used as a positive control for HIF-1α protein accumulation. In addition, incubation with 50 μM of the glycolysis inhibitor iodoacetate (IAA) under hypoxic conditions served as a negative control for HIF-1α protein accumulation. Based on the regulatory effect of DFO and IAA on the protein level of HIF-1α, no influence was seen on *HIF-1α* mRNA expression in U-251MG and U-343MG cells (Figure 4.1a and Figure 4.1b). Furthermore, an oxygen-dependent expression pattern of *CA9* mRNA was detected in both glioma cell lines (Figure 4.1c and Figure 4.1d). In normoxia, U-251MG and U-343MG showed a weak *CA9* mRNA expression (Figure 4.1c and Figure 4.1d). Compared to

normoxia the level of *CA9* mRNA was significantly increased in U-251MG (up to 56.6-fold, p<0.01) and in U-343MG (up to 42.5-fold, p<0.01) after 1 h, 6 h and 24 h in hypoxia (Figure 4.1c and Figure 4.1d). Furthermore, U-251MG cells showed an increased *CA9* mRNA expression during 48 h of reoxygenation. In U-343MG cells *CA9* mRNA expression remained elevated during 24 h of reoxygenation and decreased afterwards, reaching the normoxic *CA9* mRNA level at 48 h of reoxygenation. Treatment with DFO under normoxic conditions increased the *CA9* mRNA expression in U-251MG and U-343MG cells, whereas treatment with the negative control IAA resulted in clearly reduced *CA9* mRNA expression under hypoxic conditions (Figure 4.1c and Figure 4.1d).
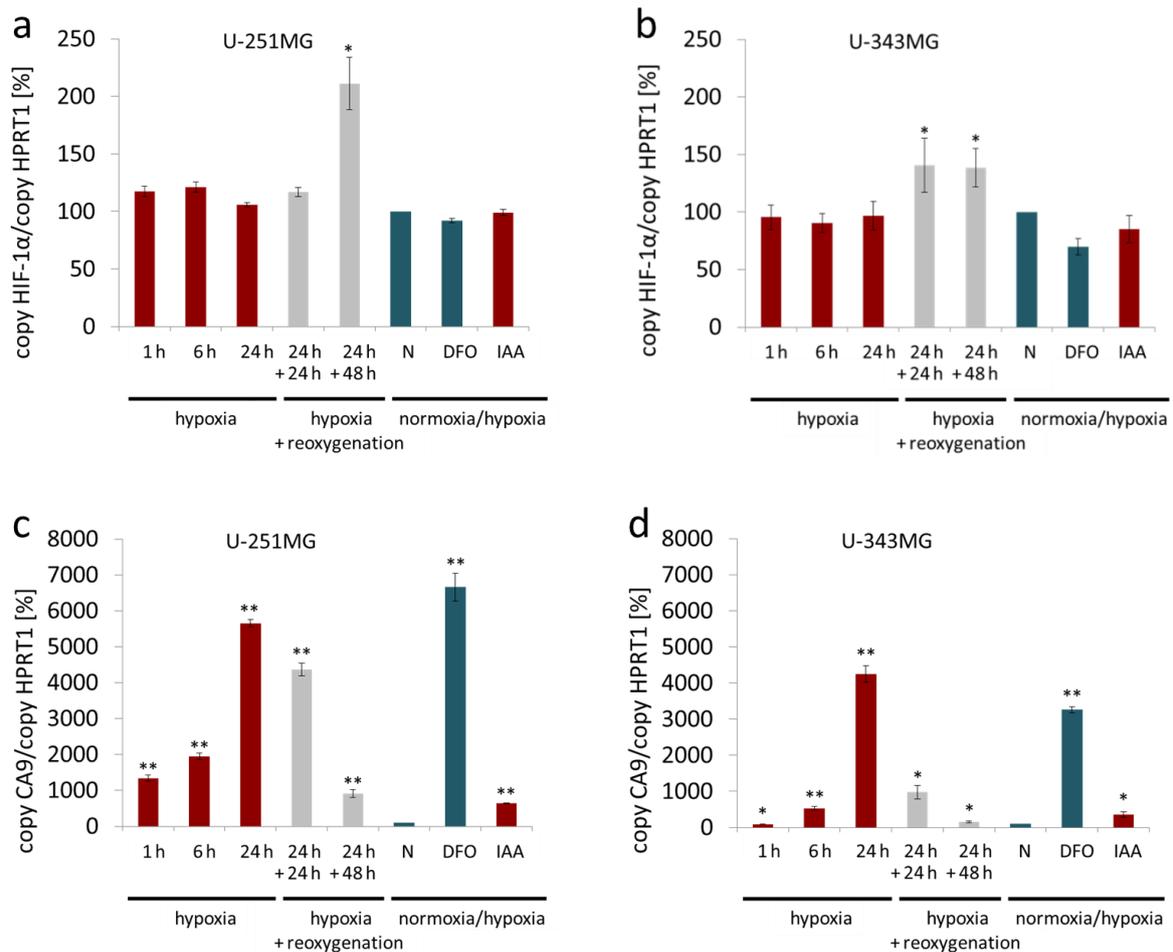


**Figure 4.1. *HIF-1α* and *CA9* mRNA expression in response to hypoxic and normoxic conditions in glioma cells.** mRNA expression levels (qPCR) of *HIF-1α* (a and b) and *CA9* (c and d) in U-251MG and U-343MG cells. Bars represent the mean values, relative to the normoxic control (set as 100 %), of three independent experiments. Error bars indicate standard deviations (±SD). *HIF-1α* and *CA9* mRNA expression under hypoxia (1 h, 6 h and 24 h, <0.1 % $O_2$); IAA: 50 µM iodoacetate in hypoxia (negative control); *HIF-1α* and *CA9* mRNA expression in response to reoxygenation (24 h hypoxia and 24 h reoxygenation or 24 h hypoxia and 48 h reoxygenation); N: *HIF-1α* and *CA9* mRNA expression in normoxia (21 % $O_2$); DFO: 100 µM desferrioxamine in normoxia (positive control); *p<0.05 and **p<0.01 (compared to the normoxic control).

### 4.1.2 Effect of hypoxia on HIF-1α and CAIX protein expression level

U-251MG and U-343MG cells showed a low level of HIF-1α protein under normoxia (Figure 4.2). After 1 h, 6 h and 24 h under hypoxic conditions, U-251MG and U-343MG cells exhibited an increased accumulation of HIF-1α protein (Figure 4.2). Reoxygenation for 24 h and 48 h in normoxia decreased the HIF-1α protein level over time in the investigated cell lines (Figure 4.2). In both cell lines induction of CAIX generally occurs during hypoxia and is dependent on HIF-1α accumulation. Further, U-251MG and U-343MG cells showed a weak CAIX protein level under normoxia (Figure 4.2). CAIX protein was stable over 48 h of reoxygenation in U-251MG cells, whereas overexpression of CAIX protein in U-343MG cells disappeared during 48 h of reoxygenation in a similar fashion to that observed under normoxia (Figure 4.2). Additionally, an increase of CAIX protein was observed using DFO under normoxic conditions and an inhibition of CAIX protein was detected using IAA in hypoxia in both cell lines, respectively (Figure 4.2).
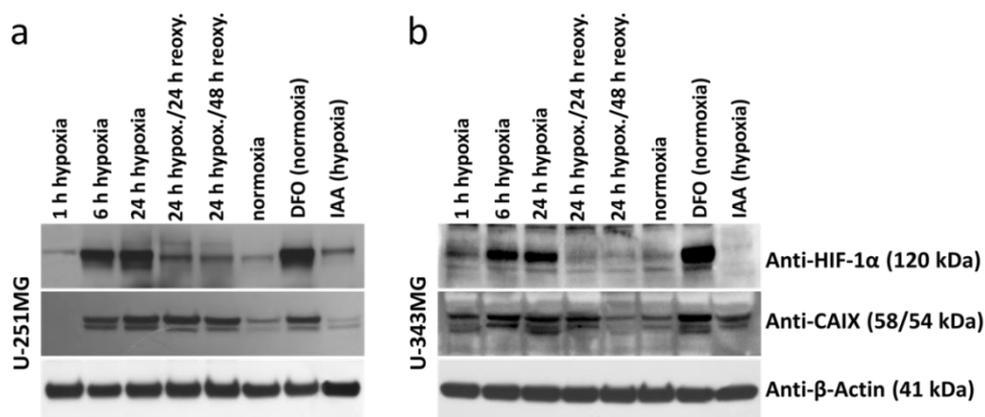


**Figure 4.2. Hypoxia-induced HIF-1α protein accumulation and CAIX protein expression in glioma cells.** Representative Western blots for HIF-1α and CAIX protein in U-251MG (a) and U-343MG (b) cells under normoxia (21 % $O_2$) and hypoxia (<0.1 % $O_2$). β-Actin served as loading control; n=3 independent experiments. HIF-1α and CAIX protein expression under hypoxia (1 h, 6 h and 24 h); IAA: 50 μM iodoacetate in hypoxia (negative control); HIF-1α and CAIX protein expression in response to reoxygenation (24 h hypoxia and 24 h reoxygenation or 24 h hypoxia and 48 h reoxygenation); N: HIF-1α and CAIX protein expression in normoxia (21 % $O_2$); DFO: 100 μM desferrioxamine in normoxia (positive control).

### 4.1.3 Effect of *HIF-1α*-specific siRNA or CTM on *HIF-1α* and *CA9* mRNA levels

In U-251MG and U-343MG cells, hypoxia did not alter the *HIF-1α* mRNA expression in comparison to the normoxic conditions. The effects of *HIF-1α*-specific siRNA or CTM on *HIF-1α* and *CA9* expression levels were compared to the control siRNA, specifically targeting the *firefly luciferase* gene, or the solvent DMSO, respectively. In both cell lines, neither control siRNA nor treatment with DMSO affected *HIF-1α* mRNA expression in normoxia or hypoxia (Figure 4.3). The effect of the *HIF-1α* siRNA or CTM on the *HIF-1α* mRNA level was analyzed 24 h after treatment and culture under normoxic and hypoxic conditions (Figure 4.3). Treatment of U-251MG cells with the

*HIF-1α*-specific siRNA resulted in a reduction of *HIF-1α* mRNA by 62.3 % ± 21.7 (p<0.05) or 57.4 % ± 18.4 (p<0.01) compared to the control siRNA under normoxic or hypoxic conditions, respectively (Figure 4.3a). In U-343MG cells *HIF-1α* siRNA decreased the *HIF-1α* mRNA level by 52.0 % ± 10.5 (p<0.01) or 53.6 % ± 18.7 (p<0.05) compared to the control siRNA under normoxic or hypoxic conditions, respectively (Figure 4.3b). Treatment of U-251MG cells with CTM increased the *HIF-1α* mRNA level by 19.6 % ± 20.2 (not significant) and by 24.1 % ± 13.6 (not significant) compared to the cells treated with DMSO in normoxia and hypoxia, respectively (Figure 4.3c). However, exposure of U-343MG cells to CTM reduced the *HIF-1α* mRNA expression by 67.0 % ± 10.4 (p<0.01) and 39.6 % ± 12.0 (p<0.01) compared to the cells treated with DMSO under normoxic and hypoxic conditions, respectively (Figure 4.3d).



**Figure 4.3. Effect of *HIF-1α* siRNA and CTM on *HIF-1α* mRNA expression in glioma cells.** mRNA expression levels (qPCR) of *HIF-1α* in U-251MG and U-343MG under normoxic (21 % $O_2$,) and hypoxic (<0.1 % $O_2$,) conditions. RNA was extracted 24 h after treatment with 75 nM *HIF-1α*-specific siRNA (a and b) or 75 nM CTM (c and d). Bars represent the mean values, relative to the control siRNA (control siRNA under normoxia was set as 100 % to elucidate the effect of hypoxia) or DMSO (DMSO under normoxia was set as 100 % to elucidate the effect of hypoxia) of three independent experiments. Error bars indicate standard deviations (±SD). UT: untreated cells, control: cells treated with 75 nM control siRNA, HIF-1α: cells treated with 75 nM *HIF-1α*-specific siRNA, DMSO: cells treated with 75 nM DMSO; CTM: cells treated with 75 nM CTM; *p<0.05 and **p<0.01 (compared to the respective control siRNA/DMSO in normoxia).

Inhibition of the transcriptional HIF-1 activity was examined by monitoring the gene expression of the HIF-1α target gene *CA9* 24 h after treatment with *HIF-1α* siRNA or CTM (Figure 4.4). In hypoxia, an elevated *CA9* mRNA expression level up to 121-fold (p<0.01) in U-251MG and up to 5.3-fold

(p<0.01) in U-343MG in comparison to the respective *CA9* mRNA level in normoxia was induced. Furthermore, neither control siRNA nor DMSO had an impact on the *CA9* mRNA expression. The influence of *HIF-1α* siRNA and CTM on *CA9* mRNA expression was compared to the respective control condition, i.e., cells treated with control siRNA or the solvent DMSO under normoxic or hypoxic conditions. In U-251MG cells, reduction of the *HIF-1α* gene expression by siRNA decreased the *CA9* mRNA expression by 90.6 % ± 1.1 (p<0.01) and by 93.6 % ± 4.8 (p<0.01) in normoxia and hypoxia (Figure 4.4a). In U-343MG cells, *HIF-1α* gene silencing reduced the *CA9* mRNA expression by 55.0 % ± 7.8 (p<0.01) and by 52.7 % ± 3.7 (p<0.05) compared to the respective control siRNA under normoxic and hypoxic conditions, respectively (Figure 4.4b). Moreover, in U-251MG cells, inhibition of HIF-1α activity in response to CTM caused a decrease in *CA9* mRNA expression by 86.4 % ± 7.5 (p<0.01) and by 50.1 % ± 12.8 (p<0.05) compared to the controls under normoxic or hypoxic conditions, respectively (Figure 4.4c). In U-343MG cells, treatment with CTM resulted in a reduction of *CA9* mRNA expression by 87.9 % ± 4.2 (p<0.01) and by 77.7 % ± 1.4 (p<0.05) compared to the controls in normoxia and hypoxia (Figure 4.4d).
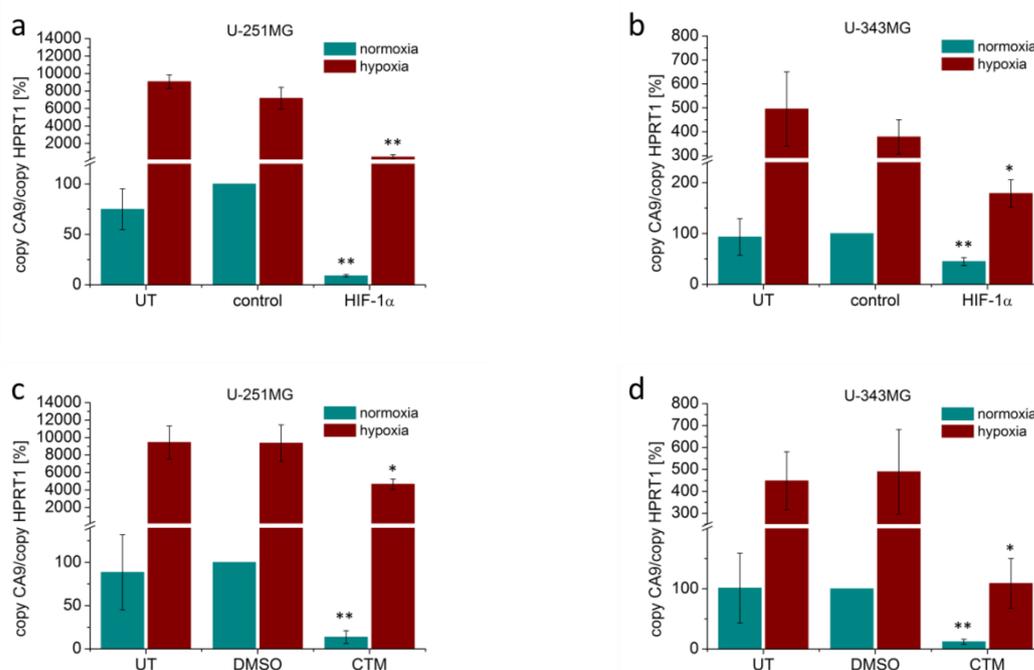


**Figure 4.4. Influence of *HIF-1α* siRNA and CTM on *CA9* mRNA expression in glioma cells.** mRNA expression levels (qPCR) of *CA9* in U-251MG and U-343MG under normoxic (21 % $O_2$) and hypoxic (<0.1 % $O_2$) conditions. RNA was extracted 24 h after treatment with 75 nM *HIF-1α*-specific siRNA (a and b) or 75 nM CTM (c and d). Bars represent the mean values, relative to the control siRNA (control siRNA under normoxia was set as 100 % to elucidate the effect of hypoxia) or DMSO (DMSO under normoxia was set as 100 % to elucidate the effect of hypoxia) of three independent experiments. Error bars indicate standard deviations (±SD). UT: untreated cells, control: cells treated with 75 nM control siRNA, HIF-1α: cells treated with 75 nM *HIF-1α*-specific siRNA, DMSO: cells treated with 75 nM DMSO; CTM: cells treated with 75 nM CTM; *p<0.05 and **p<0.01 (compared to the respective control siRNA/DMSO in normoxia).

### 4.1.4    Effect of *HIF-1α* siRNA or CTM on HIF-1α and CAIX protein level and PARP cleavage

Minimal amounts of HIF-1α protein level were detectable in U-251MG and U-343MG cell lines under normoxic conditions (Figure 4.5). On the contrary, HIF-1α protein level was considerably increased in the investigated cell lines under hypoxia. Treatment with control siRNA or DMSO did not cause a change in HIF-1α protein expression (Figure 4.5) compared to the untreated cells. Treatment of U-251MG and U-343MG cells with the *HIF-1α* siRNA resulted in a substantial decrease of HIF-1α protein expression under normoxic and hypoxic conditions (Figure 4.5a and Figure 4.5b). In U-251MG cells exposure to CTM increased HIF-1α protein expression compared to DMSO or untreated cells under normoxic and hypoxic conditions (Figure 4.5c). In contrast, U-343MG cells exhibited reduced a level of HIF-1α protein in response to CTM treatment in normoxia and hypoxia (Figure 4.5d). Furthermore, weak CAIX protein levels were detected in U-251MG and U-343MG cells in normoxia (Figure 4.5). In response to hypoxia, CAIX protein expression was substantially increased in the both cell lines. Reduction of the *HIF-1α* gene expression via siRNA resulted in a strong decrease of CAIX protein expression in U-251MG and U-343MG cells, which was independent on the culture conditions (Figure 4.5a and Figure 4.5b). Inhibition of the HIF-1α transcriptional activity by CTM resulted in a reduction of the CAIX protein level in normoxia and hypoxia compared to the respective DMSO control or untreated U-251MG and U-343MG cells (Figure 4.5c and Figure 4.5d).

In addition, the induction of apoptosis was qualitatively assessed using Western blot analysis of the proteolytic cleavage of PARP. In U-251MG cells, reduction of the *HIF-1α* gene expression via siRNA did not affect the normoxic gene expression of the large fragment of PARP, but caused cleavage of PARP under hypoxic conditions (Figure 4.5a). In U-343MG cells, reduction of the *HIF-1α* gene expression via siRNA induced apoptosis under normoxic and hypoxic conditions (Figure 4.5b). Treatment with CTM resulted in an apoptotic response under normoxic and hypoxic conditions in U-251MG cells (Figure 4.5c). In comparison, in U-343MG cells exposure to CTM had no effect on PARP cleavage under normoxic conditions but caused induction of apoptosis under hypoxic conditions (Figure 4.5d).
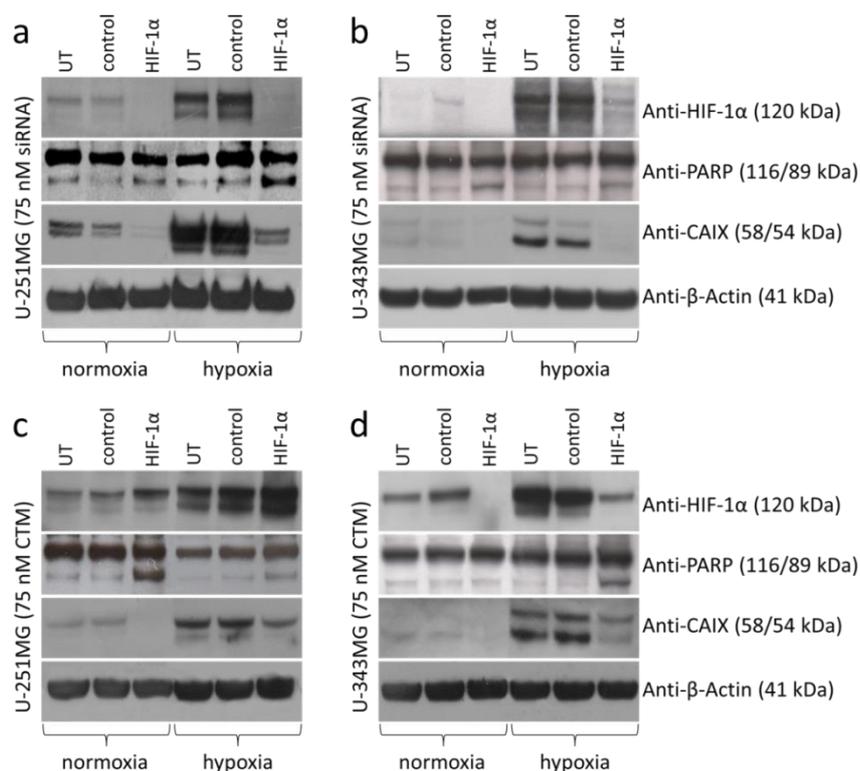
**Figure 4.5. Effect of *HIF-1α* siRNA and CTM on HIF-1α or CAIX protein and PARP cleavage in glioma cells.** Representative Western blots for HIF-1α, CAIX and PARP protein in U-251MG and U-343MG cells under normoxia (21 % $O_2$) and hypoxia (<0.1 % $O_2$). HIF-1α, CAIX protein expression and PARP cleavage after treatment with 75 nM *HIF-1α*-specific siRNA in comparison to 75 nM control siRNA or untreated U-251MG (a) and U-343MG (b) cells. HIF-1α, CAIX protein expression and PARP cleavage after treatment with 75 nM CTM in comparison to 75 nM DMSO or untreated U-251MG (c) and U-343MG (d) cells. For PARP analyses Anti-PARP antibody was used (detects full-length PARP 116 kDa and cleaved PARP 89 kDa). β-Actin served as loading control; n=3 independent experiments. UT: untreated cells, control: cells treated with 75 nM control siRNA, HIF-1α: cells treated with 75 nM *HIF-1α*-specific siRNA, DMSO: cells treated with 75 nM DMSO; CTM: cells treated with 75 nM CTM.

### 4.1.5   Effect of *HIF-1α* siRNA or CTM on clonogenic survival and radiosensitivity

The clonogenic survival assay is a crucial endpoint read-out that was used to investigate the fraction of cells surviving the treatment with *HIF-1α* siRNA or CTM (Figure 4.6) and the combined treatment of *HIF-1α* siRNA or CTM and radiation in U-251MG and U-343MG cells (Figure 4.7). In both U-251MG and U-343MG cells treatment with control siRNA or DMSO did not significantly affect the plating efficiency compared to the untreated cells (Figure 4.6). Treatment of U-251MG cells with *HIF-1α* siRNA resulted in a reduced plating efficiency by 80.4 % ± 1.2 (p<0.01) and 54.8 % ± 12.9 (p<0.05) compared to cells treated with the control siRNA under normoxic and hypoxic conditions (Figure 4.6a). In U-343MG cells treatment with *HIF-1α* siRNA decreased the plating efficiency by 32.0 % ± 10.1 (p<0.05) and by 36.1 % ± 21.3 (not significant) compared to control siRNA treated cells under normoxic and hypoxic conditions (Figure 4.6b). Furthermore, in U-251MG cells, exposure

to CTM reduced the plating efficiencies by 75.0 % ± 3.1 (p<0.01) and by 76.1 % ± 10.3 (p<0.01) compared to cells treated with DMSO in normoxia and hypoxia, respectively (Figure 4.6c). In U-343MG cells treatment with CTM decreased the plating efficiency by 44.8 % ± 5.5 (p<0.01) and by 64.0 % ± 4.3 (p<0.01) under normoxic and hypoxic conditions (Figure 4.6d).
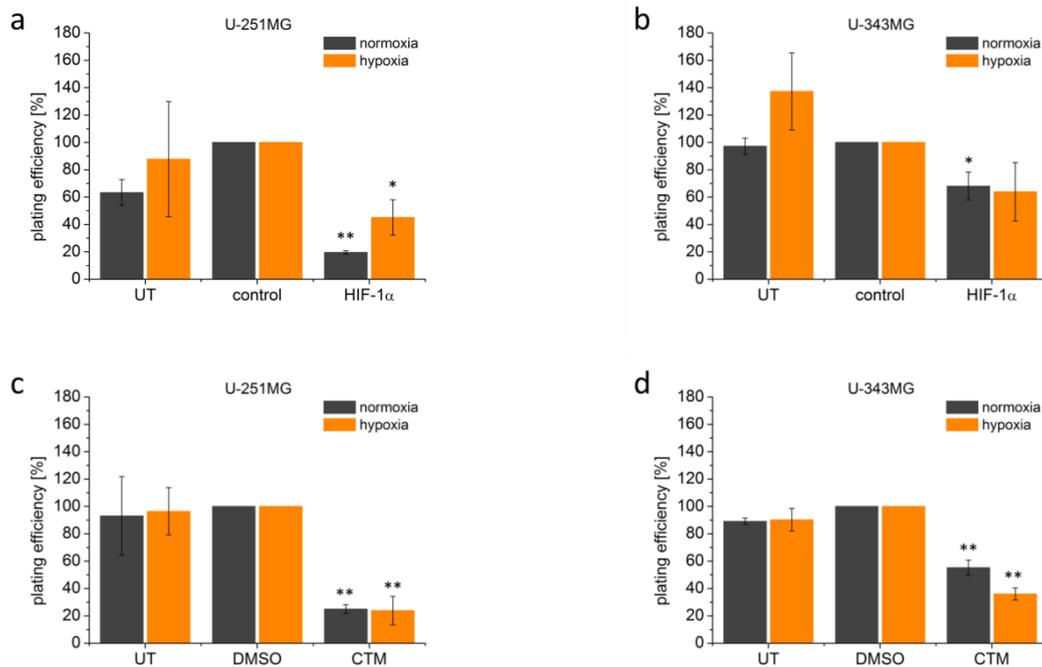


**Figure 4.6. Effect of *HIF-1α* siRNA and CTM on the clonogenic survival of glioma cells.** Effect of treatment with the *HIF-1α* siRNA (75 nM) or 75 nM CTM on the plating efficiency of non-irradiated U-251MG (a and c) and U-343MG (b and d) cells under normoxia (21 % O$_2$) and hypoxia (<0.1 % O$_2$). Bars represent the mean values, relative to the control siRNA (control siRNA in normoxia and hypoxia were set as 100 %) or DMSO (DMSO in normoxia and hypoxia were set as 100 %) of four independent experiments. Error bars indicate standard deviations (±SD). UT: untreated cells, control: cells treated with 75 nM control siRNA, HIF-1α: cells treated with 75 nM *HIF-1α*-specific siRNA, DMSO: cells treated with 75 nM DMSO; CTM: cells treated with 75 nM CTM; *p<0.05 and **p<0.01 (compared to the respective control siRNA/DMSO in normoxia or hypoxia).

A clonogenic assay was also applied to determine if *HIF-1α* siRNA or CTM sensitized U-251MG or U-343MG glioma cells to radiation (Figure 4.7). The clonogenic survival assay revealed an increased survival of U-251MG and U-343MG cells under hypoxia as compared to normoxia (Figure 4.7, untreated cells are not shown for better clarity). Survival curves showed that although treatment with *HIF-1α* siRNA slightly reduced the cytotoxic effect of radiation of U-251MG cells under normoxic conditions (DMF10: 0.86, p<0.05), it enhanced radiation sensitivity under hypoxic conditions (DMF10: 1.35, p<0.01) (Figure 4.7a). In U-343MG cells treatment with *HIF-1α* siRNA resulted in an enhanced radiosensitivity under normoxic (DMF10: 1.33, p<0.01) and hypoxic (DMF10: 1.78, p<0.01) conditions, respectively (Figure 4.7b). In addition, treatment with CTM led to an increased

radiosensitivity of U-251MG cells under normoxic (DMF10: 1.35, p<0.01) and hypoxic (DMF10: 1.18, p<0.05) conditions (Figure 4.7c). In U-343MG cells exposure to CTM did not affect radiosensitivity under normoxic (DMF10: 1.02, p<0.05) conditions, but improved response to radiation under hypoxia (DMF10: 1.48, p<0.05) (Figure 4.7d).
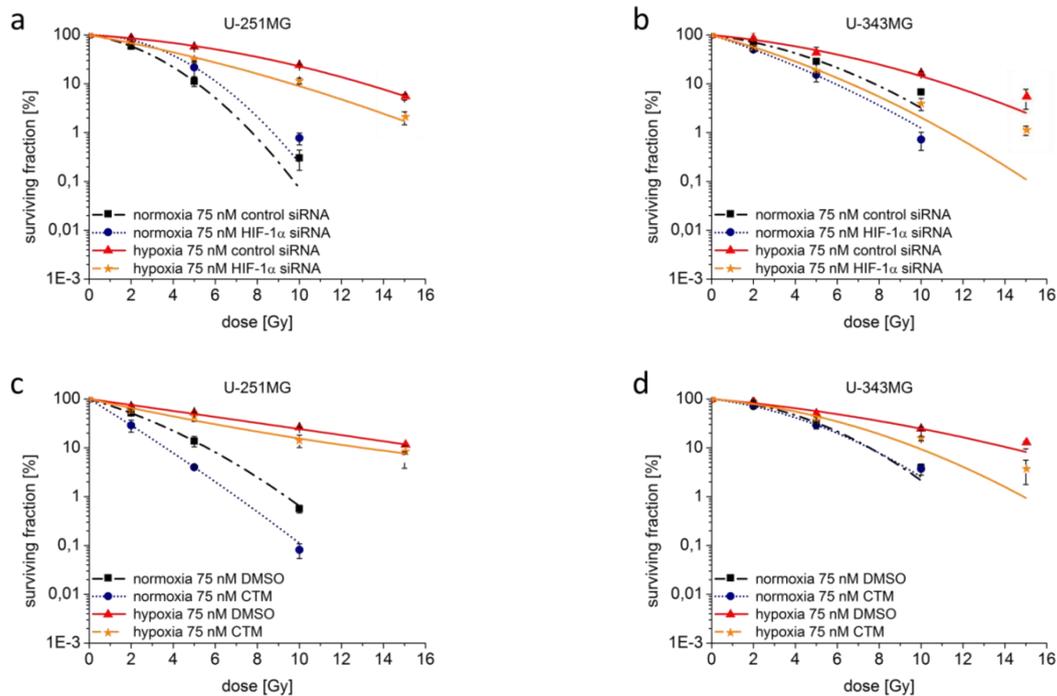


**Figure 4.7. Effect of *HIF-1α* siRNA or CTM on radiosensitivity of glioma cells.** Clonogenic survival after treatment with the *HIF-1α* siRNA (75 nM) or exposure to 75 nM CTM and radiation of U-251MG (a and c) and U-343MG (b and d) cells under normoxia (21 % $O_2$, 0-10 Gy) and hypoxia (<0.1 % $O_2$, 0-15 Gy). The plating efficiencies of non-irradiated cells were set as 100 %, respectively. Each point represents the mean values of four independent experiments. Error bars indicate standard deviations (±SD). control: cells treated with 75 nM control siRNA, HIF-1α: cells treated with 75 nM *HIF-1α*-specific siRNA, DMSO: cells treated with 75 nM DMSO; CTM: cells treated with 75 nM CTM.

In summary, both *HIF-1α*-specific siRNA and CTM obviously reduced the activity of HIF-1α in U-251MG and U-343MG malignant glioma cell lines in normoxia and hypoxia. Although siRNA and CTM inhibit HIF-1α through two rather different mechanisms, both attenuated the hypoxia-induced radioresistance of U-251MG and U-343MG cells. Nevertheless, under normoxic conditions siRNA and CTM demonstrated opposite effects on radiosensitivity in U-251MG and U-343MG cells. While under normoxia *HIF-1α* siRNA enhanced the response to radiation only in U-343MG cells, exposure to CTM increased radiosensitivity only in U-251MG cells. Furthermore, the results suggest that *CA9* could serve as an indicator of effective HIF-1-related radiosensitization.

## 4.2  Reduction of *IDH1* expression via siRNA in U-251MG, U-343MG and LN-229 malignant glioma cells under normoxic and hypoxic conditions

Mutations targeting the *IDH1* gene occur in a restricted spectrum of tumors, including gliomas and acute myeloid leukemia (Parsons et al., 2008; Paschka et al., 2010). In gliomas of all grades the presence of *IDH1* mutation is associated with better clinical outcome after standard treatments such as surgery, radiotherapy and chemotherapy (Parsons et al., 2008; Hartmann et al., 2009; Ichimura et al., 2009; Yan et al., 2009). The mutated IDH1 enzyme IDH1R132H shows a strongly decreased enzyme activity to isocitrate and gain a new enzyme function catalyzing the NADPH-depend reduction of α-KG to D-2-HG (Dang et al., 2010). However, it is unclear whether *IDH1* mutation is associated with a less aggressive phenotype or directly linked to increased sensitivity to radiotherapy. Thus, the effect of reduced *IDH1* gene expression using *IDH1*-specific siRNA on the response to radiation was investigated in U-251MG (grade IV), U-343MG (grade III) and LN-229 (grade IV) glioma cells.

### 4.2.1  Effect of *IDH1*-specific siRNA on the *IDH1* mRNA level

For *IDH1* gene silencing by siRNA also a control siRNA with no significant homology to any known gene in human cells was used. In U-251MG, U-343MG and LN-229 cells treatment with control siRNA did not affect *IDH1* mRNA expression compared to the untreated cells in normoxia or hypoxia (Figure 4.8). The effect of the *IDH1* siRNA on the *IDH1* mRNA level was examined 24 h after treatment and culture under normoxic and hypoxic conditions. Treatment of U-251MG cells with the *IDH1*-specific siRNA resulted in a reduction of the *IDH1* mRNA by 73.9 % ± 11.9 ($p<0.01$) or 78.7 % ± 7.7 ($p<0.01$) compared to the control siRNA under normoxic or hypoxic conditions, respectively (Figure 4.8a). In U-343MG cells *IDH1* siRNA reduced the *IDH1* mRNA expression by 96.7 % ± 2.9 ($p<0.01$) or 88.9 % ± 3.6 ($p<0.01$) under normoxic or hypoxic conditions, respectively (Figure 4.8b). Treatment of LN-229 cells with *IDH1*-specific siRNA decreased the *IDH1* mRNA level by 74.8 % ± 11.1 ($p<0.01$) and 85.6 % ± 2.2 ($p<0.01$) in normoxia and hypoxia (Figure 4.8c).
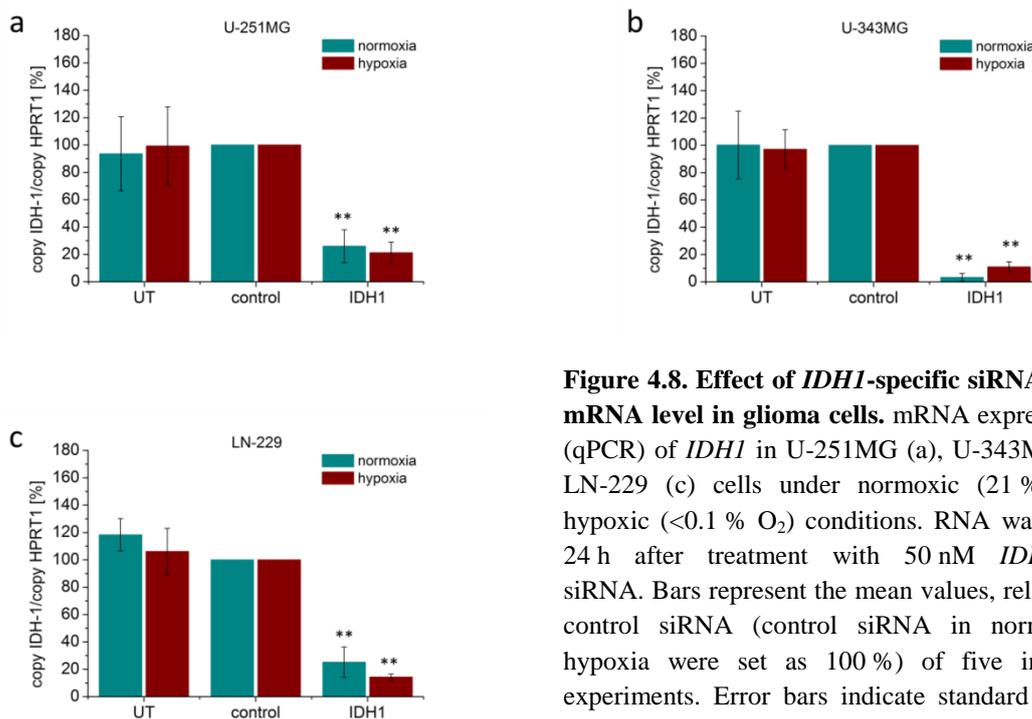
**Figure 4.8. Effect of *IDH1*-specific siRNA on *IDH1* mRNA level in glioma cells.** mRNA expression level (qPCR) of *IDH1* in U-251MG (a), U-343MG (b) and LN-229 (c) cells under normoxic (21 % O$_2$) and hypoxic (<0.1 % O$_2$) conditions. RNA was extracted 24 h after treatment with 50 nM *IDH1*-specific siRNA. Bars represent the mean values, relative to the control siRNA (control siRNA in normoxia and hypoxia were set as 100 %) of five independent experiments. Error bars indicate standard deviations (±SD). UT: untreated cells, control: cells treated with 50 nM control siRNA, IDH1: cells treated with 50 nM *IDH1*-specific siRNA; **p<0.01 (compared to the respective control siRNA in normoxia or hypoxia).

### 4.2.2 Effect of *IDH1*-specific siRNA on the IDH1 protein level and PARP cleavage

U-251MG, U-343MG and LN-229 displayed similar gene expression patterns of IDH1 protein under normoxic and hypoxic conditions (Figure 4.9). Treatment with control siRNA did not induce an altered IDH1 protein expression (Figure 4.9) compared to the untreated cells. In agreement to the qPCR experiments, Western blot analyses confirmed the decrease of IDH1 protein expression in a cell type-specific pattern under normoxic and hypoxic conditions. While in U-251MG and U-343MG cells exposure to *IDH1* siRNA almost completely suppressed the IDH1 protein, LN-229 cells exhibited a weak IDH1 protein level after treatment with *IDH1* siRNA.

Additionally, the induction of apoptosis was qualitatively assessed using Western blot analysis of the proteolytic cleavage of PARP. In U-251MG cells and LN-229 cells, a reduced *IDH1* gene expression by siRNA did not induce apoptosis under normoxic and hypoxic condition, respectively (Figure 4.9). On the contrary, in U-343MG cells, *IDH1* gene silencing via siRNA did not affect the gene expression of PARP in normoxia, but caused a slightly increased cleavage of PARP under hypoxic conditions (Figure 4.9).
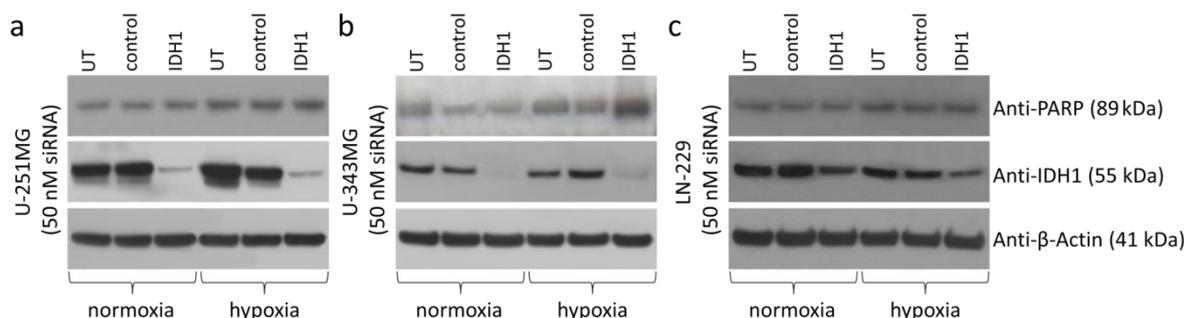
**Figure 4.9. Influence of *IDH1*-specific siRNA on the IDH1 protein expression in glioma cells.** Representative Western blots for IDH1 protein in U-251MG (a), U-343MG (b) and LN-229 (c) cells under normoxic (21 % $O_2$) and hypoxic (<0.1 % $O_2$) conditions. IDH1 protein expression 24 h after treatment with 50 nM *IDH1*-specific siRNA in comparison to 50 nM control siRNA or untreated cells. For PARP analyses cleaved PARP antibody was used (detects cleaved PARP 89 kDa and does not recognize full length PARP). β-Actin served as loading control; n=3 independent experiments. UT: untreated cells, control: cells treated with 50 nM control siRNA, IDH1: cells treated with 50 nM *IDH1*-specific siRNA.

### 4.2.3 Effect of *IDH1* siRNA on the clonogenic survival and radiosensitivity

The influence of *IDH1*-specific siRNA on the plating efficiency of non-irradiated glioma cells was investigated using the clonogenic survival assay. Treatment with the control siRNA did not significantly affect the clonogenic survival compared to the untreated U-251MG, U-343MG and LN-229 cells, respectively. In U-251MG cells, treatment with *IDH1*-specific siRNA resulted in a slightly increased plating efficiency under normoxia by 9.3 % ± 3.7 (not significant), whereas in these cells under hypoxic conditions a decreased plating efficiency by 16.8 % ± 14.9 (not significant) was observed (Figure 4.10a). Further, the reduction of the *IDH1* gene expression using siRNA resulted in a decreased plating efficiency under normoxia by 19.6 % ± 3.7 (p<0.01) in U-343MG and by 14.5 % ± 21.9 (not significant) in LN-229 cells as compared to the respective cells treated with the control siRNA (Figure 4.10b and Figure 4.10c). Furthermore, in hypoxia treatment with *IDH1* siRNA resulted in a slightly decreased clonogenic survival by 3.2 % ± 0.8 (p<0.05) in U-343MG and by 4.9 % ± 12.0 (not significant) in LN-229 cells as compared to the control siRNA treated cells, respectively (Figure 4.10b and Figure 4.10c).
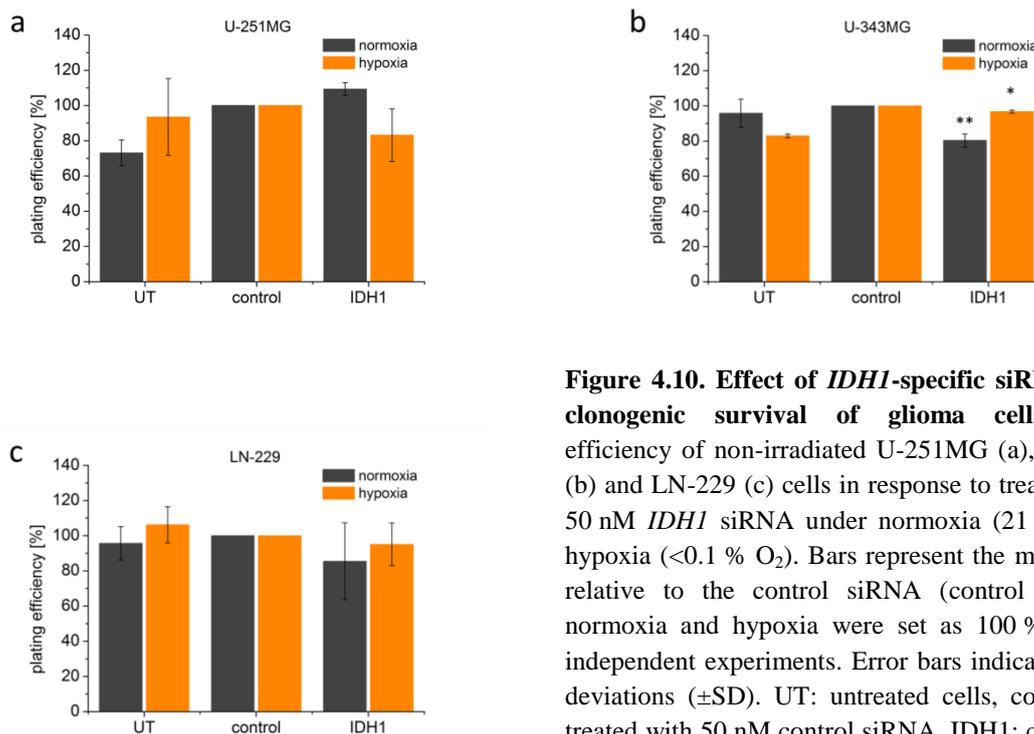
**Figure 4.10. Effect of *IDH1*-specific siRNA on the clonogenic survival of glioma cells.** Plating efficiency of non-irradiated U-251MG (a), U-343MG (b) and LN-229 (c) cells in response to treatment with 50 nM *IDH1* siRNA under normoxia (21 % $O_2$) and hypoxia (<0.1 % $O_2$). Bars represent the mean values, relative to the control siRNA (control siRNA in normoxia and hypoxia were set as 100 %) of three independent experiments. Error bars indicate standard deviations (±SD). UT: untreated cells, control: cells treated with 50 nM control siRNA, IDH1: cells treated with 50 nM *IDH1*-specific siRNA; *p<0.05 and **p<0.01 (compared to the respective control siRNA in normoxia or hypoxia).

The influence of a reduced *IDH1* gene expression via siRNA on radiosensitivity of U-251MG, U-343MG and LN-229 cells was evaluated by means of the clonogenic survival after irradiation and compared to that of non-irradiated cells (set as 100 %) (Figure 4.11). The assay revealed an increased survival of U-251MG, U-343MG and LN-229 cells under hypoxia as compared to normoxia (Figure 4.11, untreated cells are not shown for better clarity). Furthermore, the survival curves indicate that reduction of the *IDH1* gene expression did not affect the response to radiation in U-343MG grade III glioma cells under normoxic conditions (DMF10: 1.07, p<0.05). On the contrary, treatment with *IDH1* siRNA slightly attenuated the radioresistance of U-343MG cells under hypoxic conditions (DMF10: 1.63, p<0.01) (Figure 4.11b). In addition, the siRNA-mediated reduction of the IHD1 gene expression had no effect on radiosensitivity of grade IV glioblastoma cell lines U-251MG and LN-229 in normoxia (U-251MG DMF10: 0.99, not significant; LN-229 DMF10: 0.98, not significant) and hypoxia (U-251MG DMF10: 0.91, not significant; LN-229 DMF10: 1.02, not significant) (Figure 4.11a and Figure 4.11c).
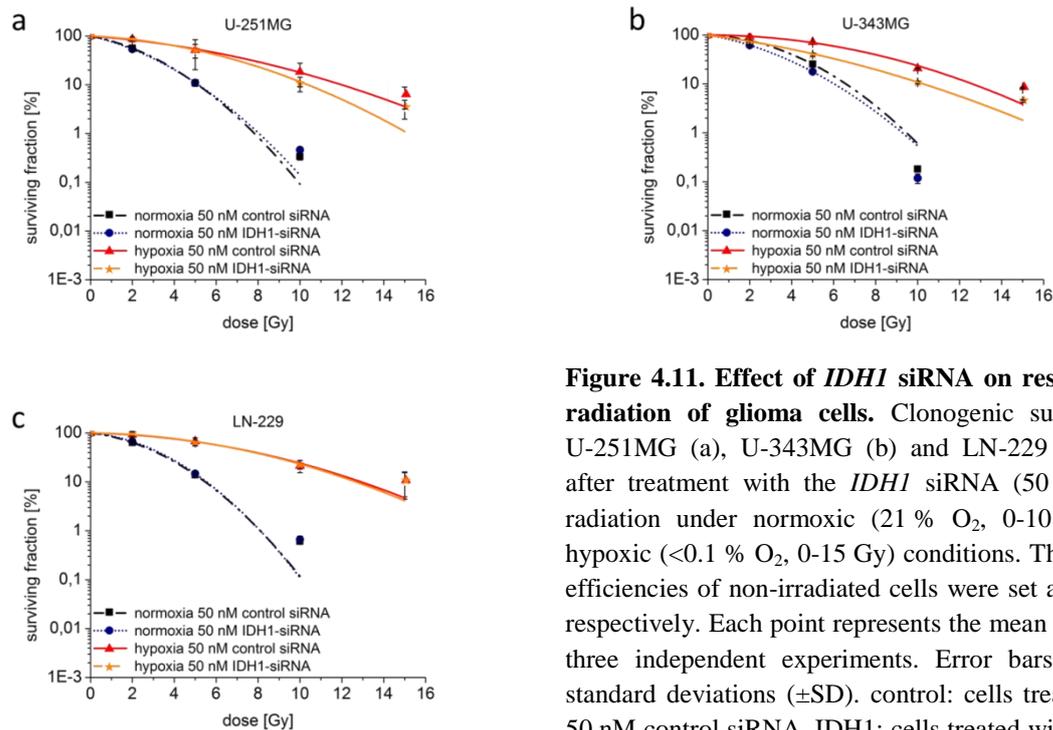
**Figure 4.11. Effect of *IDH1* siRNA on response to radiation of glioma cells.** Clonogenic survival of U-251MG (a), U-343MG (b) and LN-229 (c) cells after treatment with the *IDH1* siRNA (50 nM) and radiation under normoxic (21 % $O_2$, 0-10 Gy) and hypoxic (<0.1 % $O_2$, 0-15 Gy) conditions. The plating efficiencies of non-irradiated cells were set as 100 %, respectively. Each point represents the mean values of three independent experiments. Error bars indicate standard deviations (±SD). control: cells treated with 50 nM control siRNA, IDH1: cells treated with 50 nM *IDH1*-specific siRNA.

In summary, *IDH1*-specific siRNA clearly decreased the gene expression of IDH1 in malignant glioma cell lines U-251MG, U-343MG and LN-229 in normoxia and hypoxia. Reduction of the *IDH1* gene expression via siRNA did not affect radiosensitivity of glioblastoma grade IV U-251MG and LN-229 cells under normoxic and hypoxic conditions. On the other hand, the reduced *IDH1* gene expression decreased the radioresistance of U-343MG cells (anaplastic astrocytoma grade III) only under hypoxic conditions, whereas in normoxia no effect on the radiosensitivity of these cells was observed.

## 4.3 IDH1$^{wt}$ or IDH1$^{R132H}$ expression in U-251MG, U-343MG and LN-229 malignant glioma cells under normoxic and hypoxic conditions

In gliomas of all grades the presence of *IDH1* mutation is linked to a more favorable clinical outcome after standard treatments comprising surgery, radiotherapy and chemotherapy (Ichimura et al., 2009; Hartmann et al., 2009; Yan et al., 2009). However, it is not completely understood yet, whether the *IDH1* mutation is associated with a less aggressive phenotype or directly linked to an increased sensitivity to radiotherapy. In this work, the influence of IDH1$^{R132H}$ mutant protein on cellular behavior and radiosensitivity was analyzed *in vitro* under normoxia (21 % $O_2$) and hypoxia (<1 % $O_2$) in a panel of human glioma cell lines with different degrees of malignancy, (U-251MG (grade IV),

U-343MG (grade III) and LN-229 (grade IV)) with stable overexpression of wild type (IDH1^{wt}) or mutated IDH1 (IDH1^{R132H}).

### 4.3.1  Establishment of stable cell lines overexpressing IDH1^{wt} or IDH1^{R132H}

To determine the effect of an overexpression of IDH1 mutant protein within glioma cells, IDH1^{wt} and IDH1^{R132H} constructs were generated and U-251MG, U-343MG and LN-229 stable cell lines with empty vector (pLVX) or expression of IDH1^{wt} or IDH1^{R132H} were established using puromycin selection post transduction. Analyses by qPCR revealed a high *IDH1* mRNA level in pLVX IDH1^{wt} transduced U-251MG (normoxia: 62.9-fold (p<0.01), hypoxia: 42.9-fold (p<0.01)), U-343MG (normoxia: 56.8-fold (p<0.01), hypoxia: 68.7-fold (p<0.01)) and LN-229 (normoxia: 55.8-fold (p<0.01), hypoxia: 39.6-fold (p<0.01)) cells compared to cells stably transduced with empty vector pLVX (Figure 4.12). Furthermore, a high *IDH1* mRNA level in pLVX IDH1^{R132H} transduced U-251MG (normoxia: 78.0-fold (p<0.01), hypoxia: 57.5-fold (p<0.01)), U-343MG (normoxia: 52.2-fold (p<0.01), hypoxia: 37.7-fold (p<0.01)) and LN-229 (normoxia: 76.5-fold (p<0.01), hypoxia: 52.7-fold (p<0.01)) cells was observed compared to cells stably transduced with empty vector pLVX, respectively (Figure 4.12).
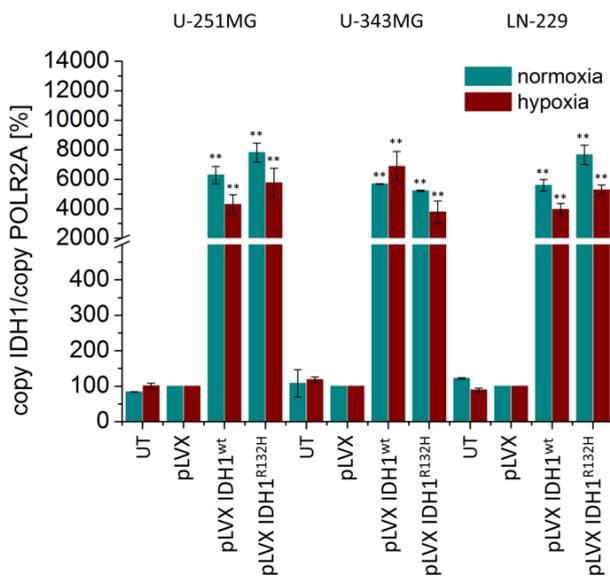


**Figure 4.12. Effect of stable transduction of IDH1^{wt} or IDH1^{R132H} on *IDH1* mRNA level in glioma cells.** U-251MG, U-343MG and LN-229 cells stably express high quantities of *IDH1* mRNA (qPCR) under normoxic (21 % O$_2$) and hypoxic (<0.1 % O$_2$) conditions. RNA was extracted 24 h after seeding. Bars represent the mean values, relative to the empty vector (empty vector in normoxia and hypoxia were set as 100 %, respectively) of five independent experiments. Error bars indicate standard deviations (±SD). UT: untreated, pLVX: cells stably transduced with empty vector, pLVX IDH1^{wt}: cells overexpressing IDH1^{wt}, pLVX IDH1^{R132H}: cells overexpressing IDH1^{R132H}; **p<0.01 (compared to the respective empty vector cells in normoxia or hypoxia).

Additionally, IDH1^{wt} and IDH1^{R132H} protein expression was analyzed via anti-human IDH1- and mutant-specific anti-IDH1R132H antibodies in Western blot analysis of untreated, empty vector and pLVX IDH1^{wt} or pLVX IDH1^{R132H} transduced U-251MG, U-343MG and LN-229 glioma cells under normoxic (21 % O$_2$) and hypoxic (<0.1 % O$_2$) conditions (Figure 4.13). The investigated glioma cells showed a moderate expression of wild type IDH1 in normoxia and hypoxia. Stable transduction with the empty vector pLVX did not affect the expression of wild type IDH1 in the investigated cell lines

(Figure 4.13). In addition to quantitative real-time PCR, Western blot analysis confirmed the overexpression of IDH1$^{wt}$ or IDH1$^{R132H}$ protein in stably transduced U-251MG, U-343MG and LN-229 glioma cells under normoxic and hypoxic conditions, respectively (Figure 4.13).
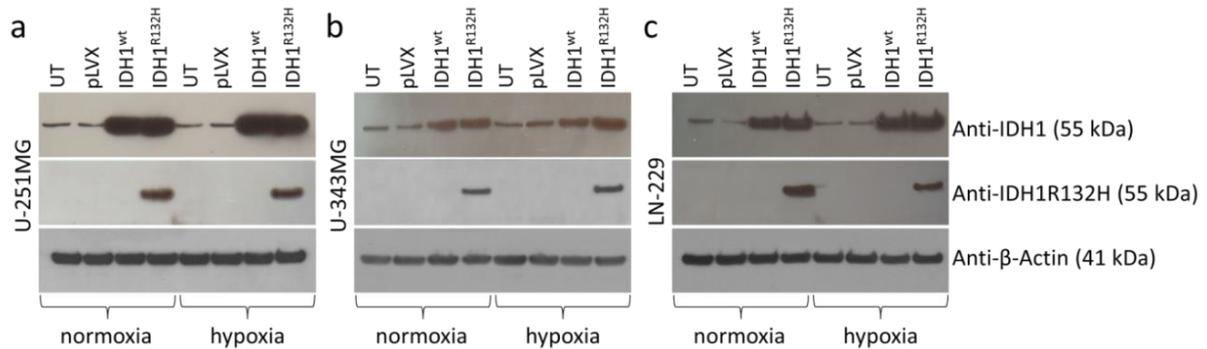


**Figure 4.13. Effect of stable transduction of IDH1$^{wt}$ or IDH1$^{R132H}$ on IDH1 protein level in glioma cells.** Representative Western blots for IDH1$^{wt}$ and IDH1$^{R132H}$ protein in stably transduced U-251MG (a), U-343MG (b) and LN-229 (c) cells under normoxia (21 % O$_2$) and hypoxia (<0.1 % O$_2$) using anti-IDH1 and anti-IDH1R132H antibodies. Anti-IDH1 antibody was used for detection of IDH1$^{wt}$ and IDH1$^{R132H}$ protein, whereas anti-IDH1R132H antibody specifically recognizes the IDH1 mutant protein. β-Actin served as loading control; n=5 independent experiments. UT: untreated cells, pLVX: cells stably transduced with empty vector, pLVX IDH1$^{wt}$: cells overexpressing IDH1$^{wt}$, pLVX IDH1$^{R132H}$: cells overexpressing IDH1$^{R132H}$.

Immunofluorescence staining was applied to analyze the IDH1$^{wt}$ and IDH1$^{R132H}$ protein expression patterns in stably transduced U-251MG, U-343MG and LN-229 cells. Immunofluorescence staining with anti-human IDH1 and mutant-specific anti-IDH1R132H antibodies confirmed overexpression and the diffuse cytoplasmic distribution of IDH1$^{wt}$ or IDH1$^{R132H}$ protein in the different glioma cell lines under normoxic and hypoxic conditions, suggesting that the oxygen concentration did not influence the expression of IDH1$^{R132H}$ protein (Figure 4.14, appendix: Figure 8.1 and Figure 8.2).
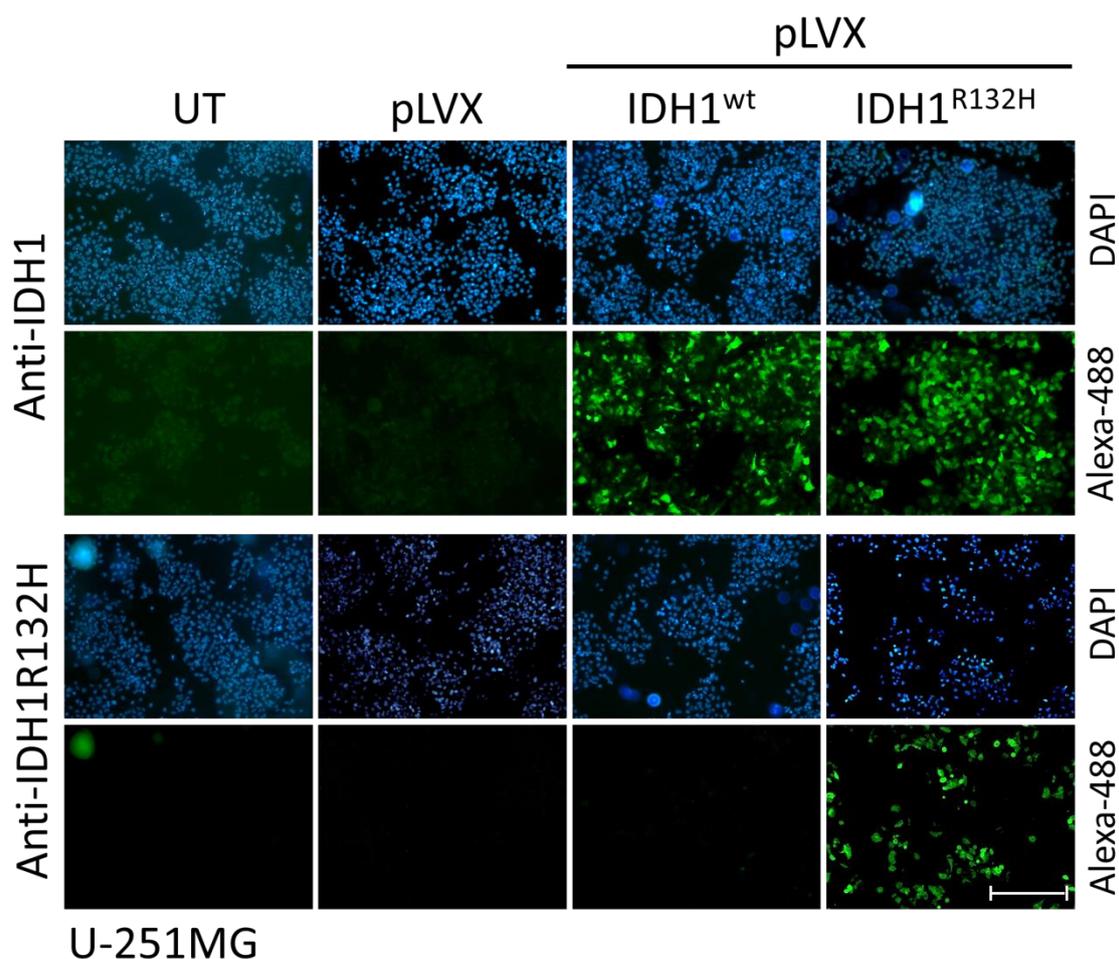
**Figure 4.14. Immunofluorescence staining of transduced U-251MG glioma cells stably expressed IDH1$^{wt}$ or IDH1$^{R312H}$ protein.** Representative immunofluorescence staining of IDH1$^{wt}$ and IDH1$^{R132H}$ protein in U-251MG cells using anti-IDH1 and anti-IDH1R132H antibodies. Stable cell lines showed a diffuse cytoplasmic distribution of IDH1$^{wt}$ or IDH1$^{R132H}$ protein. Immunofluorescence staining was achieved 24 h after seeding. Cell nuclei were counterstained with DAPI. n=3 independent experiments; scale bar=100 μm. UT: untreated cells, pLVX: cells stably transduced with empty vector, pLVX IDH1$^{wt}$: cells overexpressing IDH1$^{wt}$, pLVX IDH1$^{R132H}$: cells overexpressing IDH1$^{R132H}$.

### 4.3.2    Effect of IDH1$^{R132H}$ on the viability and proliferation in 2D culture

To determine the effect of *IDH1* mutation on viability and cell growth, untreated cells, cells stably transduced with empty vector pLVX, IDH1$^{wt}$- or IDH1$^{R132H}$-expressing cells were investigated in 2D culture under normoxic and hypoxic conditions (Figure 4.15). In 2D culture, gene expression of IDH1$^{R132H}$ resulted in a slight reduction of the viability between 2.6 % ± 1.9 and 6.0 % ± 2.9 (not significant) compared to the IDH1$^{wt}$ cells of U-251MG, U-343MG and LN-229 under normoxic and hypoxic conditions (Figure 4.15).
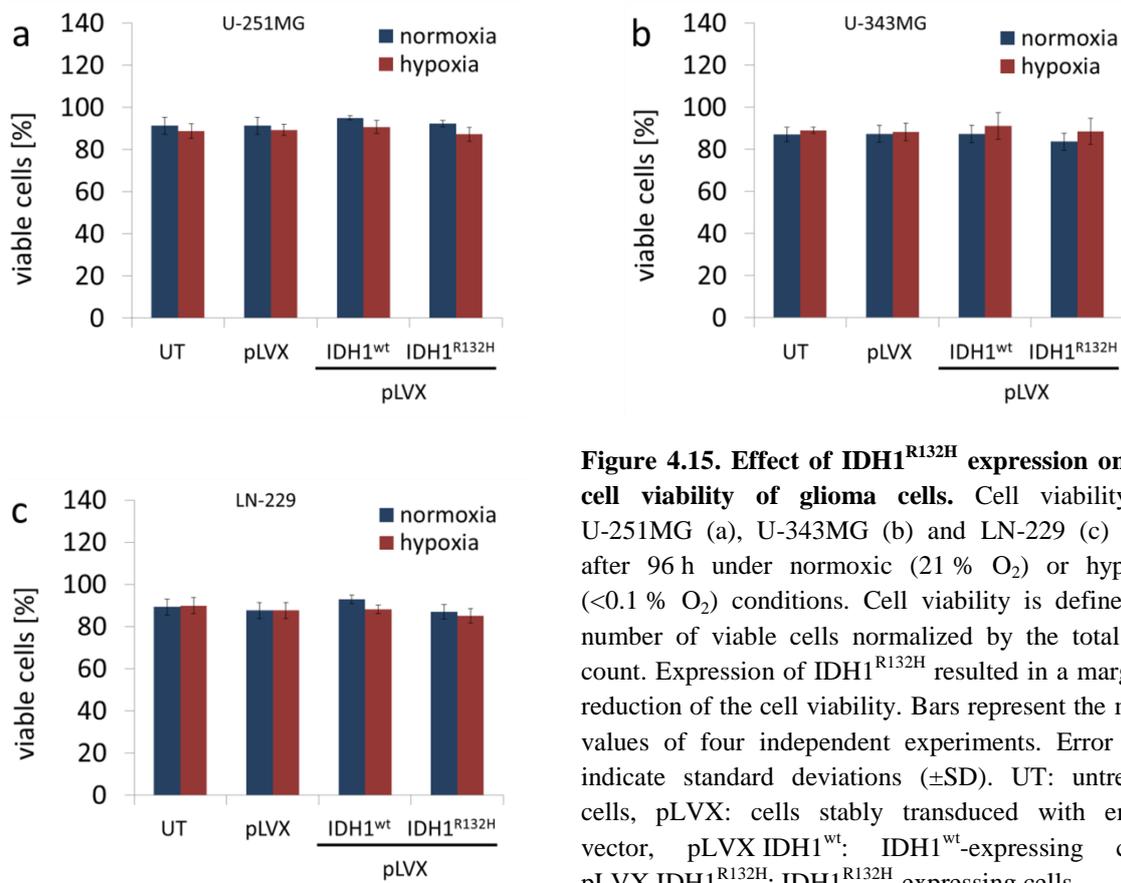
**Figure 4.15. Effect of IDH1^{R132H} expression on the cell viability of glioma cells.** Cell viability of U-251MG (a), U-343MG (b) and LN-229 (c) cells after 96 h under normoxic (21 % $O_2$) or hypoxic (<0.1 % $O_2$) conditions. Cell viability is defined as number of viable cells normalized by the total cell count. Expression of IDH1^{R132H} resulted in a marginal reduction of the cell viability. Bars represent the mean values of four independent experiments. Error bars indicate standard deviations (±SD). UT: untreated cells, pLVX: cells stably transduced with empty vector, pLVX IDH1^{wt}: IDH1^{wt}-expressing cells, pLVX IDH1^{R132H}: IDH1^{R132H}-expressing cells.

In addition to that gene expression of IDH1^{R132H} slightly reduced the proliferation of the investigated cell lines. In normoxia, the cell number was reduced by 8.1 % ± 1.9 ($p<0.05$) in U-251MG cells, by 11.9 % ± 3.9 ($p<0.05$) in U-343MG cells and by 9.5 % ± 6.8 ($p<0.05$) in LN-229 cells at 96 h as compared to the respective IDH1^{wt} cells (Figure 4.16). Under hypoxic conditions, gene expression of IDH1^{R132H} resulted in a slightly decreased proliferation of U-251MG cells by 6.9 % ± 1.1 ($p<0.05$), of U-343MG cells by 8.6 % ± 3.9 ($p<0.05$) and of LN-229 cells by 9.5 % ± 4.6 ($p<0.05$) at 96 h relative to the specific IDH1^{wt} cells (Figure 4.16).
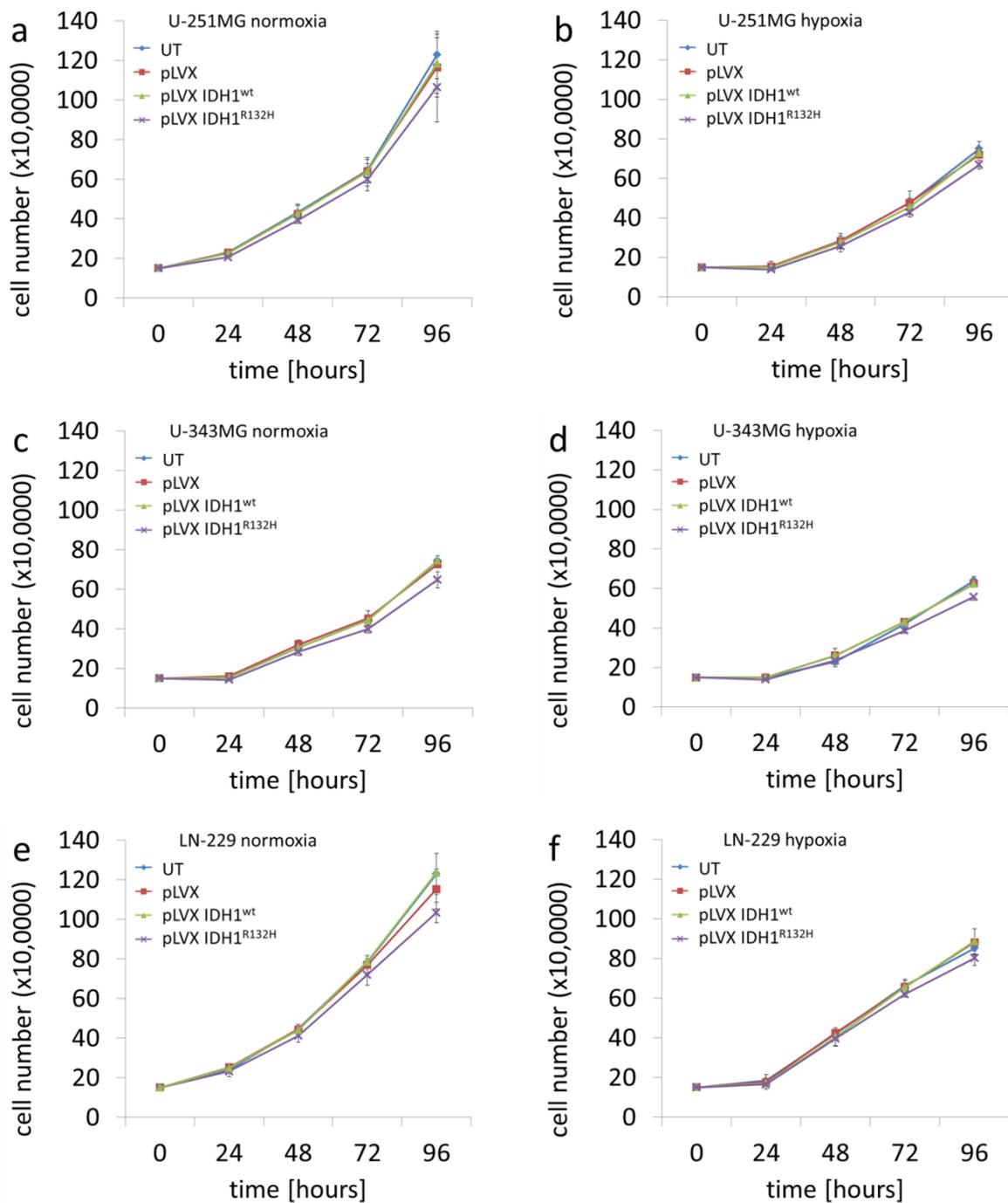
**Figure 4.16. Effect of IDH1^R132H expression on cell proliferation in 2D culture of glioma cells.** Cell proliferation of U-251MG (a and b), U-343MG (b and d) and LN-229 (e and f) cells in 2D culture was analyzed over 96 h under normoxic (21 % $O_2$) and hypoxic (<0.1 % $O_2$) conditions. Each point represents the mean values of four independent experiments. Error bars indicate standard deviations (±SD). UT: untreated cells, pLVX: cells stably transduced with empty vector, pLVX IDH1^wt: IDH1^wt-expressing cells, pLVX IDH1^R132H: IDH1^R132H-expressing cells.

### 4.3.3 Effect of IDH1$^{R132H}$ on growth characteristics 3D spheroid culture

In general, solid tumors grow in a spatial 3D array with very intimate cell–cell interactions, complex extracellular matrix organization and non-uniform oxygen and nutrient distribution. In 2D culture the micro milieu is significantly different from that found in solid tumors. Hence, it is obvious that 2D culture cannot be used to examine all aspects of tumor biology. Based on that fact, cell growth was also investigated in a multicellular 3D tumor spheroid model which simulates many of the characteristics of solid *in vivo* tumors. The experiments showed that the oxygen concentration itself had no effect on the growth properties of the different cell lines. However, IDH1$^{R132H}$ caused differences in their growth characteristics during 3D culture (Figure 4.17). On the one hand, the untreated cells, the empty vector cells and the IDH1$^{wt}$-expressing cells of all three cell lines showed a compact 3D spheroid structure, respectively. On the other hand, the IDH1$^{R132H}$-expressing cells formed more loose and uneven spheroids in normoxia (Figure 4.17a, c and e) and hypoxia (Figure 4.17b, d and f).
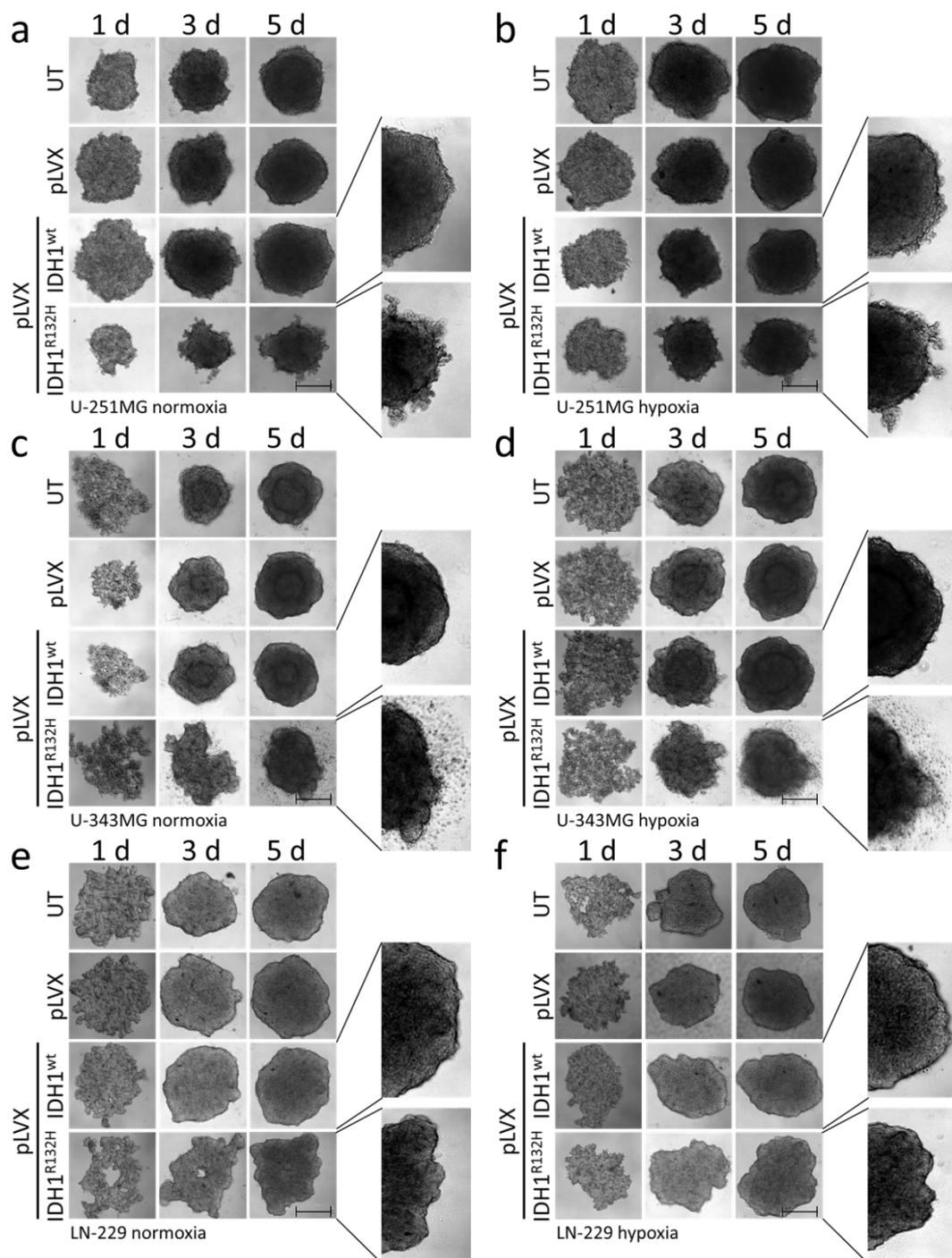
**Figure 4.17. Effect of IDH1$^{R132H}$ expression on growth characteristics in 3D spheroid cultures of glioma cells.** Representative 3D spheroid cultures of U-251MG (a and b), U-343MG (c and d) and LN-229 (e and f) cells after one, three and five days in normoxia (21 % O$_2$) and hypoxia (<0.1 % O$_2$). IDH1$^{R132H}$ cells showed different growth characteristics in 3D spheroid cultures. n=3 independent experiments; scale bar=200 μm. UT: untreated cells, pLVX: cells stably transduced with empty vector, pLVX IDH1$^{wt}$: IDH1$^{wt}$-expressing cells, pLVX IDH1$^{R132H}$: IDH1$^{R132H}$-expressing cells.

### 4.3.4 Effect of IDH1$^{R132H}$ on the cell migration of glioma cells in 2D culture

In order to evaluate the effect of IDH1$^{R132H}$ on the migration of U-251MG, U-343MG and LN-229 glioma cells a wound-healing assay (scratch assay) under normoxia and hypoxia was performed. Images were taken at 0 h, 24 h and 48 h after wounding and of incubation under normoxic or hypoxic conditions. Evaluation of the wound closure revealed that the migration of U-251MG and LN-229 cells (both grade IV) was generally higher compared to U-343MG cells (grade III) (Figure 4.18). Furthermore, migration was higher in all glioma cells under normoxia compared to hypoxia (Figure 4.18). Moreover, treatment with the empty vector or gene expression of IDH1$^{wt}$ had no effect on the migration at 48 h after wounding compared to the untreated cells in the investigated cell lines (Figure 4.18). In contrast, gene expression of IDH1$^{R132H}$ reduced the cell migration by 22.9 % ± 3.8 (p<0.01) in U-251MG, by 14.8 % ± 2.1 (p<0.05) in U-343MG and by 36.7 % ± 4.6 (p<0.01) in LN-229 cells compared to IDH1$^{wt}$ cells under normoxia (Figure 4.18). In addition, under hypoxic conditions, gene expression of IDH1$^{R132H}$ decreased the cell migration by 21.3 %± 3.9 (p<0.01) in U-251MG, by 12.1 % ± 1.2 (p<0.01) in U-343MG and by 67.5 % ± 1.0 (p<0.01) in LN-229 cells compared to the IDH1$^{wt}$ cells, respectively (Figure 4.18).
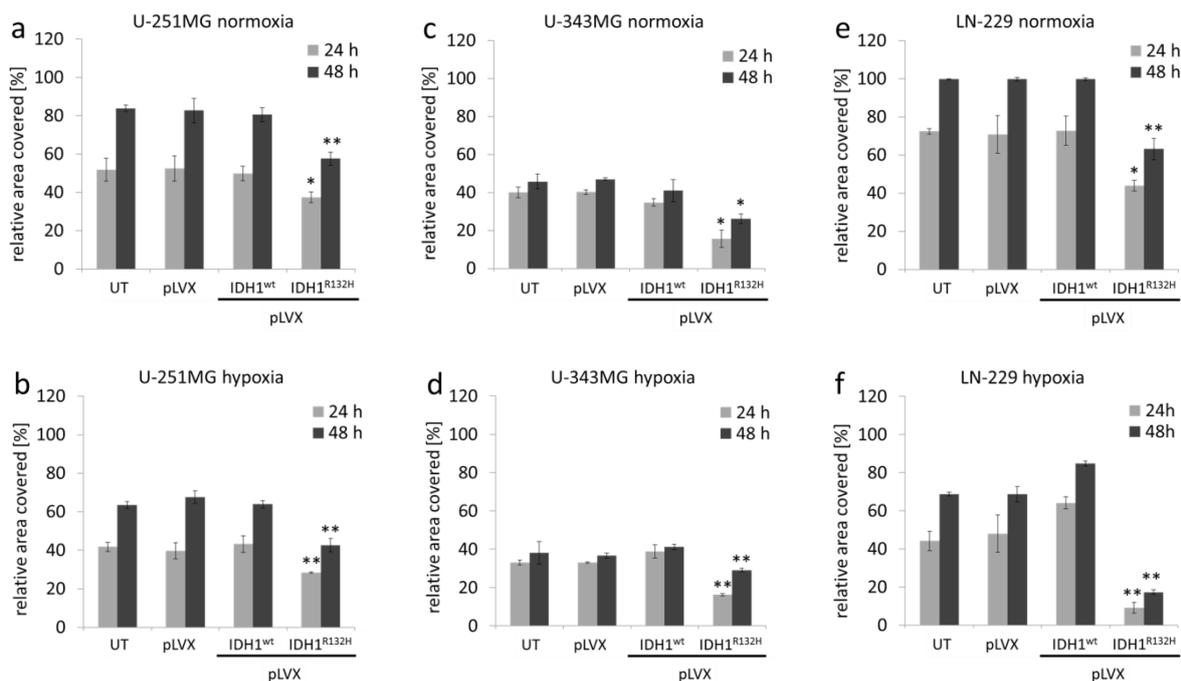


**Figure 4.18. Effect of IDH1$^{R132H}$ gene expression on wound closure in a 2D wound-healing assay of glioma cells.** Cell migration of U-251MG (a and b), U-343MG (c and d) and LN-229 (e and f) cells in a 2D wound-healing assay under normoxic (21 % O$_2$) and hypoxic (<0.1 % O$_2$) conditions. Cell migration was evaluated via measuring the wounding area (μm$^2$) 24 h and 48 h after wounding. Bars represent the mean values of four independent experiments. Error bars indicate standard deviations (±SD). UT: untreated cells, pLVX: cells stably transduced with empty vector, pLVX IDH1$^{wt}$: IDH1$^{wt}$-expressing cells, pLVX IDH1$^{R132H}$: IDH1$^{R132H}$-expressing cells; *p<0.05 and **p<0.01 (compared to the respective IDH1$^{wt}$ cells in normoxia or hypoxia).

### 4.3.5 Effect of IDH1$^{R132H}$ on cell migration of glioma cells in 3D spheroid-based culture

A 3D spheroid-based migration assay was applied to analyze the influence of IDH1$^{R132H}$ on the cell migration of U-251MG, U-343MG and LN-229 glioma cells in 3D culture under normoxic and hypoxic conditions. The results confirmed the findings of the 2D wound-healing assay (4.3.2). Also in 3D culture the cell migration of U-251MG, U-343MG and LN-229 cells was higher in normoxia compared to hypoxia (Figure 4.19). Furthermore, treatment with the empty vector or gene expression of IDH1$^{wt}$ did not affect the cell migration compared to the untreated cells of each cell line (Figure 4.19). In contrast, gene expression of IDH1$^{R132H}$ reduced the cell migration by 26.8 % ± 4.6 ($p<0.01$) in U-251MG, by 30.9 % ± 5.6 ($p<0.01$) in U-343MG and by 17.0 % ± 2.5 ($p<0.01$) in LN-229 cells at 72 h after transferring spheroids to 10 cm dishes compared to the respective IDH1$^{wt}$ cells under normoxia (Figure 4.19). In addition, under hypoxic conditions, gene expression of IDH1$^{R132H}$ also decreased the cell migration by 26.0 % ± 6.2 ($p<0.01$) in U-251MG, by 43.8 % ± 1.1 ($p<0.05$) in U-343MG and by 45.9 % ± 3.8 ($p<0.05$) in LN-229 cells at 72 h after transferring spheroids to 10 cm dishes in comparison to the respective IDH1$^{wt}$ cells (Figure 4.19).
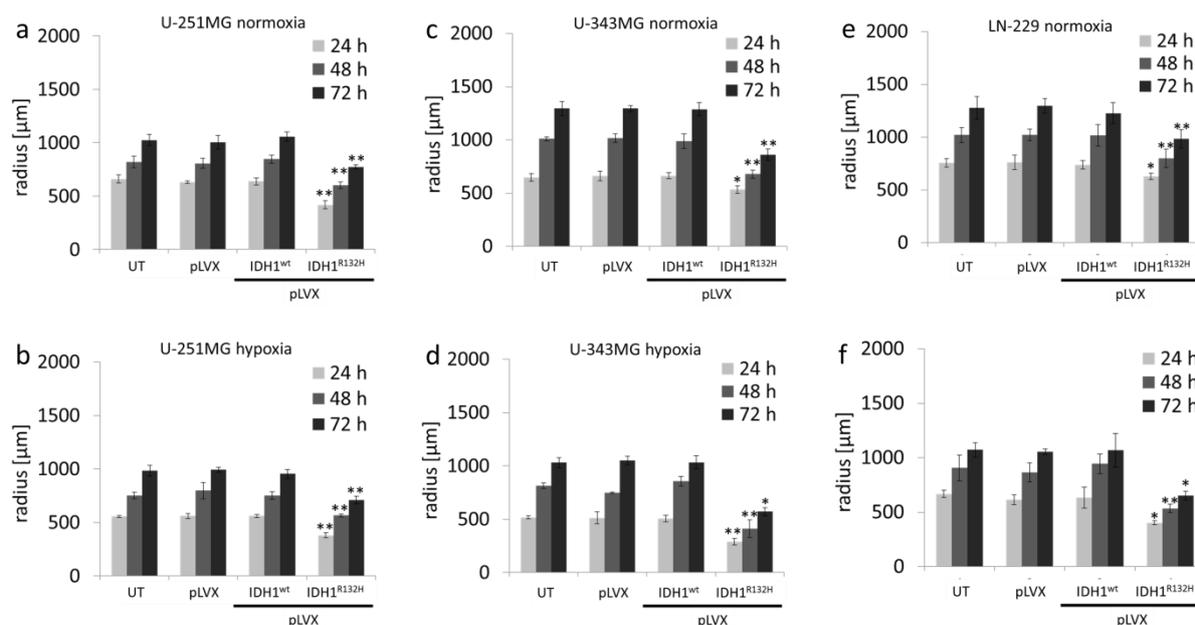


**Figure 4.19. Effect of IDH1$^{R132H}$ gene expression on migration radius in a 3D spheroid-based migration assay of glioma cells.** Cell migration of U-251MG (a and b), U-343MG (c and d) and LN-229 (e and f) cells in 3D spheroid-based migration assay under normoxia (21 % $O_2$) and hypoxia (<0.1 % $O_2$). Cell migration was evaluated via measuring the spheroid migration radius (µm) 24 h, 48 h and 72 h after transferring spheroids to 10 cm dishes. Bars represent the mean values of three independent experiments. Error bars indicate standard deviations (±SD). UT: untreated cells, pLVX: cells stably transduced with empty vector, pLVX IDH1$^{wt}$: IDH1$^{wt}$-expressing cells, pLVX IDH1$^{R132H}$: IDH1$^{R132H}$-expressing cells; *$p<0.05$ and **$p<0.01$ (compared to the respective IDH1$^{wt}$ cells in normoxia or hypoxia).

### 4.3.6 Effect of IDH1$^{R132H}$ on cellular stiffness of glioma cells

AFM is a technology to analyze mechanical properties of living cells in physiological media at nanoscale. Physical measurements obtained by AFM were utilized to quantify the relationship between several cell-specific parameters with a network analytical approach to compile the composite parameter "stiffness" (see 3.13). In order to spread and form metastases, cancer cells have to circulate through narrow blood capillaries and then ooze between other cells into normal tissue, suggesting that cancer cells with high metastatic potential might benefit from their softness and flexibility (Cross et al., 2007; Cross et al., 2008; Hayashi and Iwata, 2015). Thus, lower cell stiffness indicates higher metastatic potential whereas high stiffness is a sign of a less aggressive phenotype of cancer cells (Hayashi and Iwata, 2015). For AFM indentation measurements, single rounded cells were captured by gently pressing a functionalized tip-less AFM cantilever onto the respective cell surfaces (Figure 3.1 and Figure 3.2). Using a tip-less cantilever and measure rounded cells allow detection of cellular mechanical properties. AFM measurements revealed that gene expression of IDH1$^{wt}$ slightly increased the cell stiffness of glioma cell lines compared to untreated cells and empty vector cells, respectively (Figure 4.20). In addition, IDH1$^{R132H}$ caused a considerable increase of cell stiffness of U-251MG (p=0.1), U-343MG (p<0.01) and LN-229 (p<0.01) cells compared to untreated cells, empty vector cells (pLVX) and IDH1$^{wt}$ cells (Figure 4.20).
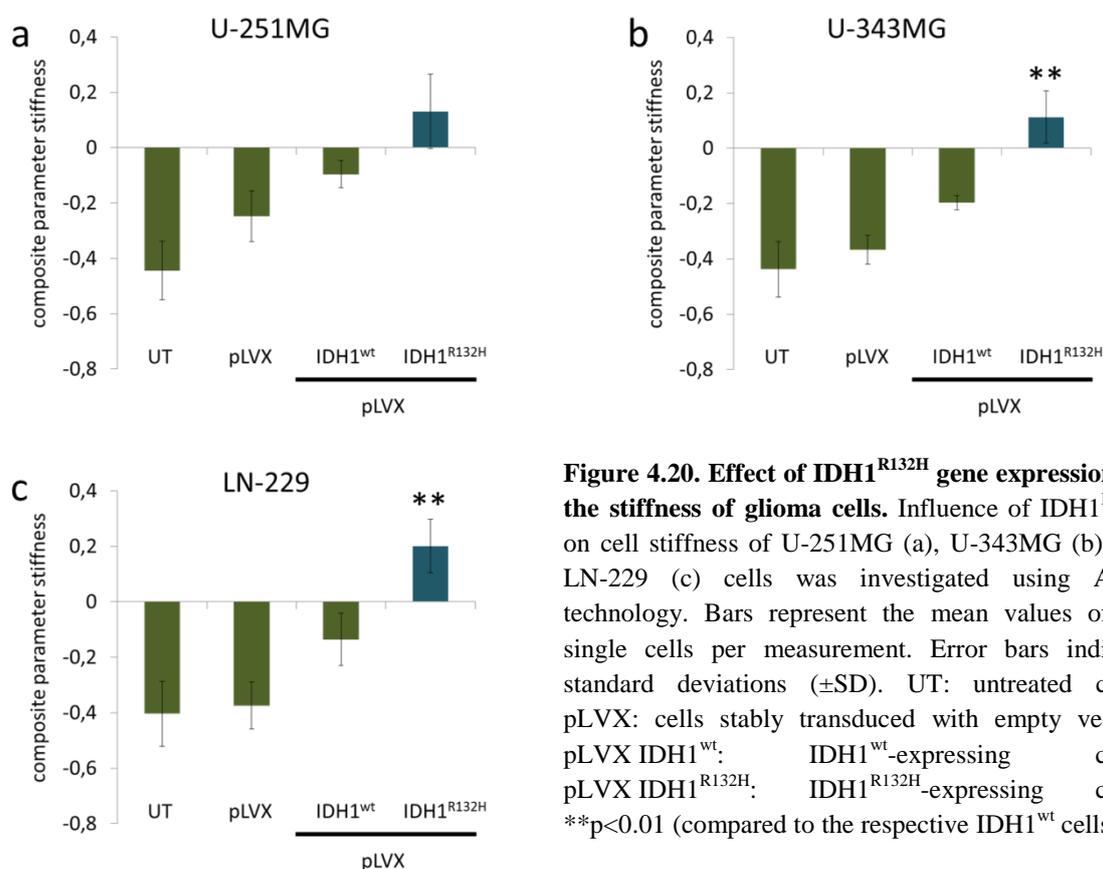


**Figure 4.20. Effect of IDH1$^{R132H}$ gene expression on the stiffness of glioma cells.** Influence of IDH1$^{R132H}$ on cell stiffness of U-251MG (a), U-343MG (b) and LN-229 (c) cells was investigated using AFM technology. Bars represent the mean values of 20 single cells per measurement. Error bars indicate standard deviations (±SD). UT: untreated cells, pLVX: cells stably transduced with empty vector, pLVX IDH1$^{wt}$: IDH1$^{wt}$-expressing cells, pLVX IDH1$^{R132H}$: IDH1$^{R132H}$-expressing cells. **p<0.01 (compared to the respective IDH1$^{wt}$ cells).

### 4.3.7 Effect of IDH1$^{R132H}$ on the clonogenic survival and radiosensitivity

The clonogenic survival assay was used to determine if the gene expression of IDH1$^{R132H}$ influences the radiosensitivity of U-251MG, U-343MG and LN-229 cells. Neither the treatment with the empty vector nor the gene expression of IDH1$^{wt}$ affected the clonogenic survival compared to the untreated U-251MG, U-343MG and LN-229 cells, respectively (Figure 4.21). On the contrary, under normoxia the gene expression of IDH1$^{R132H}$ resulted in a decreased plating efficiency by 12.3 % $\pm$ 7.1 ($p<0.05$) in U-251MG, by 10.2 % $\pm$ 4.3 ($p<0.05$) in U-343MG and by 8.8 % $\pm$ 7.7 ($p<0.01$) in LN-229 cells compared to the respective empty vector cells (Figure 4.21). Furthermore, under hypoxic conditions gene expression of IDH1$^{R132H}$ resulted in a decreased plating efficiency by 16.6 % $\pm$ 2.6 ($p<0.01$) in U-251MG, by 32.0 % $\pm$ 13.0 ($p<0.01$) in U-343MG and by 31.7 % $\pm$ 13.1 ($p<0.05$) in LN-229 cells as compared to the empty vector cells, respectively (Figure 4.21).
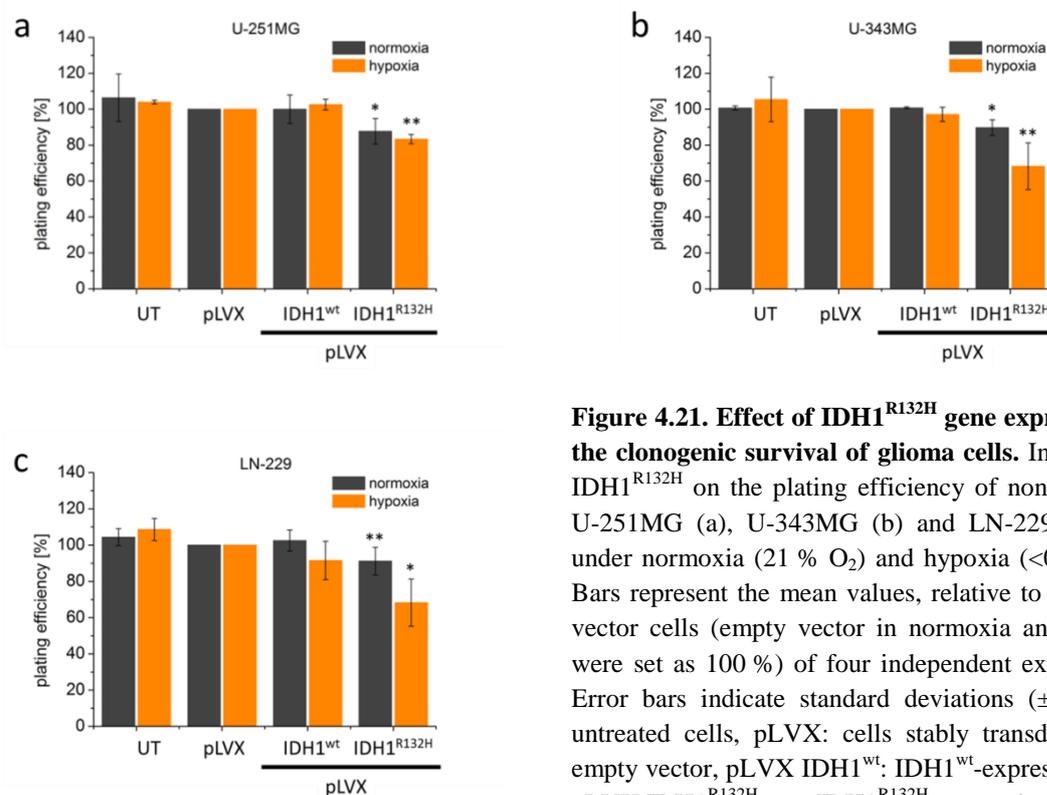


**Figure 4.21. Effect of IDH1$^{R132H}$ gene expression on the clonogenic survival of glioma cells.** Influence of IDH1$^{R132H}$ on the plating efficiency of non-irradiated U-251MG (a), U-343MG (b) and LN-229 cells (c) under normoxia (21 % $O_2$) and hypoxia (<0.1 % $O_2$). Bars represent the mean values, relative to the empty vector cells (empty vector in normoxia and hypoxia were set as 100 %) of four independent experiments. Error bars indicate standard deviations ($\pm$SD). UT: untreated cells, pLVX: cells stably transduced with empty vector, pLVX IDH1$^{wt}$: IDH1$^{wt}$-expressing cells, pLVX IDH1$^{R132H}$: IDH1$^{R132H}$-expressing cells; *$p<0.05$ and **$p<0.01$ (compared to the respective empty vector cells in normoxia or hypoxia).

In addition, the effect of IDH1$^{R132H}$ on the cellular response to radiation was investigated in U-251MG, U-343MG and LN-229 cells. In general, untreated, empty vector and IDH1$^{wt}$ cells exhibited similar radiation survival curves in normoxia and hypoxia, respectively (Figure 4.22, untreated cells and empty vector cells are not shown for better clarity). Furthermore, U-251MG, U-343MG and LN-229 showed an increased survival under hypoxia compared to normoxia. Survival curves indicate that gene

expression of IDH1$^{R132H}$ enhanced the effect of radiation in grade III glioma U-343MG cells under normoxic (DMF10: 1.78, $p<0.01$) and hypoxic (DMF10: 1.75, $p<0.01$) conditions (Figure 4.22b) In addition, expression of IDH1$^{R132H}$ caused an increased radiosensitivity of grade IV glioblastoma cell lines U-251MG and LN-229 in normoxia (U-251MG DMF10: 1.52, $p<0.01$; LN-229 DMF10: 1.41, $p<0.05$) and hypoxia (U-251MG DMF10: 1.42, $p<0.01$; LN-229 DMF10: 1.68, $p<0.01$) (Figure 4.22a and Figure 4.22c).
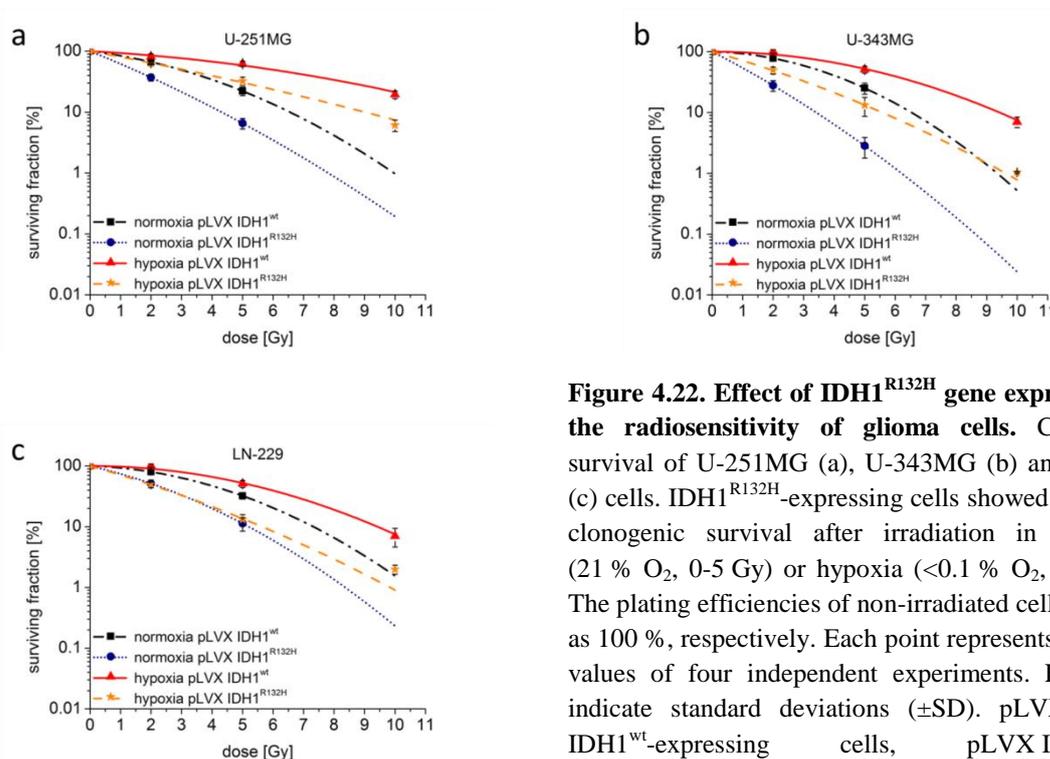


**Figure 4.22. Effect of IDH1$^{R132H}$ gene expression on the radiosensitivity of glioma cells.** Clonogenic survival of U-251MG (a), U-343MG (b) and LN-229 (c) cells. IDH1$^{R132H}$-expressing cells showed a reduced clonogenic survival after irradiation in normoxia (21 % O$_2$, 0-5 Gy) or hypoxia (<0.1 % O$_2$, 0-10 Gy). The plating efficiencies of non-irradiated cells were set as 100 %, respectively. Each point represents the mean values of four independent experiments. Error bars indicate standard deviations ($\pm$SD). pLVX IDH1$^{wt}$: IDH1$^{wt}$-expressing cells, pLVX IDH1$^{R132H}$: IDH1$^{R132H}$-expressing cells.

## 4.3.8    Effect of IDH1$^{R132H}$ on γH2AX foci formation after irradiation

In eukaryotic cells, DNA double-strand breaks (DSBs) occur frequently from endogenous cellular processes or are caused by exogenous sources such as ionizing radiation. In response to the introduction of DNA DSBs, the minor histone H2A variant is rapidly phosphorylated on Ser-139 to produce γH2AX (Paull et al., 2000). Based on the direct correlation between the number of DSBs and γH2AX foci, quantitation of γH2AX foci formation was applied as a marker of DNA damage and repair (Paull et al., 2000; Sedelnikova et al., 2002). Foci which persist for longer than 24 h, so called residual γH2AX foci, indicate unrepaired or misrepaired DSBs. These unsuccessfully repaired DSBs are generally assumed to play a major role in radiation-induced cell death (Frankenberg-Schwager, 1990). Therefore, analyzing the induction of γH2AX foci allows to indirectly evaluate the influence of IDH1$^{R132H}$ gene expression on the effect of radiation in U-251MG, U-343MG and LN-229 cells.

For this purpose, untreated, empty vector and IDH1$^{wt}$- or IDH1$^{R132H}$-expressing cells were irradiated at 0, 2 and 4 Gy under normoxia and hypoxia, respectively. Induction of DNA DSBs and the associated cellular repair capacity was investigated by visualization (Figure 4.23, representative images of U-251MG, 2 and 4 Gy) and quantitation (Figure 4.24 and Figure 4.25) of the residual γH2AX foci 24 h after radiation. Treatment with the empty vector or gene expression of IDH1$^{wt}$ did not affect the number of γH2AX foci compared to the respective untreated U-251MG, U-343MG and LN-229 cells in normoxia and hypoxia, respectively.

After irradiation with 0, 2 and 4 Gy the average number of γH2AX foci per cell increased in a dose dependent manner in U-251MG, U-343MG and LN-229 cells under normoxic and hypoxic conditions (Figure 4.24). Furthermore, in hypoxia γH2AX foci accumulation was decreased irrespective of the dose level in comparison to normoxic conditions in the investigated cell lines (Figure 4.24). Under hypoxic conditions, in untreated, empty vector and IDH1$^{wt}$ cells, the γH2AX foci formation was up to 2.5-fold lower in U-251MG, up to 1.9-fold lower in U-343MG and up to 1.4-fold lower in LN-229 cells compared to the respective cells under normoxic conditions (Figure 4.24).

In normoxia, gene expression of IDH1$^{R132H}$ increased the number of γH2AX foci by 2.3-fold ($p<0.01$) from 2 foci/nucleus to 4.6 foci/nucleus in U-251MG, by 2.1-fold ($p<0.01$) from 2.2 foci/nucleus to 4.5 foci/nucleus in U-343MG cells and by 2.3-fold ($p<0.05$) from 2.3 foci/nucleus to 5.3 foci/nucleus in LN-229 cells compared to the respective IDH1$^{wt}$ cells (Figure 4.24). In addition, after irradiation with 4 Gy IDH1$^{R132H}$ cells showed an increase of γH2AX foci formation by 2.1-fold ($p<0.01$) from 6.8 foci/nucleus to 14.5 foci/nucleus in U-251MG, by 2.2-fold ($p<0.01$) from 3.1 foci/nucleus to 6.6 foci/nucleus in U-343MG cells and by 2.3-fold ($p<0.01$) from 4.0 foci/nucleus to 9.4 foci/nucleus in LN-229 cells in normoxia (Figure 4.24).

Under hypoxic conditions, when cells were irradiated at 2 Gy, the gene expression of IDH1$^{R132H}$ increased the number of γH2AX foci by 4.7-fold ($p<0.01$) from 1.0 foci/nucleus to 4.5 foci/nucleus in U-251MG, by 2.4-fold ($p<0.01$) from 1.2 foci/nucleus to 2.9 foci/nucleus in U-343MG cells and by 2.1-fold ($p<0.01$) from 2.2 foci/nucleus to 4.5 foci/nucleus in LN-229 cells compared to the respective IDH1$^{wt}$ cells (Figure 4.24). Furthermore, in hypoxia gene expression of IDH1$^{R132H}$ increased the γH2AX foci formation about 3.0-fold ($p<0.01$) from 2.8 foci/nucleus to 8.4 foci/nucleus in U-251MG, 3.0-fold ($p<0.01$) from 2.4 foci/nucleus to 7.3 foci/nucleus in U-343MG cells and 2.2-fold ($p<0.01$) from 3.0 foci/nucleus to 6.6 foci/nucleus in LN-229 cells compared to the IDH1$^{wt}$ cells, respectively (Figure 4.24).

Further, the fraction of cells in dependence of the number of residual γH2AX foci per nucleus was evaluated (Figure 4.25). In untreated, empty vector and IDH1$^{wt}$ cells a higher percentage of cells with low amount of foci per nucleus was observed (Figure 4.25). In contrast, IDH1$^{R132H}$-expressing cells

showed an increased percentage of cells with high number of residual γH2AX foci per nucleus in normoxia and hypoxia (Figure 4.25).
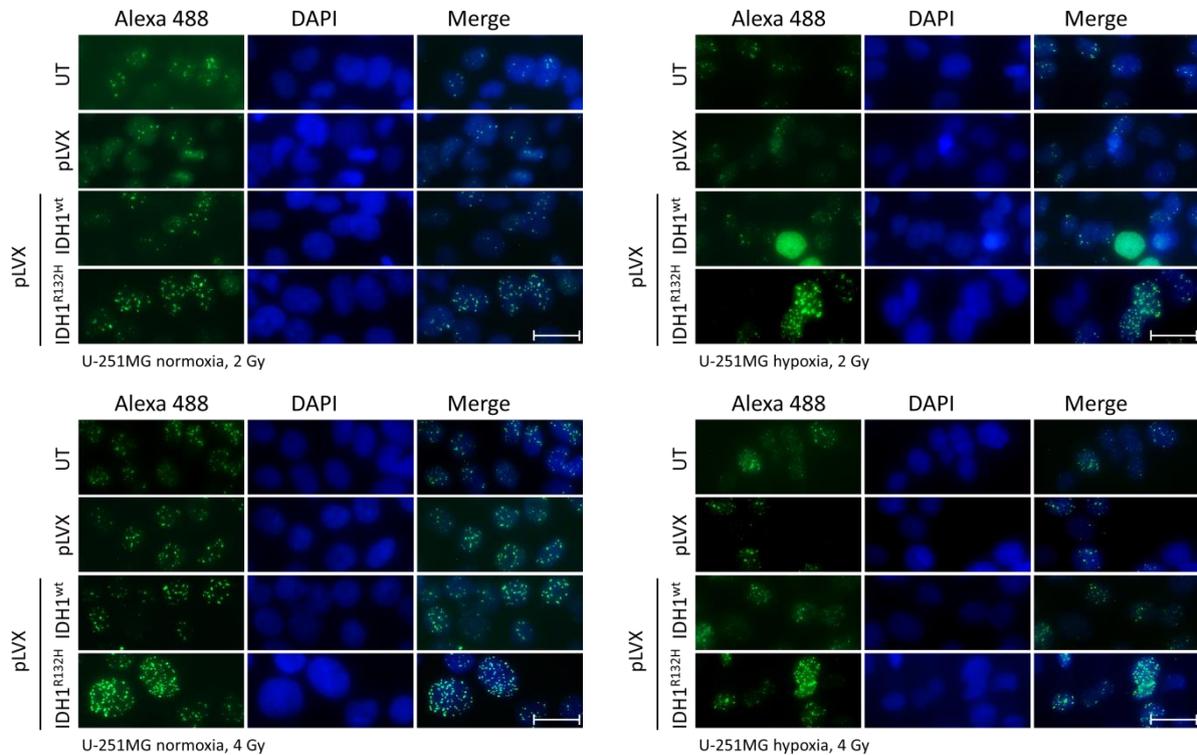


**Figure 4.23. Effect of IDH1^R132H gene expression on the accumulation of residual γH2AX foci after radiation in U-251MG cells.** Representative images of γH2AX staining of U-251MG cells 24 h after irradiation with 2 and 4 Gy under normoxia (21 % $O_2$) and hypoxia (<0.1 % $O_2$). Green: γH2AX foci; Blue: Cell nuclei (DAPI). n=3 independent experiments; bar=25 μm. UT: untreated, pLVX: cells stably transduced with empty vector, pLVX IDH1^wt: IDH1^wt-expressing cells, pLVX IDH1^R132H: IDH1^R132H-expressing cells.
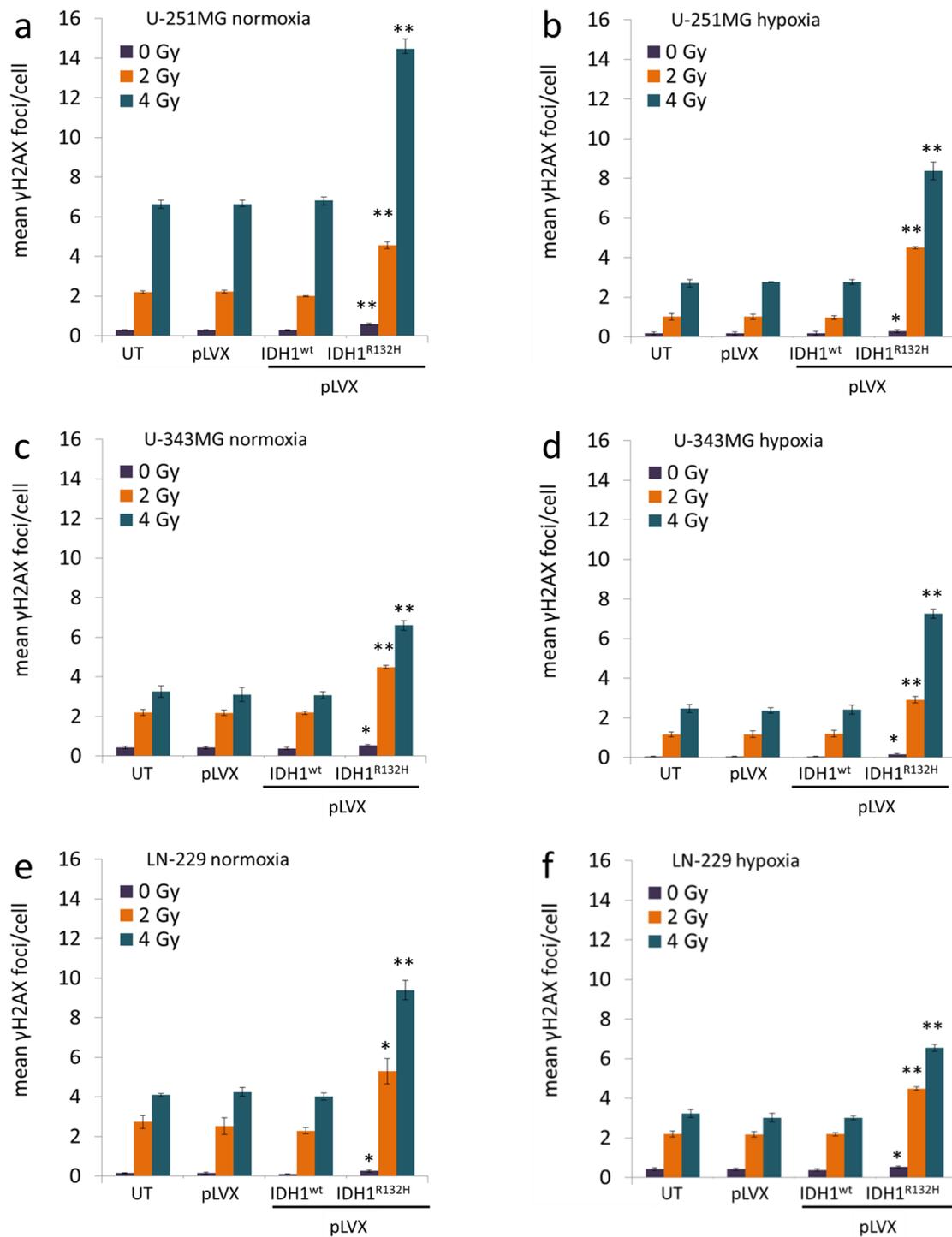
**Figure 4.24. Effect of IDH1$^{R132H}$ gene expression on the number of residual γH2AX foci after radiation in glioma cells.** Residual γH2AX foci in U-251MG (a and b), U-343MG (c and d) and LN-229 (e and f) cells. DNA damage was analyzed by H2AX staining at 24 h after irradiation with 0, 2 and 4 Gy. γH2AX foci were counted manually in the nuclei of 300-400 untreated, empty vector, IDH1$^{wt}$ or IDH1$^{R132H}$ cells under normoxia (21 % O$_2$) and hypoxia (<0.1 % O$_2$). Bars represent the mean values of three independent experiments. Error bars indicate standard deviations (±SD). UT: untreated, pLVX: cells stably transduced with empty vector, pLVX IDH1$^{wt}$: IDH1$^{wt}$-expressing cells, pLVX IDH1$^{R132H}$: IDH1$^{R132H}$-expressing cells; *p<0.05 and **p<0.01 (compared to the respective IDH1$^{wt}$ cells in normoxia or hypoxia).

66
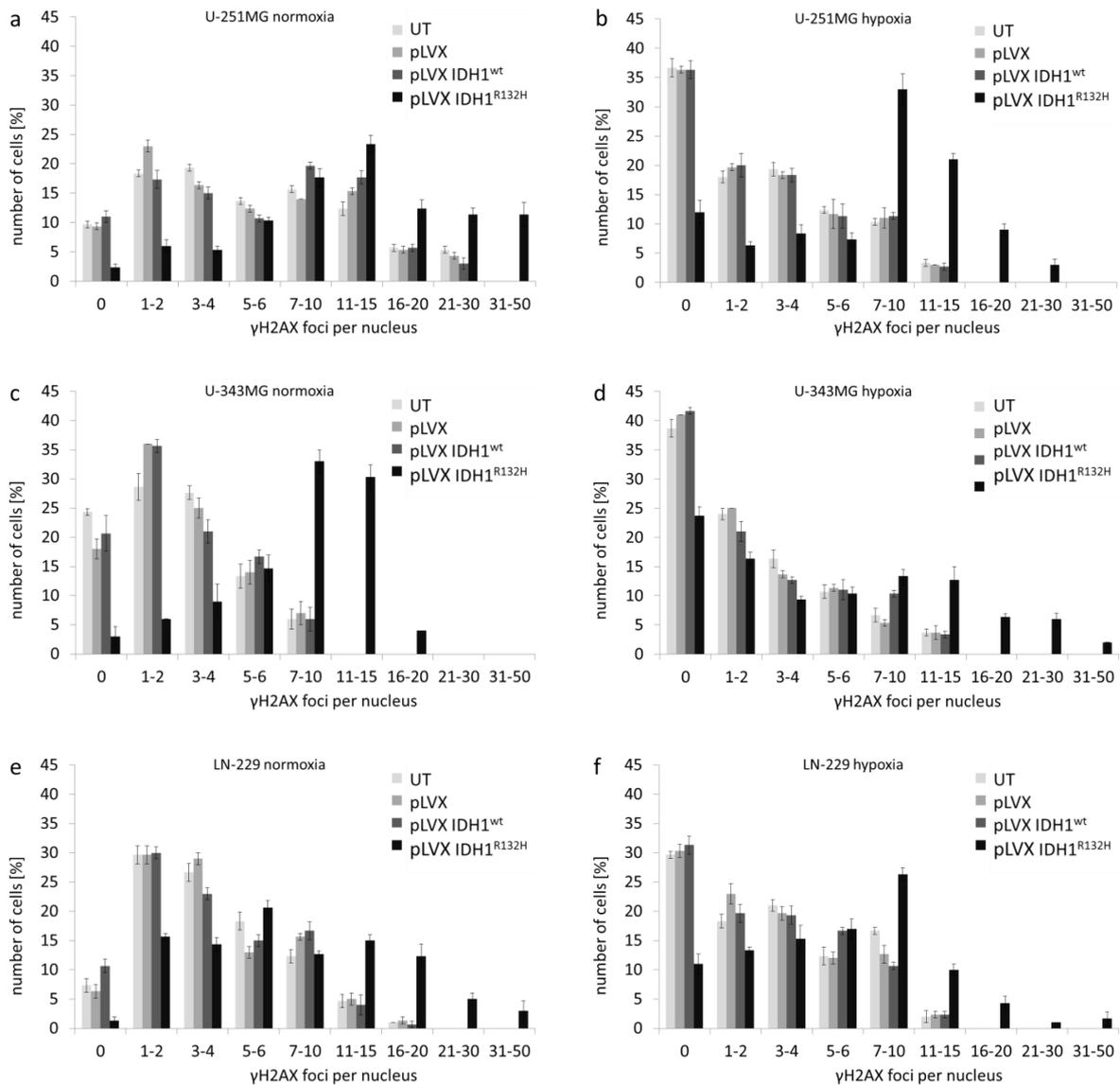
**Figure 4.25. Effect of IDH1$^{R132H}$ gene expression on the distribution of residual γH2AX foci after radiation in glioma cells.** In U-251MG (a), U-343MG (b) and LN-229 (c) cells residual γH2AX foci were quantified manually as foci per nucleus of 300-400 untreated, empty vector, IDH1$^{wt}$ or IDH1$^{R132H}$ cells under normoxia (21 % O$_2$) and hypoxia (<0.1 % O$_2$). γH2AX staining was achieved 24 h after radiation with 4 Gy. Bars represent the mean values of three independent experiments. Error bars indicate standard deviations (±SD). UT: untreated, pLVX: cells stably transduced with empty vector, pLVX IDH1$^{wt}$: IDH1$^{wt}$-expressing cells, pLVX IDH1$^{R132H}$: IDH1$^{R132H}$-expressing cells.

## 4.3.9 Effect of IDH1$^{R132H}$ on induction of apoptosis in glioma cells

The proteolytic cleavage of PARP via Western blot analysis was used to qualitatively assess the induction of apoptosis. Cleavage of PARP was not detectable in untreated, empty vector and IDH1$^{wt}$ cells of U-251MG, U-343MG and LN-229 cells under normoxic conditions (Figure 4.26a). On the contrary, cleavage of PARP was slightly increased in the investigated cell lines in hypoxia (Figure 4.26b). Furthermore, untreated, empty vector and IDH1$^{wt}$ cells exhibited similar proteolytic cleavage

of PARP under normoxia and hypoxia, respectively (Figure 4.26). After irradiation at 5 Gy untreated, empty vector and IDH1$^{wt}$ cells showed an increased induction of apoptosis in the investigated cell lines under normoxic conditions. In hypoxia, irradiation induced an elevated induction of apoptosis in the untreated, empty vector and IDH1$^{wt}$ cells of U-251MG and U-343MG cells, whereas in LN-229 cells a comparable cleavage of PARP was detected before and after irradiation at 5 Gy. In addition, a slightly increased apoptosis was observed in the non-irradiated IDH1$^{R132H}$-expressing cells compared to the particular IDH1$^{wt}$ cells of the indicated cell lines under normoxia and hypoxia, respectively (Figure 4.26). After irradiation with 5 Gy, gene expression of IDH1$^{R132H}$ clearly increased the radiation-induced apoptosis in comparison to the untreated, empty vector and IDH1$^{wt}$ cells of U-251MG, U-343MG and LN-229 glioma cell lines under normoxic and hypoxic conditions (Figure 4.26).
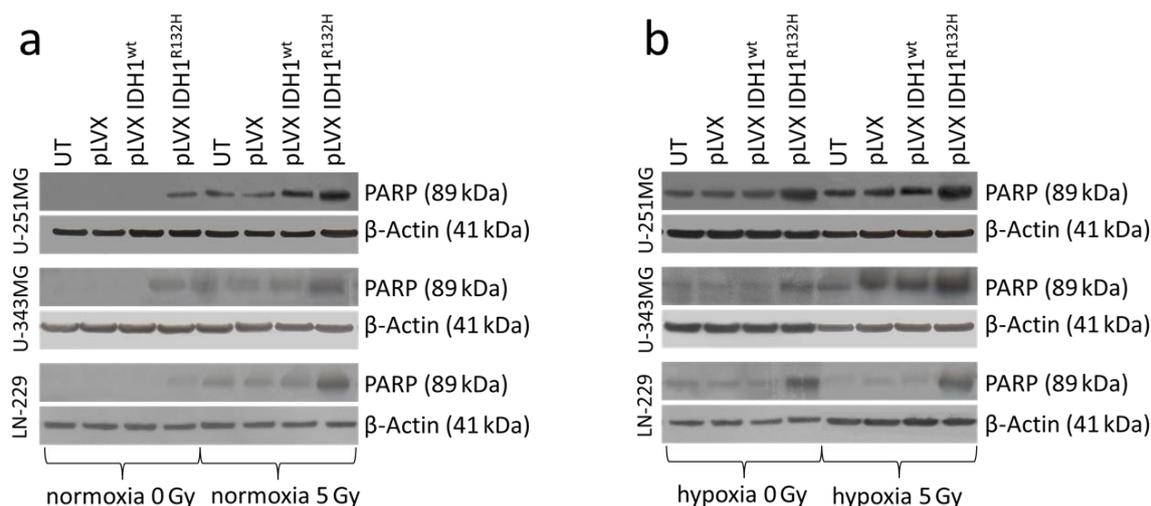


**Figure 4.26. Effect of IDH1$^{R132H}$ gene expression on the induction of apoptosis in glioma cells.** Representative Western blot analyses of cleaved PARP (89 kDa) in U-251MG, U-343MG and LN-229 cells before and after irradiation at 5 Gy under normoxia (21 % O$_2$) and hypoxia (<0.1 % O$_2$). For PARP analyses cleaved PARP antibody was used (detects cleaved PARP 89 kDa and does not recognize full length PARP). β-Actin served as loading control; n=3 independent experiments. UT: untreated, pLVX: cells stably transduced with empty vector, pLVX IDH1$^{wt}$: IDH1$^{wt}$-expressing cells, pLVX IDH1$^{R132H}$: IDH1$^{R132H}$-expressing cells.

In summary, it appears from the present data that IDH1$^{R132H}$ affected the cellular behavior of all three cell lines by slightly decreasing viability and cell proliferation. In addition, gene expression of IDH1$^{R132H}$ caused differences in growth properties in 3D spheroid culture, significantly reduced the cell migration in 2D and 3D spheroid culture and increased the cell stiffness of the investigated glioma cells. Furthermore, gene expression of IDH1$^{R132H}$ changed the response to radiation which resulted in an increase of radiosensitivity, an accumulation of residual γH2AX foci and an elevated induction of apoptosis. Furthermore, the effect of IDH1$^{R132H}$ on the cellular behavior and the radiosensitivity was comparable in both normoxic and hypoxic conditions.

## 4.4 Effect of IDH1[R132H] expression on transcriptional activity of HIF-1α in U-251MG, U-343MG and LN-229 glioma cells in normoxia and hypoxia

The influence of mutated IDH1 on the HIF-1α pathway is still controversially discussed in the literature. On the one hand, some authors have reported that gene expression of IDH1[R132H] increases the level of the subunit HIF-1α. On the other hand, contradictory results have been published demonstrating no influence of IDH1[R132H] on HIF-1α or even a reduction of the HIF-1α activity (Zhao et al., 2009; Xu et al., 2011; Chowdhury et al., 2011; Koivunen et al., 2012). Thus, the effect of IDH1[R132H] on the gene expression of HIF-1α and its target gene *CA9* was investigated in stably transduced U-251MG, U-343MG and LN-229 cells under normoxic and hypoxic conditions.

### 4.4.1 Effect of IDH1[R132H] on *HIF-1α* and *CA9* mRNA expression

The qPCR experiments revealed that neither treatment with the empty vector nor the gene expression of IDH1[wt] or IDH1[R132H] induced a significant alteration of *HIF-1α* mRNA level compared to respective untreated cells under normoxia and hypoxia in all three cell lines (Figure 4.27).
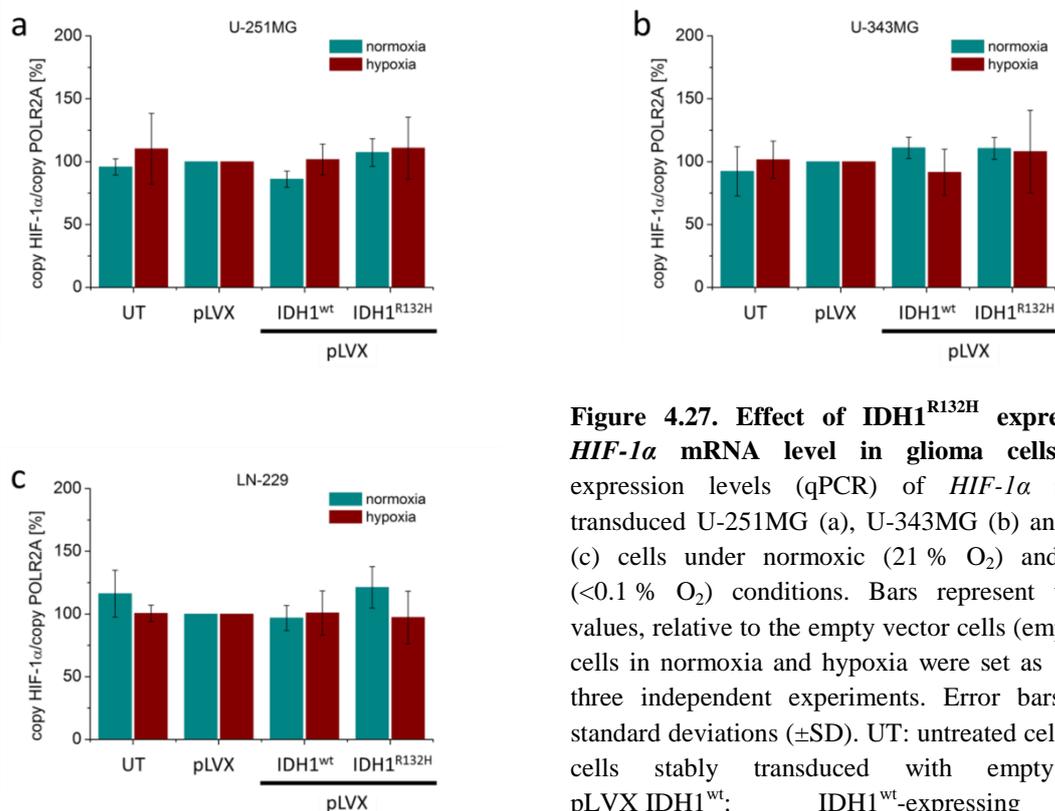


**Figure 4.27. Effect of IDH1[R132H] expression on *HIF-1α* mRNA level in glioma cells.** mRNA expression levels (qPCR) of *HIF-1α* in stably transduced U-251MG (a), U-343MG (b) and LN-229 (c) cells under normoxic (21 % O$_2$) and hypoxic (<0.1 % O$_2$) conditions. Bars represent the mean values, relative to the empty vector cells (empty vector cells in normoxia and hypoxia were set as 100 %) of three independent experiments. Error bars indicate standard deviations (±SD). UT: untreated cells, pLVX: cells stably transduced with empty vector, pLVX IDH1[wt]: IDH1[wt]-expressing cells, pLVX IDH1[R132H]: IDH1[R132H]-expressing cells.

In addition, HIF-1 activity was assessed by monitoring the gene expression of HIF-1α target gene *CA9* (Figure 4.28). Treatment with the empty vector or gene expression of IDH1[wt] had no effect on *CA9* mRNA level compared to the untreated cells of the respective cell line. However, IDH1[R132H] affected *CA9* gene expression in a cell line-specific fashion. In U-251MG cells, expression of IDH1[R132H] caused an increase of *CA9* mRNA level by 2.0-fold ($p < 0.01$) in normoxia and 1.5-fold ($p < 0.01$) in hypoxia compared to the respective empty vector cells (Figure 4.28a). Furthermore, U-343MG cells displayed an almost 1.9-fold ($p < 0.01$) and 1.3-fold ($p < 0.01$) increase of *CA9* mRNA expression compared to the empty vector cells under normoxic and hypoxic conditions, respectively (Figure 4.28b). In contrast, in LN-229 cells IDH1[R132H] induced a reduction of *CA9* mRNA level by 80 % ± 8.2 ($p < 0.01$) and 71.6 % ± 8.2 ($p < 0.01$) in comparison to the empty vector cells under normoxic and hypoxic condition, respectively (Figure 4.28c).
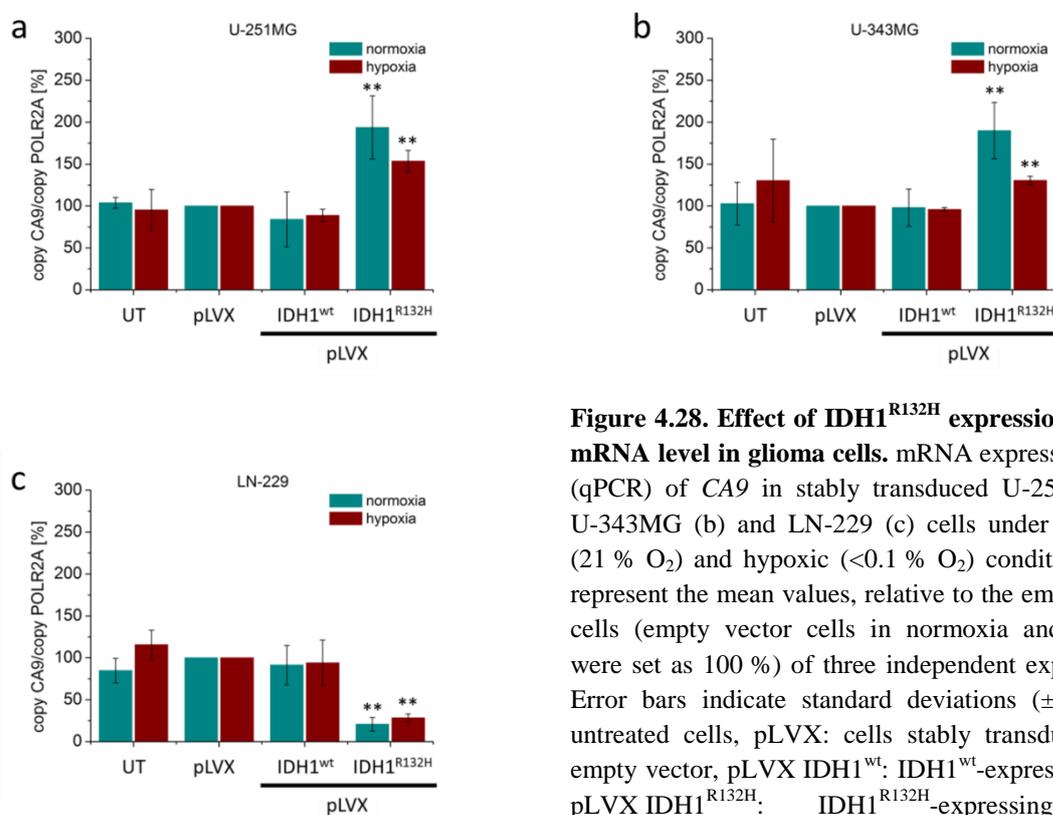


**Figure 4.28. Effect of IDH1[R132H] expression on *CA9* mRNA level in glioma cells.** mRNA expression levels (qPCR) of *CA9* in stably transduced U-251MG (a), U-343MG (b) and LN-229 (c) cells under normoxic (21 % $O_2$) and hypoxic (<0.1 % $O_2$) conditions. Bars represent the mean values, relative to the empty vector cells (empty vector cells in normoxia and hypoxia were set as 100 %) of three independent experiments. Error bars indicate standard deviations (±SD). UT: untreated cells, pLVX: cells stably transduced with empty vector, pLVX IDH1[wt]: IDH1[wt]-expressing cells, pLVX IDH1[R132H]: IDH1[R132H]-expressing cells; **$p < 0.01$ (compared to the empty vector cells in normoxia or hypoxia).

## 4.4.2 Effect of IDH1[R132H] on HIF-1α and CAIX protein expression

Under normoxia, untreated, empty vector and IDH1[wt] or IDH1[R132H] cells showed a low level of HIF-1α and CAIX protein under normoxia in U-251MG, U-343MG and LN-229 cells (Figure 4.29). After 24 h under hypoxic conditions, untreated, empty vector and IDH1[wt] or IDH1[R132H] cells exhibited an increased accumulation of HIF-1α protein and an induction of CAIX protein level (Figure 4.29).

However, treatment with the empty vector or gene expression of IDH1[wt] had no effect on HIF-1α and CAIX protein level compared to the untreated controls in the investigated glioma cell lines. In U-251MG and U-343MG cells an increase of HIF-1α and CAIX protein level in the IDH1[R132H]-expressing cells was observed under normoxic and hypoxic conditions (Figure 4.29a and Figure 4.29b). On the contrary, a reduction of HIF-1α and CAIX protein was detected under normoxic and hypoxic conditions in IDH1[R132H]-positive LN-229 cells (Figure 4.29c). In addition, immunohistochemical staining was applied to analyze the IDH1[R132H], HIF-1α and CAIX protein expression patterns in stably transduced U-251MG, U-343MG and LN-229 cells (appendix Figure 8.3, Figure 8.4 and Figure 8.5). In accordance to the qPCR and Western Blot analyses, immunohistochemical staining confirmed the HIF-1α accumulation and CAIX induction in U-251MG and U-343MG cells and the reduction of HIF-1α and CAIX protein in LN-229 cells (appendix Figure 8.3, Figure 8.4 and Figure 8.5).
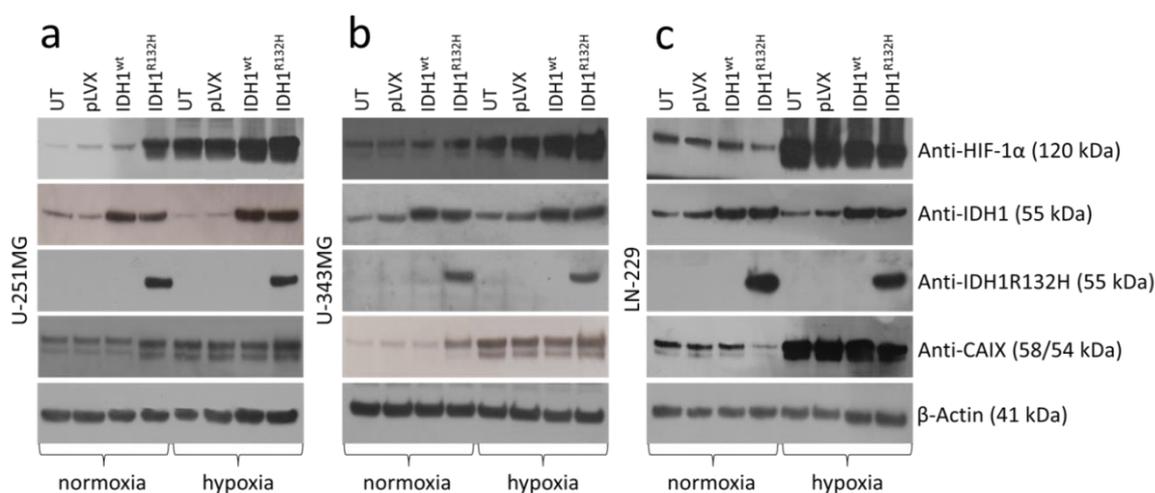


**Figure 4.29. Effect of IDH1[R132H] gene expression on HIF-1α and CAIX protein levels.** Representative Western blots for HIF-1α and CAIX protein expression in stably transduced U-251MG (a), U-343MG (b) and LN-229 (c) cells under normoxic (21 % O₂) and hypoxic (<0.1 % O₂) conditions. β-Actin served as loading control; n=3 independent experiments. UT: untreated cells, pLVX: cells stably transduced with empty vector, pLVX IDH1[wt]: IDH1[wt]-expressing cells, pLVX IDH1[R132H]: IDH1[R132H]-expressing cells.

In summary, the effect of IDH1[R132H] gene expression on HIF-1α activity and induction of its target gene *CA9* differs in a cell-line dependent fashion. In U-251MG and U-343MG gene expression of IDH1[R132H] induced an elevated HIF-1α accumulation and *CA9* gene expression, whereas in LN-229 cells, IDH1[R132H] caused a reduced HIF-1α protein level and *CA9* gene expression.

# 5 DISCUSSION

Malignant gliomas are the most common type of primary brain tumors, with an annual incidence of 5/100,000 individuals (Louis et al., 2007; Wen and Kesari, 2008). These tumors are highly aggressive and have a dismal prognosis under the current standard treatment regime, consisting of maximal surgical resection, whenever possible, followed by radiation and chemotherapy (Stupp et al., 2005; Stupp et al., 2010; Stupp et al., 2014). For patients with high-grade gliomas the median survival time ranges from 15 months to three years (Ohgaki and Kleihues, 2013; Chen et al., 2012; Westermark, 2012; Van Gool et al., 2009; Jovčevska et al., 2013). The heterogeneity of these types of tumors with respect to clinical presentation, pathology, genetic profile and the poor response to treatment, make high-grade gliomas one of the most challenging malignancies in clinical oncology (Jovčevska et al., 2013). Based on this heterogeneity and the various mutual signatures the chances for a universal treatment are reduced, particularly due to the fact that subtypes have different treatment responses, which therefore may result in both over- or undertreatment of these tumors (van den Bent, 2010).

On a molecular level, malignant gliomas are characterized by a variety of genetic and epigenetic alterations (Ohgaki and Kleihues, 2013). In high-grade gliomas the molecular markers HIF-1α and *IDH1R132H* have been identified as prognostic markers with major roles in tumorigenesis and the response to radiotherapy. In addition to their benefit in diagnosis, investigation of HIF-1α and *IDH1R132H* supports the understanding of tumorigenesis and resistance to therapy of malignant gliomas. Furthermore, both markers are attractive targets for novel therapeutic approaches to improve the response to standard treatment of high-grade glioma such as radiotherapy.

## 5.1 HIF-1α targeting via siRNA or CTM

Malignant gliomas exhibit intratumoral hypoxia, which has been linked to poor response to radio- or chemotherapy and further induces gene expression of HIF-1α, which is one of the main mediators of hypoxic response (Collingridge et al., 1999; Nordsmark et al., 2005; Brennan et al., 2006; Semenza, 2013). Additionally, in malignant gliomas, elevated levels of HIF-lα protein correlate with poor patient outcome, since it promotes tumor growth, angiogenesis and disease progression (Birner et al., 2001; Blazek et al., 2007; Eckerich et al., 2007; Kaynar et al., 2008; Reszec et al., 2013).

In the present study, the effects of hypoxia on HIF-1 and *CA9*/CAIX gene and protein expression was initially investigated by qPCR and Western blot analyses in U-251MG and U-343MG malignant glioma cells. It was observed that *HIF-1α* mRNA expression levels were comparable under normoxic and hypoxic conditions irrespective of the investigated cell line (Figure 4.1). Furthermore, both cell lines displayed weak HIF-1α protein levels under normoxia and an increase of HIF-1α protein levels,

*CA9* mRNA levels and CAIX protein levels under hypoxia (Figure 4.1 and Figure 4.2). In a previous study, using the glioma cell line U-87MG, the usefulness of HIF-1α as an endogenous marker of tumor hypoxia and the associated radioresistance of human tumor cells has already been described (Vordermark and Brown, 2003a). In a subsequent study by these authors, CAIX was also found to be a suitable marker of current or previous chronic hypoxia and was associated with radioresistance of HT 1080 human fibrosarcoma cells, proposing that the amount of CAIX-positive cells in a tumor cell suspension may be related to the radiosensitivity of this tumor *in vivo* (Vordermark et al., 2005). However, little is known about the impact of HIF-1α inhibition on radioresistance of malignant gliomas.

In the present work, inhibition of the HIF-1 pathway was performed by two alternative strategies, namely treatment with *HIF-1α* siRNA or exposure to CTM. The effect of these approaches on the gene expression of HIF-1α and its target gene *CA9* was investigated by qPCR and Western blot analyses. On the one hand, targeting *HIF-1α* via specific siRNA effectively reduced the mRNA as well as the protein expression of HIF-1α and its target *CA9*/CAIX in U-251MG and U-343MG cells in normoxia and hypoxia, respectively (Figure 4.3 and Figure 4.4).

On the other hand, the small molecule CTM was used to inhibit the transcriptional activity of HIF-1α. CTM is a metabolite from the fungal species *Chaetomium*, that has been reported to disrupt the binding of HIF-1α to the co-activator p300, which is responsible for the formation of the transcriptional active HIF-1α/p300 complex (Kung et al., 2004). Therefore, CTM impairs the gene expression of HIF-1α target genes, such as *CA9*, rather than influencing the gene or protein expression levels of HIF-1α. In the present thesis, CTM did not influence the expression of *HIF-1α* mRNA in U-251MG cells under normoxic and hypoxic conditions (Figure 4.3). In addition, exposure to CTM slightly increased the HIF-1α protein level but attenuated the HIF-1α-induced expression of *CA9* mRNA and CAIX protein in U-251MG cells in normoxia and hypoxia, respectively (Figure 4.4 and Figure 4.5).

One possible explanation for the slight increase of HIF-1α protein expression could be an auto regulatory feedback loop of HIF-1α, caused by the CTM-mediated inhibition of the transcriptional activity of HIF-1α. In this way, the U-251MG cells probably compensate the decreased transcriptional activity by an increased stabilization of HIF-1α protein. Moreover, a further explanation could be that CTM also inhibits the interaction of HIF-1α and VHL. In this case an undesirable side effect of CMT may be the inhibition of the proteasomal degradation of HIF-1α protein, leading to increased HIF-1α protein levels. On the contrary, in U-343MG cells exposure to CTM reduced the mRNA and protein expression of both HIF-1α and its target *CA9*/CAIX under normoxic and hypoxic conditions, respectively (Figure 4.3, Figure 4.4 and Figure 4.5). One reason for this behavior may be that the applied dose of CTM caused cytotoxic side effects in the lower grade III glioma cells U-343MG. The

different effects of CTM in U-251MG and U-343MG cells are assumed to be caused by their different origin. U-343MG cells originate from an anaplastic astrocytoma (grade III) and U-251MG cells were derived from a *de novo* glioblastoma (grade IV) (Ishii et al., 1999; Kleihues et al., 2002; Louis et al., 2007). Hence, both investigated glioma cell lines differ in their genetic status and regulation of different pathways and consequently in their response to treatment, including exposure to CTM. Additionally, CTM is a small molecule and the target specificity of small molecules is debatable and there might be another unknown mechanism of CTM play a role. Despite this, the results were in accordance with preliminary studies and illustrate that monitoring *CA9* mRNA and CAIX protein expression can be used as suitable marker of hypoxia and further to verify the transcriptional activity of HIF-1 (Vordermark and Brown, 2003a; Vordermark and Brown, 2003b; Vordermark et al., 2005; Kessler et al., 2010).

In this thesis, inhibition of HIF-1α by siRNA or CTM in U-251MG and U-343MG cells resulted in a reduced plating efficiency compared to cells treated with the control siRNA or DMSO under normoxic and hypoxic conditions, respectively (Figure 4.6). In accordance with these findings it has already been reported that inhibition of HIF-1α decreases tumor growth in malignant gliomas (Jensen et al., 2006). Furthermore, Dai and colleagues reported an oxygen-independent cytotoxicity induced by HIF-1α inhibition in U-87MG glioblastoma cells (Dai et al., 2003).

In the literature, a hypoxia-associated resistance to radiotherapy and chemotherapy has been described for various tumor entities, including malignant gliomas (Collingridge et al., 1999; Vaupel et al., 2002; Nordsmark et al., 2005; Anderson et al., 2014). Additionally, it has been proposed that HIF-1α gene expression is a significant prognostic indicator in glial brain tumors treated with radiotherapy (Birner et al., 2001; Korkolopoulou et al., 2004). In the present work, inhibition of HIF-1α by siRNA or by CTM under hypoxic conditions resulted in a significantly enhanced radiosensitivity of the human glioma cells (Figure 4.7). In addition, PARP cleavage was analyzed via Western Blot analyses. The proteolytic cleavage of PARP, is an early biochemical event that accompanies apoptosis in many cell types (Gu et al., 1995; Mullen, 2004). Western blot analyses of the cleavage of PARP demonstrated that inhibition of HIF-1α via siRNA or CTM induced apoptosis in U-251MG and U-343MG cells under hypoxic conditions (Figure 4.5). In previous experiments by Staab and coworkers, HIF-1α inhibition by CTM also effectively reduced the hypoxia-dependent transcription of the HIF-1α target gene *CA9* and sensitized hypoxic HT 1080 human fibrosarcoma cells to radiation under *in vitro* conditions (Staab et al., 2007). In addition to the increased radiosensitivity, silencing of *HIF-1α* by specific siRNA has also been shown to increase the sensitivity of glioma cells to the chemotherapeutic agents doxorubicin and etoposide (Chen et al., 2009).

Furthermore, in accordance with the induction of apoptosis in U-251MG and U-343MG cells observed in the present study, Dai and colleagues reported a p53-independent apoptosis induced by HIF-1α

inhibition in U-87MG glioblastoma cells (Dai et al., 2003). In addition, various studies showed that silencing of *HIF-1α* attenuates growth and inhibits hypoxia-mediated cell migration and invasion of *in vitro* and *in vivo* malignant glioma models (Gillespie et al., 2007; Fujiwara et al., 2007; Ali et al., 2009). In agreement with the increased radiosensitivity and the induced apoptosis of U-251MG and U-343MG cells under hypoxic conditions, it has previously been demonstrated in prostate carcinoma cells that the impact of HIF-1α inhibitor PX-478 on radiosensitivity in normoxia was less dramatic than under hypoxic conditions (Palayoor et al., 2008). Further studies have also reported that HIF inhibitors are more effective in attenuation of HIF-dependent transcriptional activity under hypoxic conditions as under normoxic conditions (Rapisarda et al., 2002; Zhong et al., 2004).

Based on the regulation of the HIF-1 pathway, these observations are not surprising. In normoxia, HIF-1α protein is rapidly degraded by the proteasome (Wang et al., 1995; Salceda and Caro, 1997). In contrast, under hypoxic conditions HIF-1α is stabilized and translocates from the cytoplasm into the nucleus where it interacts with transcriptional coactivators such as CBP/p300 and induces the gene expression of its transcriptional targets via binding to their HREs (Kallio et al., 1997; Huang et al., 1996; Lando et al., 2002) (Figure 1.3). Hence, the adaption of cancer cells to hypoxia is primarily dependent on the HIF-1α activity, suggesting that cancer cells are more sensitive to HIF-1α inhibition at low oxygen concentrations.

Nevertheless, tumor cells have also been shown to upregulate HIF-1α protein levels due to various factors, including elevated oxidative stress, metabolic alterations, mutations (i.e. mutations in the *IDH1/2* genes) and anti-cancer therapies such as photodynamic therapy, hyperthermia or doxorubicin chemotherapy (Pialoux et al., 2009; Isaacs et al., 2005; Selak et al., 2005; Mitra et al., 2006; Moon et al., 2010; Cao et al., 2013; Zhao et al., 2009; Xu et al., 2011; Koivunen et al., 2012). In this context, HIF-1α has been shown to be involved in the induction of autophagy due to HIF-1α-dependent gene expression of BNIP3 and BNIP3L, which promoted cell survival of U-87MG and T98G glioma cells (Hu et al., 2012). In agreement with these findings, it has also been that the hypoxic microenvironment contributes to cell survival rather than cell death by inducing autophagy in various normal as well as cancer cells (e.g. CCL39 hamster fibroblasts, LS174 colon carcinoma cells, PC3 prostate carcinoma cells) (Bellot et al., 2009). In this study, Bellot and coworkers also demonstrated that inhibition of autophagy, through a combined silencing of the two HIF-1α targets BNIP3 and BNIP3L, increased cell death under hypoxic conditions. Hence, it was suggested that the HIF-1α induced autophagy is a survival mechanism that promotes tumor progression (Papandreou et al., 2005; Pouysségur et al., 2006; Bellot et al., 2009; Zhang et al., 2008). Therefore, inhibition of HIF-1α by siRNA or CTM may suppress the hypoxia-mediated autophagy and subsequently increases radiosensitivity and induces apoptosis in U-251MG and U-343MG cells. Further investigations are necessary to analyze if HIF-1α induces autophagy and if inhibition of HIF-1α may attenuate this protective mechanism in U-251MG

and U-343MG cells. Taken together, this is the first work showing that inhibition of HIF-1a by siRNA or CTM under hypoxic conditions resulted in a significantly increased radiosensitivity of human malignant glioma cells. The present thesis and several other studies supported the fact that HIF-1α is an attractive target to overcome hypoxia-related radioresistance of various tumors entities (Moeller et al., 2005; Yeo et al., 2003; Staab et al., 2007; Bache et al., 2008; Kessler et al., 2010).

Although inhibition of HIF-1α under hypoxia increased radiosensitivity of U-251MG and U-343MG cells, the results of the present study showed that siRNA and CTM had different impacts on the radiation sensitivity of glioma cells under normoxia (Figure 4.7). On the one hand, *HIF-1α* siRNA slightly reduced the cytotoxic effect of radiation in U-251MG cells, whereas in U-343MG cells, siRNA increased the effects of radiation. On the other hand treatment with CTM increased the effect of radiation in U-251MG cells, whereas in U-343MG cells, CTM did not affect the response to irradiation (Figure 4.7). In accordance with these observations, reduction of the *HIF-1α* gene expression via siRNA did not affect the normoxic gene expression of the large fragment of PARP in U-251MG cells, whereas apoptosis was induced in U 343MG cells. On the contrary, treatment with CTM resulted in an apoptotic response under normoxic conditions in U-251MG cells, whereas in U-343MG cells exposure to CTM had no effect on PARP cleavage under normoxic conditions. In accordance with these findings it has already been reported that the basal HIF-1α levels under normoxic conditions did not predict the radiosensitivity of different human tumor cell lines (H1339, EPLC-272H, A549, SAS, XF354, FaDu, BHY and CX- tumor cell lines) under normoxia (Schilling et al., 2012).

One explanation for these different responses to treatment might be the aforementioned different origins of both cell lines. Thus, different genes involved in cellular pathways regulating proliferation, apoptosis, energy metabolism and DNA repair, could carry mutations or deletions. For example, both cell lines differ in their genetic status of *TP53* and consequently in their disease aggressiveness as well as response to treatment. U-343MG cells exhibit the wild type *TP53* gene, whereas U-251MG carry mutated *TP53* (Ishii et al., 1999).

The tumor suppressor protein p53 plays a major role in the response to damaged or abnormally structured DNA by controlling cell cycle checkpoints (Pellegata et al., 1996; Agarwal et al., 1995). Several studies have already demonstrated that p53 is responsible for cell cycle arrest and regulation of DNA repair or apoptosis when the DNA damage is too extensive. Hence, the ability to respond to HIF-1α inhibition and radiation may differ in U-251MG and U-343MG cells.

Another explanation for different responses to HIF-1α inhibition and radiation could be that *HIF-1α*-specific siRNA and CTM have different modes of action, since siRNA reduces the gene expression of *HIF-1α*, whereas CTM inhibits its transcriptional activity. Furthermore, the function of CTM is yet not fully understood. CTM is a member of the epidithiodiketopiperazine (ETP) family.

Previous studies have shown that ETPs react with p300 and cause zinc ion ejection. Additionally, the results of Cook and coworkers suggest that ETPs also interact with other zinc ion binding proteins (Cook et al., 2009). Hence, it is possible that ETPs like CTM can act by more than one mechanism in cells. Based on this hypothesis it is likely that CTM interacts with other proteins (excluding HIF-1α), which are also relevant for radiosensitivity.

In the literature various different strategies for inhibiting the HIF-1 pathway are described. In these studies, small anticancer molecules have been shown to inhibit HIF activity through different modes of action, such as reducing *HIF-1α* mRNA expression or HIF-1α protein translation or affecting HIF-1α protein degradation and stabilization, as well as HIF-1α-HIF-1β dimerization or HIF-1α DNA binding activity and interactions with other proteins (reviewed in Semenza, 2012 and Xia et al., 2012). Based on the promising strategy of indirectly inhibiting HIF-1α, several of these anticancer agents have made it to clinical trials and a few have been FDA-approved in the US for cancer treatment, such as camptothecins, bortezomib, romidepsin, temsirolimus, perifosine, 2-Methoxyestradiol, echinomycin and ansamycins (Geldanamycin, 17-AAG, 17-DMAG) (Burroughs et al., 2013).

In accordance to the present study, where siRNA and CTM showed different impacts on radiosensitivity of glioma cells under normoxia, it has been reported that the complexity of cancer metabolism, regulation and progression results in different effects of anticancer drugs (Xia et al., 2012; Burroughs et al., 2013). The very complex nature of cancer makes it difficult to separate the desired effects aimed at one pathway from another one or can cause unexpected counter-productive events. However, the complexity of cancer can also act in a synergistic manner by up- or down-regulating multiple pathways and/or targets resulting in similar net results during the design and realization of innovative therapeutics (Kola and Landis, 2004; Burroughs et al., 2013). Cancer treatment is one of the most active areas in medical research. However, it is also characterized by one of the highest attrition rates, which is caused by several factors, including the hypoxic and acidic tumor microenvironment, validity and accuracy of *in vitro* preclinical models, drug absorption and distribution, tumor and drug metabolism, drug excretion, organ toxicities, appropriate drug delivery *in vivo* and translation to the clinic (Adams, 2012; Burroughs et al., 2013; Cook et al., 2014). Thus, even though HIF-1α was discovered in 1991 and since then many studies and clinical trials have been focused on targeting this marker no specific inhibitor of HIF-1α has been brought to market up to now. However, the present study clearly demonstrates that targeting HIF-1α is a challenging but also promising strategy to reduce cancer cell survival and to increase the response of malignant gliomas to radiotherapy. Based on the complex role of HIF-1α in aggressiveness and progression of malignant gliomas, it appears reasonable to further focus on HIF-1α target genes, such as *CA9*, to prevent undesired effects in the treatment of tumors.

## 5.2 Targeting *IDH1* via siRNA

In gliomas, *IDH1* mutation (*IDH1R132H*) has been found to be a frequent event at an early stage of tumorigenesis and seems to dictate a particular path for oncogenic progression of these tumors. Mutation of the *IDH1* gene occurs in 70 % to 80 % of WHO grade II and III astrocytic and oligodendroglial tumors, as well as in the majority of WHO grade IV secondary glioblastomas that generally evolve over the time from these lower grade tumors, but not in primary glioblastomas which clinically develop *de novo* (Parsons et al., 2008; Yan et al., 2009; Hartmann et al., 2009; Ichimura et al., 2009; Juratli et al., 2012a). In gliomas of all grades the presence of *IDH1* mutation is associated with better clinical outcome after standard treatment comprising surgery, radiotherapy and chemotherapy (Parsons et al., 2008; Yan et al., 2009; Hartmann et al., 2009; Ichimura et al., 2009). The mutated IDH1 enzyme IDH1R132H shows a strongly reduced enzyme activity in catalyzing the reversible decarboxylation of isocitrate to α-KG (Zhao et al., 2009; Dang et al., 2010; Gross et al., 2010; Ward et al., 2010). On the other hand, IDH1R132H exhibits a new enzyme function leading to D-2-HG accumulation and lowering α-KG as well as NADPH levels.

In the present work, reduction of the gene expression of *IDH1* was performed by treatment with *IDH1*-specific siRNA. The effect of the *IDH1*-specific siRNA on the gene expression of IDH1 was investigated by qPCR and Western blot analyses. Furthermore, the effect of decreased IDH1 enzyme activity, via siRNA-induced reduction of the *IDH1* gene expression on the plating efficiency, sensitivity to radiation and cleavage of PARP was analyzed in glioma cells with different degrees of malignancy (U-251MG, grade IV; U-343MG, grade III and LN-229, grade IV) under normoxic and hypoxic conditions.

In this work, a reduction of *IDH1* mRNA by siRNA of up to 79 % in U-251MG, 97 % in U-343MG and 86 % in LN-229 cells was observed under normoxic and hypoxic conditions, respectively (Figure 4.8). In addition, *IDH1*-specific siRNA clearly decreased the level of IDH1 protein via gene silencing in malignant glioma cell lines U-251MG, U-343MG and LN-229 in normoxia and hypoxia (Figure 4.9). The reduction of the *IDH1* gene expression via siRNA did not significantly affect the plating efficiency in glioblastoma grade IV U-251MG and LN-229 cells under normoxic and hypoxic conditions, respectively (Figure 4.10). Furthermore, in grade III U-343MG cells a slight reduction of the plating efficiency by 3.2 % in normoxia and 4.9 % in hypoxia was observed (Figure 4.10). In a previous study, inhibition of *IDH1* with shRNA decreased the IDH1 gene expression by 90 % in HOG oligodendroglioma cells and induced a reduction of the $NADP^+$-dependent IDH activity by nearly one half, indicating that IDH1 accounts for approximately half of the cellular $NADP^+$-dependent IDH activity (Jin et al., 2011). Moreover, it has been suggested that the remaining activity in *IDH1* knockdown cells may be supplied by the residual IDH1 enzyme and by IDH2 (Jin et al., 2011).

Furthermore, in the present thesis gene silencing of *IDH1* via siRNA did not affect radiosensitivity or induce PARP cleavage in glioblastoma grade IV U-251MG and LN-229 cells under normoxic and hypoxic conditions, respectively (Figure 4.11 and Figure 4.9). In contrast, a reduction of the *IDH1* gene expression using siRNA increased the radiosensitivity and induction of apoptosis of U-343MG cells (glioma grade III) under hypoxic conditions, whereas in normoxia no impact on the radiosensitivity or cleavage of PARP was observed (Figure 4.11 and Figure 4.9).

These results suggest that the residual IDH1 enzyme and IDH2 are sufficient to compensate the reduced *IDH1* gene expression via siRNA in U-251MG and LN-229 cells (residual IDH1 enzyme in U-251MG: 21 %, residual IDH1 enzyme in LN-229: 14 %) (Figure 4.8). On the contrary, the enhanced radiosensitivity and induction of apoptosis in U-343MG cells under hypoxic conditions is possibly caused by a combination of different factors, including lower amounts of residual IDH1 enzyme (residual IDH1 enzyme in U-343MG: 3 %), stressful hypoxic conditions as well as the lower grade of malignancy and the genetic status of U-343MG cells (Figure 4.8). Hence, for example, the gene expression of wild type p53 renders U-343MG cells more sensitive to radiation and induced apoptosis.

In addition, hypoxia promotes the IDH-dependent reverse flux, i.e. the carboxylation of α-KG back to isocitrate, which is required for *de novo* lipogenesis to support cell growth and viability (Metallo et al., 2011; Wise et al., 2011; Mullen et al., 2011; Filipp et al., 2012). By using stable isotopic tracers of glutamine ($[1-^{13}C]$ glutamine) in various cell lines (e.g. A549, MDA-MB-231 and HCT116), Metallo and coworkers demonstrated a significant and robust decrease of the reductive carboxylation when *IDH1* mRNA was targeted using shRNA (Metallo et al., 2011). In contrast, no significant change of this reductive flux was observed when IDH2 mRNA was targeted. In this study it was also shown that oxygen concentrations play a critical role in regulating the carbon utilization for production of acetyl coenzyme A (AcCoA) which supports lipid synthesis in mammalian cells. Furthermore, the results revealed that VHL-deficient renal cell lines preferentially utilize the reductive glutamine metabolism for lipid biosynthesis even in normoxia.

Therefore, in the present work the remaining enzyme activity in *IDH1* siRNA treated U-343MG cells may not be sufficient to affect the reductive carboxylation of α-KG and thus U-343MG cells are more vulnerable by the altered metabolic flux of α-KG. This hypothesis is supported by the observations made for non-irradiated U-343MG cells, where reduction of the *IDH1* gene expression by siRNA induced an induction of apoptosis under hypoxic conditions.

Furthermore, the IDH enzymes appear to play a crucial role in cellular protection as well as the response to oxidative and energetic stress through NADPH, which is required to regenerate the antioxidant GSH (Lee et al., 2002; Kim et al., 2012). In addition, α-KG itself functions as an antioxidant (Lee et al., 2002; Mailloux et al., 2007). Moreover, a previous study documented an

increased gene expression of IDH enzymes and termination of proliferation when an energetic challenge was induced by substituting galactose for glucose in HT-22 neurons (Grelli et al., 2013). Thus, it appears to be useful to quantitatively analyze isocitrate and α-KG to determine the remaining IDH1 activity in *IDH1* siRNA treated cells.

Taken together, the current findings from siRNA experiments indicate that it seems unlikely that dominant negative activity is a major consequence of the *IDH1* mutations in cancer. Different other functional studies demonstrated that IDH mutations gain the neomorphic activity to reduce α-KG to D-2-HG rather than a dominant negative inhibition of wild type IDH1 (Dang et al., 2010; Gross et al., 2010; Ward et al., 2010; Jin et al., 2011). In other words, mutations targeting *IDH1* result in simultaneous loss of the normal catalytic activity to produce α-KG and gain of a new function the production of D-2-HG (Yang et al., 2012). Further, both effects seem to play a role in the improved prognosis and the prolonged overall survival of patients with malignant gliomas (Metellus et al., 2010; Leu et al., 2013; Gorovets et al., 2012; Sabha et al., 2014). Gene silencing of *IDH1* via siRNA only mimics the loss of function, but it is not the right tool to imitate the gain of function of an IDH1 mutation. This hypothesis may partially explain why reduction of *IDH1* gene expression did not increase the radiosensitivity or induce apoptosis in U-251MG and LN-229 cells under normoxic and hypoxic conditions. In agreement with this assumption it has been reported that glioma cells expressing IDH1$^{R132H}$ share metabolic profile features with cells treated with D-2-HG but not with cells in which IDH1 wild type gene expression was inhibited (Reitman et al., 2011). Hence, further experiments addressing the gene expression of IDH1$^{R132H}$ in glioma cells were carried out to mimic the gain-of-function activity that catalyzes the conversion of α-KG into D-2-HG in a manner that leads to D-2-HG accumulation and consumption of α-KG as well as NADPH.

## 5.3 Influence of IDH1$^{R132H}$ expression on cellular behavior and response to radiation

Up to now, research about the influence of *IDH1* mutation on cellular behavior and response to radiation of malignant gliomas is very limited. Furthermore, especially in clinical studies it is difficult to specifically correlate the better prognosis and prolonged overall survival of patients with *IDH* mutant gliomas with the cellular behavior itself or the improved response to therapy treatment, since patients with malignant gliomas receive standard therapy treatment in any case. Thus, it is still unclear if the known positive effects of *IDH* mutations on prognosis and overall survival of patients originates from a less aggressive phenotype or is directly linked to an increased sensitivity to radiotherapy and/or chemotherapy.

In the present work, the effect of IDH1 mutant protein on the biological behavior was evaluated by analyzing the viability and proliferation in 2D culture, plating efficiency and growth characteristics in

3D spheroid culture, cell migration in 2D or in 3D spheroid-based culture as well as cellular stiffness in malignant glioma cell lines overexpressing IDH1$^{R132H}$.

Therefore, IDH1$^{wt}$ and IDH1$^{R132H}$ constructs were generated and U-251MG, U-343MG and LN-229 stable cell lines with empty vector (pLVX) or gene expression of IDH1$^{wt}$ or IDH1$^{R132H}$ were established using puromycin selection post transduction. Characterization by qPCR and Western blot analysis revealed high levels of IDH1$^{wt}$ or IDH1$^{R132H}$ mRNA and protein in pLVX IDH1$^{wt}$ or pLVX IDH1$^{R132H}$ transduced U-251MG, U-343MG and LN-229 cells (Figure 4.12 and Figure 4.13). Additionally, immunofluorescence and immunohistochemical staining showed the diffuse cytoplasmic distribution of IDH1$^{wt}$ or IDH1$^{R132H}$ protein in the stable transduced cell lines (Figure 4.14, Figure 8.1 and Figure 8.2).

In the investigated glioma cells IDH1$^{R132H}$ gene expression slightly decreased viability between 2.6 % and 6.0 % as well as cell proliferation between 6.9 % and 11.9 % in 2D culture irrespective of the oxygen concentration (Figure 4.15 and Figure 4.16). Gene expression of IDH1$^{R132H}$ reduced the plating efficiency in the non-irradiated glioma cell lines between 8.8 % and 12.3 % under normoxic as well as between 16.6 % and 32.0 % under hypoxic conditions (Figure 4.21). In both environments, expression of the mutated IDH1 protein caused altered growth patterns in 3D spheroid culture of the investigated cells (Figure 4.17). IDH1$^{R132H}$ cells aggregated to more loose, uneven and irregular structures in 3D cultures, whereas untreated, empty vector and IDH1$^{wt}$ cells formed compact tumor spheroids (Kessler et al., 2015).

IDH enzymes play critical roles in a number of cellular processes, including glucose sensing, glutamine metabolism and lipogenesis (Ronnebaum et al., 2006; Metallo et al., 2011; Filipp et al., 2012). Mutated IDH enzymes lose their normal function and gain a new enzyme function catalyzing the NADPH-dependent reduction of α-KG to D-2-HG (Xu et al., 2004). Thereby, the profound influence of *IDH* mutations on the cellular metabolism and the interference with normal biosynthetic pathways may explain the observed effects on cell viability, proliferation in 2D and 3D spheroid culture and plating efficiency. Indeed, it has already been demonstrated that gene expression of IDH1$^{R132H}$ decreased the proliferation and migration of U-87MG cells in normoxia (Li et al., 2013b). Moreover, the data of the present work are consistent with a further study, where IDH1$^{R132H}$ overexpression in U-87MG glioma cells resulted in a decreased proliferation under normoxia and mice injected with U-87MG IDH1$^{R132H}$-expressing cells exhibited a prolonged survival compared to mice injected with U-87MG IDH1$^{wt}$-expressing cells (Bralten et al., 2011).

However, in the present work only slight effects on the viability, proliferation and plating efficiency were observed, indicating that IDH1$^{R132H}$-expressing cells compensate the altered flux of α-KG to D-2-HG (Figure 4.15, Figure 4.16 and Figure 4.21). In a study of Dang and colleagues it has been reported that gliomas carrying *IDH* mutations showed markedly elevated levels of D-2-HG, but levels

of other citric acid cycle metabolites, including α-KG, malate, fumarate, succinate and isocitrate, were not significantly altered (Dang et al., 2010). This suggests that *IDH* mutant gliomas maintain normal levels of essential cell metabolites even in case of an altered metabolic flux of α-KG (Dang et al., 2010). In a further study, metabolic profiling of human oligodendroglioma cell line HOG, which stably expresses IDH1$^{R132H}$ or IDH2$^{R172K}$, revealed that the *IDH* mutation caused widespread metabolic alterations in the level of amino acids and their derivatives as well as depletion of glutathione metabolites and metabolites of the citric acid cycle (Reitman et al., 2011). In accordance with these findings it has also been demonstrated that gene expression of mutant IDH1R132H in U-87MG cells or immortalized normal human astrocytes caused a significant drop in the concentrations of glutamate, lactate and phosphocholine as well as the expected elevation of D-2-HG levels (Izquierdo-Garcia et al., 2015). In addition, quantitative metabolome analyses also showed that *IDH1* mutation results in an activation of glutaminolysis in glioma (Ohka et al., 2014). Taken together, these findings suggest that *IDH* mutant gliomas compensate their altered flux of α-KG to unusually high amounts of D-2-HG by extensive metabolic changes. These metabolic alterations and the possible resulting depletion of metabolites may cause slight decreases in cell viability, proliferation and plating efficiency as well as changed growth patterns in 3D spheroid culture.

The altered growth patterns of IDH1$^{R132H}$-expressing cells in 3D spheroid culture may also have been induced by D-2-HG itself. α-KG and D-2-HG are structurally almost identical metabolites. Thus, D-2-HG competes with α-KG and thereby it inhibits various α-KG-dependent dioxygenases, including Jumonji C-(JmjC)-domain-containing proteins of histone demethylases and Ten-eleven translocation (TET) family members enzymes (Chowdhury et al., 2011; Xu et al., 2011). These enzymes are involved in a number of important cellular processes by hydroxylating target proteins while utilizing α-KG as a cosubstrate. In normal cells, JmjC histone demethylases and TET 5-methylcytosine hydroxylases mediate chromatin modifications in order to maintain cellular homeostasis. In *IDH* mutated gliomas the elevated D-2-HG levels appear to cause altered chromatin modifications and thus a profound change in the epigenetic status of these cells, resulting in a dysregulated gene expression, which is a frequent sign of tumorigenesis (Chowdhury et al., 2011; Xu et al., 2011; Lu et al., 2012; Rohle et al., 2013). This dysregulation may be the reason of the altered growth behavior in 3D spheroid culture observed in the current study, where IDH1$^{R132H}$-expressing U-251MG, U-343MG and LN-229 glioma cells aggregated to more lose, uneven and irregular structures.

Another group of α-KG-dependent dioxygenases are prolyl hydroxylase domain-containing proteins (PHDs; also known as EGLNs), such as prolyl-4-hydroxylases. These enzymes are required for post-translational modifications of proteins by hydroxylation of proline groups on the C4 position. Hence they are essential for important cellular processes and are for example involved in the maturation of collagen (Gorres et al., 2008; Winter and Page, 2000). In a physiological *in vivo* study of

Saski and colleagues it has been shown that D-2-HG accumulation caused by the activity of mutated IDH1 affects the collagen modification by α-KG-dependent prolyl hydroxylases in brain-specific IDH1[R132H] conditional knock-in mice (Sasaki et al., 2012). In particular, it was observed that the excess of D-2-HG attenuated the type IV collagen maturation and thereby impaired the basement membrane structure and function (Sasaki et al., 2012). Based on this, the D-2-HG-mediated perturbation of collagen maturation and basement membrane functions may have resulted in the missing capability of IDH1[R132H]-expressing U-251MG, U-343MG and LN-229 glioma cells to form regular and compact tumor aggregates in 3D spheroid culture.

In this work, investigation of cell mechanics by AFM technology revealed that IDH1[R132H] caused a considerable increase of cell stiffness compared to untreated cells, empty vector cells and IDH1[wt] cells in all three cell lines (Figure 4.20). In addition, it was also observed that gene expression of IDH1[R132H] in the three investigated glioma cell lines significantly reduced the cell migration compared to the respective untreated, empty vector and IDH1[wt] cells in 2D and 3D spheroid culture under normoxic and hypoxic conditions (Figure 4.18 and Figure 4.19).

Cell spreading has been shown to correlate with changes of important cell functions including DNA synthesis, differentiation, cell migration and cell stiffness (Bhadriraju and Hansen, 2002; Watanabe et al., 2012). Using atomic force microscopy, Cross and colleagues reported that living metastatic cancer cells extracted from the pleural fluids of patients with suspected lung, breast and pancreas cancer were more than 70 % to 80 % softer compared to benign mesothelial cells taken from the body cavities (Cross et al., 2007). This study also proved that cells of different cancer types exhibit a common stiffness, whereas the stiffness of benign mesothelial cells showed a log-normal distribution. In other words, the distribution of the stiffness of tumour cells is over five times narrower than the corresponding distribution for benign mesothelial cells. In addition, Cross and coworkers demonstrated that nanomechanical analysis correlates well with immunohistochemical testing generally used for detecting cancer (Cross et al., 2007). Based on these and other nanomechanical studies it has been suggested that cancer cells with high metastatic potential might benefit from their altered mechanical properties. Increased softness and flexibility supports spreading and formation of metastases as cancer cells have to circulate through narrow blood capillaries and then permeate into normal tissue (Cross et al., 2007; Cross et al., 2008; Hayashi and Iwata, 2015). However, the underlying mechanism which drives cancer cells to softer mechanical characteristics and thereby to a creep compliance (deformability) is not fully understood. Therefore, the relationship of increased glioma cell stiffness and mutated *IDH1* should be a topic of further reseach.

Furthermore, it has also been shown that cellular stiffness of ovarian cancer cell lines and primary cells derived from ascites of patients with advanced stage ovarian cancer is inversely proportional to migration and invasion (Swaminathan et al., 2011). This is consistent to a study by Watanabe and

coworkers who revealed that highly motile melanoma cells (B16-F10) exhibit low cell stiffness while low motile and metastatic melanoma cells (B16-F1) cells are characterized by high cell stiffness (Watanabe et al., 2012). Thus, the migration activity of cancer cells seems to correlate with their cellular stiffness.

These findings are in accordance with observations made in the current study where gene expression of IDH1$^{R132H}$ caused a reduced migration activity and an increased cellular stiffness of U-251MG, U343MG and LN-229 cells. In turn, this would suggest a less invasiveness of the IDH1$^{R132H}$-expressing cells and may explain the better prognosis of patients with *IDH1* mutant gliomas. Different studies support the relationship between the stiffness and the invasiveness of cancer cells. Additionally, several investigations have already provided evidence that stiffness, deformation and cell motility are regulated by different cellular processes, including the actomyosin contractility, the gene expression of the epithelial marker E-cadherin and the mesenchymal marker vimentin as well as alterations in the actin cytoskeleton via type III TGF-β receptor (Reichl et al., 2008; Stamenović and Coughlin, 1999; Swaminathan et al., 2011). Therefore, further work is required to elucidate the factors responsible for decreased stiffness and increased deformability of cancer cells. For example, analyses of the actin, E-cadherin and vimentin gene expression may provide additional information about the mediators of the reduced invasiveness of IDH1$^{R132H}$-expressing cells.

Another explanation for the reduced migration of IDH1$^{R132H}$-expressing cells may be an altered gene expression of matrix metalloproteinases, which are involved in the regulation of cell migration, proliferation and death by degrading matrix and non-matrix substrates (Murphy et al., 1991; Newby, 2006). Therefore, analyses of the gene expression of matrix metalloproteinases are needed to elucidate the influence of these proteinases with respect to the reduced migration of IDH1$^{R132H}$-expressing cells.

Further, it is well known that cell proliferation affects migration. Therefore, in this work the scratch assay was also performed with pre-treatment of glioma cell lines with 10 µg/mL mitomycin C for 2 h to prevent mitosis and to distinguish migration from proliferation (Data not shown). Results of scratch assay with or without mitomycin C correlated well, thus the reduced migration of IDH1$^{R132H}$-expressing cells were not caused by the altered growth of these cells.

In a recent study it has been demonstrated that overexpression of IDH1R132H in glioblastoma cell lines U-87MG and U-251MG led to reduced cell proliferation, migration and invasion, which were accompanied by increased apoptosis (Cui et al., 2016). In this study a significant reduction in the gene expression, nuclear accumulation and activity of β-catenin was observed following overexpression of IDH1R132H. Therefore, further research on the relationship between mutant *IDH1* and wingless-related integration site (Wnt)/β-catenin signaling may elucidate the altered cellular phenotype of U-251MG, U-343MG and LN-229 IDH1$^{R132H}$-expressing cells.

In the literature, clinical observations by Qi and coworkers suggest that the prolonged survival of patients with *IDH* mutated gliomas is primarily linked to a less aggressive biological behavior, which was evaluated on the basis of tumor site and magnetic resonance imaging (MRI) features (Qi et al., 2014). This study demonstrated that *IDH* mutated tumors were rarely located in the high-risk regions of the brain and were significantly more likely to exhibit a unilateral pattern of growth, sharp tumor margins, homogeneous signal intensity and less contrast enhancement on MRI (Qi et al., 2014).

In summary, the findings of the present work support former clinical observations as the gene expression of IDH1$^{R132H}$ slightly decreased cell viability, proliferation, plating efficiency and caused an altered growth in 3D culture with more loose and uneven spheroids, reduced the cell migration in 2D and 3D spheroid culture and reduced the stiffness of U-251MG, U-343MG and LN-229 cells, which is a sign of a less aggressive phenotype.

In order to investigate the effect of mutant *IDH1* on radiobiological behavior, cellular radiosensitivity was carried out with U-251MG, U-343MG and LN-229 gliomas after radiation under normoxia and hypoxia. In both environments analysis of survival curves revealed that gene expression of IDH1$^{R132H}$ significantly intensified the effect of radiation (Kessler et al., 2015) (Figure 4.22). These findings are consistent with an *in vitro* study found in the literature, which for example have demonstrated that gene expression of IDH1$^{R132H}$ increased the sensitivity to radiation of U-87MG cells under mild hypoxic conditions (Wang et al., 2014).

In a recent meta-analysis of 55 studies about the prognostic significance of *IDH1* in glioma showed that an *IDH1/2* mutation has a significant benefit for overall survival (hazard ratio (HR)=0.39, 95 % CI: 0.34-0.45; p<0.001) and progression-free survival (HR=0.42, 95 % CI: 0.35–0.51; p<0.001) (Xia et al., 2015). Moreover, based on the data collected in the prospective randomized phase III European Organization for Research and Treatment of Cancer (EORTC) study 26951 it was analyzed if *IDH* mutations can predict the outcome of chemotherapy. Additionally, the *IDH* mutation status was compared to other known outcome related markers (van den Bent et al., 2006; Bent et al., 2010). This study has shown that *IDH1* mutations were less frequent in tumors with glioblastoma features, including necrosis, *EGFR* amplification, polysomy of chromosome 7 as well as loss of chromosome 10 and the presence of mitosis. On the contrary, the presence of *IDH1* mutations was strongly associated with longer progression-free survival as well as longer overall survival and was positively correlated with the presence of 1p/19q loss, the presence of MGMT promoter methylation and with younger age. Especially these findings confirmed that there is a low incidence of *IDH1* mutations in primary glioblastoma, but a high incidence of these mutations in grade II and grade III gliomas. It was also demonstrated that patients with tumors harboring *IDH* mutations showed better outcomes compared to patients with *IDH1* wild type gliomas, whereas no significant difference was observed when the patients received adjuvant PCV after radiotherapy (59.4 Gy in fractions of 1.8 Gy) or

radiotherapy alone (Bent et al., 2010). In summary, this extensive study clearly supported the hypothesis that the presence of *IDH1* mutations is a major prognostic factor for outcome of this specific group of anaplastic oligodendroglial tumors. However, the results at that time gave no indication that the presence of *IDH1* mutations predicts the outcome to adjuvant PCV chemotherapy. On the other hand, due to the fact that all patients received radiotherapy, this clinical trial indicates that *IDH1* mutation predicts better response to radiotherapy of patients with malignant gliomas and supports the data of the present work, where gene expression of IDH1$^{R132H}$ enhanced the response of the investigated cell lines to radiation.

In a subsequent analysis of the EORTC study 26951, ten years after the completion of enrollment and a median follow-up of 140 months, it has been shown that overall survival (median OS, 42.3 vs. 30.6 months after radiotherapy alone; HR, 0.75; 95 % CI, 0.60 to 0.95) and progression-free survival (median PFS, 24.3 months after radiotherapy/PCV vs. 13.2 months with radiotherapy only; HR, 0.66; 95 % CI, 0.52 to 0.83) were significantly better after radiotherapy/PCV in patients with diagnosed anaplastic oligodendroglial tumors (van den Bent et al., 2013b). It was also observed that the three markers 1p/19q codeletion, MGMT promoter methylation and *IDH* mutation were highly prognostic for patient survival. However, consistent with the initial analyses, no predictive value of MGMT promoter methylation alone or of *IDH* mutations in the absence of 1p/19q codeletion for the benefit of adjuvant PCV chemotherapy was observed, underlining the importance of radiotherapy of these tumors (Combs et al., 2011; van den Bent et al., 2013b).

In addition to the prognostic relevance of an *IDH1* mutation in grade II and grade III glioma, *IDH* mutation is also associated with better outcomes in high-grade glioma. Different studies demonstrated that the median overall survival was 65 months for patients with *IDH* mutant anaplastic astrocytoma and 20 months for patients with wild type *IDH1*, whereas the median overall survival was 31 months for patients with glioblastoma harboring an *IDH* mutation and 15 months, for those without mutations (Hartmann et al., 2010; Combs et al., 2013; Juratli et al., 2012b; Kizilbash et al., 2014; Turkalp et al., 2014). Furthermore, an improved response to radiochemotherapy was observed using serial magnetic resonance imaging in glioblastoma patients with *IDH1* mutation in comparison to *IDH* wild type patients (Tran et al., 2014). In accordance with the effects of *IDH1* mutation described in the literature, the present work also shows that grade III U-343MG IDH1$^{R132H}$-expressing cells are more sensitive to radiation as compared to grade IV U-251MG IDH1$^{R132H}$ and LN-229 IDH1$^{R132H}$-expressing cells under normoxia and hypoxia, respectively. In summary, the present thesis and the clinical observations suggest that the survival benefit caused by *IDH1* mutation for patients with low-grade or high-grade gliomas may be an indication of the positive effect of *IDH1* mutation on the response to radiotherapy. In this context, the question may arise if *IDH1* mutated gliomas are also more sensitive to treatment with temozolomide. On the one hand, Li and coworkers demonstrated that IDH1R132H protein did

not sensitize U-87MG cells to temozolomide (Li et al., 2013b). On the contrary, at least one study has demonstrated that *IDH* mutation appears to be a significant marker of positive prognosis and increased sensitivity to temozolomide in low-grade gliomas, suggesting that *IDH* mutation may also be an indicator of enhanced chemosensitivity (Houillier et al., 2010). In glioma patients, *IDH* mutations are capable of establishing the methylation phenotype (G-CIMP). These chromatin alterations result in transcriptional silencing of the associated genes and the majority of G-CIMP malignant gliomas also exhibit MGMT promoter methylation (Lai et al., 2011; Brennan et al., 2013; Turcan et al., 2012; van den Bent et al., 2013a). Furthermore, it has been shown that decreased MGMT gene expression, caused by MGMT promoter methylation, results in an improved response to alkylating agents such as temozolomide (Esteller et al., 2000; Hegi et al., 2005). Further *in vitro* studies are needed to validate these observations and to investigate if treatment with both temozolomide and radiation may provoke additive effects on cell survival and induction of apoptosis of $IDH1^{R132H}$-expressing U-251MG, U-343MG and LN-229 cells.

In this thesis, the effect of mutant *IDH1* on induction of apoptosis and DNA damage was carried out via Western blot analysis of PARP cleavage and γH2AX assay with U-251MG, U-343MG and LN-229 gliomas after radiation under normoxia and hypoxia. In both environments gene expression of $IDH1^{R132H}$ slightly enhanced cleavage of PARP in the non-irradiated glioma cell lines (Figure 4.26). In addition, gene expression of the mutant IDH1 effectively enhanced the radiation-induced accumulation of γH2AX foci and induction of apoptosis in U-251MG, U-343MG and LN-229 glioma cells irrespective of the oxygen conditions (Figure 4.23, Figure 4.24 and Figure 4.25).

Under physiological conditions, IDH enzymes regulate a number of cellular functions and play an essential role in cellular protection as well as response to oxidative and energetic stress (Ronnebaum et al., 2006; Metallo et al., 2011; Filipp et al., 2012; Reitman et al., 2011; Bleeker et al., 2010). The mutated IDH1 enzyme exhibits a strongly decreased enzyme activity to isocitrate and $NADP^+$ and gains an abnormal NADPH-dependent catalytic activity (Dang et al., 2010; Jin et al., 2011; Bleeker et al., 2010; Gross et al., 2010; Ward et al., 2010). NADPH is required to regenerate reduced GSH, the major cellular ROS scavenger (Dang et al., 2010; Bleeker et al., 2010). Additionally, α-KG itself functions as an antioxidant (Lee et al., 2002; Mailloux et al., 2007). Thereby, it has been suggested that glioma cells expressing mutant IDH1 have a diminished antioxidant capacity and therefore may experience a subsequent loss of cytoprotection under conditions of oxidative stress (Bleeker et al., 2010). Under these circumstances low NADPH levels might sensitize malignant gliomas for oxidative stress, amplifying the response to radiotherapy and thereby may account for the prolonged survival of patients harboring the mutations. Thus, it is possible that the enhanced radiosensitivity of U-251MG, U-343MG and LN-229 cells in the present work was caused by the $IDH1^{R132H}$-induced reduction of the cytoprotection against oxidative stress. Due to the key role of NADPH in the cellular antioxidation

systems it has been supposed that *IDH1/2* mutations may increase intracellular reactive oxygen species (ROS) by the decrease of intracellular NADPH levels (Sasaki et al., 2012). Insufficient control of intracellular ROS has been associated with cellular senescence and apoptosis (Ying, 2008; Finkel and Holbrook, 2000; Lee et al., 2011). Consistent with these findings the gene expression of IDH1$^{R132H}$ slightly increased cleavage of PARP and the number of residual γH2AX foci per nucleus in the non-irradiated glioma cell lines in the present work. Further studies are in progress to evaluate the GSH/GSSH ratio and the ROS level in IDH1$^{R132H}$-expressing U-251MG, U-343MG and LN-229 cells.

It has been widely reported in literature that with increasing malignancy gliomas exhibit intratumoral hypoxia, which has been associated with poor response to radio- or chemotherapy (Gray et al., 1953; Collingridge et al., 1999; Nordsmark et al., 2005; Said et al., 2007b; Combs et al., 2013). In the present work, gene expression of IDH1$^{R132H}$ attenuated the hypoxia-induced radioresistance of malignant glioma cells U-251MG, U-343MG and LN-229. As already described, IDH1 catalyzes the reductive carboxylation of α-KG to isocitrate, which is essential for citrate synthesis under hypoxic conditions. Likewise, cells grown under hypoxia rely almost exclusively on the reductive carboxylation of glutamine-derived α-KG for *de novo* lipogenesis (Metallo et al., 2011; Wise et al., 2011). Leonardi and colleagues demonstrated that the mutated IDH1 enzyme is not sufficient to catalyze the reductive carboxylation of α-KG to isocitrate, suggesting that these metabolic alteration contribute to the reduced aggressiveness of glioma cells expressing IDH1$^{R132H}$ (Leonardi et al., 2012). Hence, the important requirement of NADPH for redox control and the widespread metabolic changes can be the reason for an increased sensitivity to radiation of the investigated glioma cells, especially under hypoxic conditions. In addition, the elevated D-2-HG levels appear to cause an altered chromatin modification and by that a profound change in the epigenetic status of these cells. Further work is therefore required to investigate possible epigenetic effects which may influence the sensitivity of IDH1$^{R132H}$-expressing glioma cells to oxidative stress under normoxic or hypoxic conditions. In this context, the present study could show that the gene expression of IDH1$^{R132H}$ increased the number of residual γH2AX foci per nucleus in U-251MG, U-343MG and LN-229 cells independent of the oxygen concentrations (Figure 4.23, Figure 4.24 and Figure 4.25).

In the literature it has been suggested that targeting IDH mutations is an attractive approach for treatment of *IDH* mutant gliomas due to that D-2-HG has been postulate to act as an oncometabolite (see 1.4.2). For example, Zheng and coworkers developed a series of mutant IDH inhibitors, which inactivate the mutant IDH1 enzyme via hydrogen bonds and electrostatic interactions with a stronger affinity to the active site of the mutated IDH1 enzyme (Zheng et al., 2013). Inhibition of IDH1R132H was, for example, described by Rohle and colleagues who used the mutation-specific molecule AGI-5198. In this study, a decreased D-2-HG level and a reversed differentiation blockage, which is

generally associated with *IDH* mutation in gliomas, was observed in murine xenografts (Rohle et al., 2013). Futher studies are required to determine the exact role of *IDH* mutation in glioma initiation and progression as well as to optimize the targeting of this pathway in cancer therapy.

In addition, a multicenter phase I trial (NOA-16/NONK-6) is ongoing to evaluate the potential of targeting IDH mutations by vaccination-based immunotherapy. From an immunological perspective IDH mutations represent ideal tumor-specific neoantigens due to their high uniformity and ubiquitous gene expression in all tumour cells (Schumacher et al., 2014a). In this study, it was demonstrated that IDH1R132H contains an immunogenic epitope suitable for mutation-specific vaccination (Schumacher et al., 2014a). Moreover they showed that IDH1R132H is presented on human MHC class II molecules and induces a mutation-specific CD4$^+$ antitumor T-cell response in humans as wells as in a syngeneic tumor model of MHC-humanized mice (Schumacher et al., 2014b). Likewise, another study recently demonstrated that immunizations by subcutaneous injections of different peptides encompassing the IDH1 mutation site, induced higher amounts of peripheral CD8$^+$ T-cells, increased production of IFN-γ and anti-IDH1R132H antibodies in a murine intracranial glioma model (Pellegatta et al., 2015). These promising studies suggest that the development of mutant IDH1-targeted immunotherapies can lead to therapeutically meaningful anti-tumor immune responses. In this respect it is worth noting that a combination of radiotherapy and immunotherapy seems to be another promising strategy for the treatment of *IDH1* mutant gliomas as both therapy forms complement each other. The positive synergistic effects of this approach have already been demonstrated in murine models and are the basis of a variety of clinical trials (Lee et al., 2009; Takeshima et al., 2010; Zeng et al., 2013).

In conclusion, the data of the present work suggests that IDH1$^{R132H}$ gene expression in all investigated glioma cells leads to a reduced aggressiveness as well as a higher radiosensitivity independent of the oxygen concentrations and the degree of tumor malignancy. The results highlight the important role of mutant *IDH1* in response to radiation and are consistent with the clinical observation of prolonged survival of patients harboring the *IDH1* mutation.

## 5.4 Influence of IDH1$^{R132H}$ expression on HIF-1α level

The transcription factor HIF-1, a dimer of an oxygen-regulated α subunit and an oxygen-independent β subunit, governs cellular adaption to low oxygen concentrations by regulating tumor-relevant genes involved in energy metabolism, cell proliferation, apoptosis and angiogenesis (Semenza, 2002; Bracken et al., 2003; Goda et al., 2003; Manalo et al., 2005). Under physiological conditions, the HIF-1α subunit is strictly regulated by proline and asparagine hydroxylation mediated by the α-KG-dependent dioxygenases PHD2 and FIH, respectively (Hirota and Semenza, 2005). The hydroxylated HIF1-α subunit is recognized by the VHL tumor suppressor E3 ligase for proteasomal

degradation (Semenza, 2014; Wenger et al., 2005). However, the relationship between gene expression of mutant IDH and HIF-1α activity in gliomas is controversially discussed in literature.

In the present work, the effect of IDH1 mutant protein expression on HIF-1α and its target gene *CA9* was evaluated by qPCR, Western blot analysis and immunohistochemical staining of U-251MG, U-343MG and LN-229 cells (Figure 4.27, Figure 4.28, Figure 4.29, Figure 8.3, Figure 8.4 and Figure 8.5). It was observed that IDH1$^{R132H}$ gene expression affects the transcriptional activity of HIF-1α in a cell-line dependent manner. In U-251MG and U-343MG cells, the gene expression of IDH1$^{R132H}$ caused an increased HIF-1α protein level and induction of its target gene *CA9* in normoxia and hypoxia, respectively (Figure 4.27 and Figure 4.28). Expression of an IDH1$^{R132H}$ transgene was already reported to increase HIF-1α protein level in HEK293T cells due to IDH1 loss of function and decreased intracellular α-KG levels (Zhao et al., 2009). Moreover, the accumulation of HIF-1α protein was reversible by using a cell-permeable α-KG derivative.

In a another study, gene expression of IDH1R132H or treatment with cell-permeable D-2-HG has also been demonstrated to increase HIF-1α protein level in HEK293T and U-87MG cells (Xu et al., 2011). D-2-HG and α-KG are almost identical metabolites, suggesting that D-2-HG can bind and function as a competitive inhibitor of α-KG-dependent dioxygenases (Iyer et al., 2009; Loenarz and Schofield, 2008; Chowdhury et al., 2011; Xu et al., 2011). This hypothesis was confirmed by Xu and colleagues, who demonstrated that the activities of α-KG-dependent PHDs are increased by the activity of wild type IDH1 and impaired by tumor-derived mutant IDH1 (Xu et al., 2011). Similarly, IDH1$^{R132H}$ knock in mice also showed high levels of D-2-HG that were associated with an inhibition of prolyl hydroxylation of HIF-1α and up-regulation of HIF-1α target gene transcription of *vascular endothelial growth factor* (*VEGF*) and *GLUT-1* (Sasaki et al., 2012). These results are comparable to the findings of the current study, where an increased HIF-1α protein level and an induction of the target gene *CA9* was observed in the IDH1$^{R132H}$-expressing U-251MG and U-343MG glioma cells independent of the oxygen concentrations.

On the contrary, D-2-HG has been reported to weakly inhibit HIF-1α prolyl hydroxylases and asparaginyl hydroxylases *in vitro*, with IC50 values higher than 1 mM (Chowdhury et al., 2011). To investigate the hypothesis that gene expression of mutated IDH1 specifically leads to accumulation of HIF-1α protein in human gliomas *in vivo*, Williams and coworkers examined a large variety of glial tumors by immunohistochemistry (Williams et al., 2011). In this study, no evident relationship between the gene expression of mutated IDH1 and HIF-1α was observed. Thus, it was suggested that other mechanisms such as hypoxia, growth factor dependent transcriptional regulation and major genetic and epigenetic alterations resulting in oncogene gain of function or tumor suppressor gene loss of function affected the HIF-1α protein level (Schofield and Ratcliffe, 2004; Semenza, 2010; Williams et al., 2011).

In contrast, in the present work, in LN-229 cells the expression of IDH1$^{R132H}$ caused a decreased HIF-1α protein level and reduction of its target gene *CA9* under normoxic and hypoxic conditions (Figure 4.27 and Figure 4.28). In accordance to these results a decreased HIF-1α activity was demonstrated due to the stimulation of prolyl-4-hydroxylases by D-2-HG in immortalized human astrocytes (Koivunen et al., 2012). Likewise, a reduced HIF-1α activity in primary patient astrocytoma samples was also reported already (Koivunen et al., 2012).

In conclusion, results from the present work and the literature have shown that activation of the HIF-1α pathway is rather regulated via other known mechanisms than via hypoxia. One explanation for this could be the IDH1R132H or D-2-HG dose-dependent increase of HIF-1α protein level. Indeed, a dose-dependent increase of HIF-1α and decrease of endostatin (a secretory peptide in inhibiting angiogenesis and tumor growth) with increasing gene expression of IDH1R132H was already observed in U-87MG cells (Xu et al., 2011). However, it is also possible that an IDHR132H-induced alteration of the cellular metabolome influences HIF-1α transcriptional activity. *IDH* mutant gliomas compensate their altered flux of α-KG to unusually high amounts of D-2-HG by substantial metabolic changes (Reitman et al., 2011; Izquierdo-Garcia et al., 2015; Ohka et al., 2014). For example, PHDs are inhibited in the presence of succinate or fumarate, leading to the hypothesis that HIF-1α is involved in the metabolic changes of *IDH1* mutant gliomas (Isaacs et al., 2005; Selak et al., 2005). Moreover, the D-2-HG synthesis catalyzed by the mutated IDH1 enzyme is limited by the concentrations of α-KG and NADPH. Therefore, also glutamine availability may influence D-2-HG synthesis and HIF-1α accumulation as IDH1$^{R132H}$ cells utilize the reductive glutamine metabolism for restocking of α-KG (Metallo et al., 2011; Wise et al., 2011). Thus, increased gene expression of HIF-1α is more likely a mechanism to adapt to the IDH1R132H-specific metabolism, possibly dose-dependent of unknown metabolites (e.g. α-KG, glutamine, glutamate or metabolites of the citric acid cycle), rather than to constitutively accumulate in *IDH1* mutated gliomas. The presence of a permanently increased HIF-1α protein level is also unlikely, because *IDH* mutated gliomas are generally not ''angiogenic'' as would be expected for tumors with dysregulated HIF-1α (Reitman et al., 2010; Jin et al., 2011). In addition, immunohistochemical staining of WHO grade II and III gliomas revealed that the gene expression of HIF-1α, CAIX and GLUT-1 was independent of the genetic status of *IDH1* (Metellus et al., 2011).

Furthermore, it is possible that the HIF-1 pathway is not primarily regulated by mutated IDH1, but rather via elevated ROS and oxidative stress in these tumors. At high levels, ROS damage cell organelles, particularly the mitochondria, which are generators of and targets for reactive species (Murphy, 2009). Through autophagy cells coordinate their energy metabolism and availability of metabolites for normal macromolecule biosynthesis, which are necessary for vital processes (Kroemer et al., 2010; Filomeni et al., 2015). Autophagy is activated by oxidative stress, oxidative damage and

carbon source availability, such as amino acids and glucose (Filomeni et al., 2015). Here, the amino acid glutamine serves as a main signal for activation of the process (Cohen and Hall, 2009; Nicklin et al., 2009). Moreover, HIF-1α-dependent gene expression of BNIP3/BNIP3L is a key mechanism in the activation of hypoxia-induced autophagy (Bellot et al., 2009; Dodson et al., 2013). Based on the aforementioned correlations, HIF-1 might be involved in activating autophagy in *IDH1* mutated cells by elevated ROS generation resulting in oxidative stress as well as by decreased amounts of glutamine. In this context, further analyses of HIF-1α gene expression in IDH1$^{R132H}$-expressing U-251MG, U-343MG and LN-229 cells over extended periods of time, investigations of autophagy activation or quantitative analyses of metabolites such as α-KG, glutamine, D-2-HG, succinate and fumarate may help to better understand the role of HIF-1α in *IDH1* mutant gliomas. If accumulation of HIF-1α occurs at specific stages of tumorigenesis in the course of adaptation to metabolic alterations or elevated oxidative stress, HIF inhibition may provide a narrower therapeutic window in the treatment of *IDH1* mutant glioma. Hence, further work is required to elucidate the relationship between mutant *IDH1* and the actions of HIF-1α in gliomas.

# 6  Summary and outlook

Malignant gliomas, the most common subtype of primary brain tumors, are aggressive, invasive and exhibit intratumoral hypoxia. Despite multimodal treatment options, comprising surgery, radiotherapy and chemotherapy, high-grade gliomas still remain incurable. Due to their heterogeneity and various mutual signatures, the chances for establishing a universal standard treatment of these tumors are limited. In this context, the identification and validation of molecular markers appear to be promising approaches for a clear stratification of patients with malignant gliomas. In addition, molecular markers represent a useful tool for the understanding of cancer biology and the development of tailored therapeutic options. Furthermore, such biomarkers permit a subclassification of malignant gliomas, which makes it possible to differentiate between patients with higher risk for toxicity and those who may benefit from a particular treatment. In high-grade gliomas the transcription factor HIF-1α, a key mediator of the cellular response to hypoxia, is associated with poor patient outcome, disease progression, an aggressive cancer phenotype and resistance to therapy. Hence, several studies have highlighted HIF-1α as a potential target for the development of novel strategies to treat malignant gliomas. In addition, *IDH1* mutations have also been successfully linked to prognostic information and thus proposed as genetic markers for glioma classification. *IDH* mutations occur in the vast majority of grade II and grade III gliomas as well as secondary glioblastomas, where they seem to predispose a particular path for oncogenic progression resulting in an increased progression-free and overall survival of affected patients, irrespective of tumor malignancy. Based on this knowledge, one aim of the present thesis was to investigate the effect of HIF-1α inhibition via siRNA or CTM as well as the effect of an *IDH1* mutation on cellular behavior and response to radiation of different malignant glioma cell lines under normoxic and hypoxic conditions.

Targeting HIF-1α via specific siRNA or CTM effectively reduced the gene expression or transcriptional activity of HIF-1α and further decreased the gene expression of its target *CA9*/CAIX in U-251MG and U-343MG cells in normoxia and hypoxia, respectively. Although siRNA and CTM inhibit HIF-1α through two rather different mechanisms, both induced apoptosis and attenuated the radioresistance of malignant glioma cell lines U-251MG (DMF10: 1.35 and 1.18) and U-343MG (DMF10: 1.78 and 1.48) under hypoxic conditions. In contrast, under normoxic conditions siRNA and CTM showed diverse effects on induction of apoptosis and radiosensitivity of U-251MG (DMF10: 0.86 and 1.35) and U-343MG (DMF10: 1.33 and 1.02) cells. The results suggest that inhibition of HIF-1α is a promising strategy to sensitize hypoxic malignant gliomas to radiotherapy and that its target gene *CA9* could serve as an indicator of effective HIF-1-related radiosensitization.

Reduction of the *IDH1* gene expression via siRNA only increased the radiosensitivity of U-343MG cells under hypoxic conditions (hypoxia, U-251MG DMF10: 0.91; U-343MG DMF10: 1.63; LN-229 DMF10: 1.02). In contrast, in normoxia no influence on the radiobiological behavior of U-251MG, U-343MG and LN-229 cells was observed (normoxia, U-251MG DMF10: 0.99; U-343MG DMF10: 1.07; LN-229 DMF10: 0.98). This implies that the better outcome of patients with malignant gliomas is not caused by a reduced enzyme function of mutated IDH1 but by the gain-of-function activity of mutated IDH1 that leads to D-2-HG accumulation and consumption of α-KG as well as NADPH.

Therefore, the gene expression of IDH1$^{R132H}$ was carried out in stable transduced glioma cells to mimic the gain-of-function activity that catalyzes the conversion of α-KG into D-2-HG. The data revealed that gene expression of mutated IDH1 causes a reduced aggressiveness based on slightly decreased cell proliferation and plating efficiency, altered growth properties in 3D spheroid culture and significantly reduced cell migration as well as increased cell stiffness. Furthermore, gene expression of IDH1$^{R132H}$ changed the response to radiation which resulted in elevated radiosensitivity (normoxia, U-251MG DMF10: 1.52; U-343MG DMF10: 1.78; LN-229 DMF10: 1.41 and hypoxia, U-251MG DMF10: 1.42; U-343MG DMF10: 1.75; LN-229 DMF10: 1.68), an accumulation of residual γH2AX foci and an increase of apoptosis. In addition, the effect of gene expression of mutated IDH1 on the cellular behavior and radiosensitivity was independent of the oxygen concentrations. The results emphasize the important role of mutant *IDH1* in the response to radiation and are consistent with the clinical observation of improved prognosis and prolonged overall survival of patients harboring the mutation.

Nevertheless, further studies have to be conducted in order to support the findings of this work. For example, analyzing the influence of *IDH1* mutations on metabolite concentrations or enzyme activitiy as well as on DNA repair mechanisms would gain a better insight into the underlying effect of increased radiosensitivity. Additionally, the observed reduction of cell stiffness and invasiveness of *IDH1* mutated gliomas should be elucidated in more detail in upcoming studies. Since *IDH1* mutated tumors almost exclusively rely on glutaminolysis in hypoxia, the ability to enhance cell radiosensitivity by inhibition of this metabolic pathway could be another clinical benefit for patients with these tumors. Moreover, further work is required to fully elucidate the relationship between *IDH1* mutations, the subsequent D-2-HG accumulation and the actions of HIF-1α in gliomas as HIF inhibition can provide a therapeutic option in the treatment of *IDH1* mutant gliomas. Finally, the findings of the present study should also be further evaluated using *in vivo* models as the clinical validity of the obtained *in vitro* results may be limited.

In conclusion, detection of the genetic status of *IDH1* before radiotherapy might help to identify patients with a radioresistant *IDH1* wild type glioma who should receive more aggressive treatments than patients with *IDH1* mutant glioma. Furthermore, continuing characterization of mutations of the

IDH enzymes and their relationship to HIF-1α will help to gain deeper insight into the understanding of tumorigenesis of malignant gliomas. This will facilitate the development of new biomarkers to allow early cancer diagnosis and opens new opportunities for treatment of these tumors.

# 7 REFERENCES

Adams, D.J. (2012). The Valley of Death in anticancer drug development: a re-assessment. Trends Pharmacol. Sci. *33*, 173–180.

Agarwal, M.L., Agarwal, A., Taylor, W.R., and Stark, G.R. (1995). p53 controls both the G2/M and the G1 cell cycle checkpoints and mediates reversible growth arrest in human fibroblasts. Proc. Natl. Acad. Sci. U. S. A. *92*, 8493–8497.

Amary, M.F., Bacsi, K., Maggiani, F., Damato, S., Halai, D., Berisha, F., Pollock, R., O'Donnell, P., Grigoriadis, A., Diss, T., et al. (2011). IDH1 and IDH2 mutations are frequent events in central chondrosarcoma and central and periosteal chondromas but not in other mesenchymal tumours. J. Pathol. *224*, 334–343.

Anderson, J.C., Duarte, C.W., Welaya, K., Rohrbach, T.D., Bredel, M., Yang, E.S., Choradia, N.V., Thottassery, J.V., Yancey Gillespie, G., Bonner, J.A., et al. (2014). Kinomic exploration of temozolomide and radiation resistance in Glioblastoma multiforme xenolines. Radiother. Oncol. J. Eur. Soc. Ther. Radiol. Oncol. *111*, 468–474.

Baba, Y., Nosho, K., Shima, K., Irahara, N., Chan, A.T., Meyerhardt, J.A., Chung, D.C., Giovannucci, E.L., Fuchs, C.S., and Ogino, S. (2010). HIF1A overexpression is associated with poor prognosis in a cohort of 731 colorectal cancers. Am. J. Pathol. *176*, 2292–2301.

Bache, M., Reddemann, R., Said, H.M., Holzhausen, H.-J., Taubert, H., Becker, A., Kuhnt, T., Hänsgen, G., Dunst, J., and Vordermark, D. (2006). Immunohistochemical detection of osteopontin in advanced head-and-neck cancer: Prognostic role and correlation with oxygen electrode measurements, hypoxia-inducible-factor-1α-related markers, and hemoglobin levels. Int. J. Radiat. Oncol. *66*, 1481–1487.

Bache, M., Kappler, M., Wichmann, H., Rot, S., Hahnel, A., Greither, T., Said, H.M., Kotzsch, M., Würl, P., Taubert, H., et al. (2010). Elevated tumor and serum levels of the hypoxia-associated protein osteopontin are associated with prognosis for soft tissue sarcoma patients. BMC Cancer *10*, 132.

Bache, M., Rot, S., Keßler, J., Güttler, A., Wichmann, H., Greither, T., Wach, S., Taubert, H., Söling, A., Bilkenroth, U., et al. (2015). mRNA expression levels of hypoxia-induced and stem cell-associated genes in human glioblastoma. Oncol. Rep. *33*, 3155–3161.

Bailey P and Cushing H: A Classification of the Tumors of the Glioma Group on a Histogenetic Basis with a Correlated Study of Prognosis. JB Lippincott & Co., Philadelphia, PA, 1926

Balcer-Kubiczek, E.K. (2012). Apoptosis in radiation therapy: a double-edged sword. Exp. Oncol. *34*, 277–285.

Balss, J., Meyer, J., Mueller, W., Korshunov, A., Hartmann, C., and Deimling, A. von (2008). Analysis of the IDH1 codon 132 mutation in brain tumors. Acta Neuropathol. (Berl.) *116*, 597–602.

Baskar, R., Lee, K.A., Yeo, R., and Yeoh, K.-W. (2012). Cancer and Radiation Therapy: Current Advances and Future Directions. Int. J. Med. Sci. *9*, 193–199.

Begg, A.C., Stewart, F.A., and Vens, C. (2011). Strategies to improve radiotherapy with targeted drugs. Nat. Rev. Cancer *11*, 239–253.

Bell, C., Dowson, N., Fay, M., Thomas, P., Puttick, S., Gal, Y., and Rose, S. (2015). Hypoxia imaging in gliomas with 18F-fluoromisonidazole PET: toward clinical translation. Semin. Nucl. Med. *45*, 136–150.

Bellot, G., Garcia-Medina, R., Gounon, P., Chiche, J., Roux, D., Pouysségur, J., and Mazure, N.M. (2009). Hypoxia-Induced Autophagy Is Mediated through Hypoxia-Inducible Factor Induction of BNIP3 and BNIP3L via Their BH3 Domains. Mol. Cell. Biol. *29*, 2570–2581.

Bent, M.J. van den, Dubbink, H.J., Marie, Y., Brandes, A.A., Taphoorn, M.J.B., Wesseling, P., Frenay, M., Tijssen, C.C., Lacombe, D., Idbaih, A., et al. (2010). IDH1 and IDH2 Mutations Are Prognostic but not Predictive for Outcome in Anaplastic Oligodendroglial Tumors: A Report of the European Organization for Research and Treatment of Cancer Brain Tumor Group. Clin. Cancer Res. *16*, 1597–1604.

van den Bent, M.J. (2010). Interobserver variation of the histopathological diagnosis in clinical trials on glioma: a clinician's perspective. Acta Neuropathol. (Berl.) *120*, 297–304.

van den Bent, M.J., Carpentier, A.F., Brandes, A.A., Sanson, M., Taphoorn, M.J.B., Bernsen, H.J.J.A., Frenay, M., Tijssen, C.C., Grisold, W., Sipos, L., et al. (2006). Adjuvant Procarbazine, Lomustine, and Vincristine Improves Progression-Free Survival but Not Overall Survival in Newly Diagnosed Anaplastic Oligodendrogliomas and Oligoastrocytomas: A Randomized European Organisation for Research and Treatment of Cancer Phase III Trial. J. Clin. Oncol. Off. J. Am. Soc. Clin. Oncol. *24*, 2715–2722.

van den Bent, M.J., Dubbink, H.J., Sanson, M., van der Lee-Haarloo, C.R., Hegi, M., Jeuken, J.W.M., Ibdaih, A., Brandes, A.A., Taphoorn, M.J.B., Frenay, M., et al. (2009). MGMT Promoter Methylation Is Prognostic but Not Predictive for Outcome to Adjuvant PCV Chemotherapy in Anaplastic Oligodendroglial Tumors: A Report From EORTC Brain Tumor Group Study 26951. J. Clin. Oncol. *27*, 5881–5886.

van den Bent, M.J., Erdem-Eraslan, L., Idbaih, A., de Rooi, J., Eilers, P.H.C., Spliet, W.G.M., den Dunnen, W.F.A., Tijssen, C., Wesseling, P., Sillevis Smitt, P.A.E., et al. (2013a). MGMT-STP27 methylation status as predictive marker for response to PCV in anaplastic Oligodendrogliomas and Oligoastrocytomas. A report from EORTC study 26951. Clin. Cancer Res. Off. J. Am. Assoc. Cancer Res. *19*, 5513–5522.

van den Bent, M.J., Brandes, A.A., Taphoorn, M.J.B., Kros, J.M., Kouwenhoven, M.C.M., Delattre, J.-Y., Bernsen, H.J.J.A., Frenay, M., Tijssen, C.C., Grisold, W., et al. (2013b). Adjuvant procarbazine, lomustine, and vincristine chemotherapy in newly diagnosed anaplastic oligodendroglioma: long-term follow-up of EORTC brain tumor group study 26951. J. Clin. Oncol. Off. J. Am. Soc. Clin. Oncol. *31*, 344–350.

Bernier, J., Hall, E.J., and Giaccia, A. (2004). Radiation oncology: a century of achievements. Nat. Rev. Cancer *4*, 737–747.

Bhadriraju, K., and Hansen, L.K. (2002). Extracellular matrix- and cytoskeleton-dependent changes in cell shape and stiffness. Exp. Cell Res. *278*, 92–100.

Bigler, E.D., and Clement, P.F. (1997). Diagnostic Clinical Neuropsychology (University of Texas Press).

Birner, P., Gatterbauer, B., Oberhuber, G., Schindl, M., Rössler, K., Prodinger, A., Budka, H., and Hainfellner, J.A. (2001). Expression of hypoxia-inducible factor-1 alpha in oligodendrogliomas: its impact on prognosis and on neoangiogenesis. Cancer *92*, 165–171.

Blazek, E.R., Foutch, J.L., and Maki, G. (2007). Daoy medulloblastoma cells that express CD133 are radioresistant relative to CD133- cells, and the CD133+ sector is enlarged by hypoxia. Int. J. Radiat. Oncol. Biol. Phys. *67*, 1–5.

Bleeker, F.E., Atai, N.A., Lamba, S., Jonker, A., Rijkeboer, D., Bosch, K.S., Tigchelaar, W., Troost, D., Vandertop, W.P., Bardelli, A., et al. (2010). The prognostic IDH1( R132 ) mutation is associated with reduced NADP+-dependent IDH activity in glioblastoma. Acta Neuropathol. (Berl.) *119*, 487–494.

Borger, D.R., Tanabe, K.K., Fan, K.C., Lopez, H.U., Fantin, V.R., Straley, K.S., Schenkein, D.P., Hezel, A.F., Ancukiewicz, M., Liebman, H.M., et al. (2012). Frequent Mutation of Isocitrate Dehydrogenase (IDH)1 and IDH2 in Cholangiocarcinoma Identified Through Broad-Based Tumor Genotyping. The Oncologist *17*, 72–79.

Bracken, C.P., Whitelaw, M.L., and Peet, D.J. (2003). The hypoxia-inducible factors: key transcriptional regulators of hypoxic responses. Cell. Mol. Life Sci. CMLS *60*, 1376–1393.

Brahimi-Horn, C., Mazure, N., and Pouysségur, J. (2005). Signalling via the hypoxia-inducible factor-1alpha requires multiple posttranslational modifications. Cell. Signal. *17*, 1–9.

Bralten, L.B.C., Kloosterhof, N.K., Balvers, R., Sacchetti, A., Lapre, L., Lamfers, M., Leenstra, S., de Jonge, H., Kros, J.M., Jansen, E.E.W., et al. (2011). IDH1 R132H decreases proliferation of glioma cell lines in vitro and in vivo. Ann. Neurol. *69*, 455–463.

Brennan, C.W., Verhaak, R.G.W., McKenna, A., Campos, B., Noushmehr, H., Salama, S.R., Zheng, S., Chakravarty, D., Sanborn, J.Z., Berman, S.H., et al. (2013). The Somatic Genomic Landscape of Glioblastoma. Cell *155*, 462–477.

Brennan, D.J., Jirstrom, K., Kronblad, Å., Millikan, R.C., Landberg, G., Duffy, M.J., Rydén, L., Gallagher, W.M., and O'Brien, S.L. (2006). CA IX is an Independent Prognostic Marker in Premenopausal Breast Cancer Patients with One to Three Positive Lymph Nodes and a Putative Marker of Radiation Resistance. Clin. Cancer Res. *12*, 6421–6431.

Bruick, R.K., and McKnight, S.L. (2001). A conserved family of prolyl-4-hydroxylases that modify HIF. Science *294*, 1337–1340.

Buckner, J.C., Brown, P.D., O'Neill, B.P., Meyer, F.B., Wetmore, C.J., and Uhm, J.H. (2007). Central nervous system tumors. Mayo Clin. Proc. *82*, 1271–1286.

Burroughs, S.K., Kaluz, S., Wang, D., Wang, K., Van Meir, E.G., and Wang, B. (2013). Hypoxia inducible factor pathway inhibitors as anticancer therapeutics. Future Med. Chem. *5*.

Cancer Genome Atlas Research Network (2015). Comprehensive, Integrative Genomic Analysis of Diffuse Lower-Grade Gliomas. N. Engl. J. Med. *372*, 2481–2498.

Cao, Y., Eble, J.M., Moon, E., Yuan, H., Weitzel, D.H., Landon, C.D., Nien, C.Y.-C., Hanna, G., Rich, J.N., Provenzale, J.M., et al. (2013). Tumor Cells Upregulate Normoxic HIF-1α in Response to Doxorubicin. Cancer Res. *73*, 6230–6242.

Carmeliet, P., Dor, Y., Herbert, J.M., Fukumura, D., Brusselmans, K., Dewerchin, M., Neeman, M., Bono, F., Abramovitch, R., Maxwell, P., et al. (1998). Role of HIF-1alpha in hypoxia-mediated apoptosis, cell proliferation and tumour angiogenesis. Nature *394*, 485–490.

Chen, J., Li, Y., Yu, T.-S., McKay, R.M., Burns, D.K., Kernie, S.G., and Parada, L.F. (2012). A restricted cell population propagates glioblastoma growth following chemotherapy. Nature *488*, 522–526.

Chen, L., Feng, P., Li, S., Long, D., Cheng, J., Lu, Y., and Zhou, D. (2009). Effect of hypoxia-inducible factor-1alpha silencing on the sensitivity of human brain glioma cells to doxorubicin and etoposide. Neurochem. Res. *34*, 984–990.

Cheng, S.Y., Huang, H.J., Nagane, M., Ji, X.D., Wang, D., Shih, C.C., Arap, W., Huang, C.M., and Cavenee, W.K. (1996). Suppression of glioblastoma angiogenicity and tumorigenicity by inhibition of endogenous expression of vascular endothelial growth factor. Proc. Natl. Acad. Sci. U. S. A. *93*, 8502–8507.

Chowdhury, R., Yeoh, K.K., Tian, Y.-M., Hillringhaus, L., Bagg, E.A., Rose, N.R., Leung, I.K.H., Li, X.S., Woon, E.C.Y., Yang, M., et al. (2011). The oncometabolite 2-hydroxyglutarate inhibits histone lysine demethylases. EMBO Rep. *12*, 463–469.

Cohen, A., and Hall, M.N. (2009). An amino acid shuffle activates mTORC1. Cell *136*, 399–400.

Collingridge, D.R., Piepmeier, J.M., Rockwell, S., and Knisely, J.P. (1999). Polarographic measurements of oxygen tension in human glioma and surrounding peritumoural brain tissue. Radiother. Oncol. J. Eur. Soc. Ther. Radiol. Oncol. *53*, 127–131.

Combs, S.E., Rieken, S., Wick, W., Abdollahi, A., von Deimling, A., Debus, J., and Hartmann, C. (2011). Prognostic significance of IDH-1 and MGMT in patients with glioblastoma: One step forward, and one step back? Radiat. Oncol. Lond. Engl. *6*, 115.

Combs, S.E., Bruckner, T., Mizoe, J.-E., Kamada, T., Tsujii, H., Kieser, M., and Debus, J. (2013). Comparison of carbon ion radiotherapy to photon radiation alone or in combination with temozolomide in patients with high-grade gliomas: explorative hypothesis-generating retrospective analysis. Radiother. Oncol. J. Eur. Soc. Ther. Radiol. Oncol. *108*, 132–135.

Conley, S.J., Baker, T.L., Burnett, J.P., Theisen, R.L., Lazarus, D., Peters, C.G., Clouthier, S.G., Eliasof, S., and Wicha, M.S. (2015). CRLX101, an investigational camptothecin-containing nanoparticle-drug conjugate, targets cancer stem cells and impedes resistance to antiangiogenic therapy in mouse models of breast cancer. Breast Cancer Res. Treat. *150*, 559–567.

Cook, D., Brown, D., Alexander, R., March, R., Morgan, P., Satterthwaite, G., and Pangalos, M.N. (2014). Lessons learned from the fate of AstraZeneca's drug pipeline: a five-dimensional framework. Nat. Rev. Drug Discov. *13*, 419–431.

Cook, K.M., Hilton, S.T., Mecinovic, J., Motherwell, W.B., Figg, W.D., and Schofield, C.J. (2009). Epidithiodiketopiperazines block the interaction between hypoxia-inducible factor-1alpha (HIF-1alpha) and p300 by a zinc ejection mechanism. J. Biol. Chem. *284*, 26831–26838.

Corroyer-Dulmont, A., Chakhoyan, A., Collet, S., Durand, L., MacKenzie, E.T., Petit, E., Bernaudin, M., Touzani, O., and Valable, S. (2015). Imaging modalities to assess oxygen status in glioblastoma. Nucl. Med. 57.

Cragg, M.S., Harris, C., Strasser, A., and Scott, C.L. (2009). Unleashing the power of inhibitors of oncogenic kinases through BH3 mimetics. Nat. Rev. Cancer *9*, 321–326.

Crews, S.T. (1998). Control of cell lineage-specific development and transcription by bHLH-PAS proteins. Genes Dev. *12*, 607–620.

Cross, S.E., Jin, Y.-S., Rao, J., and Gimzewski, J.K. (2007). Nanomechanical analysis of cells from cancer patients. Nat. Nanotechnol. *2*, 780–783.

Cross, S.E., Jin, Y.-S., Tondre, J., Wong, R., Rao, J., and Gimzewski, J.K. (2008). AFM-based analysis of human metastatic cancer cells. Nanotechnology *19*, 384003.

Cui, D., Ren, J., Shi, J., Feng, L., Wang, K., Zeng, T., Jin, Y., and Gao, L. (2016). R132H mutation in IDH1 gene reduces proliferation, cell survival and invasion of human glioma by downregulating Wnt/β-catenin signaling. Int. J. Biochem. Cell Biol. *73*, 72–81.

Dai, S., Huang, M.L., Hsu, C.Y., and Chao, K.S.C. (2003). Inhibition of hypoxia inducible factor 1alpha causes oxygen-independent cytotoxicity and induces p53 independent apoptosis in glioblastoma cells. Int. J. Radiat. Oncol. Biol. Phys. *55*, 1027–1036.

Dai, Y., Bae, K., and Siemann, D.W. (2011). Impact of Hypoxia on the Metastatic Potential of Human Prostate Cancer Cells. Int. J. Radiat. Oncol. • Biol. • Phys. *81*, 521–528.

Dang, L., White, D.W., Gross, S., Bennett, B.D., Bittinger, M.A., Driggers, E.M., Fantin, V.R., Jang, H.G., Jin, S., Keenan, M.C., et al. (2010). Cancer-associated IDH1 mutations produce 2-hydroxyglutarate. Nature *465*, 966.

De Flora, S., and Bonanni, P. (2011). The prevention of infection-associated cancers. Carcinogenesis *32*, 787–795.

Dean, M., Fojo, T., and Bates, S. (2005). Tumour stem cells and drug resistance. Nat. Rev. Cancer *5*, 275–284.

Delaney, G., Jacob, S., Featherstone, C., and Barton, M. (2005). The role of radiotherapy in cancer treatment: estimating optimal utilization from a review of evidence-based clinical guidelines. Cancer *104*, 1129–1137.

Dellas, K., Bache, M., Pigorsch, S.U., Taubert, H., Kappler, M., Holzapfel, D., Zorn, E., Holzhausen, H.-J., and Haensgen, G. (2008). Prognostic impact of HIF-1alpha expression in patients with definitive radiotherapy for cervical cancer. Strahlenther. Onkol. Organ Dtsch. Röntgenges. Al *184*, 169–174.

Denko, N.C. (2008). Hypoxia, HIF1 and glucose metabolism in the solid tumour. Nat. Rev. Cancer *8*, 705–713.

Derjaguin, B.V., Muller, V.M., and Toporov, Y.P. (1975). Effect of contact deformations on the adhesion of particles. J. Colloid Interface Sci. *53*, 314–326.

Desjardins, A., Reardon, D.A., Herndon, J.E., Marcello, J., Quinn, J.A., Rich, J.N., Sathornsumetee, S., Gururangan, S., Sampson, J., Bailey, L., et al. (2008). Bevacizumab Plus Irinotecan in Recurrent WHO Grade 3 Malignant Gliomas. Clin. Cancer Res. Off. J. Am. Assoc. Cancer Res. *14*, 7068–7073.

Dewey, W.C., Ling, C.C., and Meyn, R.E. (1995). Radiation-induced apoptosis: relevance to radiotherapy. Int. J. Radiat. Oncol. Biol. Phys. *33*, 781–796.

Dimberg, A. (2014). The glioblastoma vasculature as a target for cancer therapy. Biochem. Soc. Trans. *42*, 1647–1652.

Dodson, M., Darley-Usmar, V., and Zhang, J. (2013). Cellular Metabolic and Autophagic Pathways: Traffic Control by Redox Signaling. Free Radic. Biol. Med. *63*, 207–221.

Dubbink, H.J., Taal, W., van Marion, R., Kros, J.M., van Heuvel, I., Bromberg, J.E., Zonnenberg, B.A., Zonnenberg, C.B.L., Postma, T.J., Gijtenbeek, J.M.M., et al. (2009). IDH1 mutations in low-grade astrocytomas predict survival but not response to temozolomide. Neurology *73*, 1792–1795.

Dubbink, H.J., Atmodimedjo, P.N., Kros, J.M., French, P.J., Sanson, M., Idbaih, A., Wesseling, P., Enting, R., Spliet, W., Tijssen, C., et al. (2015). Molecular classification of anaplastic oligodendroglioma using next-generation sequencing: a report of the prospective randomized EORTC Brain Tumor Group 26951 phase III trial. Neuro-Oncol.

Dudley, A.C. (2012). Tumor Endothelial Cells. Cold Spring Harb. Perspect. Med. *2*.

Duncan, W. (1973). Exploitation of the oxygen enhancement ratio in clinical practice. Br. Med. Bull. *29*, 33–38.

Ebert, B.L., Firth, J.D., and Ratcliffe, P.J. (1995). Hypoxia and mitochondrial inhibitors regulate expression of glucose transporter-1 via distinct Cis-acting sequences. J. Biol. Chem. *270*, 29083–29089.

Eckerich, C., Zapf, S., Fillbrandt, R., Loges, S., Westphal, M., and Lamszus, K. (2007). Hypoxia can induce c-Met expression in glioma cells and enhance SF/HGF-induced cell migration. Int. J. Cancer *121*, 276–283.

Ema, M., Taya, S., Yokotani, N., Sogawa, K., Matsuda, Y., and Fujii-Kuriyama, Y. (1997). A novel bHLH-PAS factor with close sequence similarity to hypoxia-inducible factor 1α regulates the VEGF expression and is potentially involved in lung and vascular development. Proc. Natl. Acad. Sci. U. S. A. *94*, 4273–4278.

Epstein, A.C.R., Gleadle, J.M., McNeill, L.A., Hewitson, K.S., O'Rourke, J., Mole, D.R., Mukherji, M., Metzen, E., Wilson, M.I., Dhanda, A., et al. (2001). C. elegans EGL-9 and Mammalian Homologs Define a Family of Dioxygenases that Regulate HIF by Prolyl Hydroxylation. Cell *107*, 43–54.

Esteller, M., Garcia-Foncillas, J., Andion, E., Goodman, S.N., Hidalgo, O.F., Vanaclocha, V., Baylin, S.B., and Herman, J.G. (2000). Inactivation of the DNA-repair gene MGMT and the clinical response of gliomas to alkylating agents. N. Engl. J. Med. *343*, 1350–1354.

Evans, S.M., Jenkins, K.W., Chen, H.I., Jenkins, W.T., Judy, K.D., Hwang, W.-T., Lustig, R.A., Judkins, A.R., Grady, M.S., Hahn, S.M., et al. (2010). The Relationship among Hypoxia, Proliferation, and Outcome in Patients with De Novo Glioblastoma: A Pilot Study. Transl. Oncol. *3*, 160–169.

Ewing, D. (1998). The oxygen fixation hypothesis: a reevaluation. Am. J. Clin. Oncol. *21*, 355–361.

Filipp, F.V., Scott, D.A., Ronai, Z.A., Osterman, A.L., and Smith, J.W. (2012). Reverse TCA cycle flux through isocitrate dehydrogenases 1 and 2 is required for lipogenesis in hypoxic melanoma cells. Pigment Cell Melanoma Res. *25*, 375–383.

Filomeni, G., De Zio, D., and Cecconi, F. (2015). Oxidative stress and autophagy: the clash between damage and metabolic needs. Cell Death Differ. *22*, 377–388.

Finkel, T., and Holbrook, N.J. (2000). Oxidants, oxidative stress and the biology of ageing. Nature *408*, 239–247.

Firth, J.D., Ebert, B.L., Pugh, C.W., and Ratcliffe, P.J. (1994). Oxygen-regulated control elements in the phosphoglycerate kinase 1 and lactate dehydrogenase A genes: similarities with the erythropoietin 3' enhancer. Proc. Natl. Acad. Sci. U. S. A. *91*, 6496–6500.

Firth, J.D., Ebert, B.L., and Ratcliffe, P.J. (1995). Hypoxic regulation of lactate dehydrogenase A. Interaction between hypoxia-inducible factor 1 and cAMP response elements. J. Biol. Chem. *270*, 21021–21027.

Flamme, I., Fröhlich, T., von Reutern, M., Kappel, A., Damert, A., and Risau, W. (1997). HRF, a putative basic helix-loop-helix-PAS-domain transcription factor is closely related to hypoxia-inducible factor-1α and developmentally expressed in blood vessels. Mech. Dev. *63*, 51–60.

Frankenberg-Schwager, M. (1990). Induction, repair and biological relevance of radiation-induced DNA lesions in eukaryotic cells. Radiat. Environ. Biophys. *29*, 273–292.

Gambarota, G., Leenders, W., Maass, C., Wesseling, P., van der Kogel, B., van Tellingen, O., and Heerschap, A. (2008). Characterisation of tumour vasculature in mouse brain by USPIO contrast-enhanced MRI. Br. J. Cancer *98*, 1784–1789.

Gatenby, R.A., and Gillies, R.J. (2004). Why do cancers have high aerobic glycolysis? Nat. Rev. Cancer *4*, 891–899.

Geisbrecht, B.V., and Gould, S.J. (1999). The Human PICD Gene Encodes a Cytoplasmic and Peroxisomal NADP+-dependent Isocitrate Dehydrogenase. J. Biol. Chem. *274*, 30527–30533.

Gilbert, M.R., Wang, M., Aldape, K.D., Stupp, R., Hegi, M.E., Jaeckle, K.A., Armstrong, T.S., Wefel, J.S., Won, M., Blumenthal, D.T., et al. (2013). Dose-Dense Temozolomide for Newly Diagnosed Glioblastoma: A Randomized Phase III Clinical Trial. J. Clin. Oncol. *31*, 4085–4091.

Goda, N., Dozier, S.J., and Johnson, R.S. (2003). HIF-1 in cell cycle regulation, apoptosis, and tumor progression. Antioxid. Redox Signal. *5*, 467–473.

Goldberg, M.A., Dunning, S.P., and Bunn, H.F. (1988). Regulation of the erythropoietin gene: evidence that the oxygen sensor is a heme protein. Science *242*, 1412–1415.

Gorovets, D., Kannan, K., Shen, R., Kastenhuber, E.R., Islamdoust, N., Campos, C., Pentsova, E., Heguy, A., Jhanwar, S.C., Mellinghoff, I.K., et al. (2012). IDH Mutation and Neuroglial Developmental Features Define Clinically Distinct Subclasses of Lower Grade Diffuse Astrocytic Glioma. Clin. Cancer Res. *18*, 2490–2501.

Gorres, K.L., Edupuganti, R., Krow, G.R., and Raines, R.T. (2008). Conformational Preferences of Substrates for Human Prolyl 4-Hydroxylase. Biochemistry (Mosc.) *47*, 9447–9455.

Graeber, T.G., Osmanian, C., Jacks, T., Housman, D.E., Koch, C.J., Lowe, S.W., and Giaccia, A.J. (1996). Hypoxia-mediated selection of cells with diminished apoptotic potential in solid tumours. Nature *379*, 88–91.

Gray, L.H., Conger, A.D., Ebert, M., Hornsey, S., and Scott, O.C. (1953). The concentration of oxygen dissolved in tissues at the time of irradiation as a factor in radiotherapy. Br. J. Radiol. *26*, 638–648.

Grelli, K.N., Palubinsky, A.M., Kale, A.C., Lizama-Manibusan, B.N., Stankowski, J.N., Milne, G.L., Singer, R., and McLaughlin, B. (2013). Alteration of Isocitrate Dehydrogenase Following Acute Ischemic Injury as a Means to Improve Cellular Energetic Status in Neuroadaptation. CNS Neurol. Disord. Drug Targets *12*, 849–860.

Gross, S., Cairns, R.A., Minden, M.D., Driggers, E.M., Bittinger, M.A., Jang, H.G., Sasaki, M., Jin, S., Schenkein, D.P., Su, S.M., et al. (2010). Cancer-associated metabolite 2-hydroxyglutarate accumulates in acute myelogenous leukemia with isocitrate dehydrogenase 1 and 2 mutations. J. Exp. Med. *207*, 339–344.

Gu, Y.Z., Moran, S.M., Hogenesch, J.B., Wartman, L., and Bradfield, C.A. (1998). Molecular characterization and chromosomal localization of a third alpha-class hypoxia inducible factor subunit, HIF3alpha. Gene Expr. *7*, 205–213.

Harris, A.L. (2002). Hypoxia--a key regulatory factor in tumour growth. Nat. Rev. Cancer *2*, 38–47.

Harris, C.C. (1991). Chemical and physical carcinogenesis: advances and perspectives for the 1990s. Cancer Res. *51*, 5023s–5044s.

Hartmann, C., and von Deimling, A. (2005). Oligodendrogliomas: impact of molecular genetics on treatment. Neurol. India *53*, 140–148.

Hartmann, C., Meyer, J., Balss, J., Capper, D., Mueller, W., Christians, A., Felsberg, J., Wolter, M., Mawrin, C., Wick, W., et al. (2009). Type and frequency of IDH1 and IDH2 mutations are related to astrocytic and oligodendroglial differentiation and age: a study of 1,010 diffuse gliomas. Acta Neuropathol. (Berl.) *118*, 469–474.

Hartmann, C., Hentschel, B., Wick, W., Capper, D., Felsberg, J., Simon, M., Westphal, M., Schackert, G., Meyermann, R., Pietsch, T., et al. (2010). Patients with IDH1 wild type anaplastic astrocytomas exhibit worse prognosis than IDH1-mutated glioblastomas, and IDH1 mutation status accounts for the unfavorable prognostic effect of higher age: implications for classification of gliomas. Acta Neuropathol. (Berl.) *120*, 707–718.

Hayashi, K., and Iwata, M. (2015). Stiffness of cancer cells measured with an AFM indentation method. J. Mech. Behav. Biomed. Mater. *49*, 105–111.

Hegi, M.E., Diserens, A.-C., Gorlia, T., Hamou, M.-F., de Tribolet, N., Weller, M., Kros, J.M., Hainfellner, J.A., Mason, W., Mariani, L., et al. (2005). MGMT gene silencing and benefit from temozolomide in glioblastoma. N. Engl. J. Med. *352*, 997–1003.

Hellevik, T., and Martinez-Zubiaurre, I. (2014). Radiotherapy and the Tumor Stroma: The Importance of Dose and Fractionation. Front. Oncol. *4*.

Hertz, H. (1882). Ueber die Berührung fester elastischer Körper. J. Für Reine Angew. Math. *92*, 156–171.

Hirota, K., and Semenza, G.L. (2005). Regulation of hypoxia-inducible factor 1 by prolyl and asparaginyl hydroxylases. Biochem. Biophys. Res. Commun. *338*, 610–616.

Höckel, M., and Vaupel, P. (2001). Biological consequences of tumor hypoxia. Semin. Oncol. *28*, 36–41.

Höckel, M., Knoop, C., Schlenger, K., Vorndran, B., Baussmann, E., Mitze, M., Knapstein, P.G., and Vaupel, P. (1993). Intratumoral pO2 predicts survival in advanced cancer of the uterine cervix. Radiother. Oncol. J. Eur. Soc. Ther. Radiol. Oncol. *26*, 45–50.

Hogenesch, J.B., Chan, W.K., Jackiw, V.H., Brown, R.C., Gu, Y.-Z., Pray-Grant, M., Perdew, G.H., and Bradfield, C.A. (1997). Characterization of a Subset of the Basic-Helix-Loop-Helix-PAS Superfamily That Interacts with Components of the Dioxin Signaling Pathway. J. Biol. Chem. *272*, 8581–8593.

Hohmann, T., Grabiec, U., Feese, K., Ghadban, C., and Dehghani, F. (submitted 2016) The Influence of Biomechanical Properties and Cannabinoids on Tumor Invasion.

Hotchkiss, R.S., Strasser, A., McDunn, J.E., and Swanson, P.E. (2009). Cell death. N. Engl. J. Med. *361*, 1570–1583.

Houillier, C., Wang, X., Kaloshi, G., Mokhtari, K., Guillevin, R., Laffaire, J., Paris, S., Boisselier, B., Idbaih, A., Laigle-Donadey, F., et al. (2010). IDH1 or IDH2 mutations predict longer survival and response to temozolomide in low-grade gliomas. Neurology *75*, 1560–1566.

Hu, C.-J., Sataur, A., Wang, L., Chen, H., and Simon, M.C. (2007). The N-Terminal Transactivation Domain Confers Target Gene Specificity of Hypoxia-inducible Factors HIF-1α and HIF-2α. Mol. Biol. Cell *18*, 4528–4542.

Hu, Y.-L., DeLay, M., Jahangiri, A., Molinaro, A.M., Rose, S.D., Carbonell, W.S., and Aghi, M.K. (2012). Hypoxia-induced autophagy promotes tumor cell survival and adaptation to anti-angiogenic treatment in glioblastoma. Cancer Res. *72*, 1773–1783.

Huang, L.E., Arany, Z., Livingston, D.M., and Bunn, H.F. (1996). Activation of Hypoxia-inducible Transcription Factor Depends Primarily upon Redox-sensitive Stabilization of Its α Subunit. J. Biol. Chem. *271*, 32253–32259.

Ichimura, K., Pearson, D.M., Kocialkowski, S., Bäcklund, L.M., Chan, R., Jones, D.T.W., and Collins, V.P. (2009). IDH1 mutations are present in the majority of common adult gliomas but rare in primary glioblastomas. Neuro-Oncol. *11*, 341–347.

Isaacs, J.S., Jung, Y.J., Mole, D.R., Lee, S., Torres-Cabala, C., Chung, Y.-L., Merino, M., Trepel, J., Zbar, B., Toro, J., et al. (2005). HIF overexpression correlates with biallelic loss of fumarate hydratase in renal cancer: novel role of fumarate in regulation of HIF stability. Cancer Cell *8*, 143–153.

Ishii, N., Maier, D., Merlo, A., Tada, M., Sawamura, Y., Diserens, A.C., and Van Meir, E.G. (1999). Frequent co-alterations of TP53, p16/CDKN2A, p14ARF, PTEN tumor suppressor genes in human glioma cell lines. Brain Pathol. Zurich Switz. *9*, 469–479.

Iyer, L.M., Tahiliani, M., Rao, A., and Aravind, L. (2009). Prediction of novel families of enzymes involved in oxidative and other complex modifications of bases in nucleic acids. Cell Cycle Georget. Tex *8*, 1698–1710.

Izquierdo-Garcia, J.L., Viswanath, P., Eriksson, P., Chaumeil, M.M., Pieper, R.O., Phillips, J.J., and Ronen, S.M. (2015). Metabolic Reprogramming in Mutant IDH1 Glioma Cells. PLoS ONE *10*.

Jain, R.K. (2008). Lessons from multidisciplinary translational trials on anti-angiogenic therapy of cancer. Nat. Rev. Cancer *8*, 309–316.

Jensen, R.L., Ragel, B.T., Whang, K., and Gillespie, D. (2006). Inhibition of hypoxia inducible factor-1alpha (HIF-1alpha) decreases vascular endothelial growth factor (VEGF) secretion and tumor growth in malignant gliomas. J. Neurooncol. *78*, 233–247.

Jeong, J.W., Bae, M.K., Ahn, M.Y., Kim, S.H., Sohn, T.K., Bae, M.H., Yoo, M.A., Song, E.J., Lee, K.J., and Kim, K.W. (2002). Regulation and destabilization of HIF-1alpha by ARD1-mediated acetylation. Cell *111*, 709–720.

Jiang, Y., and Uhrbom, L. (2012). On the origin of glioma. Ups. J. Med. Sci. *117*, 113–121.

Jiang, B.H., Rue, E., Wang, G.L., Roe, R., and Semenza, G.L. (1996). Dimerization, DNA binding, and transactivation properties of hypoxia-inducible factor 1. J. Biol. Chem. *271*, 17771–17778.

Jiang, B.H., Zheng, J.Z., Leung, S.W., Roe, R., and Semenza, G.L. (1997). Transactivation and inhibitory domains of hypoxia-inducible factor 1alpha. Modulation of transcriptional activity by oxygen tension. J. Biol. Chem. *272*, 19253–19260.

Jin, G., Reitman, Z.J., Spasojevic, I., Batinic-Haberle, I., Yang, J., Schmidt-Kittler, O., Bigner, D.D., and Yan, H. (2011). 2-Hydroxyglutarate Production, but Not Dominant Negative Function, Is Conferred by Glioma-Derived NADP+-Dependent Isocitrate Dehydrogenase Mutations. PLoS ONE *6*.

Jonathan, E.C., Bernhard, E.J., and McKenna, W.G. (1999). How does radiation kill cells? Curr. Opin. Chem. Biol. *3*, 77–83.

Jordan, B.F., and Sonveaux, P. (2012). Targeting Tumor Perfusion and Oxygenation to Improve the Outcome of Anticancer Therapy1. Front. Pharmacol. *3*.

Jovčevska, I., Kočevar, N., and Komel, R. (2013). Glioma and glioblastoma - how much do we (not) know? Mol. Clin. Oncol. *1*, 935–941.

Juratli, T.A., Kirsch, M., Robel, K., Soucek, S., Geiger, K., von Kummer, R., Schackert, G., and Krex, D. (2012a). IDH mutations as an early and consistent marker in low-grade astrocytomas WHO grade II and their consecutive secondary high-grade gliomas. J. Neurooncol. *108*, 403–410.

Juratli, T.A., Kirsch, M., Geiger, K., Klink, B., Leipnitz, E., Pinzer, T., Soucek, S., Schrok, E., Schackert, G., and Krex, D. (2012b). The prognostic value of IDH mutations and MGMT promoter status in secondary high-grade gliomas. J. Neurooncol. *110*, 325–333.

Kallio, P.J., Pongratz, I., Gradin, K., McGuire, J., and Poellinger, L. (1997). Activation of hypoxia-inducible factor 1α: Posttranscriptional regulation and conformational change by recruitment of the Arnt transcription factor. Proc. Natl. Acad. Sci. U. S. A. *94*, 5667–5672.

Kaya, A.O., Gunel, N., Benekli, M., Akyurek, N., Buyukberber, S., Tatli, H., Coskun, U., Yildiz, R., Yaman, E., and Ozturk, B. (2012). Hypoxia inducible factor-1 alpha and carbonic anhydrase IX overexpression are associated with poor survival in breast cancer patients. J. BUON Off. J. Balk. Union Oncol. *17*, 663–668.

Kaynar, M.Y., Sanus, G.Z., Hnimoglu, H., Kacira, T., Kemerdere, R., Atukeren, P., Gumustas, K., Canbaz, B., and Tanriverdi, T. (2008). Expression of hypoxia inducible factor-1alpha in tumors of patients with glioblastoma multiforme and transitional meningioma. J. Clin. Neurosci. Off. J. Neurosurg. Soc. Australas. *15*, 1036–1042.

Ke, Q., and Costa, M. (2006). Hypoxia-Inducible Factor-1 (HIF-1). Mol. Pharmacol. *70*, 1469–1480.

Keith, B., Johnson, R.S., and Simon, M.C. (2011). HIF1α and HIF2α: sibling rivalry in hypoxic tumor growth and progression. Nat. Rev. Cancer *12*, 9–22.

Kessler, J., Hahnel, A., Wichmann, H., Rot, S., Kappler, M., Bache, M., and Vordermark, D. (2010). HIF-1α inhibition by siRNA or chetomin in human malignant glioma cells: effects on hypoxic radioresistance and monitoring via CA9 expression. BMC Cancer *10*, 605.

Kessler, J., Güttler, A., Wichmann, H., Rot, S., Kappler, M., Bache, M., and Vordermark, D. (2015). IDH1(R132H) mutation causes a less aggressive phenotype and radiosensitizes human malignant glioma cells independent of the oxygenation status. Radiother. Oncol. J. Eur. Soc. Ther. Radiol. Oncol. *116*, 381–387.

Kettenmann, H., and Verkhratsky, A. (2011). [Neuroglia--living nerve glue]. Fortschr. Neurol. Psychiatr. *79*, 588–597.

Kieffer, S. (The Johns Hopkins University). John Hopkins Medicine. Neurology and Neurosurgery. Radiation Therapy for Brain Tumors. http://www.hopkinsmedicine.org/neurology_neurosurgery/centers_clinics/brain_tumor/treatment/radiation-therapy.html. [Date of last access 14.03.2016]

Kieffer, S. Treatment for Gliomas | Johns Hopkins Glioma Center.

Kim, J.Y., Shin, J.Y., Kim, M., Hann, S.-K., and Oh, S.H. (2012). Expression of cytosolic NADP(+)-dependent isocitrate dehydrogenase in melanocytes and its role as an antioxidant. J. Dermatol. Sci. *65*, 118–125.

Kim, K.J., Li, B., Winer, J., Armanini, M., Gillett, N., Phillips, H.S., and Ferrara, N. (1993). Inhibition of vascular endothelial growth factor-induced angiogenesis suppresses tumour growth in vivo. Nature *362*, 841–844.

Kizilbash, S.H., Giannini, C., Voss, J.S., Decker, P.A., Jenkins, R.B., Hardie, J., Laack, N.N., Parney, I.F., Uhm, J.H., and Buckner, J.C. (2014). The impact of concurrent temozolomide with adjuvant radiation and IDH mutation status among patients with anaplastic astrocytoma. J. Neurooncol. *120*, 85–93.

Kleihues, P., Louis, D.N., Scheithauer, B.W., Rorke, L.B., Reifenberger, G., Burger, P.C., and Cavenee, W.K. (2002). The WHO classification of tumors of the nervous system. J. Neuropathol. Exp. Neurol. *61*, 215-225-229.

Kohli, R.M., and Zhang, Y. (2013). TET enzymes, TDG and the dynamics of DNA demethylation. Nature *502*, 472–479.

Koivunen, P., Lee, S., Duncan, C.G., Lopez, G., Lu, G., Ramkissoon, S., Losman, J.A., Joensuu, P., Bergmann, U., Gross, S., et al. (2012). Transformation by the (R)-enantiomer of 2-hydroxyglutarate linked to EGLN activation. Nature *483*, 484–488.

Kola, I., and Landis, J. (2004). Can the pharmaceutical industry reduce attrition rates? Nat. Rev. Drug Discov. *3*, 711–715.

Kondo, Y., Kanzawa, T., Sawaya, R., and Kondo, S. (2005). The role of autophagy in cancer development and response to therapy. Nat. Rev. Cancer *5*, 726–734.

Korkolopoulou, P., Patsouris, E., Konstantinidou, A.E., Pavlopoulos, P.M., Kavantzas, N., Boviatsis, E., Thymara, I., Perdiki, M., Thomas-Tsagli, E., Angelidakis, D., et al. (2004). Hypoxia-inducible factor 1alpha/vascular endothelial growth factor axis in astrocytomas. Associations with microvessel morphometry, proliferation and prognosis. Neuropathol. Appl. Neurobiol. *30*, 267–278.

Kroemer, G., Mariño, G., and Levine, B. (2010). Autophagy and the integrated stress response. Mol. Cell *40*, 280–293.

Kung, A.L., Zabludoff, S.D., France, D.S., Freedman, S.J., Tanner, E.A., Vieira, A., Cornell-Kennon, S., Lee, J., Wang, B., Wang, J., et al. (2004). Small molecule blockade of transcriptional coactivation of the hypoxia-inducible factor pathway. Cancer Cell *6*, 33–43.

Lai, A., Kharbanda, S., Pope, W.B., Tran, A., Solis, O.E., Peale, F., Forrest, W.F., Pujara, K., Carrillo, J.A., Pandita, A., et al. (2011). Evidence for Sequenced Molecular Evolution of IDH1 Mutant Glioblastoma From a Distinct Cell of Origin. J. Clin. Oncol. *29*, 4482–4490.

Lando, D., Peet, D.J., Whelan, D.A., Gorman, J.J., and Whitelaw, M.L. (2002). Asparagine hydroxylation of the HIF transactivation domain a hypoxic switch. Science *295*, 858–861.

Lee, J.-J., Kim, B.C., Park, M.-J., Lee, Y.-S., Kim, Y.-N., Lee, B.L., and Lee, J.-S. (2011). PTEN status switches cell fate between premature senescence and apoptosis in glioma exposed to ionizing radiation. Cell Death Differ. *18*, 666–677.

Lee, S.M., Koh, H.-J., Park, D.-C., Song, B.J., Huh, T.-L., and Park, J.-W. (2002). Cytosolic NADP+-dependent isocitrate dehydrogenase status modulates oxidative damage to cells. Free Radic. Biol. Med. *32*, 1185–1196.

Lee, Y., Auh, S.L., Wang, Y., Burnette, B., Wang, Y., Meng, Y., Beckett, M., Sharma, R., Chin, R., Tu, T., et al. (2009). Therapeutic effects of ablative radiation on local tumor require CD8+ T cells: changing strategies for cancer treatment. Blood *114*, 589–595.

Leonardi, R., Subramanian, C., Jackowski, S., and Rock, C.O. (2012). Cancer-associated Isocitrate Dehydrogenase Mutations Inactivate NADPH-dependent Reductive Carboxylation. J. Biol. Chem. *287*, 14615–14620.

Leu, S., von Felten, S., Frank, S., Vassella, E., Vajtai, I., Taylor, E., Schulz, M., Hutter, G., Hench, J., Schucht, P., et al. (2013). IDH/MGMT-driven molecular classification of low-grade glioma is a strong predictor for long-term survival. Neuro-Oncol. *15*, 469–479.

Li, C., Lu, H.-J., Na, F.-F., Deng, L., Xue, J.-X., Wang, J.-W., Wang, Y.-Q., Li, Q.-L., and Lu, Y. (2013a). Prognostic role of hypoxic inducible factor expression in non-small cell lung cancer: a meta-analysis. Asian Pac. J. Cancer Prev. APJCP *14*, 3607–3612.

Li, H., Ko, H.P., and Whitlock, J.P. (1996). Induction of phosphoglycerate kinase 1 gene expression by hypoxia. Roles of Arnt and HIF1alpha. J. Biol. Chem. *271*, 21262–21267.

Li, S., Chou, A.P., Chen, W., Chen, R., Deng, Y., Phillips, H.S., Selfridge, J., Zurayk, M., Lou, J.J., Everson, R.G., et al. (2013b). Overexpression of isocitrate dehydrogenase mutant proteins renders glioma cells more sensitive to radiation. Neuro-Oncol. *15*, 57.

Linkous, A.G., and Yazlovitskaya, E.M. (2011). Angiogenesis in glioblastoma multiforme: navigating the maze. Anticancer Agents Med. Chem. *11*, 712–718.

Liu, Q., and Cao, P. (2015). Clinical and prognostic significance of HIF-1α in glioma patients: a meta-analysis. Int. J. Clin. Exp. Med. *8*, 22073–22083.

Loenarz, C., and Schofield, C.J. (2008). Expanding chemical biology of 2-oxoglutarate oxygenases. Nat. Chem. Biol. *4*, 152–156.

Lopez, G.Y., Reitman, Z.J., Solomon, D., Waldman, T., Bigner, D.D., McLendon, R.E., Samuels, Y., and Yan, H. (2010). IDH1 mutation identified in human melanoma. Biochem. Biophys. Res. Commun. *398*, 585–587.

Louis, D.N., Holland, E.C., and Cairncross, J.G. (2001). Glioma Classification. Am. J. Pathol. *159*, 779–786.

Louis, D.N., Ohgaki, H., Wiestler, O.D., Cavenee, W.K., Burger, P.C., Jouvet, A., Scheithauer, B.W., and Kleihues, P. (2007). The 2007 WHO Classification of Tumours of the Central Nervous System. Acta Neuropathol. (Berl.) *114*, 97–109.

Lu, C., Ward, P.S., Kapoor, G.S., Rohle, D., Turcan, S., Abdel-Wahab, O., Edwards, C.R., Khanin, R., Figueroa, M.E., Melnick, A., et al. (2012). IDH mutation impairs histone demethylation and results in a block to cell differentiation. Nature *483*, 474–478.

Mahaffy, R.E., Park, S., Gerde, E., Käs, J., and Shih, C.K. (2004). Quantitative Analysis of the Viscoelastic Properties of Thin Regions of Fibroblasts Using Atomic Force Microscopy. Biophys. J. *86*, 1777–1793.

Maher, E.A., Furnari, F.B., Bachoo, R.M., Rowitch, D.H., Louis, D.N., Cavenee, W.K., and DePinho, R.A. (2001). Malignant glioma: genetics and biology of a grave matter. Genes Dev. *15*, 1311–1333.

Maher, E.A., Brennan, C., Wen, P.Y., Durso, L., Ligon, K.L., Richardson, A., Khatry, D., Feng, B., Sinha, R., Louis, D.N., et al. (2006). Marked Genomic Differences Characterize Primary and Secondary Glioblastoma Subtypes and Identify Two Distinct Molecular and Clinical Secondary Glioblastoma Entities. Cancer Res. *66*, 11502–11513.

Mailloux, R.J., Bériault, R., Lemire, J., Singh, R., Chénier, D.R., Hamel, R.D., and Appanna, V.D. (2007). The tricarboxylic acid cycle, an ancient metabolic network with a novel twist. PloS One *2*, e690.

Makino, Y., Cao, R., Svensson, K., Bertilsson, G., Asman, M., Tanaka, H., Cao, Y., Berkenstam, A., and Poellinger, L. (2001). Inhibitory PAS domain protein is a negative regulator of hypoxia-inducible gene expression. Nature *414*, 550–554.

Malik, B., and Nie, D. (2012). Cancer stem cells and resistance to chemo and radio therapy. Front. Biosci. Elite Ed. *4*, 2142–2149.

Manalo, D.J., Rowan, A., Lavoie, T., Natarajan, L., Kelly, B.D., Ye, S.Q., Garcia, J.G.N., and Semenza, G.L. (2005). Transcriptional regulation of vascular endothelial cell responses to hypoxia by HIF-1. Blood *105*, 659–669.

Mariotti, L.G., Pirovano, G., Savage, K.I., Ghita, M., Ottolenghi, A., Prise, K.M., and Schettino, G. (2013). Use of the γ-H2AX Assay to Investigate DNA Repair Dynamics Following Multiple Radiation Exposures. PLoS ONE *8*, e79541.

Mashiko, R., Takano, S., Ishikawa, E., Yamamoto, T., Nakai, K., and Matsumura, A. (2011). Hypoxia-inducible factor 1α expression is a prognostic biomarker in patients with astrocytic tumors associated with necrosis on MR image. J. Neurooncol. *102*, 43–50.

Masoud, G.N., and Li, W. (2015). HIF-1α pathway: role, regulation and intervention for cancer therapy. Acta Pharm. Sin. B *5*, 378–389.

Masson, N., and Ratcliffe, P.J. (2003). HIF prolyl and asparaginyl hydroxylases in the biological response to intracellular O2 levels. J. Cell Sci. *116*, 3041–3049.

Masson, N., Willam, C., Maxwell, P.H., Pugh, C.W., and Ratcliffe, P.J. (2001). Independent function of two destruction domains in hypoxia-inducible factor-α chains activated by prolyl hydroxylation. EMBO J. *20*, 5197–5206.

Maxwell, P.H., Wiesener, M.S., Chang, G.W., Clifford, S.C., Vaux, E.C., Cockman, M.E., Wykoff, C.C., Pugh, C.W., Maher, E.R., and Ratcliffe, P.J. (1999). The tumour suppressor protein VHL targets hypoxia-inducible factors for oxygen-dependent proteolysis. Nature *399*, 271–275.

Metallo, C.M., Gameiro, P.A., Bell, E.L., Mattaini, K.R., Yang, J., Hiller, K., Jewell, C.M., Johnson, Z.R., Irvine, D.J., Guarente, L., et al. (2011). Reductive glutamine metabolism by IDH1 mediates lipogenesis under hypoxia. Nature *481*, 380–384.

Metellus, P., Coulibaly, B., Colin, C., Paula, A.M. de, Vasiljevic, A., Taieb, D., Barlier, A., Boisselier, B., Mokhtari, K., Wang, X.W., et al. (2010). Absence of IDH mutation identifies a novel radiologic and molecular subtype of WHO grade II gliomas with dismal prognosis. Acta Neuropathol. (Berl.) *120*, 719–729.

Metellus, P., Colin, C., Taieb, D., Guedj, E., Nanni-Metellus, I., Paula, A.M. de, Colavolpe, C., Fuentes, S., Dufour, H., Barrie, M., et al. (2011). IDH mutation status impact on in vivo hypoxia biomarkers expression: new insights from a clinical, nuclear imaging and immunohistochemical study in 33 glioma patients. J. Neurooncol. *105*, 591–600.

Millauer, B., Shawver, L.K., Plate, K.H., Risau, W., and Ullrich, A. (1994). Glioblastoma growth inhibited in vivo by a dominant-negative Flk-1 mutant. Nature *367*, 576–579.

Minardi, D., Lucarini, G., Santoni, M., Mazzucchelli, R., Burattini, L., Conti, A., Principi, E., Bianconi, M., Scartozzi, M., Milanese, G., et al. (2015). Survival in patients with clear cell renal cell carcinoma is predicted by HIF-1α expression. Anticancer Res. *35*, 433–438.

Mitra, S., Cassar, S.E., Niles, D.J., Puskas, J.A., Frelinger, J.G., and Foster, T.H. (2006). Photodynamic therapy mediates the oxygen-independent activation of hypoxia-inducible factor 1alpha. Mol. Cancer Ther. *5*, 3268–3274.

Modrek, A.S., Bayin, N.S., and Placantonakis, D.G. (2014). Brain stem cells as the cell of origin in glioma. World J. Stem Cells *6*, 43–52.

Moeller, B.J., Dreher, M.R., Rabbani, Z.N., Schroeder, T., Cao, Y., Li, C.Y., and Dewhirst, M.W. (2005). Pleiotropic effects of HIF-1 blockade on tumor radiosensitivity. Cancer Cell *8*, 99–110.

Moon, E.J., Sonveaux, P., Porporato, P.E., Danhier, P., Gallez, B., Batinic-Haberle, I., Nien, Y.-C., Schroeder, T., and Dewhirst, M.W. (2010). NADPH oxidase-mediated reactive oxygen species production activates hypoxia-inducible factor-1 (HIF-1) via the ERK pathway after hyperthermia treatment. Proc. Natl. Acad. Sci. U. S. A. *107*, 20477–20482.

Mullen, A.R., Wheaton, W.W., Jin, E.S., Chen, P.-H., Sullivan, L.B., Cheng, T., Yang, Y., Linehan, W.M., Chandel, N.S., and DeBerardinis, R.J. (2011). Reductive carboxylation supports growth in tumor cells with defective mitochondria. Nature *481*, 385–388.

Murphy, M.P. (2009). How mitochondria produce reactive oxygen species. Biochem. J. *417*, 1–13.

Murphy, G., Cockett, M.I., Ward, R.V., and Docherty, A.J. (1991). Matrix metalloproteinase degradation of elastin, type IV collagen and proteoglycan. A quantitative comparison of the activities of 95 kDa and 72 kDa gelatinases, stromelysins-1 and -2 and punctuated metalloproteinase (PUMP). Biochem. J. *277*, 277–279.

National Cancer Institute (29.04.2015). Radiation Therapy. URL:http://www.cancer.gov/about-cancer/treatment/types/radiation-therapy. [Date of last access: 14.03.2016]

Network glia. URL:http://www.networkglia.eu/sites/networkglia.eu/files/docs/history_glia_engl.pdf. [Date of last access: 18.03.2016]

Newby, A.C. (2006). Matrix metalloproteinases regulate migration, proliferation, and death of vascular smooth muscle cells by degrading matrix and non-matrix substrates. Cardiovasc. Res. *69*, 614–624.

Newton, H.B. (2007). Handbook of Neuro-Oncology Neuroimaging (Academic Press).

Nicklin, P., Bergman, P., Zhang, B., Triantafellow, E., Wang, H., Nyfeler, B., Yang, H., Hild, M., Kung, C., Wilson, C., et al. (2009). Bidirectional Transport of Amino Acids Regulates mTOR and Autophagy. Cell *136*, 521–534.

Nordsmark, M., Bentzen, S.M., Rudat, V., Brizel, D., Lartigau, E., Stadler, P., Becker, A., Adam, M., Molls, M., Dunst, J., et al. (2005). Prognostic value of tumor oxygenation in 397 head and neck tumors after primary radiation therapy. An international multi-center study. Radiother. Oncol. J. Eur. Soc. Ther. Radiol. Oncol. *77*, 18–24.

Noushmehr (2011). Integrated genomic & epigenomic analyses of glioblastoma multiforme: Methods development and application.

Noushmehr, H., Weisenberger, D.J., Diefes, K., Phillips, H.S., Pujara, K., Berman, B.P., Pan, F., Pelloski, C.E., Sulman, E.P., Bhat, K.P., et al. (2010). Identification of a CpG island methylator phenotype that defines a distinct subgroup of glioma. Cancer Cell *17*, 510–522.

Nowell, P.C. (1976). The clonal evolution of tumor cell populations. Science *194*, 23–28.

Ohgaki, H., and Kleihues, P. (2013). The Definition of Primary and Secondary Glioblastoma. Clin. Cancer Res. *19*, 764–772.

Ohka, F., Ito, M., Ranjit, M., Senga, T., Motomura, A., Motomura, K., Saito, K., Kato, K., Kato, Y., Wakabayashi, T., et al. (2014). Quantitative metabolome analysis profiles activation of glutaminolysis in glioma with IDH1 mutation. Tumour Biol. J. Int. Soc. Oncodevelopmental Biol. Med. *35*, 5911–5920.

Okada, H., Kohanbash, G., Zhu, X., Kastenhuber, E.R., Hoji, A., Ueda, R., and Fujita, M. (2009). Immunotherapeutic Approaches for Glioma. Crit. Rev. Immunol. *29*, 1–42.

Olson, J.D., Riedel, E., and DeAngelis, L.M. (2000). Long-term outcome of low-grade oligodendroglioma and mixed glioma. Neurology *54*, 1442–1448.

O'Rourke, J.F., Tian, Y.-M., Ratcliffe, P.J., and Pugh, C.W. (1999). Oxygen-regulated and Transactivating Domains in Endothelial PAS Protein 1: Comparison with Hypoxia-inducible Factor-1α. J. Biol. Chem. *274*, 2060–2071.

Ostrom, Q.T., Gittleman, H., Fulop, J., Liu, M., Blanda, R., Kromer, C., Wolinsky, Y., Kruchko, C., and Barnholtz-Sloan, J.S. (2015). CBTRUS Statistical Report: Primary Brain and Central Nervous System Tumors Diagnosed in the United States in 2008-2012. Neuro-Oncol. *17*, iv1-iv62.

Ozben, T. (2007). Oxidative stress and apoptosis: impact on cancer therapy. J. Pharm. Sci. *96*, 2181–2196.

Palayoor, S.T., Mitchell, J.B., Cerna, D., DeGraff, W., John-Aryankalayil, M., and Coleman, C.N. (2008). PX-478, an inhibitor of hypoxia-inducible factor-1α, enhances radiosensitivity of prostate carcinoma cells. Int. J. Cancer J. Int. Cancer *123*, 2430–2437.

Papandreou, I., Krishna, C., Kaper, F., Cai, D., Giaccia, A.J., and Denko, N.C. (2005). Anoxia is necessary for tumor cell toxicity caused by a low-oxygen environment. Cancer Res. *65*, 3171–3178.

Parker, S.J., and Metallo, C.M. (2015). Metabolic consequences of oncogenic IDH mutations. Pharmacol. Ther. *152*, 54–62.

Parkin, D.M. (2006). The global health burden of infection-associated cancers in the year 2002. Int. J. Cancer *118*, 3030–3044.

Parsons, D.W., Jones, S., Zhang, X., Lin, J.C.-H., Leary, R.J., Angenendt, P., Mankoo, P., Carter, H., Siu, I.-M., Gallia, G.L., et al. (2008). An integrated genomic analysis of human glioblastoma multiforme. Science *321*, 1807–1812.

Paschka, P., Schlenk, R.F., Gaidzik, V.I., Habdank, M., Krönke, J., Bullinger, L., Späth, D., Kayser, S., Zucknick, M., Götze, K., et al. (2010). IDH1 and IDH2 mutations are frequent genetic alterations in acute myeloid leukemia and confer adverse prognosis in cytogenetically normal acute myeloid leukemia with NPM1 mutation without FLT3 internal tandem duplication. J. Clin. Oncol. Off. J. Am. Soc. Clin. Oncol. *28*, 3636–3643.

Paull, T.T., Rogakou, E.P., Yamazaki, V., Kirchgessner, C.U., Gellert, M., and Bonner, W.M. (2000). A critical role for histone H2AX in recruitment of repair factors to nuclear foci after DNA damage. Curr. Biol. *10*, 886–895.

Pellegata, N.S., Antoniono, R.J., Redpath, J.L., and Stanbridge, E.J. (1996). DNA damage and p53-mediated cell cycle arrest: A reevaluation. Proc. Natl. Acad. Sci. U. S. A. *93*, 15209–15214.

Pellegatta, S., Valletta, L., Corbetta, C., Patanè, M., Zucca, I., Riccardi Sirtori, F., Bruzzone, M.G., Fogliatto, G., Isacchi, A., Pollo, B., et al. (2015). Effective immuno-targeting of the IDH1 mutation R132H in a murine model of intracranial glioma. Acta Neuropathol. Commun. *3*, 4.

Pérès, E.A., Gérault, A.N., Valable, S., Roussel, S., Toutain, J., Divoux, D., Guillamo, J.-S., Sanson, M., Bernaudin, M., and Petit, E. (2014). Silencing erythropoietin receptor on glioma cells reinforces efficacy of temozolomide and X-rays through senescence and mitotic catastrophe. Oncotarget *6*, 2101–2119.

Pialoux, V., Mounier, R., Brown, A.D., Steinback, C.D., Rawling, J.M., and Poulin, M.J. (2009). Relationship between oxidative stress and HIF-1 alpha mRNA during sustained hypoxia in humans. Free Radic. Biol. Med. *46*, 321–326.

Poeck, K., and Hacke, W. (2013). Neurologie (Springer-Verlag).

Poirier, M.C. (2004). Chemical-induced DNA damage and human cancer risk. Nat. Rev. Cancer *4*, 630–637.

Pouysségur, J., Dayan, F., and Mazure, N.M. (2006). Hypoxia signalling in cancer and approaches to enforce tumour regression. Nature *441*, 437–443.

Pugh, C.W., O'Rourke, J.F., Nagao, M., Gleadle, J.M., and Ratcliffe, P.J. (1997). Activation of Hypoxia-inducible Factor-1; Definition of Regulatory Domains within the α Subunit. J. Biol. Chem. *272*, 11205–11214.

Qi, S., Yu, L., Li, H., Ou, Y., Qiu, X., Ding, Y., Han, H., and Zhang, X. (2014). Isocitrate dehydrogenase mutation is associated with tumor location and magnetic resonance imaging characteristics in astrocytic neoplasms. Oncol. Lett. *7*, 1895–1902.

Rabinovich, G.A., Gabrilovich, D., and Sotomayor, E.M. (2007). Immunosuppressive Strategies that are Mediated by Tumor Cells. Annu. Rev. Immunol. *25*, 267–296.

Rankin, E.B., and Giaccia, A.J. (2008). The role of hypoxia-inducible factors in tumorigenesis. Cell Death Differ. *15*, 678–685.

Recht, L.D., Lew, R., and Smith, T.W. (1992). Suspected low-grade glioma: is deferring treatment safe? Ann. Neurol. *31*, 431–436.

Reichl, E.M., Ren, Y., Morphew, M.K., Delannoy, M., Effler, J.C., Girard, K.D., Divi, S., Iglesias, P.A., Kuo, S.C., and Robinson, D.N. (2008). Interactions between myosin and actin crosslinkers control cytokinesis contractility dynamics and mechanics. Curr. Biol. CB *18*, 471–480.

Reijneveld, J.C., Sitskoorn, M.M., Klein, M., Nuyen, J., and Taphoorn, M.J. (2001). Cognitive status and quality of life in patients with suspected versus proven low-grade gliomas. Neurology *56*, 618–623.

Reitman, Z.J., and Yan, H. (2010). Isocitrate Dehydrogenase 1 and 2 Mutations in Cancer: Alterations at a Crossroads of Cellular Metabolism. JNCI J. Natl. Cancer Inst. *102*, 932–941.

Reitman, Z.J., Parsons, D.W., and Yan, H. (2010). IDH1 and IDH2: Not Your Typical Oncogenes. Cancer Cell *17*, 215–216.

Reitman, Z.J., Jin, G., Karoly, E.D., Spasojevic, I., Yang, J., Kinzler, K.W., He, Y., Bigner, D.D., Vogelstein, B., and Yan, H. (2011). Profiling the effects of isocitrate dehydrogenase 1 and 2 mutations on the cellular metabolome. Proc. Natl. Acad. Sci. U. S. A. *108*, 3270–3275.

Reszec, J., Hermanowicz, A., Rutkowski, R., Bernaczyk, P., Mariak, Z., and Chyczewski, L. (2013). Evaluation of mast cells and hypoxia inducible factor-1 expression in meningiomas of various grades in correlation with peritumoral brain edema. J. Neurooncol. *115*, 119–125.

Reyes, H., Reisz-Porszasz, S., and Hankinson, O. (1992). Identification of the Ah receptor nuclear translocator protein (Arnt) as a component of the DNA binding form of the Ah receptor. Science *256*, 1193–1195.

Rohle, D., Popovici-Muller, J., Palaskas, N., Turcan, S., Grommes, C., Campos, C., Tsoi, J., Clark, O., Oldrini, B., Komisopoulou, E., et al. (2013). An Inhibitor of Mutant IDH1 Delays Growth and Promotes Differentiation of Glioma Cells. Science *340*, 626.

Roninson, I.B. (2003). Tumor cell senescence in cancer treatment. Cancer Res. *63*, 2705–2715.

Ronnebaum, S.M., Ilkayeva, O., Burgess, S.C., Joseph, J.W., Lu, D., Stevens, R.D., Becker, T.C., Sherry, A.D., Newgard, C.B., and Jensen, M.V. (2006). A Pyruvate Cycling Pathway Involving Cytosolic NADP-dependent Isocitrate Dehydrogenase Regulates Glucose-stimulated Insulin Secretion. J. Biol. Chem. *281*, 30593–30602.

Ruas, J.L., Poellinger, L., and Pereira, T. (2002). Functional analysis of hypoxia-inducible factor-1 alpha-mediated transactivation. Identification of amino acid residues critical for transcriptional activation and/or interaction with CREB-binding protein. J. Biol. Chem. *277*, 38723–38730.

Rupnow, B.A., and Knox, S.J. (1999). The role of radiation-induced apoptosis as a determinant of tumor responses to radiation therapy. Apoptosis Int. J. Program. Cell Death *4*, 115–143.

Sabha, N., Knobbe, C.B., Maganti, M., Al Omar, S., Bernstein, M., Cairns, R., Çako, B., von Deimling, A., Capper, D., Mak, T.W., et al. (2014). Analysis of IDH mutation, 1p/19q deletion, and PTEN loss delineates prognosis in clinical low-grade diffuse gliomas. Neuro-Oncol. *16*, 914–923.

Safavi-Abbasi, S., Reis, C., Talley, M.C., Theodore, N., Nakaji, P., Spetzler, R.F., and Preul, M.C. (2006). Rudolf Ludwig Karl Virchow: pathologist, physician, anthropologist, and politician. Implications of his work for the understanding of cerebrovascular pathology and stroke. Neurosurg. Focus *20*, E1.

Said, H.M., Staab, A., Hagemann, C., Vince, G.H., Katzer, A., Flentje, M., and Vordermark, D. (2007a). Distinct patterns of hypoxic expression of carbonic anhydrase IX (CA IX) in human malignant glioma cell lines. J. Neurooncol. *81*, 27–38.

Said, H.M., Hagemann, C., Staab, A., Stojic, J., Kühnel, S., Vince, G.H., Flentje, M., Roosen, K., and Vordermark, D. (2007b). Expression patterns of the hypoxia-related genes osteopontin, CA9, erythropoietin, VEGF and HIF-1alpha in human glioma in vitro and in vivo. Radiother. Oncol. J. Eur. Soc. Ther. Radiol. Oncol. *83*, 398–405.

Salceda, S., and Caro, J. (1997). Hypoxia-inducible factor 1alpha (HIF-1alpha) protein is rapidly degraded by the ubiquitin-proteasome system under normoxic conditions. Its stabilization by hypoxia depends on redox-induced changes. J. Biol. Chem. *272*, 22642–22647.

Sancar, A., Lindsey-Boltz, L.A., Unsal-Kaçmaz, K., and Linn, S. (2004). Molecular mechanisms of mammalian DNA repair and the DNA damage checkpoints. Annu. Rev. Biochem. *73*, 39–85.

Sanson, M., Marie, Y., Paris, S., Idbaih, A., Laffaire, J., Ducray, F., Hallani, S.E., Boisselier, B., Mokhtari, K., Hoang-Xuan, K., et al. (2009). Isocitrate Dehydrogenase 1 Codon 132 Mutation Is an Important Prognostic Biomarker in Gliomas. J. Clin. Oncol. *27*, 4150–4154.

Sasaki, M., Knobbe, C.B., Itsumi, M., Elia, A.J., Harris, I.S., Chio, I.I.C., Cairns, R.A., McCracken, S., Wakeham, A., Haight, J., et al. (2012). D-2-hydroxyglutarate produced by mutant IDH1 perturbs collagen maturation and basement membrane function. Genes Dev. *26*, 2038–2049.

Schilling, D., Bayer, C., Emmerich, K., Molls, M., Vaupel, P., Huber, R.M., and Multhoff, G. (2012). Basal HIF-1α expression levels are not predictive for radiosensitivity of human cancer cell lines. Strahlenther. Onkol. Organ Dtsch. Röntgenges. Al *188*, 353–358.

Schmitt, C.A. (2007). Cellular senescence and cancer treatment. Biochim. Biophys. Acta *1775*, 5–20.

Schödel, J., Oikonomopoulos, S., Ragoussis, J., Pugh, C.W., Ratcliffe, P.J., and Mole, D.R. (2011). High-resolution genome-wide mapping of HIF-binding sites by ChIP-seq. Blood *117*, e207-217.

Schofield, C.J., and Ratcliffe, P.J. (2004). Oxygen sensing by HIF hydroxylases. Nat. Rev. Mol. Cell Biol. *5*, 343–354.

Schumacher, T., Bunse, L., Pusch, S., Sahm, F., Wiestler, B., Quandt, J., Menn, O., Osswald, M., Oezen, I., Ott, M., et al. (2014a). A vaccine targeting mutant IDH1 induces antitumour immunity. Nature *512*, 324–327.

Schumacher, T., Bunse, L., Wick, W., and Platten, M. (2014b). Mutant IDH1: An immunotherapeutic target in tumors. Oncoimmunology *3*, e974392.

Sedelnikova, O.A., Rogakou, E.P., Panyutin, I.G., and Bonner, W.M. (2002). Quantitative Detection of 125IdU-Induced DNA Double-Strand Breaks with γ-H2AX Antibody. Radiat. Res. *158*, 486–492.

Selak, M.A., Armour, S.M., MacKenzie, E.D., Boulahbel, H., Watson, D.G., Mansfield, K.D., Pan, Y., Simon, M.C., Thompson, C.B., and Gottlieb, E. (2005). Succinate links TCA cycle dysfunction to oncogenesis by inhibiting HIF-alpha prolyl hydroxylase. Cancer Cell *7*, 77–85.

Semenza, G.L. (2000). Hypoxia, clonal selection, and the role of HIF-1 in tumor progression. Crit. Rev. Biochem. Mol. Biol. *35*, 71–103.

Semenza, G.L. (2002). Involvement of Hypoxia-Inducible Factor 1 in Human Cancer. Intern. Med. *41*, 79–83.

Semenza, G.L. (2003). Targeting HIF-1 for cancer therapy. Nat. Rev. Cancer *3*, 721–732.

Semenza, G.L. (2007). Hypoxia and cancer. Cancer Metastasis Rev. *26*, 223–224.

Semenza, G.L. (2010). Defining the role of hypoxia-inducible factor 1 in cancer biology and therapeutics. Oncogene *29*, 625–634.

Semenza, G.L. (2012). Hypoxia-inducible factors: mediators of cancer progression and targets for cancer therapy. Trends Pharmacol. Sci. *33*, 207–214.

Semenza, G.L. (2013). HIF-1 mediates metabolic responses to intratumoral hypoxia and oncogenic mutations. J. Clin. Invest. *123*, 3664–3671.

Semenza, G.L. (2014). Oxygen sensing, hypoxia-inducible factors, and disease pathophysiology. Annu. Rev. Pathol. *9*, 47–71.

Semenza, G.L., Nejfelt, M.K., Chi, S.M., and Antonarakis, S.E. (1991). Hypoxia-inducible nuclear factors bind to an enhancer element located 3' to the human erythropoietin gene. Proc. Natl. Acad. Sci. U. S. A. *88*, 5680–5684.

Semenza, G.L., Roth, P.H., Fang, H.M., and Wang, G.L. (1994). Transcriptional regulation of genes encoding glycolytic enzymes by hypoxia-inducible factor 1. J. Biol. Chem. *269*, 23757–23763.

Semenza, G.L., Jiang, B.H., Leung, S.W., Passantino, R., Concordet, J.P., Maire, P., and Giallongo, A. (1996). Hypoxia response elements in the aldolase A, enolase 1, and lactate dehydrogenase A gene promoters contain essential binding sites for hypoxia-inducible factor 1. J. Biol. Chem. *271*, 32529–32537.

Shibata, T., Kokubu, A., Miyamoto, M., Sasajima, Y., and Yamazaki, N. (2011). Mutant IDH1 Confers an in Vivo Growth in a Melanoma Cell Line with BRAF Mutation. Am. J. Pathol. *178*, 1395–1402.

Siebert, G., Carsiotis, M., and Plaut, G.W. (1957). [The enzymatic properties of isocitric dehydrogenase]. J. Biol. Chem. *226*, 977–991.

Soffietti, R., Baumert, B. g., Bello, L., Von Deimling, A., Duffau, H., Frénay, M., Grisold, W., Grant, R., Graus, F., Hoang-Xuan, K., et al. (2010). Guidelines on management of low-grade gliomas: report of an EFNS–EANO* Task Force. Eur. J. Neurol. *17*, 1124–1133.

Spitz, D.R., Sim, J.E., Ridnour, L.A., Galoforo, S.S., and Lee, Y.J. (2000). Glucose deprivation-induced oxidative stress in human tumor cells. A fundamental defect in metabolism? Ann. N. Y. Acad. Sci. *899*, 349–362.

Srinivas, V., Zhang, L.P., Zhu, X.H., and Caro, J. (1999). Characterization of an oxygen/redox-dependent degradation domain of hypoxia-inducible factor alpha (HIF-alpha) proteins. Biochem. Biophys. Res. Commun. *260*, 557–561.

Staab, A., Loeffler, J., Said, H.M., Diehlmann, D., Katzer, A., Beyer, M., Fleischer, M., Schwab, F., Baier, K., Einsele, H., et al. (2007). Effects of HIF-1 inhibition by chetomin on hypoxia-related transcription and radiosensitivity in HT 1080 human fibrosarcoma cells. BMC Cancer *7*, 213.

Stamenović, D., and Coughlin, M.F. (1999). The role of prestress and architecture of the cytoskeleton and deformability of cytoskeletal filaments in mechanics of adherent cells: a quantitative analysis. J. Theor. Biol. *201*, 63–74.

Stupp, R., Mason, W.P., van den Bent, M.J., Weller, M., Fisher, B., Taphoorn, M.J.B., Belanger, K., Brandes, A.A., Marosi, C., Bogdahn, U., et al. (2005). Radiotherapy plus Concomitant and Adjuvant Temozolomide for Glioblastoma. N. Engl. J. Med. *352*, 987–996.

Stupp, R., Hegi, M.E., van den Bent, M.J., Mason, W.P., Weller, M., Mirimanoff, R.O., Cairncross, J.G., European Organisation for Research and Treatment of Cancer Brain Tumor and Radiotherapy Groups, and National Cancer Institute of Canada Clinical Trials Group (2006). Changing paradigms--an update on the multidisciplinary management of malignant glioma. The Oncologist *11*, 165–180.

Stupp, R., Tonn, J.-C., Brada, M., Pentheroudakis, G., and Group, O. behalf of the E.G.W. (2010). High-grade malignant glioma: ESMO Clinical Practice Guidelines for diagnosis, treatment and follow-up. Ann. Oncol. *21*, v190–v193.

Stupp, R., Brada, M., Bent, M.J. van den, Tonn, J.-C., and Pentheroudakis, G. (2014). High-grade glioma: ESMO Clinical Practice Guidelines for diagnosis, treatment and follow-up. Ann. Oncol. *25*, iii93-iii101.

Sturm, D., Witt, H., Hovestadt, V., Khuong-Quang, D.-A., Jones, D.T.W., Konermann, C., Pfaff, E., Tönjes, M., Sill, M., Bender, S., et al. (2012). Hotspot Mutations in H3F3A and IDH1 Define Distinct Epigenetic and Biological Subgroups of Glioblastoma. Cancer Cell *22*, 425–437.

Suzuki, K., Ojima, M., Kodama, S., and Watanabe, M. (2003). Radiation-induced DNA damage and delayed induced genomic instability. Oncogene *22*, 6988–6993.

Swaminathan, V., Mythreye, K., O'Brien, E.T., Berchuck, A., Blobe, G.C., and Superfine, R. (2011). Mechanical stiffness grades metastatic potential in patient tumor cells and in cancer cell lines. Cancer Res. *71*, 5075–5080.

Takeshima, T., Chamoto, K., Wakita, D., Ohkuri, T., Togashi, Y., Shirato, H., Kitamura, H., and Nishimura, T. (2010). Local radiation therapy inhibits tumor growth through the generation of tumor-specific CTL: its potentiation by combination with Th1 cell therapy. Cancer Res. *70*, 2697–2706.

Taylor, L.P. (2010). Diagnosis, treatment, and prognosis of glioma Five new things. Neurology *75*, S28–S32.

Teresa Pinto, A., Laranjeiro Pinto, M., Patrícia Cardoso, A., Monteiro, C., Teixeira Pinto, M., Filipe Maia, A., Castro, P., Figueira, R., Monteiro, A., Marques, M., et al. (2016). Ionizing radiation modulates human macrophages towards a pro-inflammatory phenotype preserving their pro-invasive and pro-angiogenic capacities. Sci. Rep. *6*.

Tian, H., McKnight, S.L., and Russell, D.W. (1997). Endothelial PAS domain protein 1 (EPAS1), a transcription factor selectively expressed in endothelial cells. Genes Dev. *11*, 72–82.

Tian, H., Hammer, R.E., Matsumoto, A.M., Russell, D.W., and McKnight, S.L. (1998). The hypoxia-responsive transcription factor EPAS1 is essential for catecholamine homeostasis and protection against heart failure during embryonic development. Genes Dev. *12*, 3320–3324.

Tonn, J.-C., Westphal, M., Rutka, J.T., and Grossman, S.A. (2006). Neuro-Oncology of CNS Tumors (Springer Science & Business Media).

Torre, L.A., Bray, F., Siegel, R.L., Ferlay, J., Lortet-Tieulent, J., and Jemal, A. (2015). Global cancer statistics, 2012. CA. Cancer J. Clin. *65*, 87–108.

Tran, A.N., Lai, A., Li, S., Pope, W.B., Teixeira, S., Harris, R.J., Woodworth, D.C., Nghiemphu, P.L., Cloughesy, T.F., and Ellingson, B.M. (2014). Increased sensitivity to radiochemotherapy in IDH1 mutant glioblastoma as demonstrated by serial quantitative MR volumetry. Neuro-Oncol. *16*, 414–420.

Turcan, S., Rohle, D., Goenka, A., Walsh, L.A., Fang, F., Yilmaz, E., Campos, C., Fabius, A.W.M., Lu, C., Ward, P.S., et al. (2012). IDH1 mutation is sufficient to establish the glioma hypermethylator phenotype. Nature *483*, 479–483.

Turkalp Z, Karamchandani J, and Das S (2014). Idh mutation in glioma: New insights and promises for the future. JAMA Neurol. *71*, 1319–1325.

Van Gool, S., Maes, W., Ardon, H., Verschuere, T., Van Cauter, S., and De Vleeschouwer, S. (2009). Dendritic cell therapy of high-grade gliomas. Brain Pathol. Zurich Switz. *19*, 694–712.

Van Meir, E.G., Hadjipanayis, C.G., Norden, A.D., Shu, H.-K., Wen, P.Y., and Olson, J.J. (2010). Exciting New Advances in Neuro-Oncology. CA. Cancer J. Clin. *60*, 166–193.

Vander Heiden, M.G., Cantley, L.C., and Thompson, C.B. (2009). Understanding the Warburg Effect: The Metabolic Requirements of Cell Proliferation. Science *324*, 1029–1033.

Vaupel, P. (1996). Oxygen transport in tumors: characteristics and clinical implications. Adv. Exp. Med. Biol. *388*, 341–351.

Vaupel, P., and Mayer, A. (2007). Hypoxia in cancer: significance and impact on clinical outcome. Cancer Metastasis Rev. *26*, 225–239.

Vaupel, P., and Mayer, A. (2014). Hypoxia in tumors: pathogenesis-related classification, characterization of hypoxia subtypes, and associated biological and clinical implications. Adv. Exp. Med. Biol. *812*, 19–24.

Vaupel, P., Kallinowski, F., and Okunieff, P. (1989). Blood Flow, Oxygen and Nutrient Supply, and Metabolic Microenvironment of Human Tumors: A Review. Cancer Res. *49*, 6449–6465.

Vaupel, P., Kelleher, D.K., and Höckel, M. (2001). Oxygen status of malignant tumors: pathogenesis of hypoxia and significance for tumor therapy. Semin. Oncol. *28*, 29–35.

Vaupel, P., Briest, S., and Höckel, M. (2002). Hypoxia in breast cancer: pathogenesis, characterization and biological/therapeutic implications. Wien. Med. Wochenschr. 1946 *152*, 334–342.

Verhaak, R.G.W., Hoadley, K.A., Purdom, E., Wang, V., Qi, Y., Wilkerson, M.D., Miller, C.R., Ding, L., Golub, T., Mesirov, J.P., et al. (2010). An integrated genomic analysis identifies clinically relevant subtypes of glioblastoma characterized by abnormalities in PDGFRA, IDH1, EGFR and NF1. Cancer Cell *17*, 98.

Vordermark, D., and Brown, J.M. (2003a). Evaluation of hypoxia-inducible factor-1alpha (HIF-1alpha) as an intrinsic marker of tumor hypoxia in U87 MG human glioblastoma: in vitro and xenograft studies. Int. J. Radiat. Oncol. Biol. Phys. *56*, 1184–1193.

Vordermark, D., and Brown, J.M. (2003b). Endogenous markers of tumor hypoxia predictors of clinical radiation resistance? Strahlenther Onkol *179*, 801–811.

Vordermark, D., Katzer, A., Baier, K., Kraft, P., and Flentje, M. (2004). Cell type-specific association of hypoxia-inducible factor-1 alpha (HIF-1 alpha) protein accumulation and radiobiologic tumor hypoxia. Int. J. Radiat. Oncol. Biol. Phys. *58*, 1242–1250.

Vordermark, D., Kaffer, A., Riedl, S., Katzer, A., and Flentje, M. (2005). Characterization of carbonic anhydrase IX (CA IX) as an endogenous marker of chronic hypoxia in live human tumor cells. Int. J. Radiat. Oncol. Biol. Phys. *61*, 1197–1207.

Waitkus, M.S., Diplas, B.H., and Yan, H. (2016). Isocitrate dehydrogenase mutations in gliomas. Neuro-Oncol. *18*, 16–26.

Walsh, J.C., Lebedev, A., Aten, E., Madsen, K., Marciano, L., and Kolb, H.C. (2014). The Clinical Importance of Assessing Tumor Hypoxia: Relationship of Tumor Hypoxia to Prognosis and Therapeutic Opportunities. Antioxid. Redox Signal. *21*, 1516–1554.

Wang, G.L., and Semenza, G.L. (1995). Purification and characterization of hypoxia-inducible factor 1. J. Biol. Chem. *270*, 1230–1237.

Wang, G.L., Jiang, B.H., Rue, E.A., and Semenza, G.L. (1995). Hypoxia-inducible factor 1 is a basic-helix-loop-helix-PAS heterodimer regulated by cellular O2 tension. Proc. Natl. Acad. Sci. U. S. A. *92*, 5510–5514.

Wang, X.-W., Labussière, M., Valable, S., Pérès, E.A., Guillamo, J.-S., Bernaudin, M., and Sanson, M. (2014). IDH1R132H Mutation Increases U87 Glioma Cell Sensitivity to Radiation Therapy in Hypoxia. BioMed Res. Int. *2014*.

Warburg, O. (1956). On the origin of cancer cells. Science *123*, 309–314.

Ward, P.S., Patel, J., Wise, D.R., Abdel-Wahab, O., Bennett, B.D., Coller, H.A., Cross, J.R., Fantin, V.R., Hedvat, C.V., Perl, A.E., et al. (2010). The common feature of leukemia-associated IDH1 and IDH2 mutations is a neomorphic enzyme activity converting alpha-ketoglutarate to 2-hydroxyglutarate. Cancer Cell *17*, 225–234.

Watanabe, T., Kuramochi, H., Takahashi, A., Imai, K., Katsuta, N., Nakayama, T., Fujiki, H., and Suganuma, M. (2012). Higher cell stiffness indicating lower metastatic potential in B16 melanoma cell variants and in (-)-epigallocatechin gallate-treated cells. J. Cancer Res. Clin. Oncol. *138*, 859–866.

Weinhouse, S. (1956). On respiratory impairment in cancer cells. Science *124*, 267–269.

Weller, M., Stupp, R., Hegi, M.E., van den Bent, M., Tonn, J.C., Sanson, M., Wick, W., and Reifenberger, G. (2012). Personalized care in neuro-oncology coming of age: why we need MGMT and 1p/19q testing for malignant glioma patients in clinical practice. Neuro-Oncol. *14*, iv100-iv108.

Wen, P.Y., and Kesari, S. (2008). Malignant gliomas in adults. N. Engl. J. Med. *359*, 492–507.

Wenger, R.H., Stiehl, D.P., and Camenisch, G. (2005). Integration of oxygen signaling at the consensus HRE. Sci. STKE Signal Transduct. Knowl. Environ. *2005*, re12.

Wesseling, P., Kros, J.M., and Jeuken, J.W.M. (2011). The pathological diagnosis of diffuse gliomas: towards a smart synthesis of microscopic and molecular information in a multidisciplinary context. Diagn. Histopathol. *17*, 486–494.

Westermark, B. (2012). Glioblastoma—a moving target. Ups. J. Med. Sci. *117*, 251–256.

Wick, W., Naumann, U., and Weller, M. (2006). Transforming growth factor-beta: a molecular target for the future therapy of glioblastoma. Curr. Pharm. Des. *12*, 341–349.

Williams, S.C., Karajannis, M.A., Chiriboga, L., Golfinos, J.G., von Deimling, A., and Zagzag, D. (2011). R132H-mutation of Isocitrate Dehydrogenase-1 is not Sufficient for HIF-1α Upregulation in Adult Glioma. Acta Neuropathol. (Berl.) *121*, 279–281.

Winter, A.D., and Page, A.P. (2000). Prolyl 4-Hydroxylase Is an Essential Procollagen-Modifying Enzyme Required for Exoskeleton Formation and the Maintenance of Body Shape in the Nematode Caenorhabditis elegans. Mol. Cell. Biol. *20*, 4084–4093.

Wise, D.R., Ward, P.S., Shay, J.E.S., Cross, J.R., Gruber, J.J., Sachdeva, U.M., Platt, J.M., DeMatteo, R.G., Simon, M.C., and Thompson, C.B. (2011). Hypoxia promotes isocitrate dehydrogenase-dependent carboxylation of α-ketoglutarate to citrate to support cell growth and viability. Proc. Natl. Acad. Sci. U. S. A. *108*, 19611–19616.

World Health Organization/International Agency for Research of Cancer. THE GLOBOCAN PROJECT. URL:http://globocan.iarc.fr/. [Date of last access: 18.03.2016]

Xia, L., Wu, B., Fu, Z., Feng, F., Qiao, E., Li, Q., Sun, C., and Ge, M. (2015). Prognostic role of IDH mutations in gliomas: a meta-analysis of 55 observational studies. Oncotarget *6*, 17354–17365.

Xia, Y., Choi, H.-K., and Lee, K. (2012). Recent advances in hypoxia-inducible factor (HIF)-1 inhibitors. Eur. J. Med. Chem. *49*, 24–40.

Xu, W., Yang, H., Liu, Y., Yang, Y., Wang, P., Kim, S.-H., Ito, S., Yang, C., Wang, P., Xiao, M.-T., et al. (2011). Oncometabolite 2-hydroxyglutarate is a competitive inhibitor of α-ketoglutarate-dependent dioxygenases. Cancer Cell *19*, 17–30.

Xu, X., Zhao, J., Xu, Z., Peng, B., Huang, Q., Arnold, E., and Ding, J. (2004). Structures of human cytosolic NADP-dependent isocitrate dehydrogenase reveal a novel self-regulatory mechanism of activity. J. Biol. Chem. *279*, 33946–33957.

Yan, H., Parsons, D.W., Jin, G., McLendon, R., Rasheed, B.A., Yuan, W., Kos, I., Batinic-Haberle, I., Jones, S., Riggins, G.J., et al. (2009). IDH1 and IDH2 Mutations in Gliomas. N. Engl. J. Med. *360*, 765–773.

Yang, H., Ye, D., Guan, K.-L., and Xiong, Y. (2012). IDH1 and IDH2 Mutations in Tumorigenesis: Mechanistic Insights and Clinical Perspectives. Clin. Cancer Res. *18*, 5562–5571.

Ye, L.-Y., Zhang, Q., Bai, X.-L., Pankaj, P., Hu, Q.-D., and Liang, T.-B. (2014). Hypoxia-inducible factor 1α expression and its clinical significance in pancreatic cancer: a meta-analysis. Pancreatol. Off. J. Int. Assoc. Pancreatol. IAP Al *14*, 391–397.

Yeo, E.-J., Chun, Y.-S., Cho, Y.-S., Kim, J., Lee, J.-C., Kim, M.-S., and Park, J.-W. (2003). YC-1: A Potential Anticancer Drug Targeting Hypoxia-Inducible Factor 1. J. Natl. Cancer Inst. *95*, 516–525.

Ying, W. (2008). NAD+/NADH and NADP+/NADPH in cellular functions and cell death: regulation and biological consequences. Antioxid. Redox Signal. *10*, 179–206.

Yoshihara, T., Hamamoto, T., Munakata, R., Tajiri, R., Ohsumi, M., and Yokota, S. (2001). Localization of Cytosolic NADP-dependent Isocitrate Dehydrogenase in the Peroxisomes of Rat Liver Cells Biochemical and Immunocytochemical Studies. J. Histochem. Cytochem. *49*, 1123–1131.

Zeng, J., See, A.P., Phallen, J., Jackson, C.M., Belcaid, Z., Ruzevick, J., Durham, N., Meyer, C., Harris, T.J., Albesiano, E., et al. (2013). Anti-PD-1 blockade and stereotactic radiation produce long-term survival in mice with intracranial gliomas. Int. J. Radiat. Oncol. Biol. Phys. *86*, 343–349.

Zhang, H., Bosch-Marce, M., Shimoda, L.A., Tan, Y.S., Baek, J.H., Wesley, J.B., Gonzalez, F.J., and Semenza, G.L. (2008). Mitochondrial Autophagy Is an HIF-1-dependent Adaptive Metabolic Response to Hypoxia. J. Biol. Chem. *283*, 10892–10903.

Zhao, S., Lin, Y., Xu, W., Jiang, W., Zha, Z., Wang, P., Yu, W., Li, Z., Gong, L., Peng, Y., et al. (2009). Glioma-Derived Mutations in IDH1 Dominantly Inhibit IDH1 Catalytic Activity and Induce HIF-1α. Science *324*, 261.

Zheng, B., Yao, Y., Liu, Z., Deng, L., Anglin, J.L., Jiang, H., Prasad, B.V.V., and Song, Y. (2013). Crystallographic Investigation and Selective Inhibition of Mutant Isocitrate Dehydrogenase. ACS Med. Chem. Lett. *4*, 542–546.

Zhong, H., Marzo, A.M.D., Laughner, E., Lim, M., Hilton, D.A., Zagzag, D., Buechler, P., Isaacs, W.B., Semenza, G.L., and Simons, J.W. (1999). Overexpression of Hypoxia-inducible Factor 1α in Common Human Cancers and Their Metastases. Cancer Res. *59*, 5830–5835.

## 7.1    List of figures

## 7.2   List of tables

# 8 APPENDIX

## 8.1 Supplementary material

### 8.1.1 Immunofluorescence staining of IDH1$^{wt}$ and IDH1$^{R132H}$ protein expression patterns in stably transduced U-343MG cells
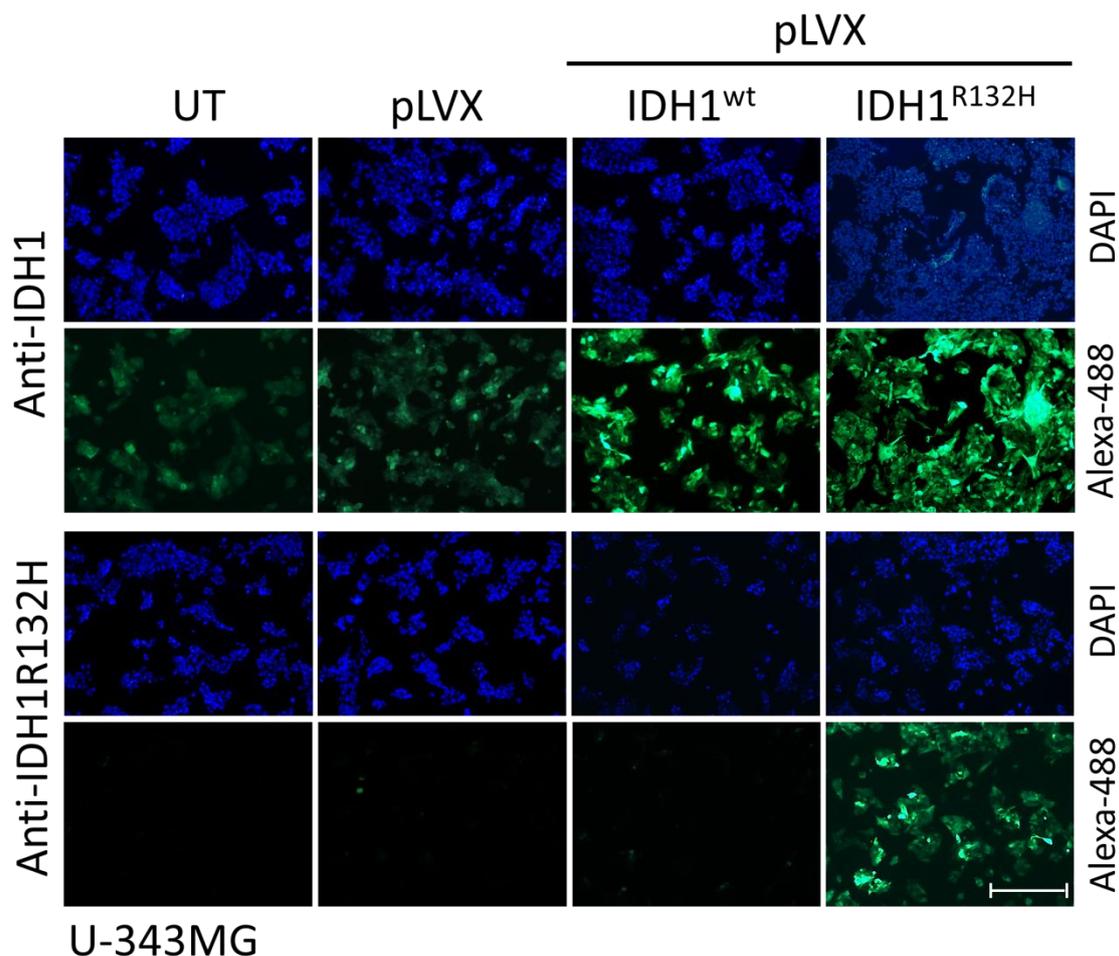


**Figure 8.1. Immunofluorescence staining of transduced U-343MG glioma cells stably expressed IDH1$^{wt}$ or IDH1$^{R312H}$ protein.** Representative immunofluorescence staining of IDH1$^{wt}$ and IDH1$^{R132H}$ protein in U-343MG cells using anti-IDH1 and anti-IDH1R132H antibodies. Stable cell lines showed a diffuse cytoplasmic distribution of IDH1$^{wt}$ or IDH1$^{R132H}$ protein. Immunofluorescence staining was achieved 24 h after seeding. Cell nuclei were counterstained with DAPI. n=3 independent experiments; scale bar=100 μm. UT: untreated cells, pLVX: cells stably transduced with empty vector, pLVX IDH1$^{wt}$: cells overexpressing IDH1$^{wt}$, pLVX IDH1$^{R132H}$: cells overexpressing IDH1$^{R132H}$.
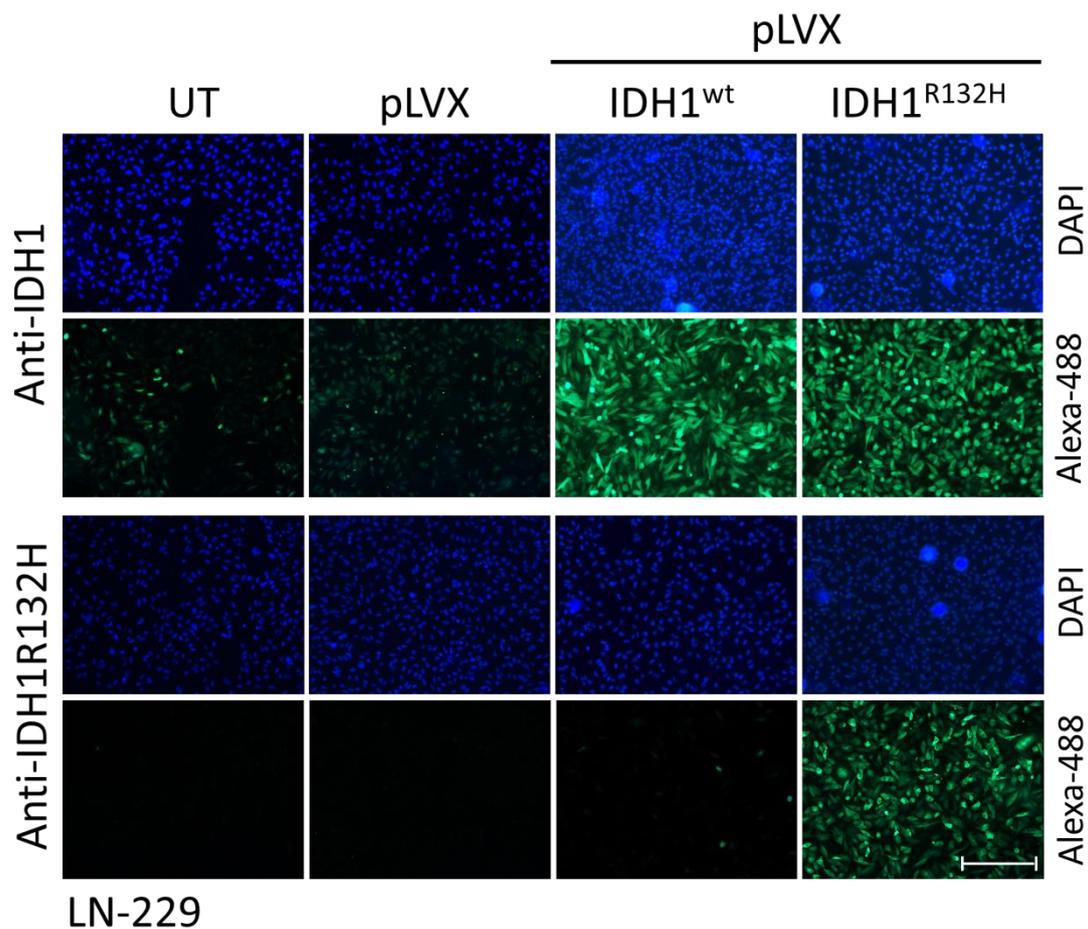
**Figure 8.2. Immunofluorescence staining of transduced LN-229 glioma cells stably expressed IDH1<sup>wt</sup> or IDH1<sup>R312H</sup> protein.** Representative immunofluorescence staining of IDH1$^{wt}$ and IDH1$^{R132H}$ protein in LN-229 cells using anti-IDH1 and anti-IDH1R132H antibodies. Stable cell lines showed a diffuse cytoplasmic distribution of IDH1$^{wt}$ or IDH1$^{R132H}$ protein. Immunofluorescence staining was achieved 24 h after seeding. Cell nuclei were counterstained with DAPI. n=3 independent experiments; scale bar=100 μm. UT: untreated cells, pLVX: cells stably transduced with empty vector, pLVX IDH1$^{wt}$: cells overexpressing IDH1$^{wt}$, pLVX IDH1$^{R132H}$: cells overexpressing IDH1$^{R132H}$.

### 8.1.2 Evaluation of HIF-1α and CAIX expression by immunohistochemical staining

Immunohistochemical staining of IDH1$^{R132H}$, HIF-1α and CAIX protein expression patterns, in stably transduced U-251MG, U-343MG and LN-229 cells (Figure 8.3 Figure 8.4 Figure 8.5). IDH1$^{R132H}$-, HIF-1α- and CAIX scoring results of the investigated cell lines are listed in Table 8.1.

**Table 8.1. IDH1$^{R132H}$, HIF-1α and CAIX protein expression in stably transduced glioma cells.** HIF-1α score: 0, no staining; 1, nuclear staining in 1–10 % of cells and/or with weak cytoplasmic staining; 2, nuclear staining in 11–50 % of cells and/or with distinct cytoplasmic staining; 3, nuclear staining in more than 50 % of cells and/or with distinct cytoplasmic staining; 4, nuclear staining in more than 50 % of cells and/or with strong cytoplasmic staining. IDH1$^{R132H}$ and CAIX score: 0, no cells stained; 1, less than 10 % of cells stained; 2, 11-50 % of cells stained; 3, more than 50 % of cells show a distinct staining; 4, more than 50 % of cells show a strong staining.

**IDH1$^{R132H}$ protein expression in stably transduced U-251MG, U-343MG and LN-229 cells**

| Cells | conditions | UT | pLVX | IDH1$^{wt}$ | IDH1$^{R132H}$ |
|---|---|---|---|---|---|
| U-251MG | normoxia | 0 | 0 | 0 | 4 |
| U-251MG | hypoxia | 0 | 0 | 0 | 4 |
| U-343MG | normoxia | 0 | 0 | 0 | 4 |
| U-343MG | hypoxia | 0 | 0 | 0 | 4 |
| LN-229 | normoxia | 0 | 0 | 0 | 4 |
| LN-229 | hypoxia | 0 | 0 | 0 | 4 |

**HIF-1α protein expression in stably transduced U-251MG, U-343MG and LN-229 cells**

| Cells | conditions | UT | pLVX | IDH1$^{wt}$ | IDH1$^{R132H}$ |
|---|---|---|---|---|---|
| U-251MG | normoxia | 0 | 0 | 0 | 3 |
| U-251MG | hypoxia | 3 | 3 | 3 | 4 |
| U-343MG | normoxia | 0 | 0 | 0 | 2 |
| U-343MG | hypoxia | 1 | 1 | 1 | 2 |
| LN-229 | normoxia | 0 | 0 | 0 | 0 |
| LN-229 | hypoxia | 3 | 3 | 3 | 2 |

**CAIX protein expression in stably transduced U-251MG, U-343MG and LN-229 cells**

| Cells | conditions | UT | pLVX | IDH1$^{wt}$ | IDH1$^{R132H}$ |
|---|---|---|---|---|---|
| U-251MG | normoxia | 3 | 3 | 3 | 4 |
| U-251MG | hypoxia | 3 | 3 | 3 | 4 |
| U-343MG | normoxia | 2 | 2 | 2 | 3 |
| U-343MG | hypoxia | 3 | 3 | 3 | 4 |
| LN-229 | normoxia | 4 | 4 | 4 | 3 |
| LN-229 | hypoxia | 4 | 4 | 4 | 2 |
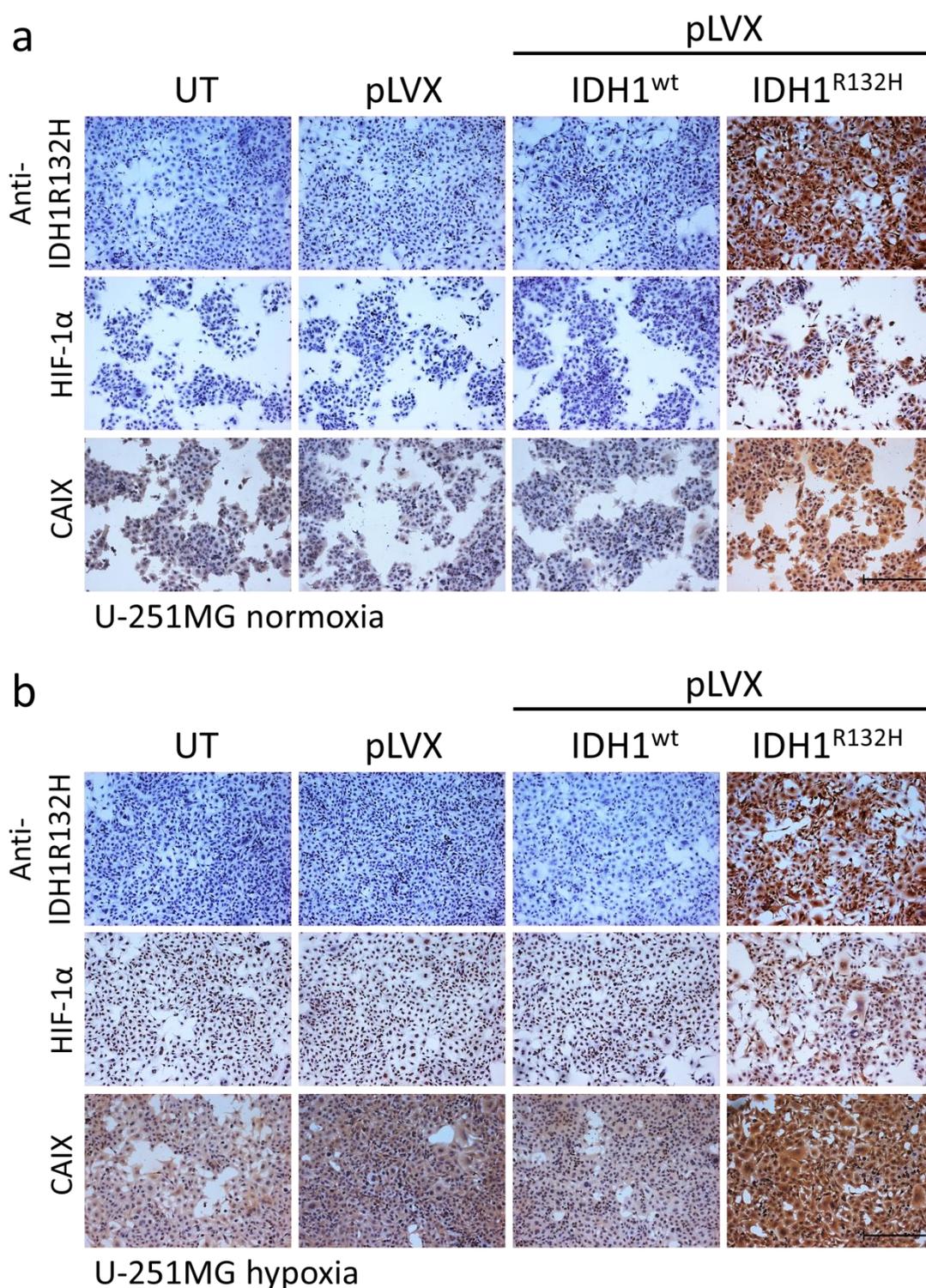
**Figure 8.3. Effect of IDH1$^{R132H}$ gene expression on HIF-1α and CAIX gene expression in U-251MG cells.**
Representative immunohistochemical staining of IDH1$^{R132H}$, HIF-1α and CAIX protein in stably transduced U-251MG cells under normoxic (a, 21 % O$_2$) and hypoxic (b, <0.1 % O$_2$) conditions. Cell nuclei were counterstained with 20 % hematoxylin. n=3 independent experiments; scale bar=100 µm. UT: untreated, pLVX: cells stably transduced with empty vector, pLVX IDH1$^{wt}$: IDH1$^{wt}$-expressing cells, pLVX IDH1$^{R132H}$: IDH1$^{R132H}$-expressing cells.
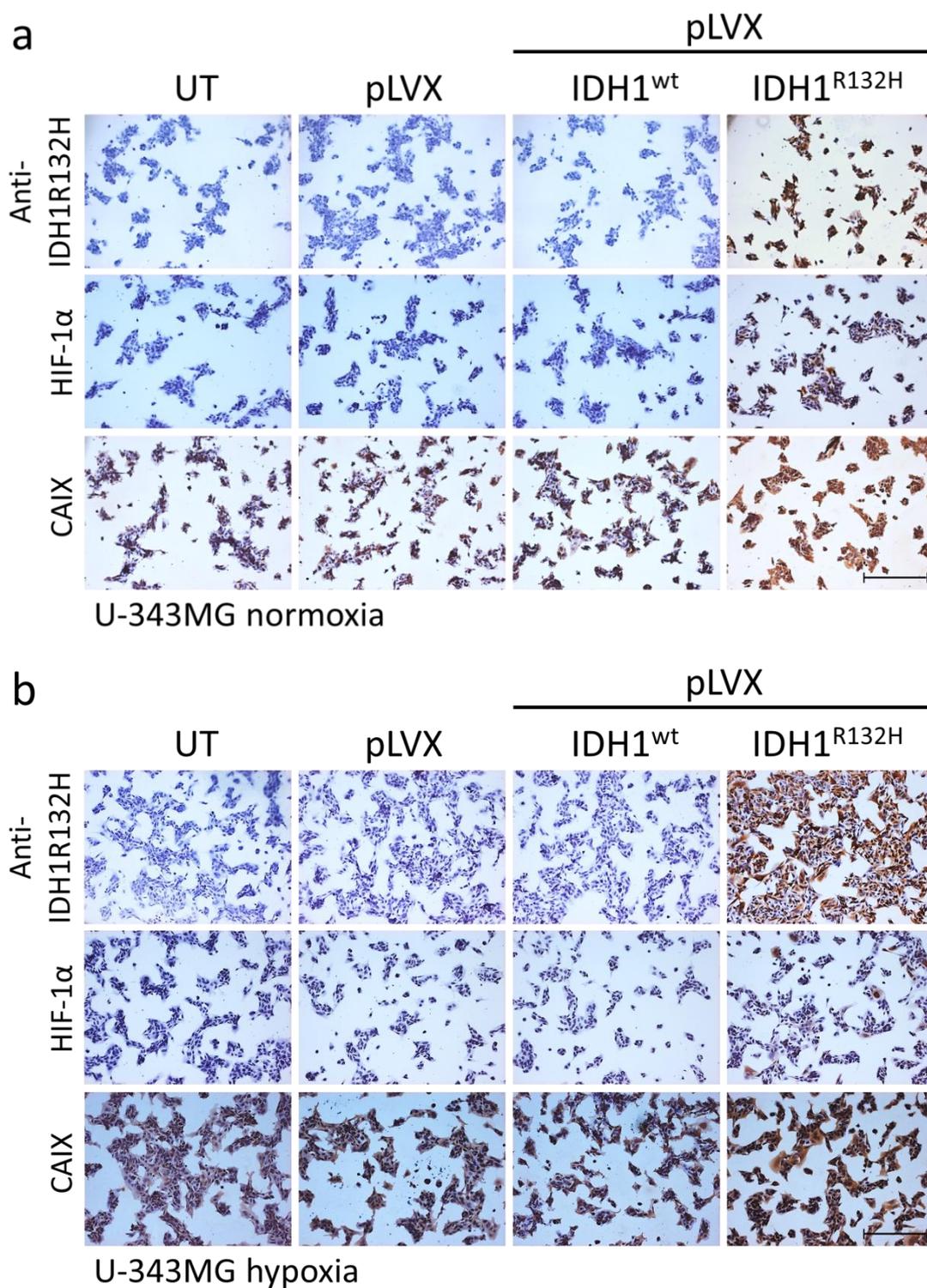
**Figure 8.4. Effect of IDH1$^{R132H}$ gene expression on HIF-1α and CAIX gene expression in U-343MG cells.** Representative immunohistochemical staining of IDH1$^{R132H}$, HIF-1α and CAIX protein in stably transduced U-343MG cells under normoxic (a, 21 % O$_2$) and hypoxic (b, <0.1 % O$_2$) conditions. Cell nuclei were counterstained with 20 % hematoxylin. n=3 independent experiments; scale bar=100 μm. UT: untreated, pLVX: cells stably transduced with empty vector, pLVX IDH1$^{wt}$: IDH1$^{wt}$-expressing cells, pLVX IDH1$^{R132H}$: IDH1$^{R132H}$-expressing cells.
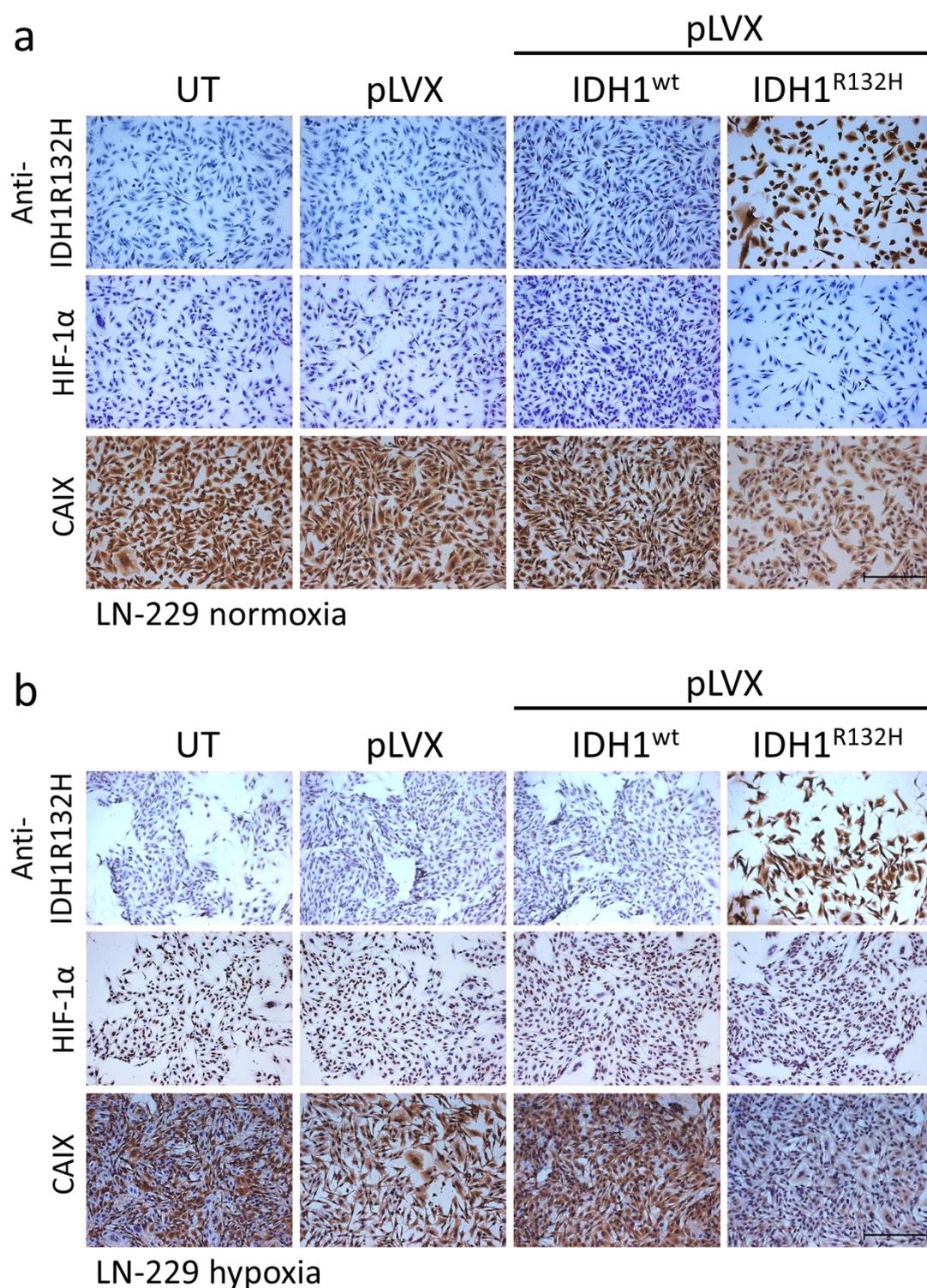
**Figure 8.5. Effect of IDH1$^{R132H}$ gene expression on HIF-1α and CAIX gene expression in LN-229 cells.** Representative immunohistochemical staining of IDH1$^{R132H}$, HIF-1α and CAIX protein in stably transduced LN-229 cells under normoxic (a, 21 % O$_2$) and hypoxic (b, <0.1 % O$_2$) conditions. Cell nuclei were counterstained with 20 % hematoxylin. n=3 independent experiments; scale bar=100 µm. UT: untreated, pLVX: cells stably transduced with empty vector, pLVX IDH1$^{wt}$: IDH1$^{wt}$-expressing cells, pLVX IDH1$^{R132H}$: IDH1$^{R132H}$-expressing cells.

# Eidesstattliche Erklärung

Hiermit erkläre ich, dass ich die vorliegende Dissertation selbstständig und nur unter Verwendung der angegebenen Quellen und Hilfsmittel angefertigt habe. Textstellen, die aus diesen Werken inhaltlich oder wörtlich übernommen wurden, sind als solche gekennzeichnet.

Weiterhin versichere ich, dass die Dissertation ausschließlich der Naturwissenschaftlichen Fakultät I der Martin-Luther-Universität Halle-Wittenberg vorgelegt wurde und ich mich erstmals für die Erlangung des Doktorgrades bewerbe.

Halle (Saale), den                                        Jacqueline Keßler

# DANKSAGUNG

# Curriculum Vitae

**Persönliche Daten**

| | |
|---|---|
| Name | Jacqueline Keßler |
| Geburtsdatum | 28.10.1981 |
| Geburtsort | Apolda |
| Familienstand | ledig, ein Kind |
| Staatsangehörigkeit | deutsch |

**Ausbildung**

| | |
|---|---|
| 10/2000-03/2008 | Studium der Biologie an der Martin-Luther-Universität Halle-Wittenberg, Thema: „Charakterisierung von adulten humanen mesenchymalen Stammzellen in ihrer mRNA-Expression und ihrem strahlenbiologischen Verhalten", Abschluss: Diplom-Biologin |
| 09/1992-06/2000 | Domgymnasium, Merseburg, Abschluss: Allgemeine Hochschulreife |
| 09/1988-06/1991 | Grundschule, Leuna |

**Arbeitserfahrung**

| | |
|---|---|
| seit 04/2008 | wissenschaftliche Mitarbeiterin, Universitätsklinik und Poliklinik für Strahlentherapie, Medizinische Fakultät der Martin-Luther-Universität Halle-Wittenberg<br>Untersuchungen zur Modulation der Strahlensensibilität humaner Gliome durch IDH1R132H und HIF-1α-targeting |
| 08/2004-02/2008 | wissenschaftliche Hilfskraft, Institut für Biologie, Abteilung Entwicklungsgenetik (Prof. Reuter) der Martin-Luther-Universität Halle-Wittenberg |

# PUBLICATIONS

**Publications related to this thesis.**

Kessler, J., Hahnel, A., Wichmann, H., Rot, S., Kappler, M., Bache, M., and Vordermark, D. (2010). HIF-1α inhibition by siRNA or chetomin in human malignant glioma cells: effects on hypoxic radioresistance and monitoring via CA9 expression. BMC Cancer *10*, 605.

Kessler, J., Güttler, A., Wichmann, H., Rot, S., Kappler, M., Bache, M., and Vordermark, D. (2015). IDH1(R132H) mutation causes a less aggressive phenotype and radiosensitizes human malignant glioma cells independent of the oxygenation status. Radiother. Oncol. J. Eur. Soc. Ther. Radiol. Oncol. *116*, 381–387.

**Publications not related to this thesis.**

Keßler, J., Rot, S., Bache, M., Kappler, M., Würl, P., Vordermark, D., Taubert, H., Greither,T. (2016). miR-199a regulates Hif-1a and OSGIN 2 mRNA and is correlated to soft-tissue sarcoma patients outcome. Oncol. Lett. (in press)

Bache, M., Rot, S., Keßler, J., Güttler, A., Wichmann, H., Greither, T., Wach, S., Taubert, H., Söling, A., Bilkenroth, U., et al. (2015). mRNA expression levels of hypoxia-induced and stem cell-associated genes in human glioblastoma. Oncol. Rep. *33*, 3155–3161.

Wichmann, H., Güttler, A., Bache, M., Taubert, H., Rot, S., Kessler, J., Eckert, A.W., Kappler, M., and Vordermark, D. (2015). Targeting of EGFR and HER2 with therapeutic antibodies and siRNA: a comparative study in glioblastoma cells. Strahlenther. Onkol. Organ Dtsch. Röntgenges. Al *191*, 180–191.

Güttler, A., Giebler, M., Cuno, P., Wichmann, H., Keßler, J., Ostheimer, C., Söling, A., Strauss, C., Illert, J., Kappler, M., et al. (2013). Osteopontin and splice variant expression level in human malignant glioma: radiobiologic effects and prognosis after radiotherapy. Radiother. Oncol. J. Eur. Soc. Ther. Radiol. Oncol. *108*, 535–540.

Bache, M., Zschornak, M.P., Passin, S., Keßler, J., Wichmann, H., Kappler, M., Paschke, R., Kaluđerović, G.N., Kommera, H., Taubert, H., et al. (2011). Increased betulinic acid induced cytotoxicity and radiosensitivity in glioma cells under hypoxic conditions. Radiat. Oncol. Lond. Engl. *6*, 111.

# POSTER, TALKS AND AWARDS

**J Keßler, A Güttler, M Bache, T Hohmann, F Dehghanie, D Vordermark:** Expression of IDH1R132H mutant protein causes a less aggressive phenotype and radiosensitizes human malignant glioma cells independent of the oxygenation status „25. Symposium Experimentelle Strahlentherapie und Klinische Strahlenbiologie", 11.-13.02.2016, Dresden.

**J Keßler, A Güttler, H Wichmann, M Bache, D Vordermark:** Einfluss von IDH1R132H auf das zellbiologische Verhalten und Strahlenempfindlichkeit von Gliomzelllinien in Abhängigkeit vom Oxygenierungszustand „Netzwerk Tumormikromillieu", 12.11.2015, Frankfurt.

**J Keßler, A Güttler, H Wichmann, K Theuerkorn, S Roth, M Kappler, M Bache, D Vordermark:** Radiosensitization of human malignant glioma cells expressing isocitrate dehydrogenase 1 (IDH1) mutant protein under normoxia and hypoxia „14th International Wolfsberg Meeting on Molecular Radiation Biology/Oncology", 20.-22.06.2015, Wolfsberg, Schweiz.

**J Keßler, H Wichmann, A Güttler, S Rot, M Bache, D Vordermark:** IDH1 Mutation in Gliomen Radiosensitivierung von IDH1R132H-positiven malignen Gliomzelllinien unter normoxischen und hypoxischen Bedingungen „24. Symposium Experimentelle Strahlentherapie und Klinische Strahlenbiologie", 26.-28.02.2015, Hamburg.

**J Keßler, A Güttler, H Wichmann, M Bache, D Vordermark:** Überexpression von IDH1R132H und die Strahlenresistenz maligner Gliome „3. Forschungstag der Medizinischen Fakultät der Martin-Luther-Universität Halle-Wittenberg", 10.10.2014, Halle.

**J Keßler, A Güttler, H Wichmann, M Bache, D Vordermark:** Einfluss einer IDH1R132H Überexpression auf die Strahlenresistenz maligner Gliome „19. Jahreskongress der Deutschen Gesellschaft für Radioonkologie (DEGRO)", 09.-12.05.2013, Berlin.

**J Keßler, A Güttler, H Wichmann, M Bache, D Vordermark:** Radiosensitization of normoxic and hypoxic U251 malignant glioma cells expressing IDH1R132H mutant protein „EORTC-EANO-ESMO conference 2013 Trends in Central Nervous System Malignancies", 22.-23.03.2013, Prag, Tschechische Republik.

**J Keßler, A Güttler, H Wichmann, M Bache, D Vordermark:** Überexpression von IDH1R132H und die Strahlenresistenz maligner Gliome „22. Symposium Experimentelle Strahlentherapie und Klinische Strahlenbiologie", 21.-23.02.2013, Dresden.

**J Keßler, A Hahnel, T Greither, S Rot, M Bache, D Vordermark:** Einfluss von IDH1 auf HIF-1α und die Strahlenresistenz maligner Gliome „18. Jahreskongress der Deutschen Gesellschaft für Radioonkologie (DEGRO)", 07.-10.06.2012, Rhein-Main-Hallen Wiesbaden.

**J Keßler, A Hahnel, S Rot, M Bache, D Vordermark:** Einfluss von IDH1 auf HIF-1α und die Strahlenresistenz maligner Gliome „21. Symposium Experimentelle Strahlentherapie und Klinische Strahlenbiologie", 09.-11.02.2012, Hamburg.

**J Keßler, M Bache, D Vordermark:** Inhibition of HIF-1α and its impact on radioresistance in malignant glioma cell lines „International Brain Tumor Research Conference", 24.-26.03.2010, Frankfurt.

**J Keßler, M Bache, D Vordermark:** Einfluss einer HIF-1α-Inhibierung durch siRNA oder chetomin auf die Strahlenresistenz maligner Gliom-Zelllinien „19. Symposium Experimentelle Strahlentherapie und Klinische Strahlenbiologie", 04.-06.03.2010, Dresden.

**J Keßler, S Rot, M Kappler, D Vordermark, H Taubert, M Bache:** Bestrahlung und Survivin-spezifische siRNA in mesenchymalen Stammzellen (MSC) und Weichteilsarkomen (WTS) „18. Symposium Experimentelle Strahlentherapie und Klinische Strahlenbiologie", 26.-28.02.2009, Dresden.


OncoRay-Posterpreis

**J Keßler, A Güttler, H Wichmann, M Bache, D Vordermark:** Überexpression von IDH1R132H und die Strahlenresistenz maligner Gliome „22. Symposium Experimentelle Strahlentherapie und Klinische Strahlenbiologie", 21.-23.02.2013, Dresden.

Nachwuchsstipendium Experimentelle Strahlentherapie

**J Keßler, A Hahnel, S Rot, M Bache, D Vordermark:** Einfluss von IDH1 auf HIF-1α und die Strahlenresistenz maligner Gliome „21. Symposium Experimentelle Strahlentherapie und Klinische Strahlenbiologie", 09.-11.02.2012, Hamburg